

Collation and Analysis of Oceanographic Datasets for National Marine Bioregionalisation

- Donna Hayes ■ Vincent Lyne
- Scott Condie ■ Brian Griffiths
- Simon Pigot ■ Gustaaf Hallegraeff

Project team: Donna Hayes, Vincent Lyne, Scott Condie, Brian Griffiths, Simon Pigot, Gustaaf Hallegraeff, Rick Smith, David McDonald, Madeleine Cahill, Peter Rothlisberg, Linda Thomas, Roger Scott, Jeff Dunn, Chris Rathbone, Philip Bohm, Franzis Althaus, Ken Ridgway, Ken Suber



Australian Government

Department of the Environment and Heritage



CSIRO Marine Research

Collation and Analysis of Oceanographic Datasets for National Marine Bioregionalisation.
A report to the Australian Government, National Oceans Office.

May 2005
CSIRO Marine Research

Donna Hayes CSIRO Marine Research
Vincent Lyne CSIRO Marine Research
Scott Condie CSIRO Marine Research
Brian Griffiths CSIRO Marine Research
Simon Pigot Department of Primary Industries, Water and Environment, Tasmania.
Gustaaf Hallegraeff University of Tasmania

Contents

1	SUMMARY	1
2	PROJECT OBJECTIVES	3
3	PROJECT BACKGROUND	4
4	DATA STORAGE AND METADATA	7
4.1	Introduction	7
4.2	Neptune Metadata records	8
4.3	Data compatibility with other data projects	15
5	NATIONAL DATASETS	16
5.1	Geographic Extent of Project	16
	<i>Depth</i>	17
	<i>Temporal coverage</i>	17
5.2	CARS: Temperature, Salinity, Oxygen, Phosphate, Nitrate and Silicate	18
	<i>Methods</i>	18
	<i>Description</i>	20
	<i>Data Provided</i>	21
5.3	Sea-surface Temperature	41
	<i>Methods</i>	41
	<i>Description</i>	42
5.4	Eddies and Fields based on SST	48
	<i>Data provided</i>	49
5.5	Sea-surface Steric Height	58
	<i>Methods</i>	58
	<i>Description</i>	59
	<i>Data Provided</i>	59
5.6	Sea-surface Height Variability	60
	<i>Methods</i>	60
	<i>Description</i>	60
	<i>Data Provided</i>	60
5.7	Geostrophic Currents	66
	<i>Methods</i>	66
	<i>Description</i>	66
	<i>Data Provided</i>	67
5.8	Mixed-layer Depth	70
	<i>Methods</i>	70
	<i>Description</i>	71
	<i>Data Provided</i>	71
5.9	Wind Stress	73
	<i>Methods</i>	73
	<i>Description</i>	73
	<i>Data provided</i>	74
5.10	Wind-stress Curl	77
	<i>Methods</i>	77
	<i>Description</i>	77
	<i>Data Provided</i>	78
5.11	Surface Waves	81
	<i>Methods</i>	81
	<i>Description</i>	81
	<i>Data Provided</i>	81
5.12	Tides	84
	<i>Methods</i>	84

<i>Description</i>	84
<i>Data Provided</i>	84
5.13 Photosynthetically Active Radiation	86
5.14 Chlorophyll- <i>a</i> from the MODIS Aqua Ocean Colour Satellite	89
5.15 Seasonal and Interannual Variations in Surface Chlorophyll from SeaWiFS Ocean-colour Satellite	94
5.16 Primary Production Estimates from the MODIS AQUA Ocean Colour Satellite and the Behrenfeld–Falkowski Vertical Generalised Production Model	97
<i>Primary Production Historical Data</i>	102
5.17 Zooplankton Biomass – Historical Data	107
<i>Summary</i>	113
6 MARINE PHYTOPLANKTON PERSPECTIVE ON AUSTRALIAN PELAGIC BIOREGIONALISATION	114
6.1 Background	114
6.2 Characterisation of Australian Marine Phytoplankton Provinces	120
7 WATER MASS FORMATION AND SUBDUCTION	125
7.1 Introduction	125
7.2 Mode Waters	126
7.3 Large-scale Setting: WOCE Section P11	128
7.4 Water Masses of the South-west Pacific	130
7.5 Subantarctic Mode Water (SAMW)	135
7.6 Summary	141
8 THE DYNAMICS OF THE EAST AUSTRALIAN CURRENT AND ITS EDDIES	142
8.1 Introduction	142
8.2 Large-scale setting: Oceanographic context	143
8.3 Circulation patterns and processes	145
8.4 East Australian Current Eddy Field and Energetics	147
8.5 Features of the EAC and the biological context	150
8.6 Overview of impacts of eddies and the East Australian Current on bioregionalisation processes in the Tasman Sea	151
8.7 Eddy formation and disappearance	153
8.8 Natural History of Eddies F and J.	155
<i>History of Eddy F</i>	155
<i>Results from the Eddy F survey</i>	156
<i>History of Eddy J</i>	157
<i>Micronekton distribution in relation to Eddy J structure and age</i>	157
8.9 Zoogeographic Surveys	164
<i>Eddy P, 1982</i>	164
<i>Latitudinal Survey 1983</i>	165
8.10 Summary	167
9 RECOMMENDATIONS FOR FUTURE RESEARCH	168
10 ACKNOWLEDGMENTS	170
11 REFERENCES	171
APPENDIX A PRODUCT LIST	178
A.1 NATIONAL (longitude: 90-180E; latitude: 0-60S)	178
A.2 The Northern Marine Region	200
A.3 CASE STUDY Albatross Bay	210
APPENDIX B DATA CENTRE DIRECTORY STRUCTURE	215
APPENDIX C CARS STATION LOCATIONS	217

APPENDIX D MAJOR OCEANOGRAPHIC FEATURES WITHIN THE AUSTRALIAN MARINE JURISDICTION	220
APPENDIX E 3-D/4-D DATA ISSUES	222
E.1 Executive Summary	222
E.2 Introduction	223
<i>Evolution of the regionalisations</i>	223
<i>Distribution of the regionalisations and other oceanographic data through web based portals</i>	224
E.3 3-D/4-D Data Properties and Data Formats	225
E.4 Software to visualise the data	226
E.5 Computer hardware to run these visualisations	228
E.6 Conclusions	229
E.7 References	229

Figures

Figure 4.1	Metadata structure for National Oceans Office data holdings.	8
Figure 4.2	Locating metadata records on Neptune.	9
Figure 5.1	The geographic region of interest for the national study.	16
Figure 5.2	Depth contours of depths chosen to present CARS data.	19
Figure 5.3	Nitrate Annual Mean at (a) the surface, (b) 150 m, (c) 500 m, (d) 1000 m and (e) 2000 m.	23
Figure 5.4	Oxygen Annual Mean at (a) the surface, (b) 150 m, (c) 500 m, (d) 1000 m and (e) 2000 m.	26
Figure 5.5	Phosphate Annual Mean at (a) the surface, (b) 150 m, (c) 500 m, (d) 1000 m and (e) 2000 m.	29
Figure 5.6	Salinity Annual Mean at (a) the surface, (b) 150 m, (c) 500 m, (d) 1000 m and (e) 2000 m.	32
Figure 5.7	Silicate Annual Mean at (a) the surface, (b) 150 m, (c) 500 m, (d) 1000 m and (e) 2000 m.	35
Figure 5.8	Temperature Annual Mean at (a) the surface, (b) 150 m, (c) 500 m, (d) 1000 m and (e) 2000 m.	38
Figure 5.9	SST image of the East Australian Current and associated eddies.	42
Figure 5.10	Sea-surface Temperature Monthly Means for (a) January, (b) April, (c) July and (d) October	44
Figure 5.11	Sea-surface Temperature Monthly Means for (a) January, (b) April, (c) July and (d) October	46
Figure 5.12	Eddies and fields based on sea-surface Temperature in January. (a) low heterogeneity, (b) medium heterogeneity, (c) high heterogeneity, (d) high heterogeneity and high gradients.	50
Figure 5.13	Eddies and fields based on sea-surface temperature in July. (a) low heterogeneity, (b) medium heterogeneity, (c) high heterogeneity, (d) high heterogeneity and high gradients	54
Figure 5.14	Eddies and fields based on sea-surface temperature in October. (a) low heterogeneity, (b) medium heterogeneity, (c) high heterogeneity, (d) high heterogeneity and high gradients.	56
Figure 5.15	Sea-surface steric height for (a) January, (b) April, (c) July and (d) October.	61
Figure 5.16	Sea-surface height monthly variability for (a) January, (b) April, (c) July and (d) October.	63
Figure 5.17	Sea-surface height annual variability.	65
Figure 5.18	Geostrophic surface currents for (a) January, (b) April, (c) July and (d) October.	68
Figure 5.19	Mixed Layer (a) mean depth and (b) annual amplitude	72
Figure 5.20	Wind stress (a) January, (b) April, (c) July and (d) October	75
Figure 5.21	Wind-stress curl (a) January, (b) April, (c) July and (d) October	79
Figure 5.22	Wave height for the Australian Region (a) Maximum wave height, (b) Mean wave height.	82
Figure 5.23	Wave period for the Australian Region (a) Maximum wave period, (b) Mean wave period.	83
Figure 5.24	Tidal Velocities in the Australian Region (a) Maximum tidal velocity, (b) Mean tidal velocity.	85
Figure 5.25	Photosynthetically Active Radiation for (a) January, (b) April, (c) July and (d) October.	87
Figure 5.26	Monthly mean Chlorophyll for (a) January, (b) April, (c) July and (d) October.	90
Figure 5.27	Monthly means for primary production for (a) January, (b) April, (c) July and (d) October.	98
Figure 5.28	Areal coverage of 27 research voyages measuring primary production in Australian waters between 1959 and 1965.	102
Figure 5.29	Primary productivity ($\text{grams C m}^{-2} \text{ d}^{-1}$) from 1959 to 1964.	104
Figure 5.30	Primary productivity in southern Australian waters by southern season	105

Figure 5.31 Primary productivity in northern Australian waters by northern season	106
Figure 5.32 Zooplankton biomass (mg wet weight m ⁻³) by category	107
Figure 5.33 Zooplankton biomass (mg wet weight m ⁻³) in southern Australian waters by southern season.	109
Figure 5.34 Zooplankton biomass (mg wet weight m ⁻³) in the Timor triangle by northern season.	110
Figure 5.35 Zooplankton biomass seasonality (Jan. to Aug.) along 110° E.	111
Figure 5.36 Zooplankton biomass seasonality (July to Oct.) along 110° E.	112
Figure 6.1 An early effort towards pelagic bioregionalisation by Wood (1954) based on dinoflagellate communities.	114
Figure 6.2 Three main phytoplankton bioregions recognised by Jeffrey & Hallegraeff (1990): 1. tropical neritic; 2. tropical oceanic; 3. temperate neritic.	115
Figure 6.3 The phytoplankton dataset available for the present work.	116
Figure 6.4 Examples of key phytoplankton indicator species used to discriminate between tropical and temperate, neritic and oceanic, cosmopolitan and subantarctic communities.	117
Figure 6.5 The results of comprehensive Australia-wide cyst surveys support the biogeographic boundary between warm-water species	118
Figure 6.6 Examples of typical SeaWiFs images of surface phytoplankton chlorophyll	119
Figure 6.7 Phytoplankton provinces in Australia	124
Figure 7.1 Section of salinity (in PSU units) along the 160°E section down to a depth of 2000 m based on the CARS. Major water masses are also indicated.	126
Figure 7.2 Longitude section along 160°E of the regionalisation of Lyne and Hayes (2005) showing the structuring by depth and longitude of the so-called Level 1b regionalisations.	127
Figure 7.3 Position of the Track of <i>RV Franklin</i> 9306 (WOCE section P11).	128
Figure 7.4 Salinity at the (a) surface, (b) 150 m, and (c) 800 m, based CARS. Major water masses are also indicated (definitions in Appendix C).	131
Figure 7.5 Vertical sections of water properties along WOCE section p11.	134
Figure 7.6 Water properties on the isopycnal corresponding to the Subantarctic Mode Water (SAMW)	136
Figure 7.7 Salinity on the isopycnal corresponding to the Subantarctic Mode Water (SAMW)	137
Figure 7.8 Water property anomalies along WOCE section P11 plotted in neutral density coordinates.	138
Figure 7.9 Properties of the Subantarctic Mode Water along P11.	139
Figure 7.10 Circulation of SAMW. Paths of water masses are shown by solid lines with arrows, and transports are indicated in circles (Sv) (Sokolov & Rintoul 2000)©Journal of Marine Research.	140
Figure 8.1 Map of the waters off eastern Australia showing surface regionalisations of water properties from Lyne and Hayes (2005).	144
Figure 8.2 Longitude section along 160°E of the regionalisation of Lyne and Hayes (2005) showing the structuring by depth and longitude of the so-called Level 1b regionalisations.	146
Figure 8.3 Map showing superposition of “energetics” field onto the regionalisation of Figure 8.1	148
Figure 8.4 Movement of Eddy J and the position of Eddy F during sampling periods (After Tranter et al, 1983).	156
Figure 8.5 Pattern of surface mean temperatures around Australia obtained from the CSIRO CARS oceanographic atlas.	163
Figure 8.6 Sampling sites (●) during August 1982 on the first zoogeography cruise.	164
Figure 8.7 Sampling sites (●) along 155 °E during June and July 1983.	165

1 Summary

The collation and analysis of oceanographic datasets reported here was one of the projects commissioned by the National Oceans Office, to support the National Marine Bioregionalisation. The main aim of this project was to provide oceanographic datasets to the Pelagic Integration Project during 2004; some were also provided to the Benthic Bioregionalisation Project coordinated by Geoscience Australia.

The oceanographic information collated was at two broad scales: a national scale (Section 5) and a more detailed scale in the Northern Large Marine Domain (Rothlisberg et al 2005). The extent of the national study was the region 90°– 180°E and 0°–60°S. The data collected over this region provided information on temperature, salinity, dissolved oxygen, nitrate, silicate, phosphate, remotely sensed sea-surface temperature, winds (stress and curl), waves, tides, eddies and fields, currents, ocean colour, primary production and photosynthetically available radiation. There were very few biological datasets on a national scale; this has been identified as a priority area for further research.

The Northern Large Marine Domain extends from Cape Talbot in Western Australia to Cape York in Queensland, encompassing part of Torres Strait, the Gulf of Carpentaria, Arafura Sea, Joseph Bonaparte Gulf and the Timor Sea. The datasets provided were similar to those listed above, with the addition of some finer-scale biological data for the Gulf of Carpentaria and Albatross Bay.

To provide a more detailed look at specific processes in Australia's oceans, two case studies are included in this report: Water-mass formation and subduction (Section 7) and Dynamics of the East Australian Current (Section 8).

The first case study provides a general discussion of water-mass formation and a detailed look at the formation of one South Pacific water mass, the Subantarctic Mode Water. This water mass is formed by deep winter convection between the subtropical front and the subantarctic front. It spreads equatorward in the subtropical gyres centred approximately 600 m depth.

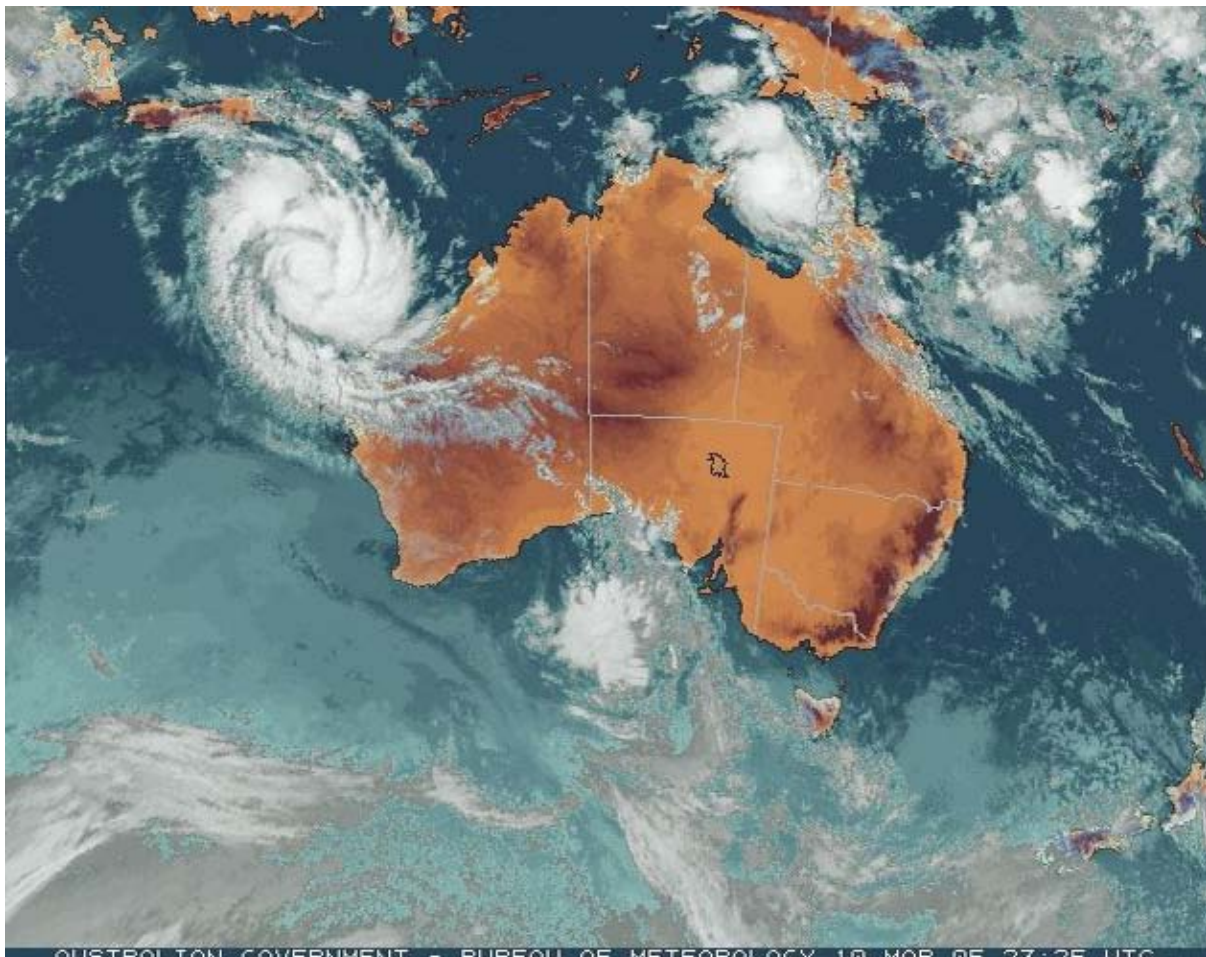
The second case study, on the dynamics of the East Australian Current, gives a detailed overview of this western boundary current and its associated eddies. The discussion brings together the physical and biological processes associated with this feature.

A third case study, of Albatross Bay, is included in the accompanying report of the Northern Large Marine Domain (Rothlisberg et al 2005). It explores both physical oceanography and biology. The Albatross Bay Region in the north-eastern Gulf of Carpentaria supports local fisheries for three species of commercially important penaeid prawns. This case study discusses both seasonal and inter-annual variability in biological and hydrographic parameters in tropical Australia.

In addition to providing inputs for the National Marine Bioregionalisation project, this work has facilitated public access to fundamental marine data. All the data collated have been delivered to the National Oceans Office as GIS layers and maps. These, and comprehensive metadata, will be freely available from Neptune (<http://neptune.oceans.gov.au>).



**Australia's Marine National Facility RV
Southern Surveyor ©CSIRO**



AUSTRALIAN GOVERNMENT - BUREAU OF METEOROLOGY 10 MAR 05 23:25 UTC
JMA and NOAA GOES-9 image via Bureau of Meteorology©. GMS-5 backup with GOES-9 operated by the joint effort of JMA and US NOAA NESDIS over the western Pacific¹.
Captured: Thursday 10 March 2005 23:30 UTC
(<http://www.bom.gov.au/gms/IDE00035.200503102130.shtml>)

¹ Satellite image processed by the Bureau of Meteorology from the Geostationary Meteorological Satellite GOES-9 operated by the National Oceanographic and Atmospheric Administration for the Japan Meteorological Agency (reproduced with permission).

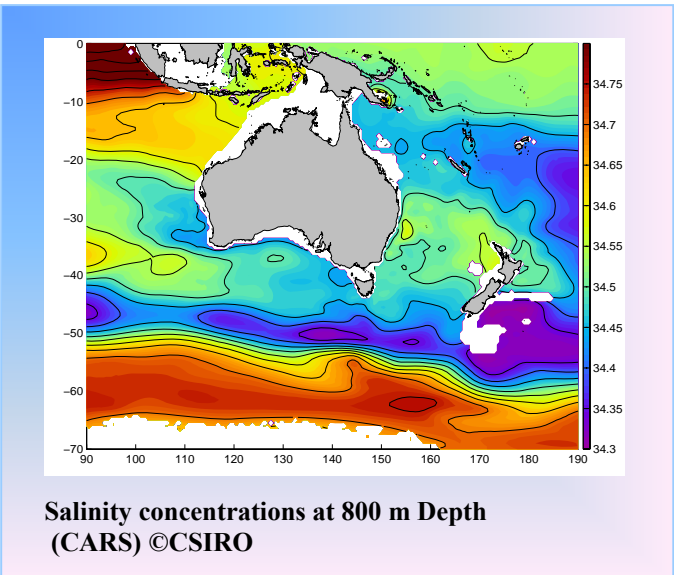
2 Project Objectives

The project aimed to collate and analyse relevant oceanographic datasets as specified by the National Oceans Office to provide information on pelagic oceanographic characteristics in Australia's marine jurisdiction, and to provide expert advice on the use of this information in defining and describing bioregions in the development of the National Marine Bioregionalisation. In addition, this project delivered benthic and oceanographic datasets to the providers of the benthic and pelagic bioregionalisation projects (Geoscience Australia and CSIRO Marine Research).

The data gathered in this project was crucial to the National Marine Bioregionalisation Project, which commenced in May 2004 and delivered draft products to the National Oceans Office in December 2004.

The oceanographic information will contribute to the definition and description of marine bioregions at two scales – a broad national scale and a more detailed scale in the northern region. This information includes biological, chemical and physical oceanographic data.

Specific oceanographic information is provided to define finer-scale bioregions for northern Australia (see Rothlisberg et al 2005). The outputs for Northern Australia are similar to the national outputs, but with information presented in more detail. Some of the datasets provided for northern Australia were not available nationally.



3 Project Background

According to Australia's Oceans Policy "...the Australian Government is committed to an ecosystem-based approach to oceans management". This approach requires planning and management to be based on ecosystem characteristics. Bioregionalisation is one way of defining ecosystem regions, as it defines regions based on physical and biological properties.

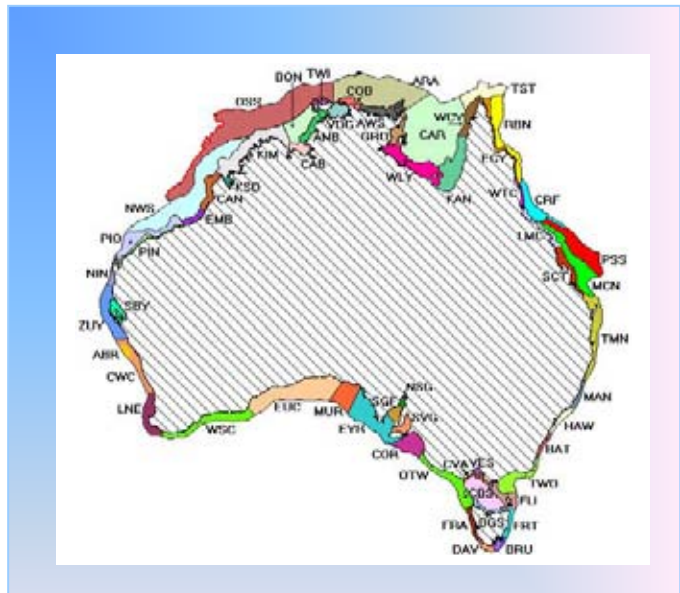
Ecosystem-based management has been implemented through regional marine planning. At a broad scale, regional marine plans have been based on the Large Marine Domains (Lyne et al 1998), while at smaller scales, they have been based on the Interim Marine and Coastal Regionalisation for Australia (IMCRA) (IMCRA Technical Group, 1998) (see insert).

The current National Marine Bioregionalisation project, coordinated by the Nation Oceans Office, consists of both pelagic (water column) and benthic (seafloor) components. The intended outcome of the National Marine Bioregionalisation is a set of bioregions for the Australian Marine Jurisdiction that will underpin a spatial framework to support planning and management of Australia's oceans.

This project builds on previous work undertaken in the project National Oceanographic Description and Information Review for National Bioregionalisation (Condie et al 2003), which produced the following data management services: a metadata catalogue; initial data products; spatial analytical and mapping services; spatial data products; and exploratory data analysis.

The pelagic bioregionalisation framework is hierarchical. Datasets to define the different levels of bioregions are identified in this report. The bioregionalisation framework is shown in Table 3.1.

The datasets identified, collated, analysed and interpreted by this project have been used in the Benthic and Pelagic Bioregionalisation projects, which delivered draft products in December 2004 and final products in April 2005.



Interim Marine and Coastal Regionalisation for Australia: Meso-scale regionalisation
[\(<http://www.deh.gov.au/parks/nrs/capad/1997/paaust/imera3.html>\)](http://www.deh.gov.au/parks/nrs/capad/1997/paaust/imera3.html)

Table 3-1 Pelagic classification framework presented as a hierarchy of levels with names, definitions, example units at each level and explanations of how these units are defined for this project. Note that temporal variability, combined with transitional adjustments between and within levels, results in overlaps between levels and units so that, in application, the framework is not strictly hierarchical.

Level	Name	Definition	Examples	Defined by CMR ² using
0	Oceans	In a global context, partitioning at this level recognises the distinction between fauna (collective ecosystems) of the Indian, Pacific and Southern oceans. Regionalisation at this level needs to be at global scales (since the distinctions are global in context). For this project, a descriptive narrative is used to distinguish the differences and transitions between the Indian, Pacific and Southern Oceans.	Pacific, Indian and Southern Oceans	Literature
1a	Oceanic Zones	Winds, solar forcing and geostrophy dynamically combine to drive a series of largely circumferential and latitudinally oriented water masses within oceans, each of which can be characterised by its water properties, circulation and assemblages of biota. Transitional zones between some water masses are generally characterised by higher plankton production, which influences trophic structure and interactions. For this project, the classifications based on physical properties are guided and corroborated by the distribution of phytoplankton and pelagic fish on the continental shelf.	The dominant water masses surrounding Australia are the South-west Pacific Central Water, Indonesian Throughflow Water (Australasian Mediterranean Water) and Indian Central Water.	CARS ³ , but for zones that extend across ocean basins, datasets that are global, or at the very least basin-wide, should ideally be used.
1b	Oceanic Substructure–Water Masses	Within the Oceanic Zones, substructure is characterised by largely latitudinal bands of water masses extending through the water column. These bands represent segments of circulatory systems that may span ocean basins.	Antarctic Intermediate Water, Subtropical Lower Water, Tropical Surface Water	CARS, full suite of variables

² CSIRO Marine Research

³ CSIRO Atlas of Regional Seas

2	Seas: Circulation Regimes	Within latitudinal bands, different ocean circulations and air/sea moisture exchanges result in different retention, mixing and transport of water properties and biological organisms. Such regions respond differently to seasonal and interannual climate variations. Consequently, there may be temporal changes in the location, extent and strength of circulation regimes and their biota. Transitional zones characterise the temporal changes and adjustments between the different circulation regimes—and, again, may be characterised by higher productivity.	Sea between Tasmania and New Zealand; circulation associated with the East Australian Current (EAC); Arafura Sea off NW Australia; Great Australia Bight offshore circulation; circulation associated with Leeuwin Current.	CARS: nested analysis of temperature, salinity and oxygen within the level above
3	Fields of Features	Within Circulation Regimes, structure can be characterised by regions of different energetics; for example, mixing due to eddy activity, frontal oscillations and boundary currents. Transition regions represent changes in the energetics at the boundary of the field and seasonal movements and variations in strength.	Fields of eddies—Eddies of the EAC. The seasonal movements of the eddy fields of the EAC.	SST, geostrophic currents
4a	Features	Description of structure and dynamics of individual features.	Individual eddies: Eddy J of the EAC	
4b	Feature Structure	Internal structure and dynamics of individual features.	The semipermanent eddies of the EAC	

4 Data storage and Metadata

4.1 Introduction

The oceanographic data collation project relied on existing datasets, most of which were in a readily accessible format. However, some existed only in paper cruise reports and had to be entered manually, while others required transcribing from old formats.

We have archived the data as collected from the various contributors. When the file size of these '*base data*' is less than 100 MB, they are stored on Neptune (<http://neptune.oceans.gov.au>), the National Oceans Office's metadata system. When the file size exceeds 100 MB, the corresponding metadata record will direct a user to the data off-line. The off-line data are currently being stored on LTO-2 tapes in 'tar' format and housed by CSIRO Marine Research. The '*base data*' will be made available to the public where there are license agreements; however, some of the base datasets will remain confidential as stipulated in the current access agreements.

Derived datasets, GIS layers and maps were created from the base data. Details of the enhanced data and visualisation products are described in Section 5. The GIS layers and maps are web-accessible on Neptune (<http://neptune.oceans.gov.au>) and are available to the public. Individual GIS and map products are connected to their unique metadata record.

A schematic diagram illustrating the metadata structure for this project on Neptune is shown in Figure 4.1.



MODIS Aqua

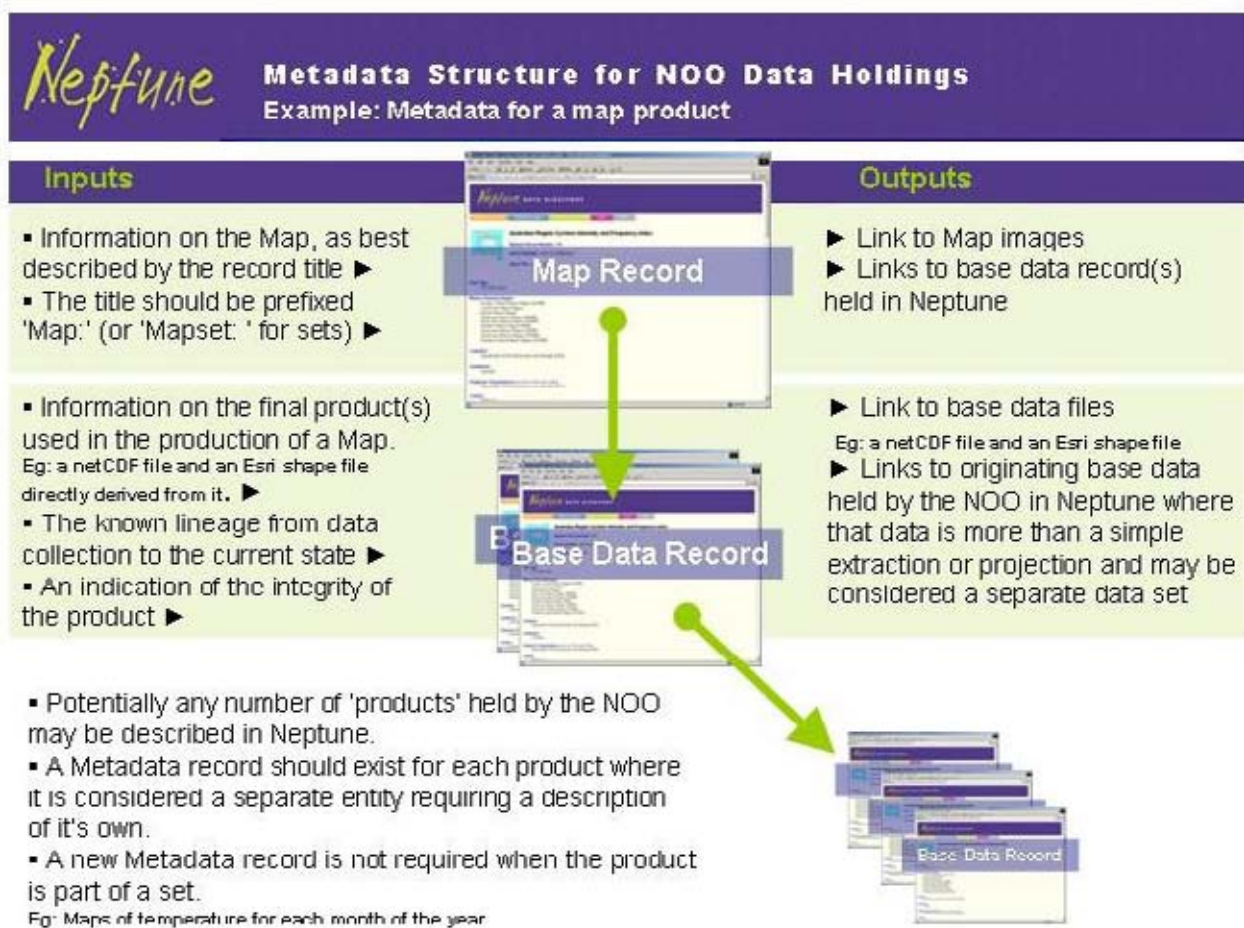


Figure 4.1 Metadata structure for National Oceans Office data holdings.

4.2 Neptune Metadata records

A record for each dataset/GIS layer/grid/coverage and map was created for Neptune (National Oceans Office database). Table 4.1 shows the Neptune record numbers and dataset titles.

To locate any of these metadata records (see Figure 4.2), go to <http://neptune.oceans.gov.au>, select 'Text or Number Search', then 'quick record retrieval' and enter the Neptune record number (see column 1 in Table 4.1).

COLLATION AND ANALYSIS OF OCEANOGRAPHIC DATASETS FOR MARINE BIOREGIONALISATION

a

The screenshot shows the 'SEARCH NEPTUNE' page. At the top, there's a purple header bar with the Neptune logo and 'DATA DIRECTORY'. Below it is a navigation bar with tabs: 'SEARCH NEPTUNE' (highlighted in orange), 'NEPTUNE HOME', 'OCEAN OFFICE HOME', 'HELP', and 'EDIT'. On the left, there's a sidebar with the Australian Government National House Office logo. The main content area contains text explaining three search methods: 'User-defined search', 'List datasets', and 'Text or number search'. It also includes instructions for navigating the search results and details about dataset types, time periods, and geographic regions.

b

The screenshot shows the 'TEXT OR NUMBER SEARCH' page. At the top, there's a purple header bar with the Neptune logo and 'DATA DIRECTORY'. Below it is a navigation bar with tabs: 'SEARCH NEPTUNE' (highlighted in orange), 'NEPTUNE HOME', 'OCEAN OFFICE HOME', 'HELP', and 'EDIT'. On the left, there's a sidebar with the Australian Government National House Office logo. The main content area contains sections for 'Free Text Search', 'Quick Title Search', and 'Quick Record Retrieval'. It includes instructions for each method and a search form with fields for 'Search for' (containing '801'), 'Search type' (set to 'Text or number search'), and a 'Continue' button. Below the search form, there's an optional section for entering user ID and password.

Figure 4.2 Locating metadata records on Neptune.

Follow link <http://neptune.oceans.gov.au>. (a) select text or number search (b) select ‘quick record retrieval’ and enter Neptune record number (listed in Table 4.1).

Table 4.1 Neptune record numbers, dataset titles and the stored data volume for each record.

Neptune Record No.	Title	Stored data volume
801	Sea-surface Height Monthly Standard Variability in the Australian Region	1.07 MB
805	Wind Stress Monthly Mean Fields in the Australian Region	netCDF format: 85.2 MB
806	Sea-surface Height Annual Standard Deviation in the Australian Region	netCDF format: 95.4KB
807	Benthic Nutrients and Physical Water Properties Annual Amplitude in the Australian Region (0.025 grid)	netCDF format: 14.8 MB
808	Sea Temperature at depth in the Australian Region	netCDF format: 46.4 MB
809	Sea-surface Silicate in the Australian Region	netCDF format: 53.3 MB
810	Sea Salinity in the Australian Region	netCDF format: 30.2 MB
811	Sea-surface Phosphate in the Australian Region	netCDF format: 55.2 MB
812	Sea-surface Dissolved Oxygen in the Australian Region	netCDF format: 54.2 MB
813	Sea-surface Nitrate in the Australian Region	netCDF format: 57.2 MB
814	Mixed Layer Depth in the Australian Region	netCDF format: 625 KB
815	GIS Layer: Wind Curl in the Australian Region	mapinfo: 1.81 MB
818	Sea-surface Mean Height and Currents in the Australian Region	netCDF format: 39.1 MB
830	Mapset: Sea-surface Temperature Quarterly Means (in the Australian Region)	pdf format: 6.34 MB jpg format: 1.84 MB
831	Mapset: Wind Stress on Australian Oceans Quarterly Means (in the Australian Region)	pdf format: 2.76 MB jpg format: 2.39 MB
832	Mapset: Wind Curl on Australian Oceans Quarterly Means (in the Australian Region)	pdf format: 1.62 MB jpg format: 1.27 MB
833	Mapset: Mean Sea-surface Currents each Quarter (in the Australian Region)	pdf format: 3.78 MB jpg format: 3.44 MB
834	Mapset: Sea-surface Height Monthly Variability (in the Australian Region)	pdf format: 13.7 MB jpg format: 3.31 MB
844	Mapset: Sea-surface Temperature Quarterly and Overall Means in the Northern Marine Region	pdf format: 18.9 MB jpg format: 1.33 MB
848	Map: Salinity Annual Means in the Northern Marine Region	pdf format: 6.14 MB jpg format: 443 KB
849	Map: Dissolved Oxygen Annual Mean in Northern Marine Region	pdf format: 6,292 KB jpg format: 439 KB
852	Map: Zooplankton Biomass in Albatross Bay	pdf format: 1.83 MB jpg format: 469 KB
854	Half Lunar Cycle Mean and Maximum Tidal Currents in the Australian Region	16.3 MB
855	Mapset: Sea-surface Height Quarterly Means (in the Australian Region)	pdf format: 3.77 MB jpg format: 3.44 MB
859	Wave Height Direction and Period in the Australian Region	1.08 GB (1,159,970,816 bytes)
868	Sea-surface Temperature Monthly Means and Variance in the Australian Region	
869	Eddies and Fields Based on Sea-surface Temperature in the Australian Region	412 MB

Neptune Record No.	Title	Stored data volume
870	Mapset: Eddies and Fields Based on Sea-surface Temperatures Quarterly (classes 1–4) (in the Australian Region)	pdf format: 35 MB jpg format: 12.6 MB
872	Incident Light and Photosynthetically Active Radiation (PAR) Monthly Means in the Australian Region	netCDF format: 216 KB
873	Mapset: Incident Light Quarterly Means (in the Australian Region)	pdf format: 1.58 MB jpg format: 1.27 MB
874	Bottom Stress from the Northern Region Circulation Model	netCDF format: 331 KB
875	Mapset: Currents in the Northern Marine Region	pdf format: 15.2 MB jpg format: 1.85 MB arc/info: 4.5 MB
879	Map: Phytoplankton Provinces in the Australian Region	pdf format: 285 KB jpg format: 218 KB text documents: 23.48 KB
880	Ocean Colour Monthly Means and Variances (MODIS) in the Australian Region	netCDF format: 713 MB
884	Zooplankton Biomass 1986–1992 in Albatross Bay	887 KB
885	Map: Sea-surface Height Annual Variability (in the Australian Region)	pdf format: 3.45 MB jpg format: 865 KB
889	Map: Silicate Annual Means in the Northern Marine Region	pdf format: 6,296 KB jpg format: 454 KB
890	Map: Phosphate Annual Means in the Northern Marine Region	pdf format: 6.14 MB jpg format: 445 KB
891	Map: Nitrate Annual Means in the Northern Marine Region	pdf format: 6,294 KB jpg format: 425 KB
894	Geostrophic Subsurface Currents in the Australian Region	netCDF format: 81.4 MB
899	Map: Sea-surface Temperature Total Mean (in the Australian Region)	pdf format: 0.99 MB jpg format: 402 KB
904	Mapset: Ocean Colour Chlorophyll Quarterly Means (in the Australian Region)	pdf format: 3.02 MB jpg format: 2.83 MB
906	Mapset: Primary Production each Quarter (in the Australian Region)	pdf format: 10 MB jpg format: 1.76 MB
907	Mapset: Sea-surface Temperature wet/dry Season Means in the Northern Marine Region	pdf format: 18.5 MB jpg format: 1.36 MB
908	Mapset: Ocean Colour Chlorophyll wet/dry Season Means in the Northern Marine Region	pdf format: 12.4 MB jpg format: 1.18 MB
912	Mapset: Bottom Stress in the Northern Marine Region	pdf format: 14,561 KB jpg format: 1,459 KB
929	Map: Primary Production Annual Mean (in the Australian Region)	pdf format: 2,549 KB jpg format: 412 KB
936	Mapset: Dissolved Oxygen by Depth Annual Means (in the Australian Region)	pdf format: 17.2 MB jpg format: 2.15 MB
937	Mapset: Nitrate by Depth Annual Means (in the Australian Region)	pdf format: 16.8 MB jpg format: 1.93 MB
938	Mapset: Phosphate by Depth Annual Means (in the Australian Region)	pdf format: 15.8 MB jpg format: 1.78 MB
939	Mapset: Salinity by Depth Annual Means (in the Australian Region)	pdf format: 3.18 MB jpg format: 2.43 MB

Neptune Record No.	Title	Stored data volume
940	Mapset: Silicate by Depth Annual Means (in the Australian Region)	pdf format: 16.7 MB jpg format: 1.44 MB
941	Mapset: Sea Temperature by Depth Annual Means (in the Australian Region)	pdf format: 8.53 MB jpg format: 2.25 MB
946	Benthic Nutrients and Physical Water Properties Annual Mean (0.1 grid) in the Australian Region	5.79 MB
948	Mapset: Primary Production wet/dry Seasonal Mean in the Northern Marine Region	pdf format: 12.3 MB jpg format: 1.02 MB
964	Maps of Pelagic Regionalisation Level 1B Classification (in the Australian Region)	report: 40.2 MB map images: 23 MB
965	Map: Mixed Layer Depth Annual Amplitude (in the Australian Region)	pdf format: 417 KB jpg format: 344 KB
968	Map: Half Lunar Mean Tidal Currents (in the Australian Region)	pdf format: 651 KB jpg format: 292 KB
969	Map: Half Lunar Maximum Tidal Currents (in the Australian Region)	pdf format: 663 KB jpg format: 292 KB
970	Map: Annual Maximum Wave Height (in the Australian Region)	pdf format: 311 KB jpg format: 334 KB
971	Map: Annual Mean Wave Height (in the Australian Region)	pdf format: 289 KB jpg format: 286 KB
972	Map: Annual Maximum Wave Period (in the Australian Region)	pdf format: 285 KB jpg format: 281 KB
973	Map: Annual Mean Wave Period (in the Australian Region)	pdf format: 287 KB jpg format: 257 KB
975	Currents from the Northern Region Circulation Model	netCDF format: 126 KB
976	Mapset: Prawn Larval Distributions in Albatross Bay for Wet and Dry Seasons	pdf format: 2,105 KB jpg format: 328 KB
977	Chlorophyll a concentrations in Albatross Bay	excel format: 141 KB
978	Map: Chlorophyll a concentrations in Albatross Bay	pdf format: 1,667 KB jpg format: 347 KB
979	Copepod Abundance in Albatross Bay	excel format: 4.73 MB
980	Map: Copepod Abundance in Albatross Bay	pdf format: 2,910 KB jpg format: 254 KB
981	Map: Phytoplankton Abundance in Albatross Bay	pdf format: 1,345 KB jpg format: 316 KB
982	Phytoplankton Abundance in Albatross Bay	5.97 MB
983	Mapset: Commercial Prawn Larval Distribution in the Gulf of Carpentaria for Wet and Dry Seasons	pdf format: 6,681 KB jpg format: 811 KB
984	Map: Mean Chlorophyll in Albatross Bay	pdf format: 1,048 KB jpg format: 252 KB
985	Mapset: Non-commercial Prawn Larval Distribution in the Gulf of Carpentaria for Wet and Dry Seasons	pdf format: 6,850 KB jpg format: 877 KB
986	Mapset: Prawn Larval Distribution in the Gulf of Carpentaria for Wet and Dry Seasons	pdf format: 6,857 KB jpg format: 876 KB
987	Zooplankton Biomass in the Gulf of Carpentaria for the Wet and Dry Seasons	excel format: 67.8 KB
988	Zooplankton Biomass in Albatross Bay for Wet and Dry Seasons	4 KB
989	Mapset: Total Zooplankton Biomass in the Gulf of Carpentaria for Wet and Dry Seasons	pdf format: 6,855 KB jpg format: 861 KB

Neptune Record No.	Title	Stored data volume
990	Mapset: Zooplankton Biomass in Albatross Bay for Wet and Dry seasons	pdf format: 2,143 KB jpg format: 432 KB
991	Mapset: Commercial Prawn Larval Distribution in Albatross Bay Wet and Dry seasons	pdf format: 1,937 KB jpg format: 396 KB
992	Mapset: Non-commercial Prawn Larval Distribution in Albatross Bay Wet and Dry seasons	pdf format: 2,208 KB jpg format: 460 KB
993	Map: Primary Production and Chlorophyll at two sites in Albatross Bay	pdf format: 1,049 KB jpg format: 252 KB
994	Mean Chlorophyll and Primary Production at two sites in Albatross Bay	37 KB
995	Prawn Larval Distribution in the Gulf of Carpentaria for Wet and Dry seasons	excel format: 33.5 KB
996	Prawn Larval Distribution in Albatross Bay for Wet and Dry seasons	excel: 6 KB
998	Map: Maximum Tidal Range for the Northern Marine Region	pdf format: 4,992 KB jpg format: 427 KB
999	Tidal Range from the Northern Marine Circulation Model	332 KB
1003	Seagrass Sites in the Port of Weipa, Gulf of Carpentaria	map/info: 437 KB word: 101 KB
1004	Map: Mixed Layer Depth Annual Mean (in the Australian Region)	pdf format: 431 KB jpg format: 375 KB
1005	Mapset: Primary productivity in northern Australian waters by northern season	jpg format: 623 KB pdf format: 4.9 MB
1006	Map: Zooplankton biomass (in the Australian Region)	jpg format: 616 KB
1007	Mapset: Primary productivity in southern Australian waters by southern season	jpg format: 568 KB pdf format: 3.26 MB
1008	Mapset: Zooplankton biomass in southern Australian waters by southern season	jpg format: 527 KB pdf format: 3.26 MB
1009	Mapset: Zooplankton biomass in the Timor triangle by northern season	jpg format: 584 KB pdf format: 4.88 MB
1010	Mapset: Zooplankton biomass seasonality (along 110° E)	jpg format: 0.99 MB pdf format: 5.81 MB
1011	Primary Production around Australia 1959–1965	excel file: 2 MB
1021	SeaWiFS movie of surface Chlorophyll, 1997–2001 in the Australian Region	GIF images assembled as a movie loop: 42.8 MB
1030	GIS Layer: Zooplankton biomass seasonality (along 110° E)	MapInfo: 7.67 KB excel: 42 KB
1031	GIS Layer: Monthly Sea-surface Temperature in the Australian Region	arcinfo: 87.4 MB
1032	GIS Layer: Sea-surface Temperature in the Australian Region	arcinfo: 6.11 MB
1033	GIS Layer: Wind Stress on Australian Oceans	arcinfo: 10.66 MB
1034	GIS Layer: Sea-surface Currents in the Australian Region	arcinfo: 1.3 MB
1035	GIS Layer: Sea-surface Height in the Australian Region	arcinfo: 11.4 MB
1036	GIS Layer: Mixed Layer Depth in the Australian Region	arcinfo: 859 KB
1037	GIS Layer: Eddies and Fields Based on Sea-surface Temperature in the Australian Region	arcinfo: 125 MB

Neptune Record No.	Title	Stored data volume
1038	GIS Layer: Wave Height Direction and Period in the Australian Region	arcinfo: 800 KB
1039	GIS Layer: Half Lunar Cycle Tidal Currents in the Australian Region	arcinfo: 16.3 MB
1040	GIS Layer: Sea-surface Silicate in the Australian Region	arcinfo: 8.23 MB arcreport: 12.6 MB
1041	GIS Layer: Sea-surface Phosphate in the Australian Region	arcinfo: 8.51 MB arcreport: 12.2 MB
1042	GIS Layer: Sea-surface Nitrate in the Australian Region	arcinfo: 8.81 MB arcreport: 13 MB
1043	GIS Layer: Sea-surface Dissolved Oxygen in the Australian Region	arcinfo: 8.08 MB arcreport: 12 MB
1044	GIS Layer: Sea Temperature in the Australian Region	arcinfo: 7.05 MB arcreport: 11 MB
1045	GIS Layer: Sea Salinity in the Australian Region	arcinfo: 4.4 MB arcreport: 7.9 MB
1046	GIS Layer: Phytoplankton Provinces in the Australian Region	arcinfo: 1.28 MB arcreport: 4.041 MB text documents: 23.48 KB
1047	GIS Layer: Ocean Colour Chlorophyll (MODIS) in the Australian Region	arcinfo: 107.49 MB
1048	GIS Layer: Primary Production (MODIS) in the Australian Region	arcinfo: 37 MB
1049	GIS Layer: Incident Light (PAR) in the Australian Region	arcinfo: 19.7 MB
1050	GIS Layer: Primary Productivity in Australian waters by season	MapInfo: 37.2 KB excel format: 150 KB
1051	GIS Layer: Zooplankton Biomass in the Australian Region	MapInfo: 23.4 KB excel format: 170 KB
1052	GIS Layer: Zooplankton biomass in southern Australian waters by southern season	MapInfo: 112 KB excel format: 71.5 KB
1053	GIS Layer: Zooplankton biomass in the Timor triangle by northern season	MapInfo: 7.76 KB excel format: 49.5 KB
1054	GIS Layer: Biomass Distribution in the Gulf of Carpentaria	arcinfo: 825.7 KB
1055	Mapset: Incident Light for the Wet and Dry Seasons in the Northern Marine Region	pdf format: 12.2 MB jpg format: 898 KB
1056	GIS Layer: Biomass in Albatross Bay	arcinfo: 774 KB
1056	Primary Production Data from MODIS in the Australian Region	104 MB

4.3 Data compatibility with other data projects

One of the objectives of this project was to make data and maps web-accessible to the public and scientists from Australia and around the world.

The project has collated a large quantity of data, created GIS layers and maps. Common data formats have been used to ensure data compatibility with other national marine bioregionalisation data providers. Data formats used are Microsoft Excel spreadsheets, ASCII grids, CSV, netCDF and ESRI shape files, coverages and grids. Maps have been produced using ESRI ArcGIS, with map images exported as JPG and PDF formats as agreed by the National Oceans Office.

The National Oceans Office's Oceans Portal is still in the development phase and does not yet have defined data formats. The standard data formats used in this project will allow the products to be delivered via the Oceans Portal once it has been developed.

CSIRO Marine Research is a partner in the Wealth from Oceans project. Oceanography Collation Data Project staff have combined resources with Wealth from Oceans staff to transcribe some of the paper datasets to computer-accessible formats. The standard data formats used allow data to be exchanged easily between this project and Wealth from Oceans projects.

5 National Datasets

5.1 Geographic Extent of Project

The geographic area of interest for this project is the entire Australian Marine Jurisdiction (Territorial Sea and Exclusive Economic Zone and territorial waters around off-shore islands, but excluding territorial waters around Antarctica). The geographic region of interest for the project is shown in Figure 5.1. The geographical extent of the datasets is this region where data are available. Where data were available over a smaller extent, this is reflected in the maps (for example, see sections on waves and tides).

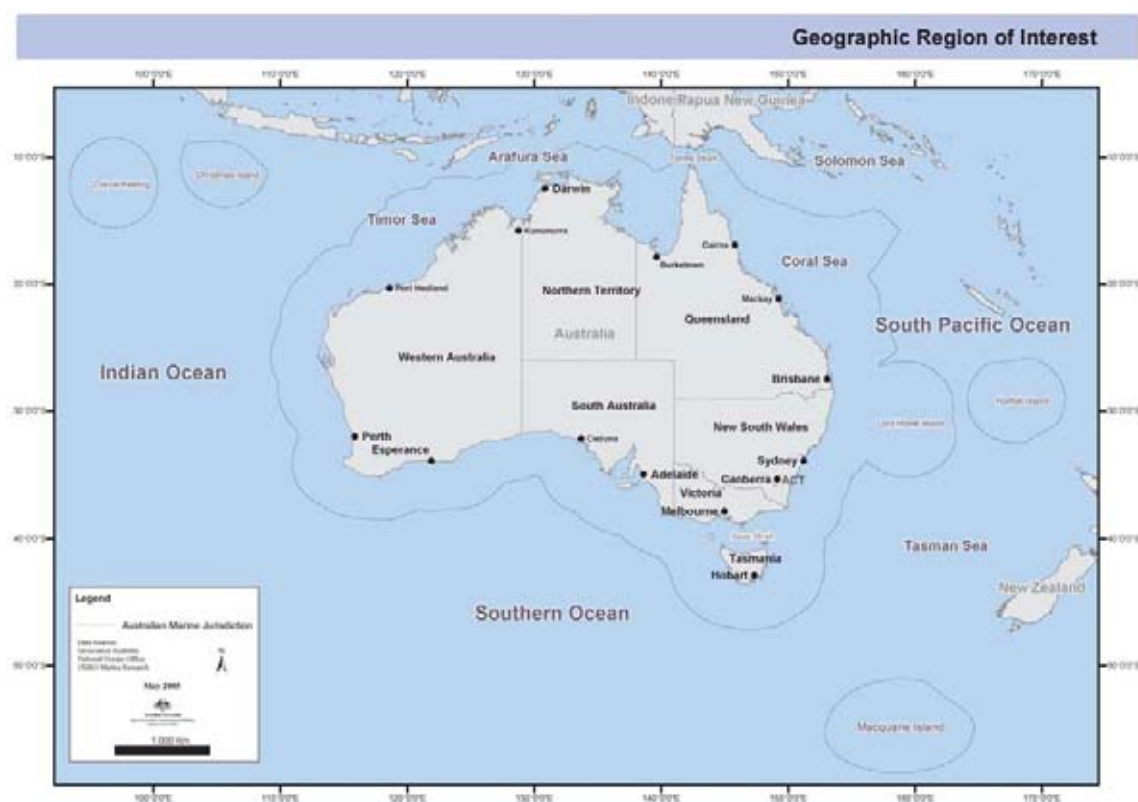
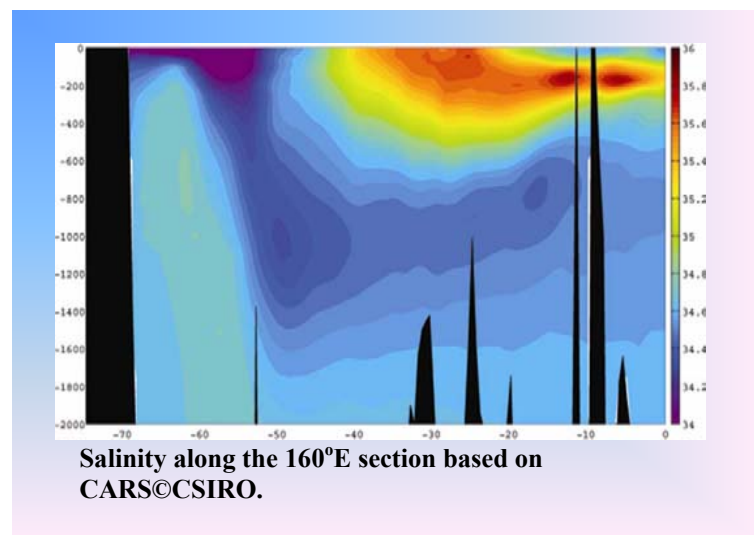


Figure 5.1 The geographic region of interest for the national study.
The geographic extent for datasets is determined by the available data.

Depth

Where available, data from all depths from the sea-surface to the sea floor were collected. The depths selected for mapping were surface, 150, 500, 1000 and 2000 metres. Benthic data were provided directly to Geoscience Australia. The benthic data and metadata are available on Neptune (<http://neptune.oceans.gov.au>) (see Appendix A for the full product list).



Temporal coverage

Most datasets are provided as monthly means and variances. Data are mapped quarterly for national datasets and six monthly for the northern datasets (see Rothlisberg et al 2005) to illustrate the seasonal variability of the data.

Data identification and acquisition

Datasets and sources were identified mainly from the Bioregionalisation Oceanographic Information System (BOIS) developed during the National Description and Information Review for National Bioregionalisation project (Condie et al 2003). This database holds pointers to data, metadata, data products, model outputs, funded existing and future research programs.

During a series of workshops and meetings held at CSIRO Marine Research early in 2004 a comprehensive list of datasets and custodians was developed. Datasets were tagged as being useful for ‘National’, ‘Regional’, ‘Interpretative’ and ‘Future use’. Datasets were then assigned a priority rating of ‘high’ or ‘low’.

Datasets identified with custodians outside of CSIRO Marine Research needed to have access agreements negotiated by the National Oceans Office before 30 May 2004. This proved difficult: very few access agreements were actually negotiated during the life of the project and none before 30 May 2004. In some cases the custodian organisation gave access but did not have the resources to mine the data. Discussions between National Oceans Office, CSIRO Marine Research and custodians had few positive outcomes for the project. However, custodians were generally willing to assist, and with more resources and time it will be possible to access many of the identified datasets for future bioregionalisation updates.

5.2 CARS: Temperature, Salinity, Oxygen, Phosphate, Nitrate and Silicate

The CSIRO Atlas of Regional Seas (CARS and CARS2000 at http://www.marine.csiro.au/~dunn/eez_data/atlas.html) (Dunn & Ridgway 2002; Ridgway et al 2002) is a set of seasonal maps of temperature, salinity, dissolved oxygen, nitrate, phosphate and silicate, generated using a weighted least squares (Loess) mapping from all available hydrographic data in the region. It covers the region 100–200°E, 5°0-0°S, on a 0.5 degree grid, and on 56 standard depth levels. Higher-resolution versions are also available for the Australian continental shelf. The data were obtained from the World Ocean Atlas 98 and CSIRO Marine Research and NIWA archives. It was designed to improve the Levitus WOA98 Atlas in the Australian region and interpolated versions of the data at a 0.1 degree resolution were used to match with other datasets.

Methods

Water column

Temperature, salinity, oxygen, silicate, phosphate and nitrate were linearly interpolated from CARS2000 mean and seasonal fields to 0.1 degree spaced grid, at all standard depth levels from sea-surface to 5500 m.

The Loess filter used to create CARS2000 resolves at each point a mean value and a sinusoid with 1 year period (and in some cases a 6 month period sinusoid—the “semi-annual cycle”.) The provided “annual amplitude” is simply the magnitude of that annual sinusoid. Data were extracted from the CARS database nCDF files for depths 0, 150, 500, 1000 and 2000 m. Annual mean and variances were calculated for these depths on a 0.1° grid.

Data Currency:	Beginning 1900 Ending 2000
Dataset status:	Progress: complete Update: occasional
Data source & Quality:	CARS2000

Positional accuracy:

Errors may occur in location of cast data, which especially arises when data are passed from originator to accumulator organisations. For example, 1100 WOA94 casts were landward of the coastline.

Parameter accuracy:

Loess mapping does not provide an error field. The data source radius (for the mapping at each grid point) is stored to give some insight into relative accuracy at different locations, and fields of data variance and RMS mapping-residuals are available.

Completeness:

All known reliable published data were used, but they were still very sparse in the south-west and at the greater depths, and especially for some nutrients. In many places strong interannual signals (which in many cases we do not attempt to resolve or compensate for) may be aliased into spatial or seasonal signals.

Benthic

Temperature, salinity, oxygen, silicate, phosphate and nitrate, linearly interpolated from 1/8 degree spaced “high resolution” CARS2000 mean and seasonal fields to 0.025 degree spaced grid. Values were obtained for seafloor by vertical linear interpolation, which is possible because CARS2000 is mapped to one depth level below seafloor by least squares quadratic filter projection of horizontally and vertically adjacent data points.

The Loess filter used to create CARS2000 resolves at each point a mean value and a sinusoid with 1 year period (and in some cases a 6 month period sinusoid—the “semi-annual cycle”.) The provided “annual amplitude” is simply the magnitude of that annual sinusoid.

Limitations:

CARS2000 is derived from ocean cast data, which is always measured above the seafloor. However, this would not lead to a significant error, for properties that do not change rapidly near the seafloor. All the limitations of CARS2000 also apply here.

Parameter accuracy:

Loess mapping does not provide an error field. The data source radius (for the mapping at each grid point) is stored to give some insight into relative accuracy at different locations, and fields of data variance and RMS mapping-residuals are available.

Completeness:

All known reliable published data are used, but they are still very sparse in the south-west and at the greater depths, and especially for some nutrients. In many places strong interannual signals (which in many cases we do not attempt to resolve nor compensate for) may be aliased into spatial or seasonal signals.

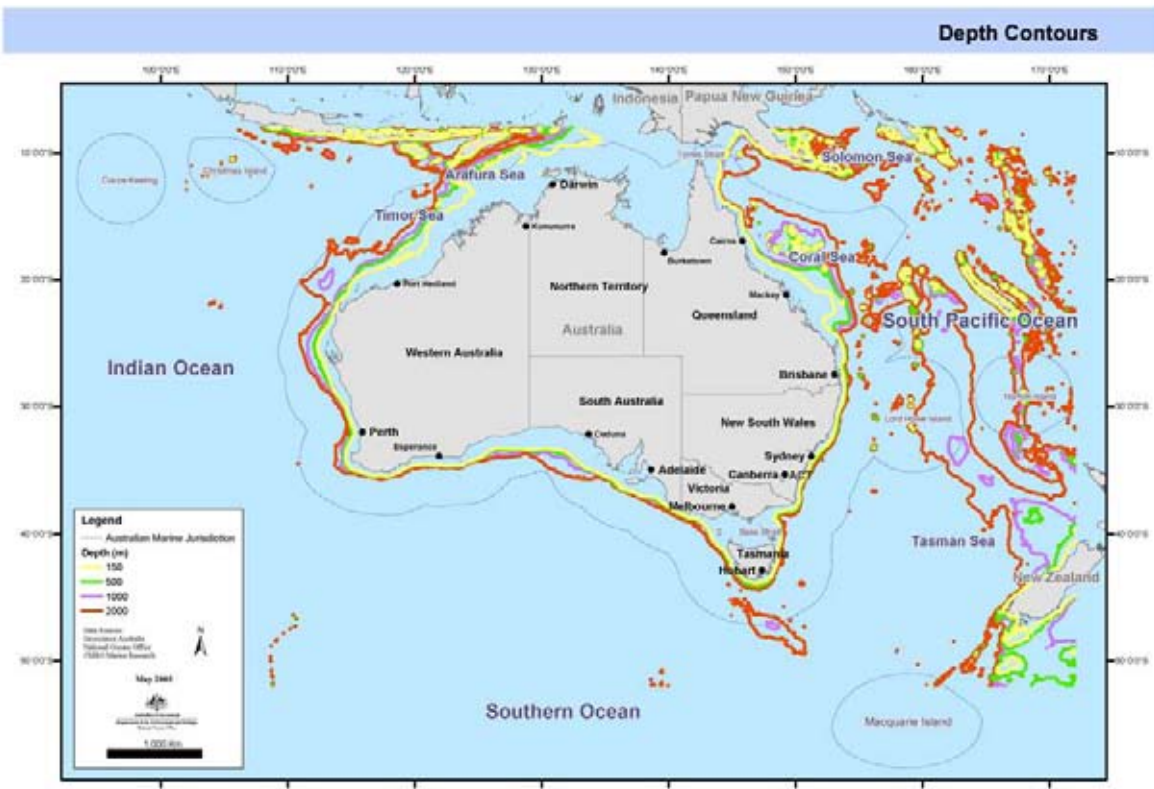


Figure 5.2 Depth contours of depths chosen to present CARS data.

Description

Annual mean maps of these properties at 0, 150, 500, 1000 and 2000 m depth are presented in Figures 5.3 through 5.8. The depth contours for the depths chosen (150, 500, 100 and 2000 m) are shown in Figure 5.2. The station locations for each of the fields are shown in Appendix C.

Temperature fields are strongly dominated by decreasing temperature with depth and a zonal pattern varying from warm tropical waters in the north ($> 28^{\circ}\text{C}$ near the surface), through Subtropical, temperate, and finally cold Subantarctic waters in the Southern Ocean ($< 2^{\circ}\text{C}$). Temperature differences between tropical and Subantarctic waters also decrease with depth, and by 500 m the warmest waters ($\sim 12^{\circ}\text{C}$) are found in the subtropics where the thermocline shallows towards the equator. Below the thermocline (> 1000 m) significant temperature differences occur largely in the Southern Ocean, where cold water masses are first formed. These features suggest that temperature is to a large extent controlled by solar-driven processes and that near the surface, the effect of ocean dynamical processes is limited to meridional (along-longitude) mixing and diffusive exchanges responsible for temperature gradients from the tropics to the Southern Ocean. Below the surface, subduction and water-formation processes can counter the relatively slow diffusive and surface heat-exchange processes so that the deep water patterns have a significant signature due to ocean circulatory processes. Our assessment, therefore, is that at broad scales, surface temperature fields reflect a strong component of global climatic processes, while the deeper fields more strongly reflect global water-formation and transport processes.

At regional scales, departure of surface-temperature fields from the expected climatic patterns reflect influences of basin-scale circulatory processes, as seen for example in the southward extension of warm water advected by the East Australian Current system and the associated mixing fields caused by eddies. Taken together, these patterns suggest that the temperature field contains patterns ranging from global (Level 0/1) down to at least feature scale (Level 3/4).

The salinity fields show a broad zonal pattern, with highest salinities in the subtropics. In relatively shallow depths (< 200 m) these high-salinity regions define Subtropical Lower Water in the Pacific and the South Indian Central Water in the Indian Ocean (both ~ 35.6). Surface salinities in the tropics tend to be much lower due to higher precipitation rates, with terrestrial run-off having a strong local influence in regions such as the Java Sea, Gulf of Papua and Gulf of Carpentaria. Relatively low salinities also occur in the Southern Ocean, where high precipitation and low evaporation determine the characteristics of Antarctic Intermediate Water (~ 34.5). At depths below 500 m, this water mass extends north throughout the subtropical and tropical regions. In comparison to temperature, salinity therefore has a strong climatic evaporative component (which also affects temperature) but it is also influenced by runoff processes that impart a dynamic salinity signature. Our assessment is that salinity is relevant at all the same Levels that temperature is and that there is a component in salinity that reflects runoff and regional-circulation processes.

The dissolved oxygen distribution near the surface remains near equilibrium with the atmosphere, so that the observed increase with latitude is predominantly a function of water temperature. However, the influence of water-mass movements can be seen even at 150 m, where low-oxygen Subtropical Lower Water is carried south by the East Australian Current system. At greater depths (> 500 m), Subantarctic Mode Water and Antarctic Intermediate Water carry high oxygen levels well into the Subtropical regions. Oxygen distribution is therefore expected to follow temperature closely, but we also recognise that biological activity, particularly phytoplankton production, will impart a signature that will subsequently be advected and mixed with surrounding waters. Thus oxygen, as is temperature, is seen to be relevant at all Levels.

The nutrient data in these maps are plotted to highlight the biologically active concentration ranges (Table 5.1). Additional information can be obtained from these datasets by plotting them using finer,

nonlinear scaling. Nutrients tend to be very low in the surface waters of the tropics and subtropics, where they are rapidly consumed by phytoplankton. This is particularly true of nitrate, which most commonly limits primary production in these waters. In contrast, phosphate and silicate distributions tend to reflect localised terrestrial inputs in tropical waters such as around Java and Papua New Guinea and the Kimberly coast. All nutrients are higher in Southern Ocean, where primary production is light-limited rather than nutrient-limited for at least part of the year. Levels increase rapidly below the surface mixed-layer, so that from 150 to 500 m, nitrate and phosphate are higher in the tropics than the subtropics, where the mixed layer is seasonally much deeper. Below 1000 m, the spread of Antarctic Intermediate Water carries nutrient-rich water throughout the region. Here again, a strong relationship with temperature is expected in tropical and temperate waters and a different relationship in the Subantarctic and Antarctic, where nutrient levels are more influenced by physical processes. The rapid response of phytoplankton to local enrichment/upwellings and their ability to strip out nutrients down to very low levels implies that tropical and temperate waters may be subject to considerable temporal and hence spatial variability. Thus some consideration needs to be given to sampling issues in assessing the value of nutrients as tracers.

Table 5.1 Biologically significant ranges for nutrients

Nutrient	Biologically Significant Range
Silicate	2 – 10 µM
Nitrate	0.5 – 2 µM
Phosphate	0.2 – 0.4 µM

Data Provided

Water column

For region 90–180E, 60S to the equator for 0.1° grid

- Annual Mean Silicate at 0, 150, 500, 1000, 2000 m
- Annual Mean Nitrate 0, 500, 1000, 2000 m
- Annual Mean Phosphate 0, 500, 1000, 2000 m
- Annual Mean Temperature 0, 150, 500, 1000, 2000 m
- Annual Mean Dissolved Oxygen at 0, 150, 500, 1000, 2000 m
- Annual Mean Salinity at 0, 150, 500, 1000, 2000 m
- Annual Variance Silicate at 0, 150, 500, 1000, 2000 m
- Annual Variance Nitrate 0, 500, 1000, 2000 m
- Annual Variance Phosphate 0, 500, 1000, 2000 m
- Annual Variance Temperature 0, 150, 500, 1000, 2000 m
- Annual Variance Dissolved Oxygen at 0, 150, 500, 1000, 2000 m
- Annual Variance Salinity at 0, 150, 500, 1000, 2000 m

Benthic

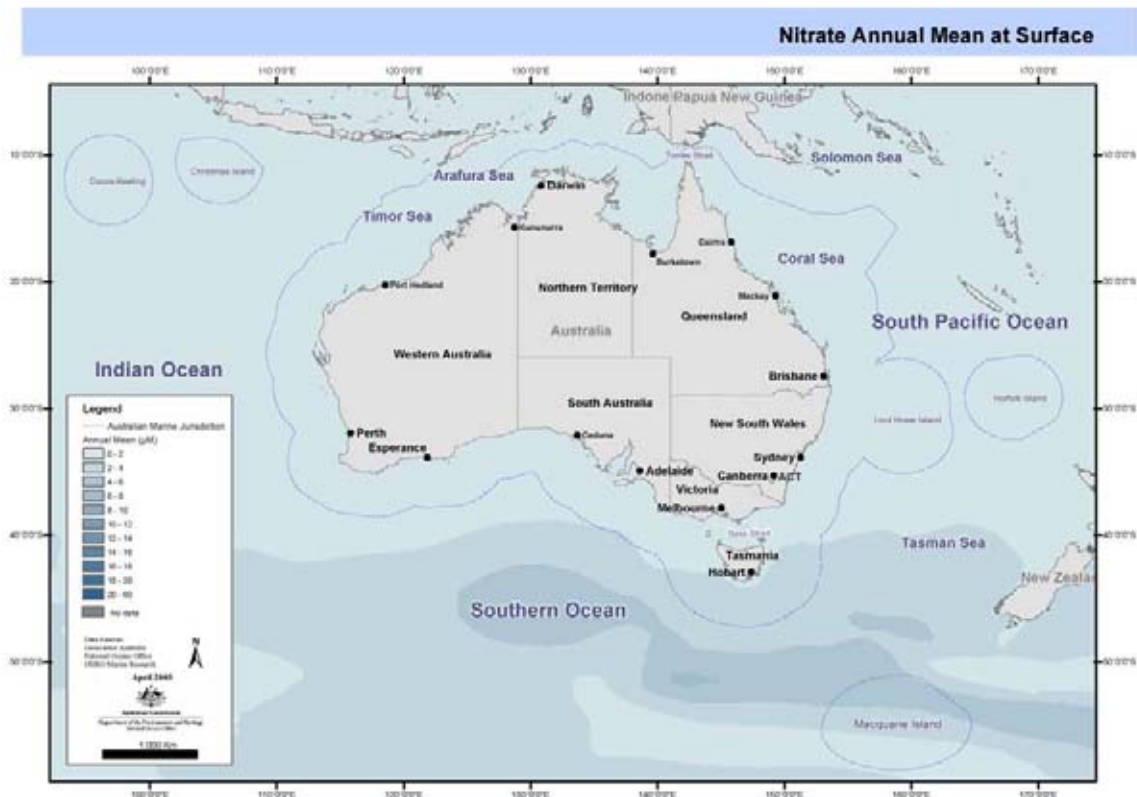
The benthic datasets delivered to Geoscience Australia in July 2004 for use in the Benthic Regionalisation were:

- Bottom Temperature at 2 km resolution on shelf and slope and at 0.1° grid for the rest of the EEZ
- Bottom salinity at 0.025° grid on shelf and slope and at 0.1° grid for the rest of the EEZ
- Bottom silicate at 0.025° grid on shelf and slope and at 0.1° grid for the rest of the EEZ
- Bottom phosphate at 0.025° grid on shelf and slope and at 0.1° grid for the rest of the EEZ
- Bottom nitrate at 0.025° grid on shelf and slope and at 0.1° grid for the rest of the EEZ
- Bottom dissolved oxygen at 0.025° grid on shelf and slope and at 0.1° grid for the rest of the EEZ
- Location of data points

For region 90–180E, 60S to equator for 0.5° grid:

- Bottom temperature
- Bottom silicate
- Bottom phosphate
- Bottom nitrate
- Bottom dissolved oxygen
- Benthic salinity

a



b

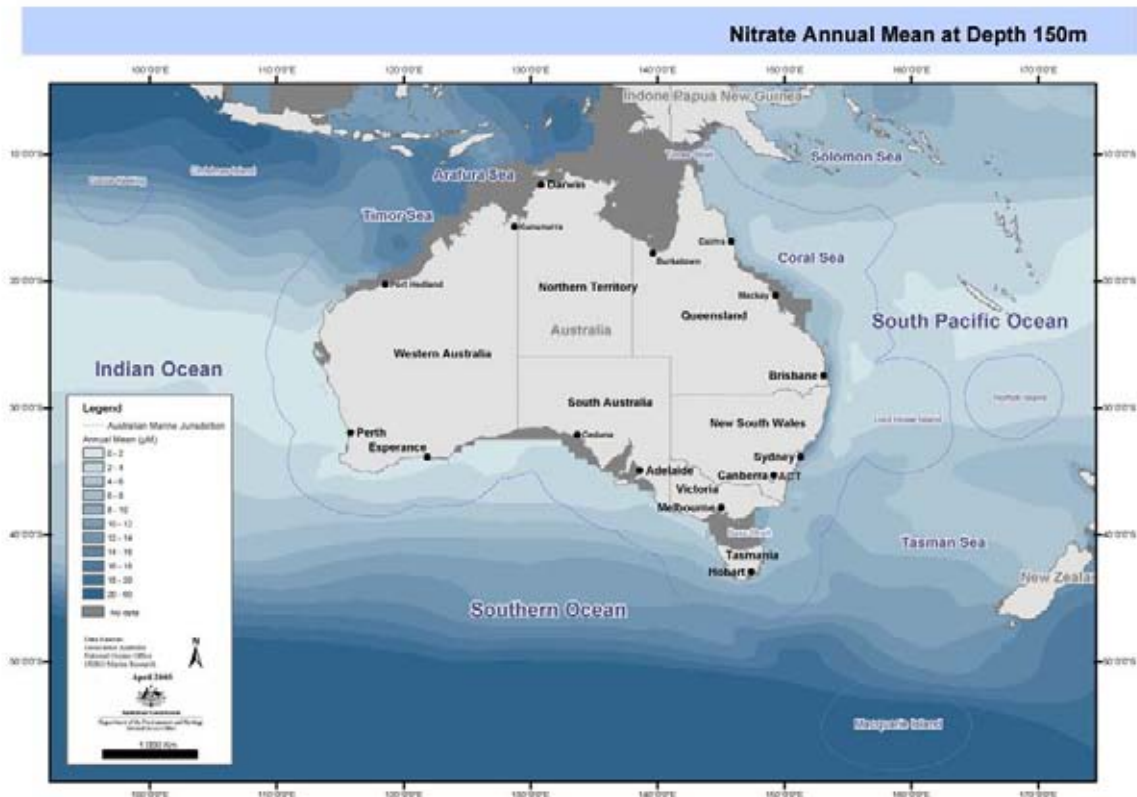
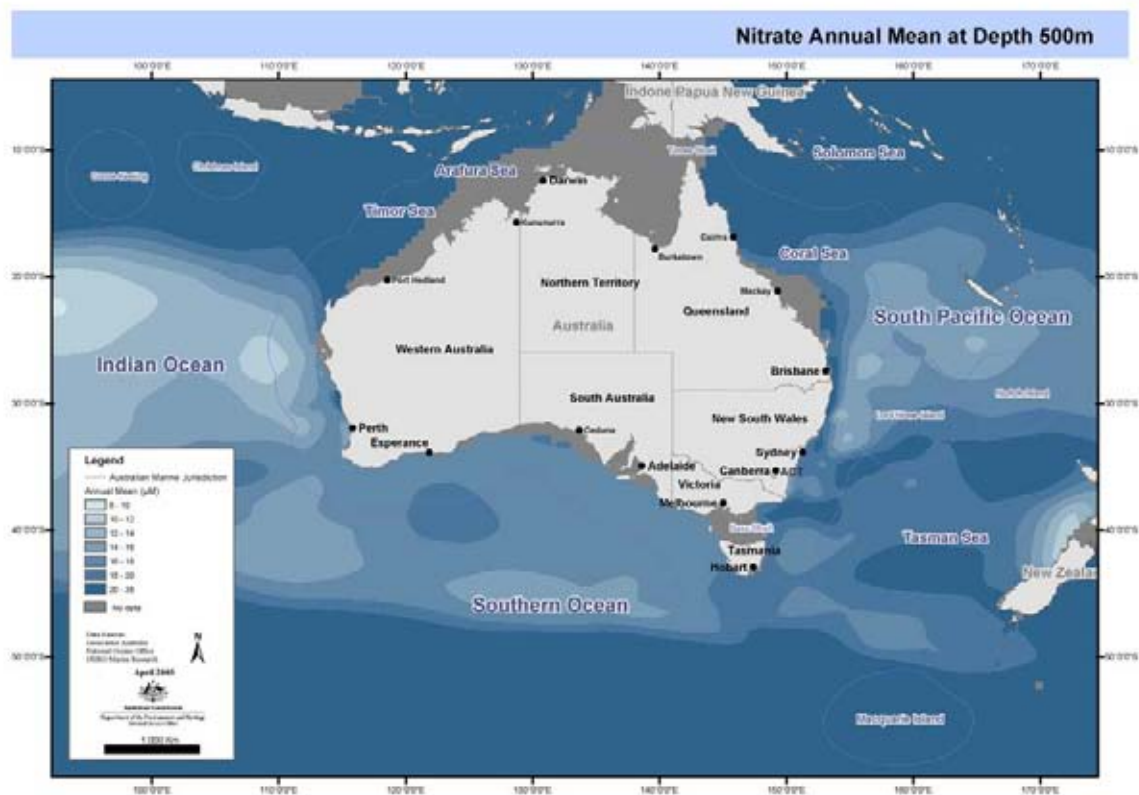


Figure 5.3 Nitrate Annual Mean at (a) the surface, (b) 150 m, (c) 500 m, (d) 1000 m and (e) 2000 m. Derived from CARS.

c



d

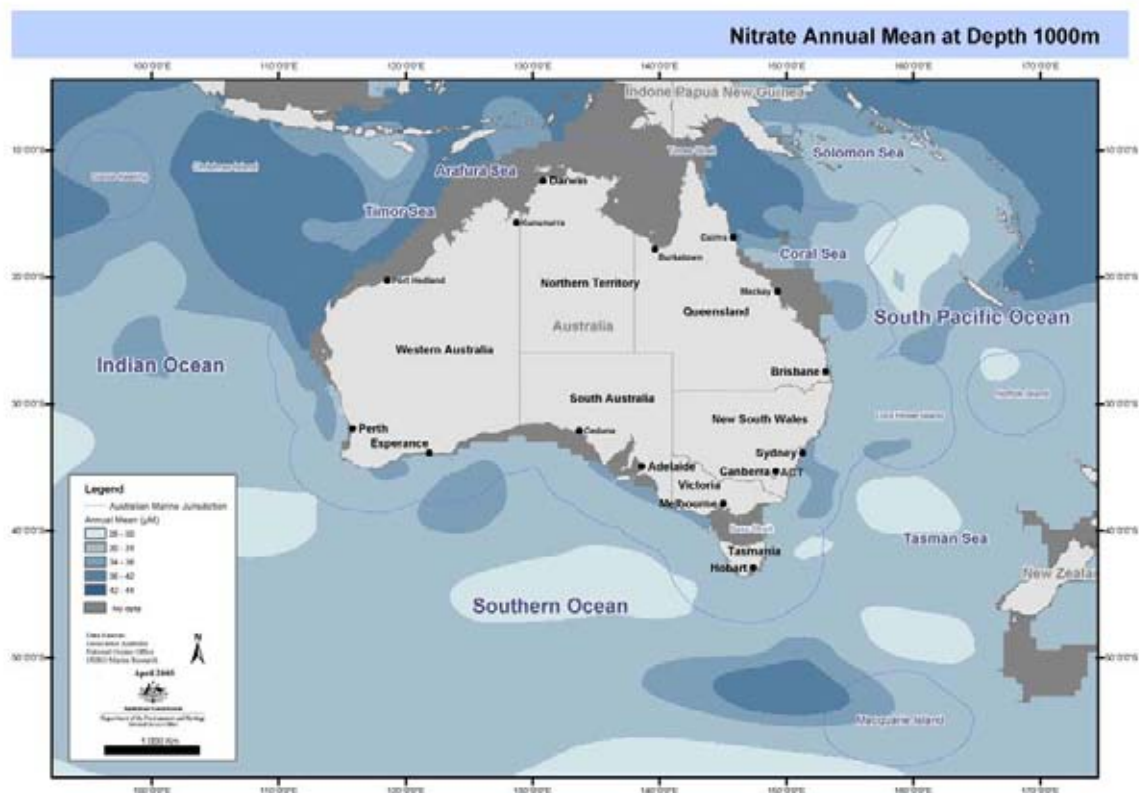


Figure 5.3 Nitrate Annual Mean at (a) the surface, (b) 150 m, (c) 500 m, (d) 1000 m and (e) 2000 m.
Derived from CARS (cont).

e

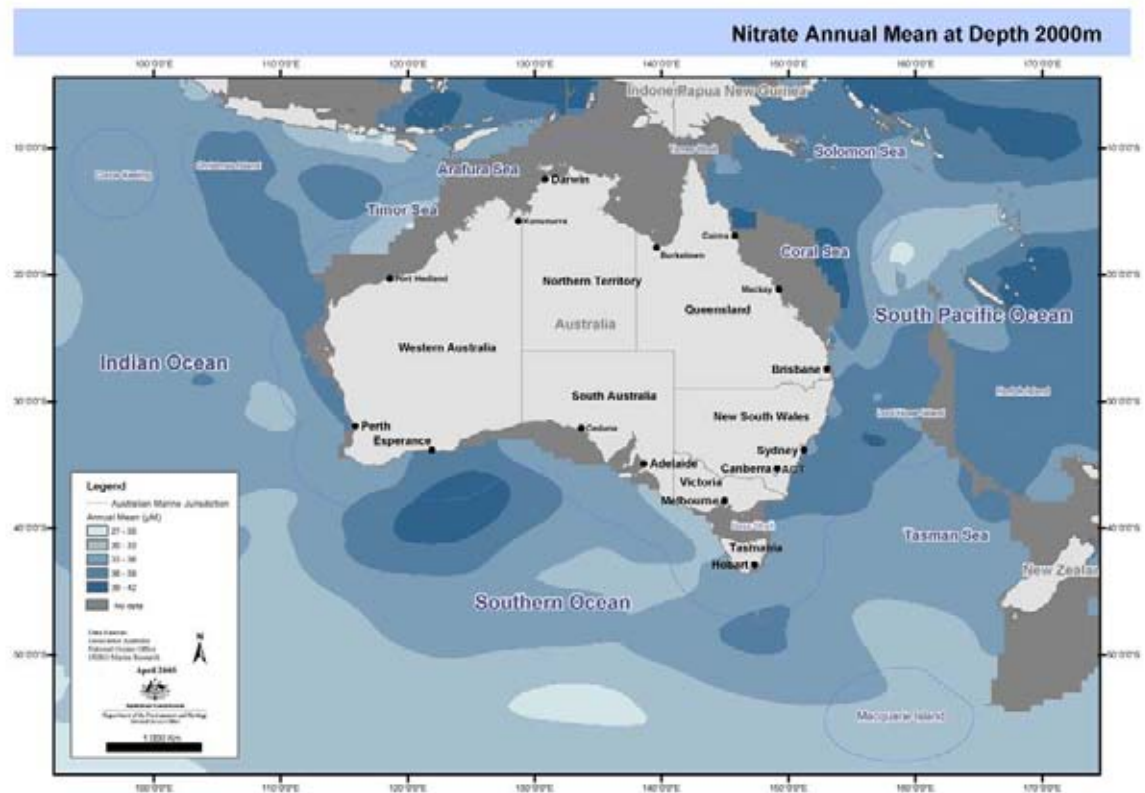
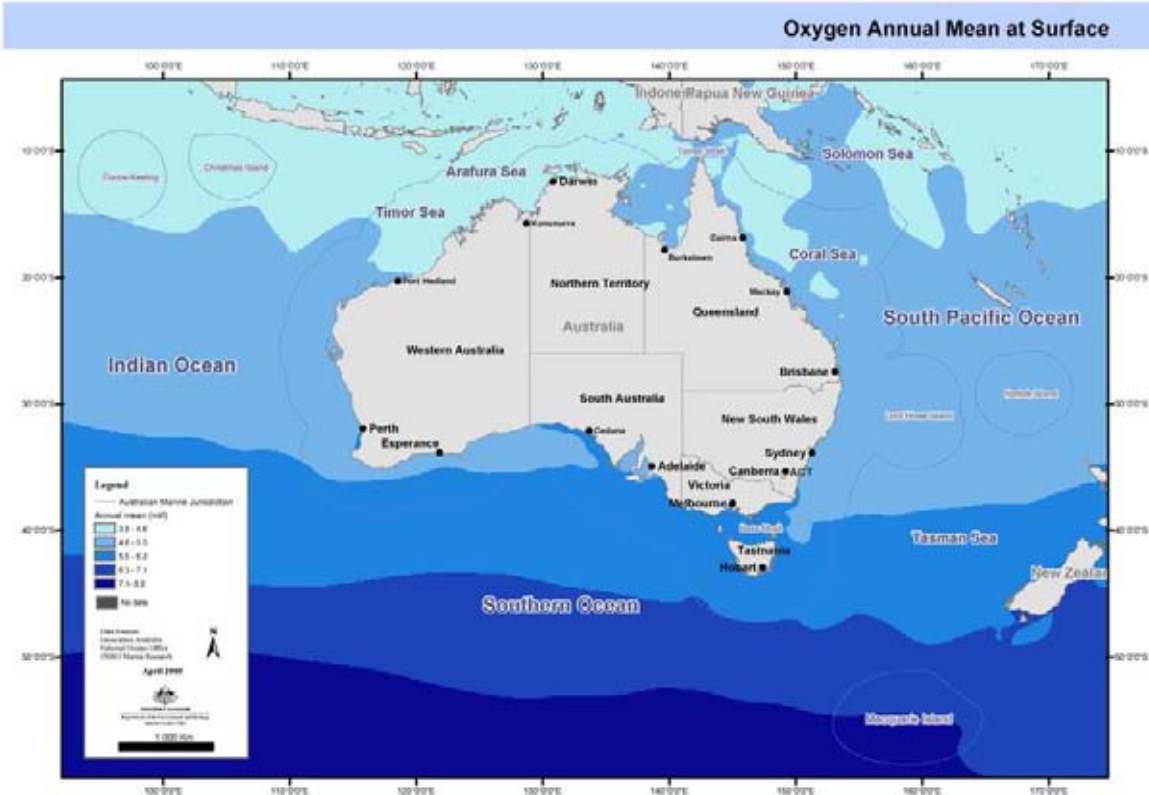


Figure 5.3 Nitrate Annual Mean at (a) the surface, (b) 150 m, (c) 500 m, (d) 1000 m and (e) 2000 m.
Derived from CARS (cont.).

a



b

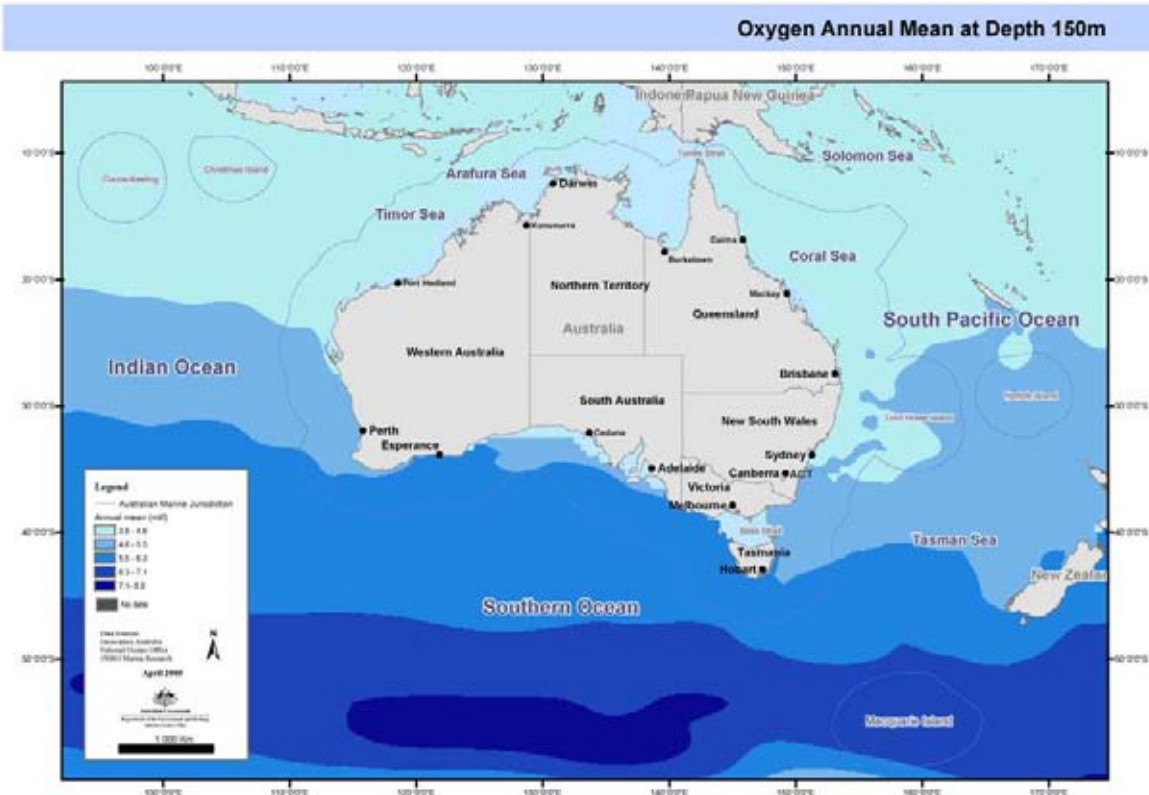
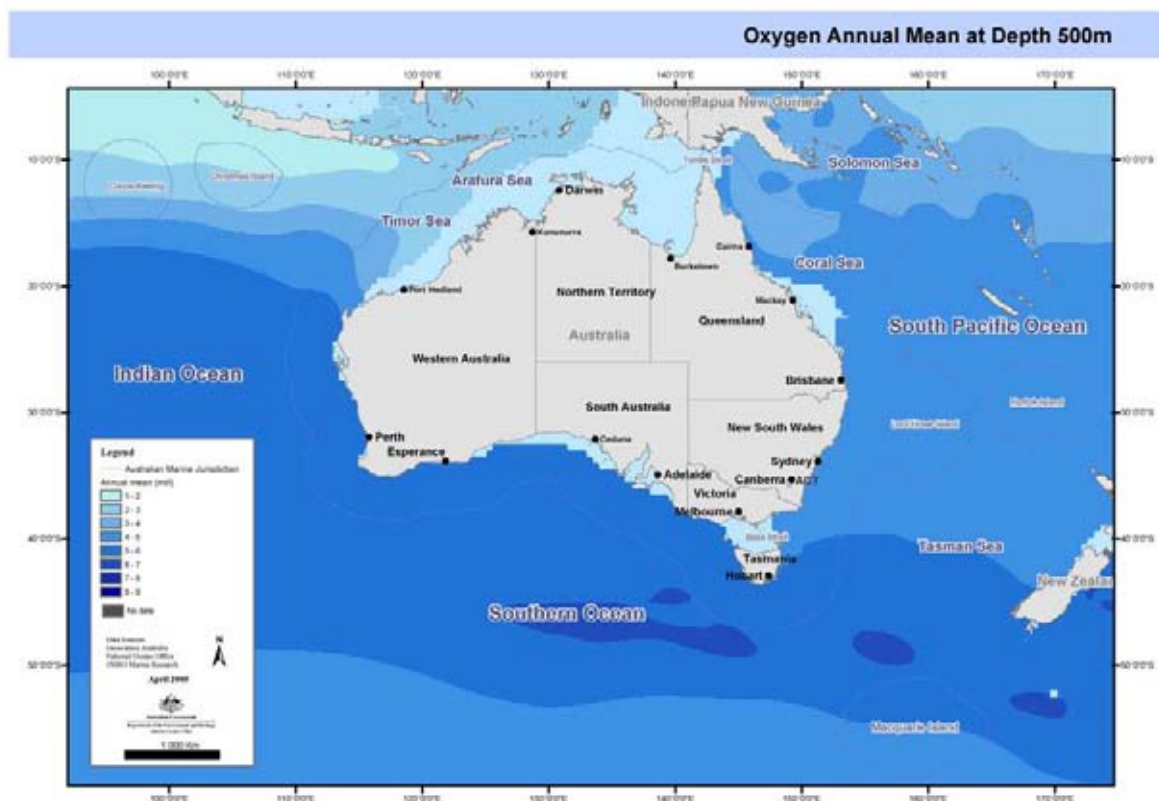
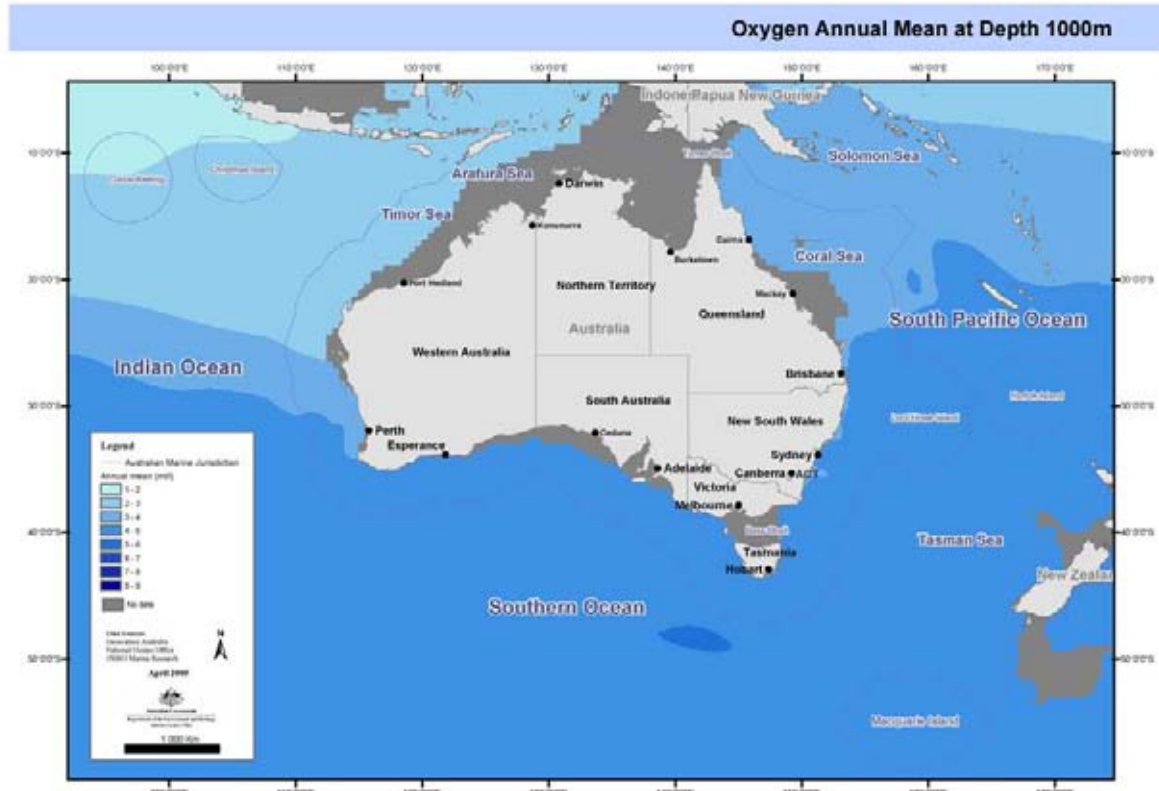


Figure 5.4 Oxygen Annual Mean at (a) the surface, (b) 150 m, (c) 500 m, (d) 1000 m and (e) 2000 m.
Derived from CARS

c



d



**Figure 5.4 Oxygen Annual Mean at (a) the surface, (b) 150 m, (c) 500 m, (d) 1000 m and (e) 2000 m.
Derived from CARS (cont)**

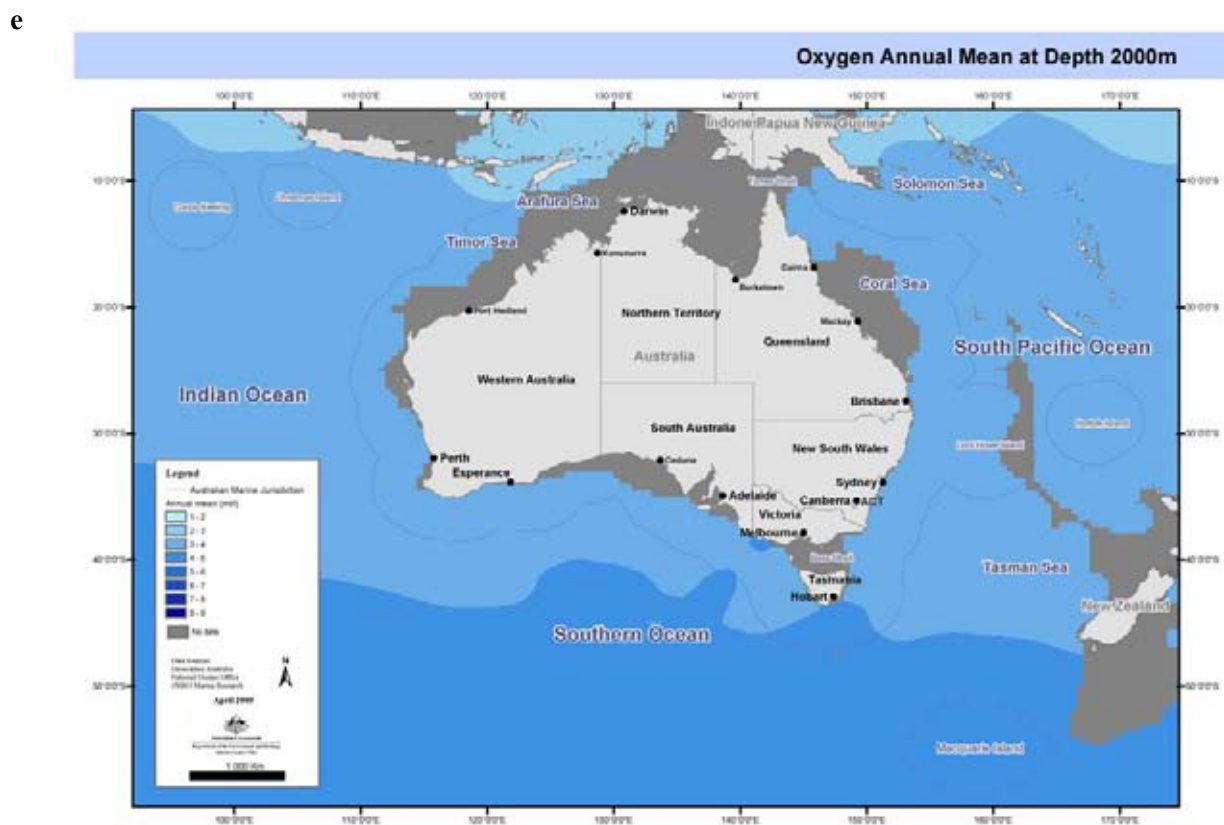
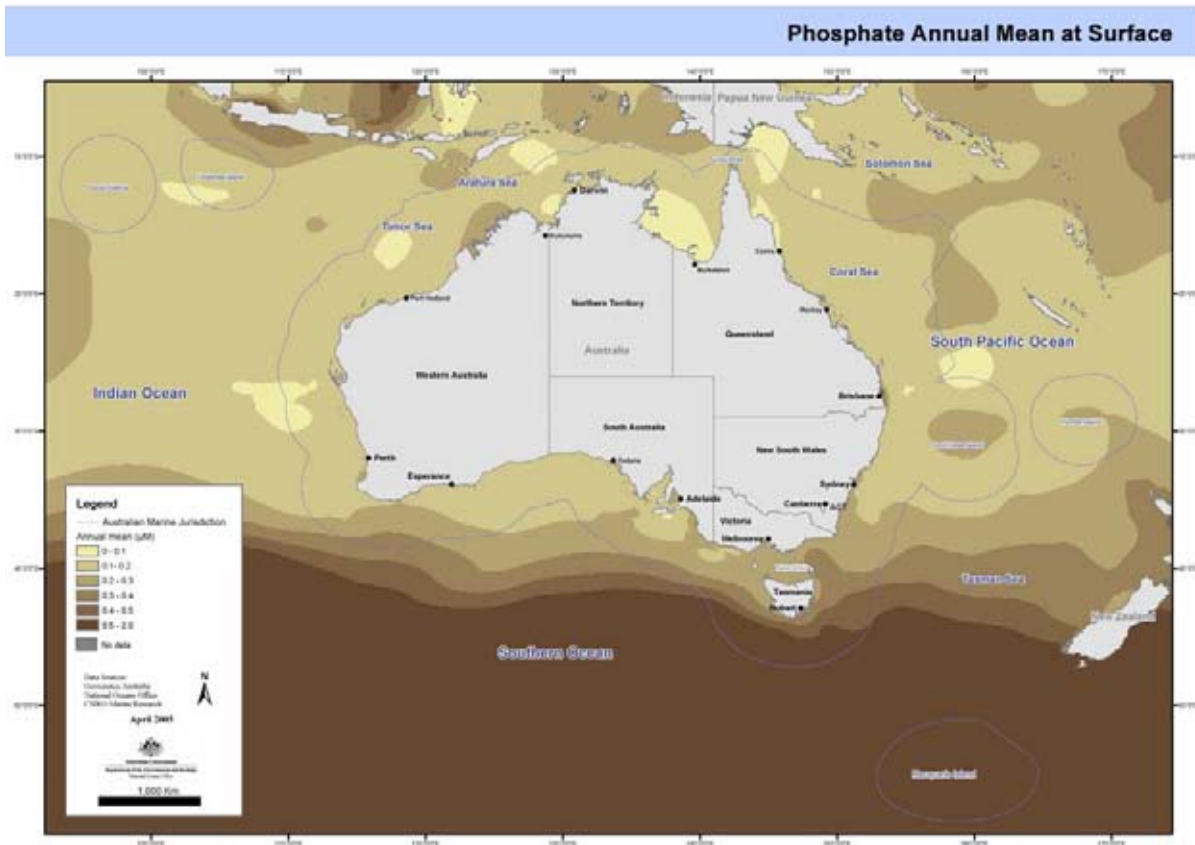


Figure 5.4 Oxygen Annual Mean at (a) the surface, (b) 150 m, (c) 500 m, (d) 1000 m and (e) 2000 m. Derived from CARS (cont)

a



b

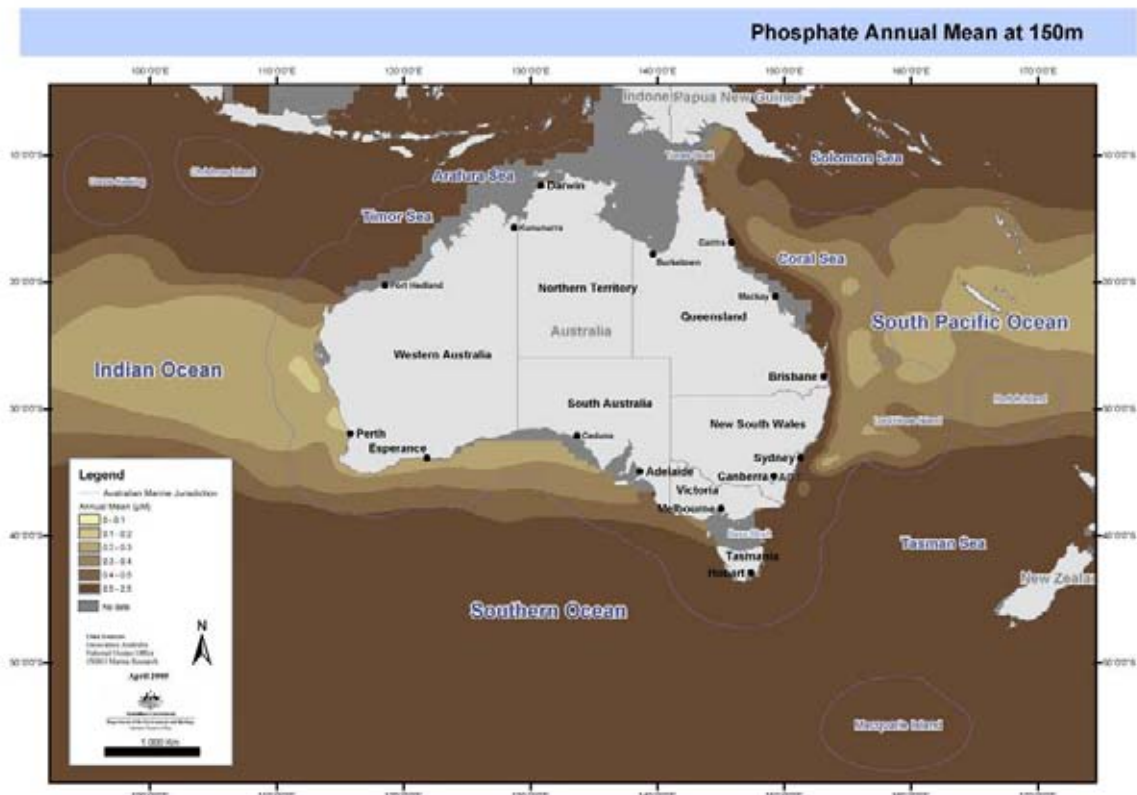
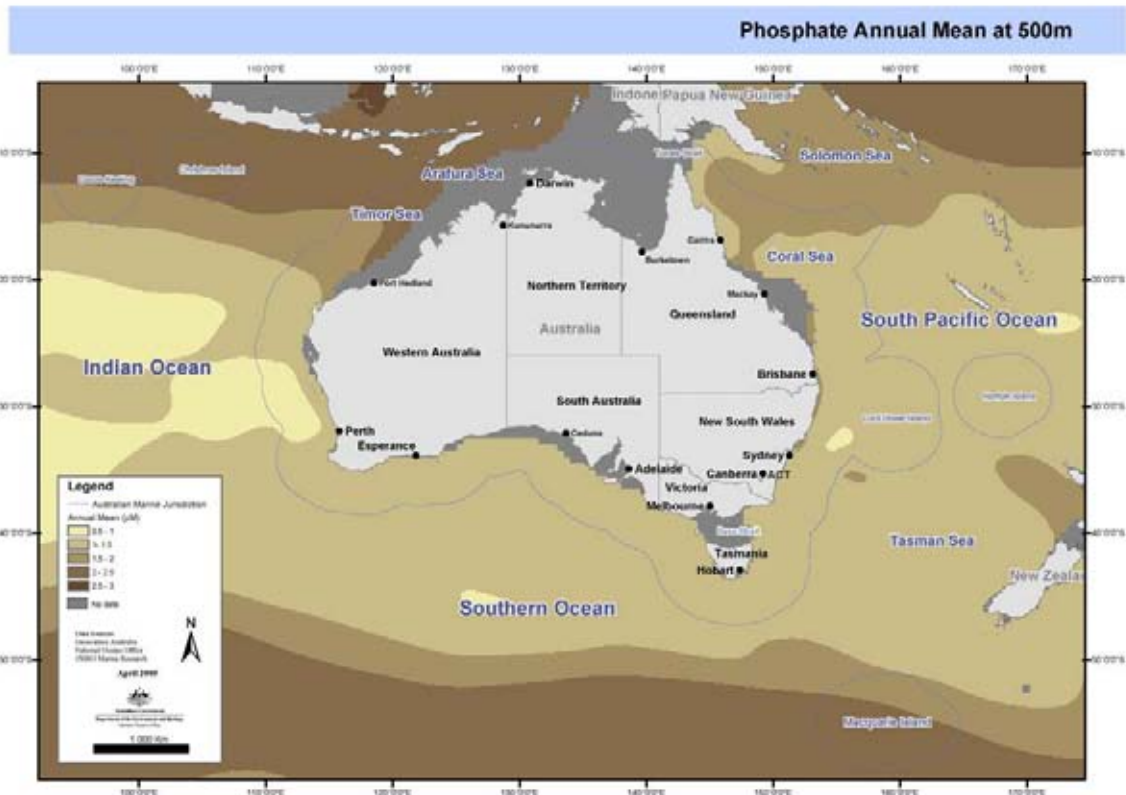
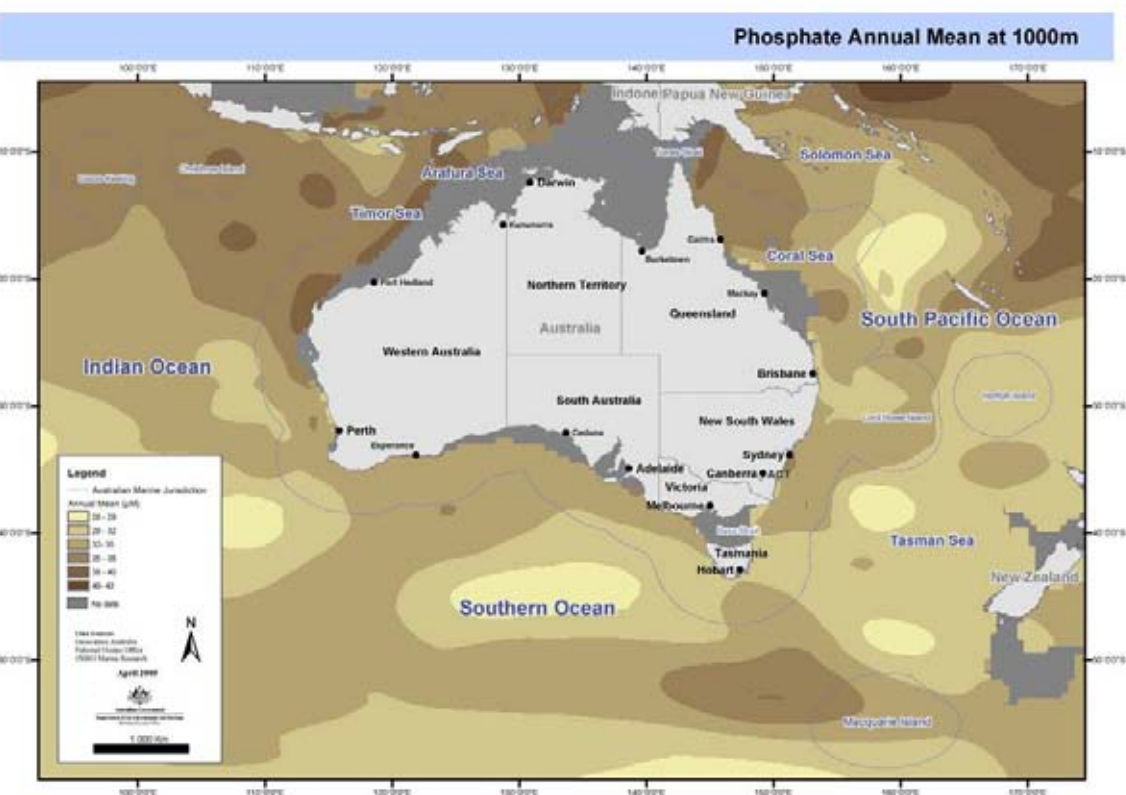


Figure 5.5 Phosphate Annual Mean at (a) the surface, (b) 150 m, (c) 500 m, (d) 1000 m and (e) 2000 m. Derived from CARS.

c



d



e

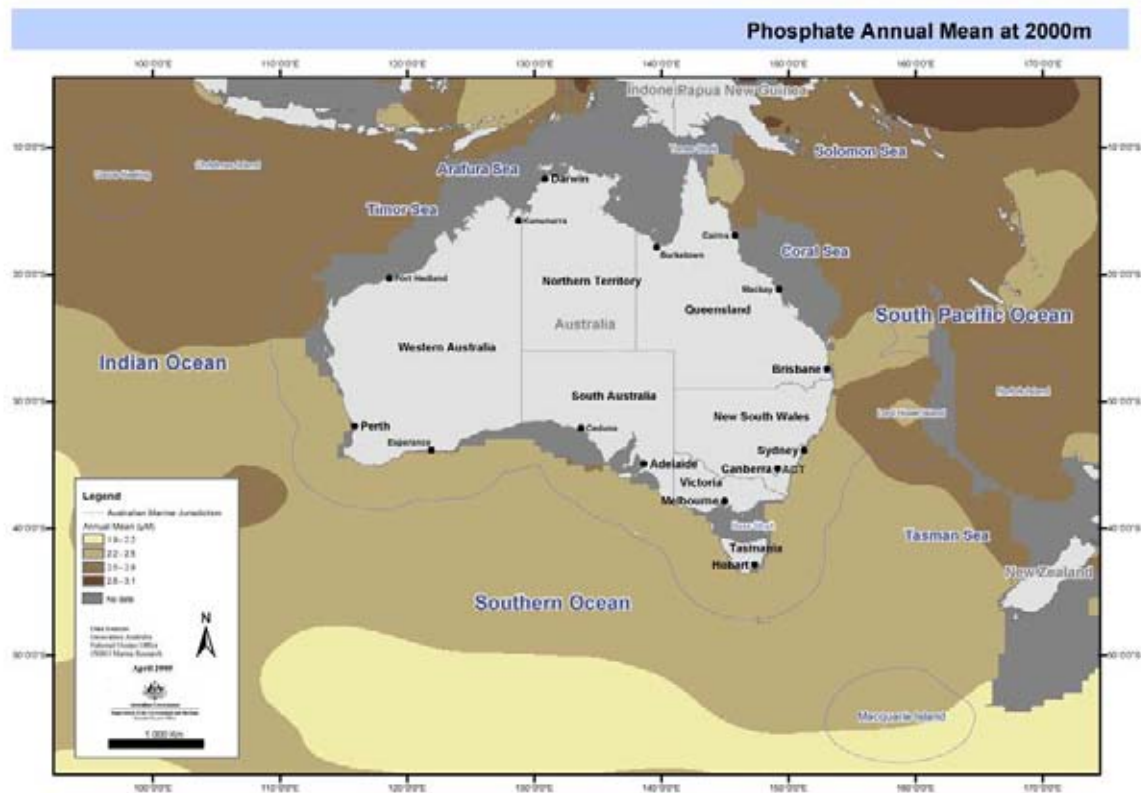
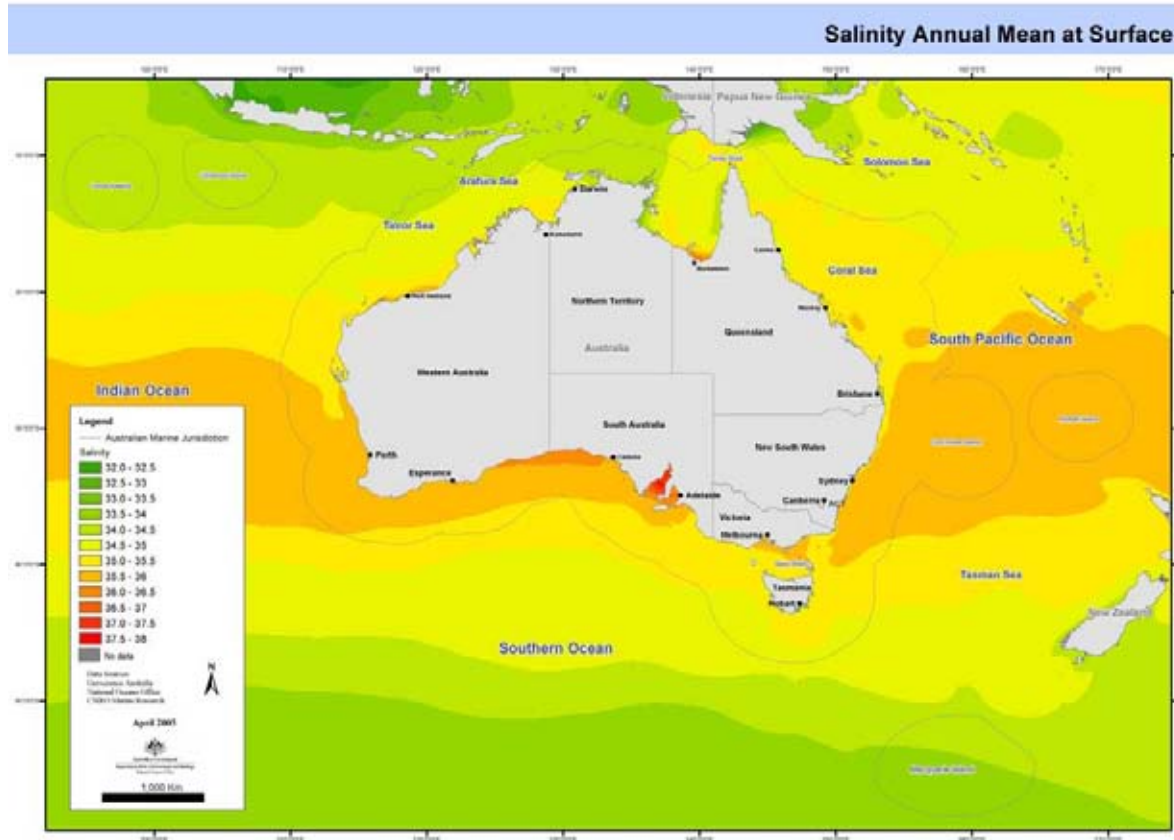


Figure 5.5 Phosphate (cont.) Annual Mean at (a) the surface, (b) 150 m, (c) 500 m, (d) 1000 m and (e) 2000 m. Derived from CARS.

a



b

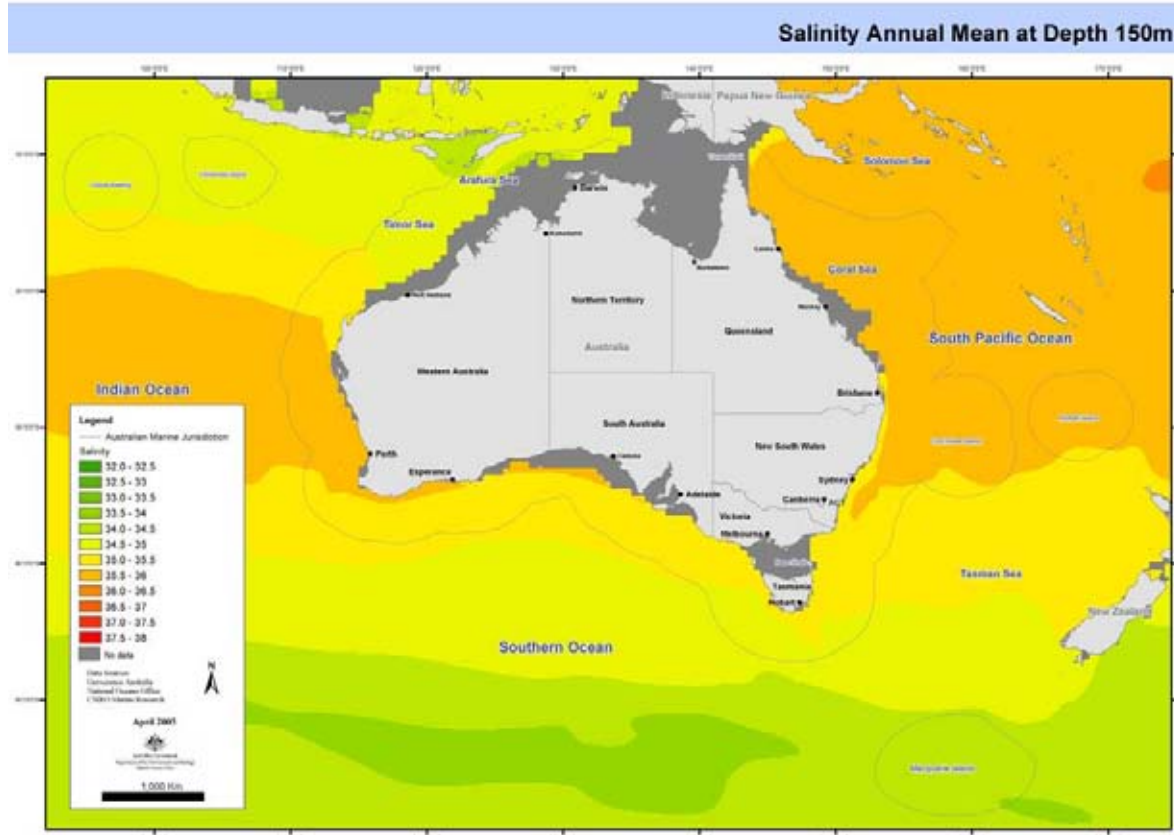
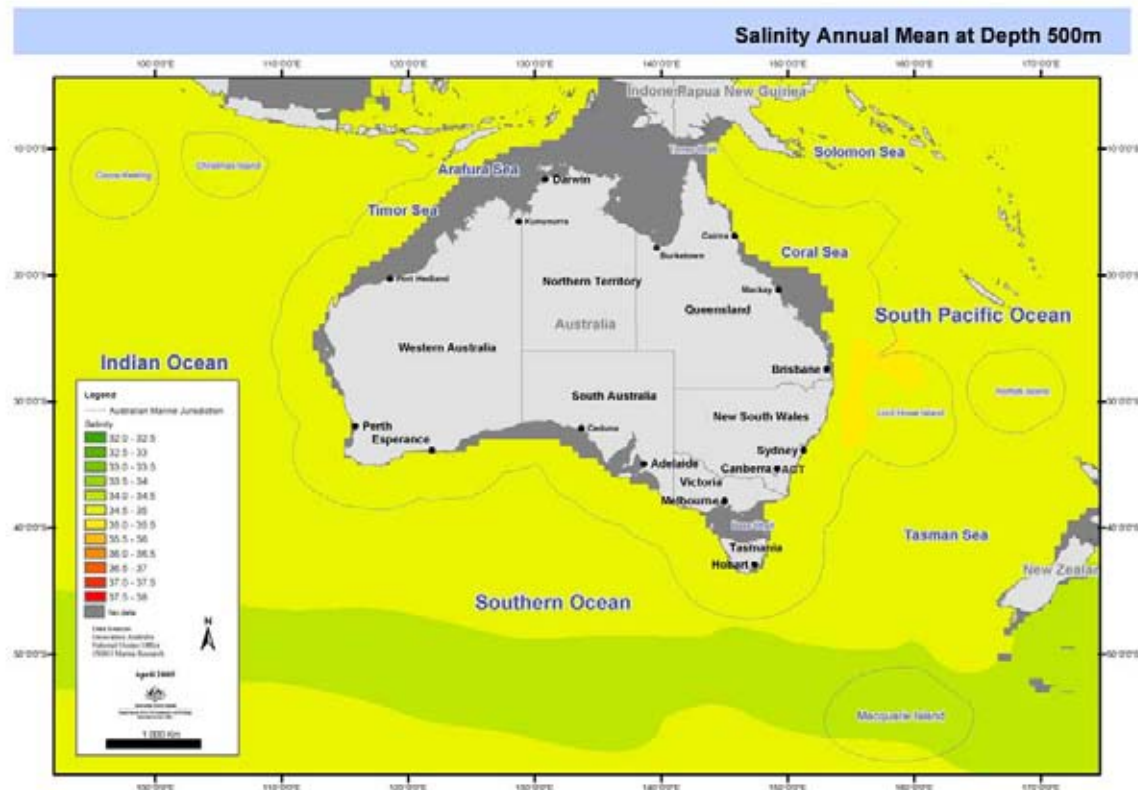


Figure 5.6 Salinity Annual Mean at (a) the surface, (b) 150 m, (c) 500 m, (d) 1000 m and (e) 2000 m.
Derived from CARS

c



d

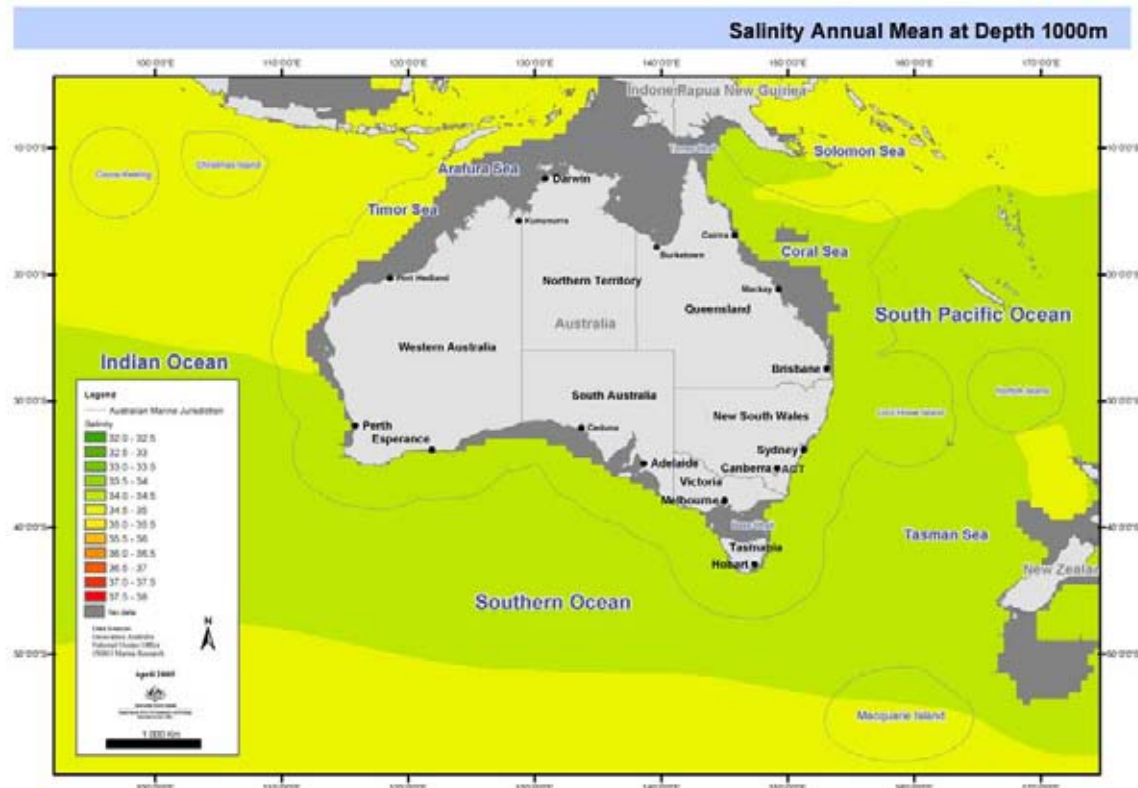


Figure 5.6 Salinity Annual Mean at (a) the surface, (b) 150 m, (c) 500 m, (d) 1000 m and (e) 2000 m.
Derived from CARS (cont)

e

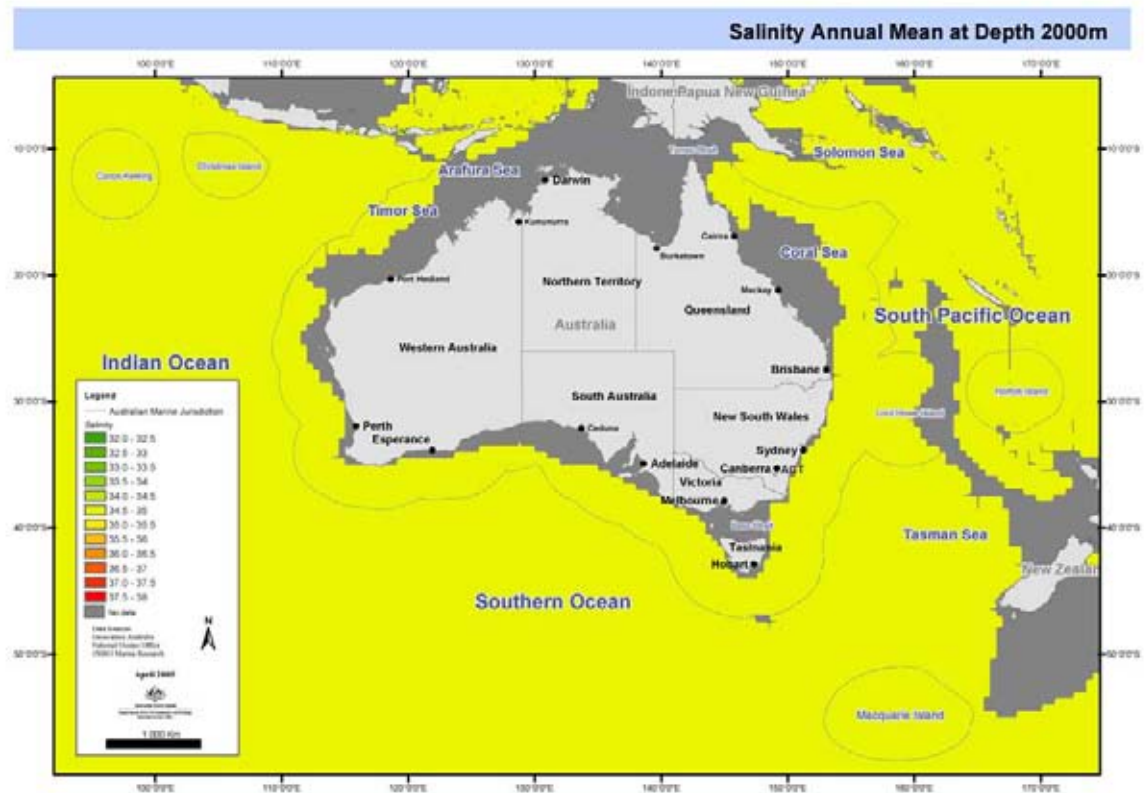
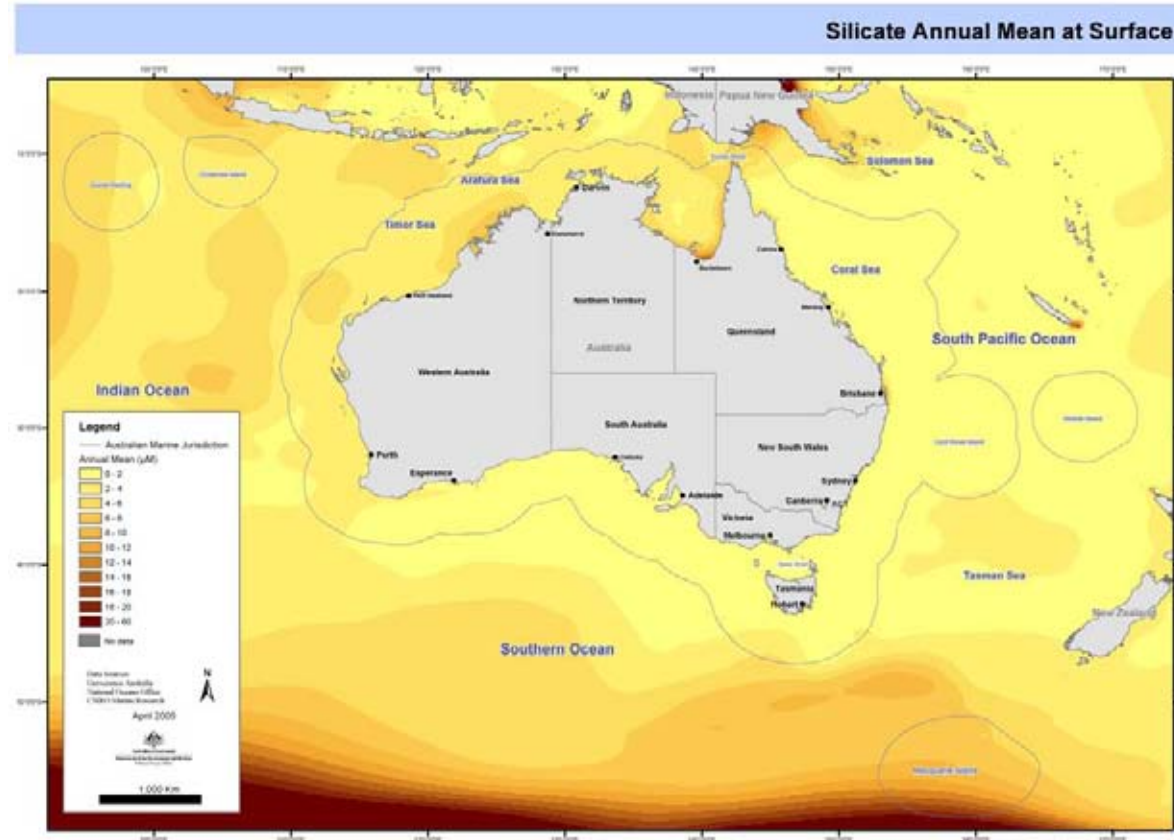


Figure 5.6 Salinity Annual Mean at (a) the surface, (b) 150 m, (c) 500 m, (d) 1000 m and (e) 2000 m.
Derived from CARS (cont)

a



b

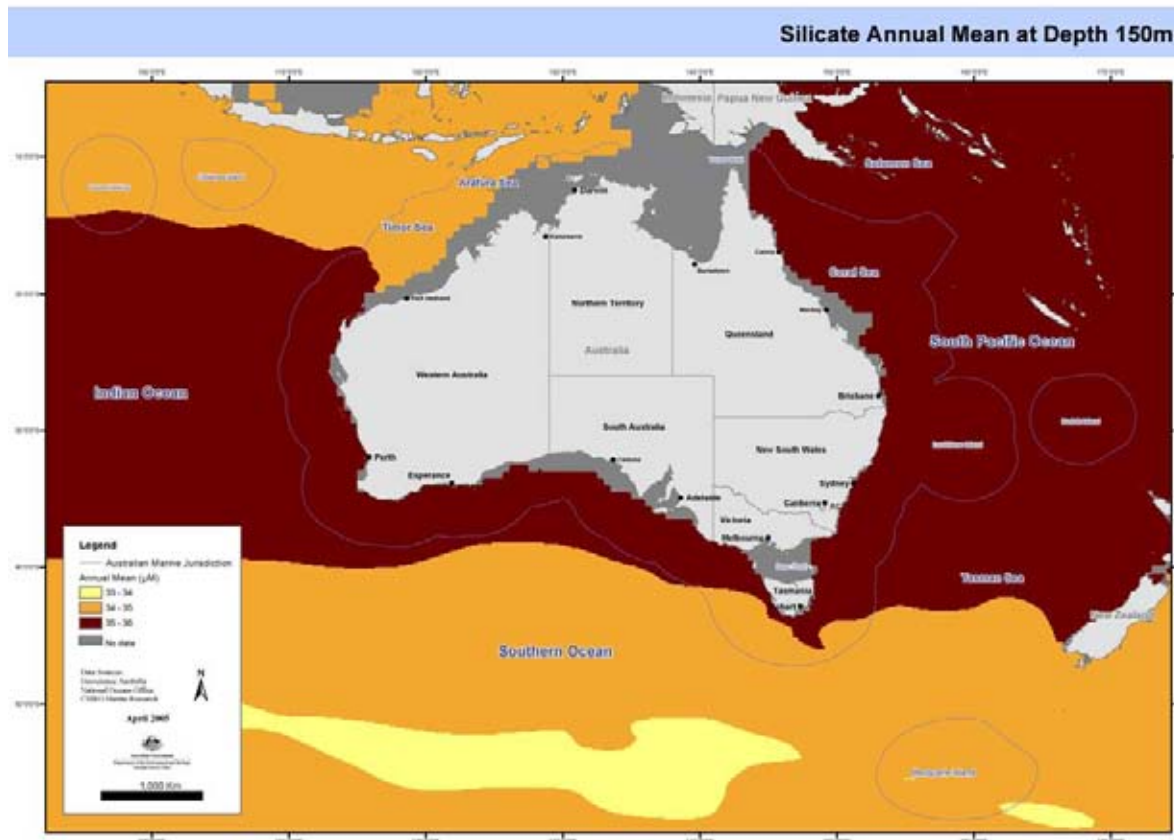
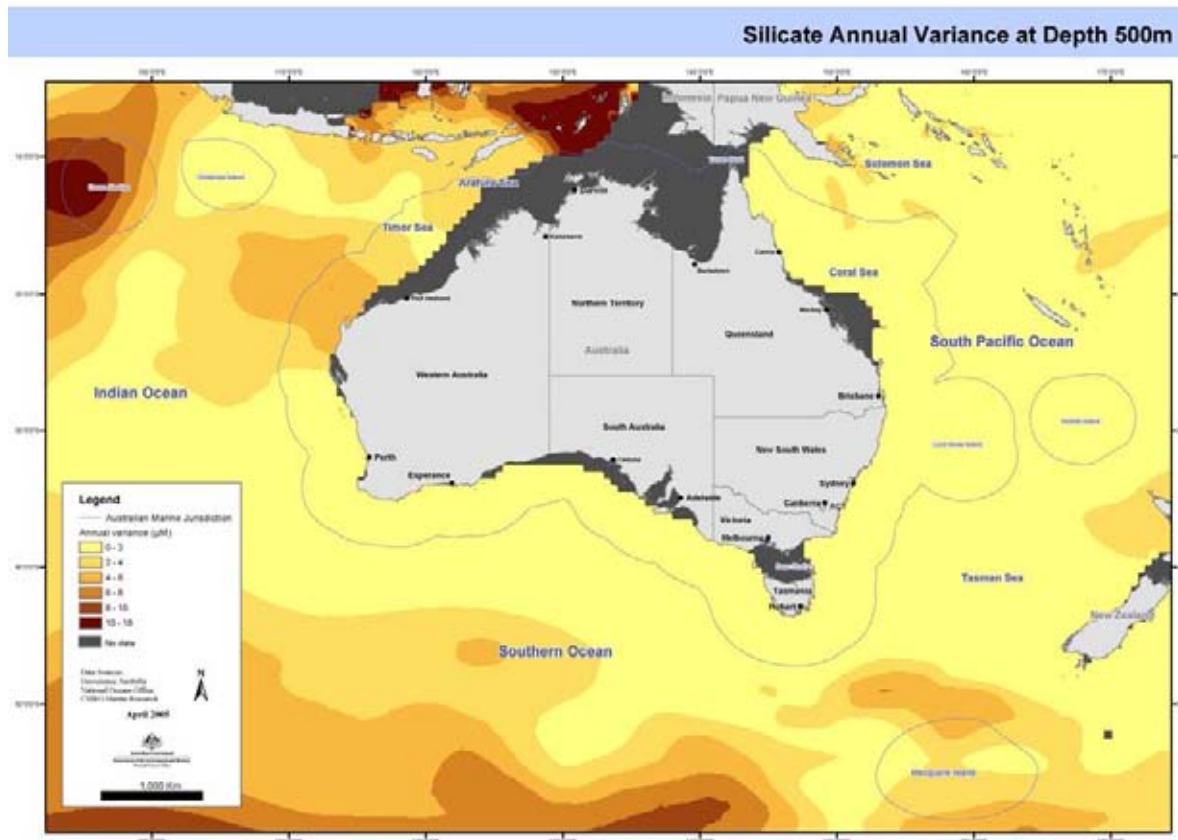
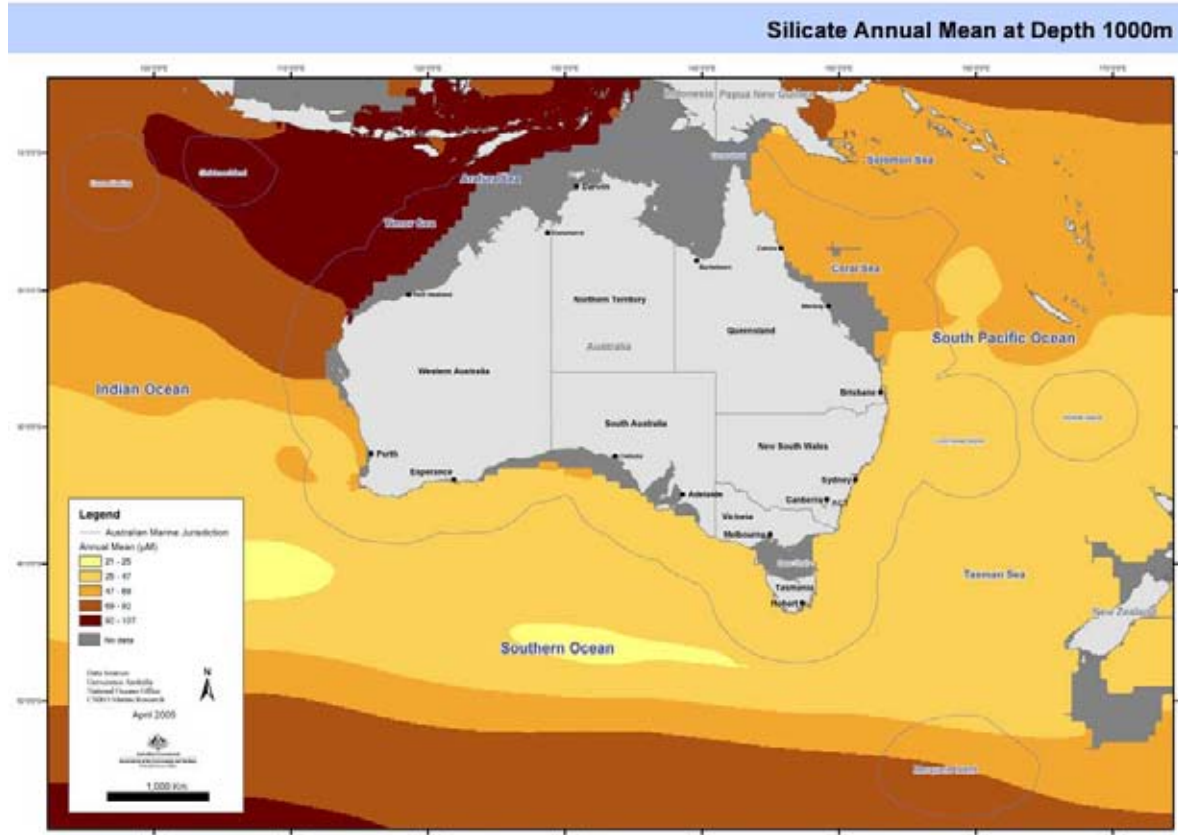


Figure 5.7 Silicate Annual Mean at (a) the surface, (b) 150 m, (c) 500 m, (d) 1000 m and (e) 2000 m. Derived from CARS.

c



d



**Figure 5.7 Silicate Annual Mean at (a) the surface, (b) 150 m, (c) 500 m, (d) 1000 m and (e) 2000 m.
Derived from CARS (cont)**

e

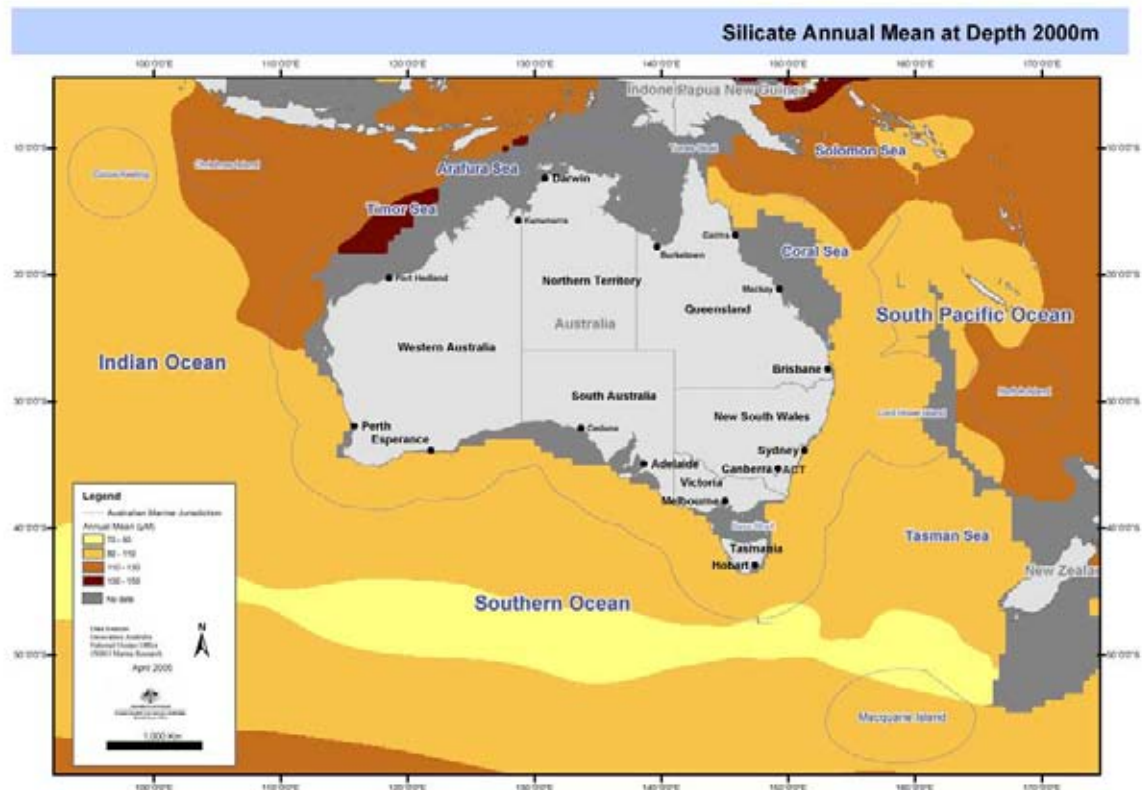
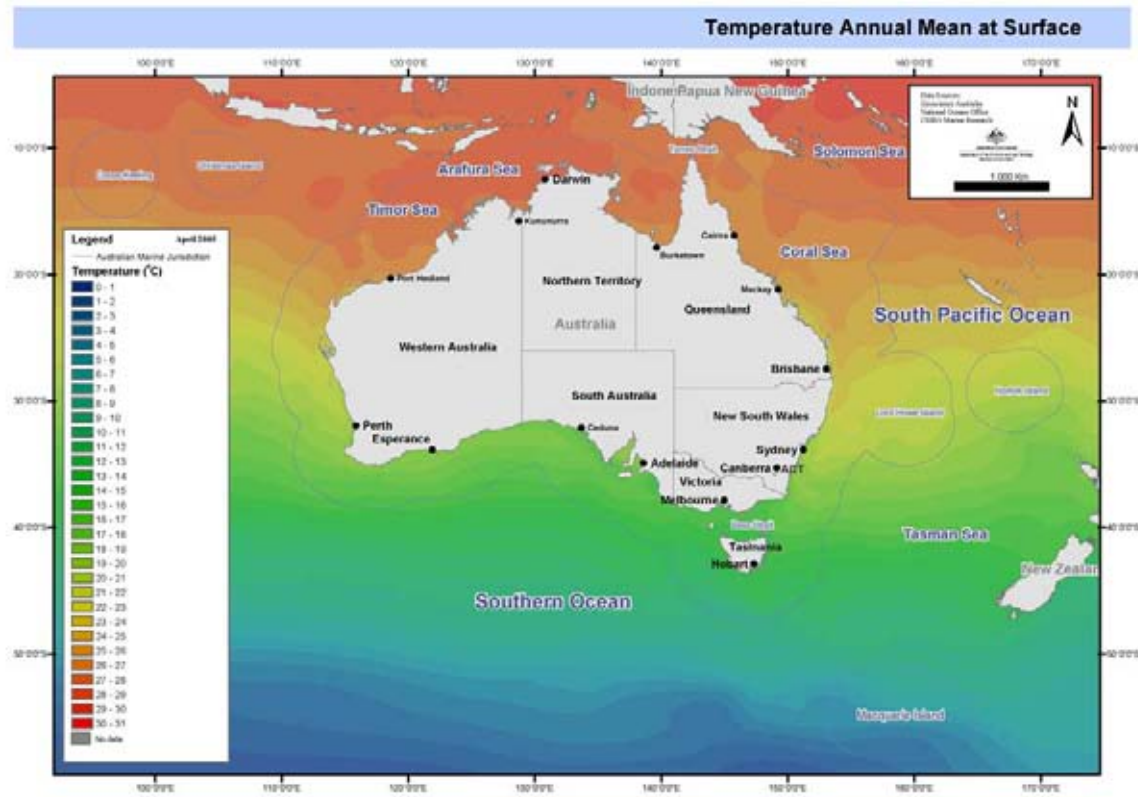


Figure 5.7 Silicate Annual Mean at (a) the surface, (b) 150 m, (c) 500 m, (d) 1000 m and (e) 2000 m.
Derived from CARS (cont)

a



b

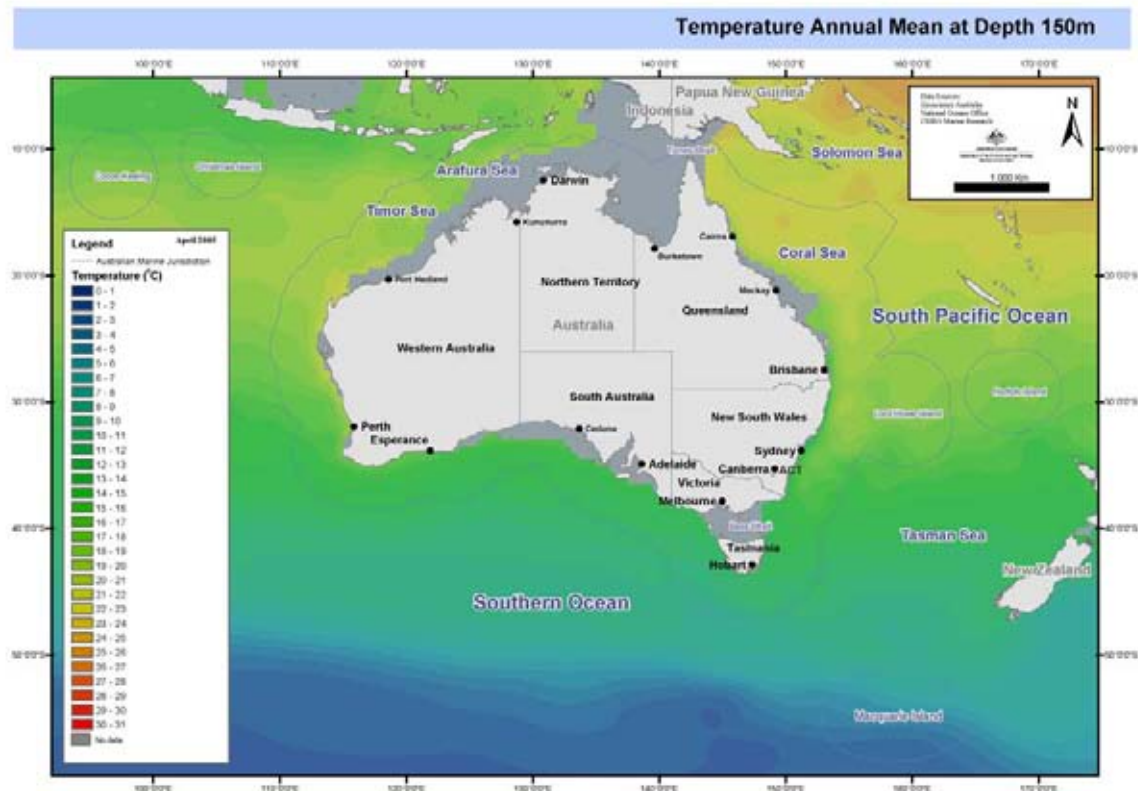
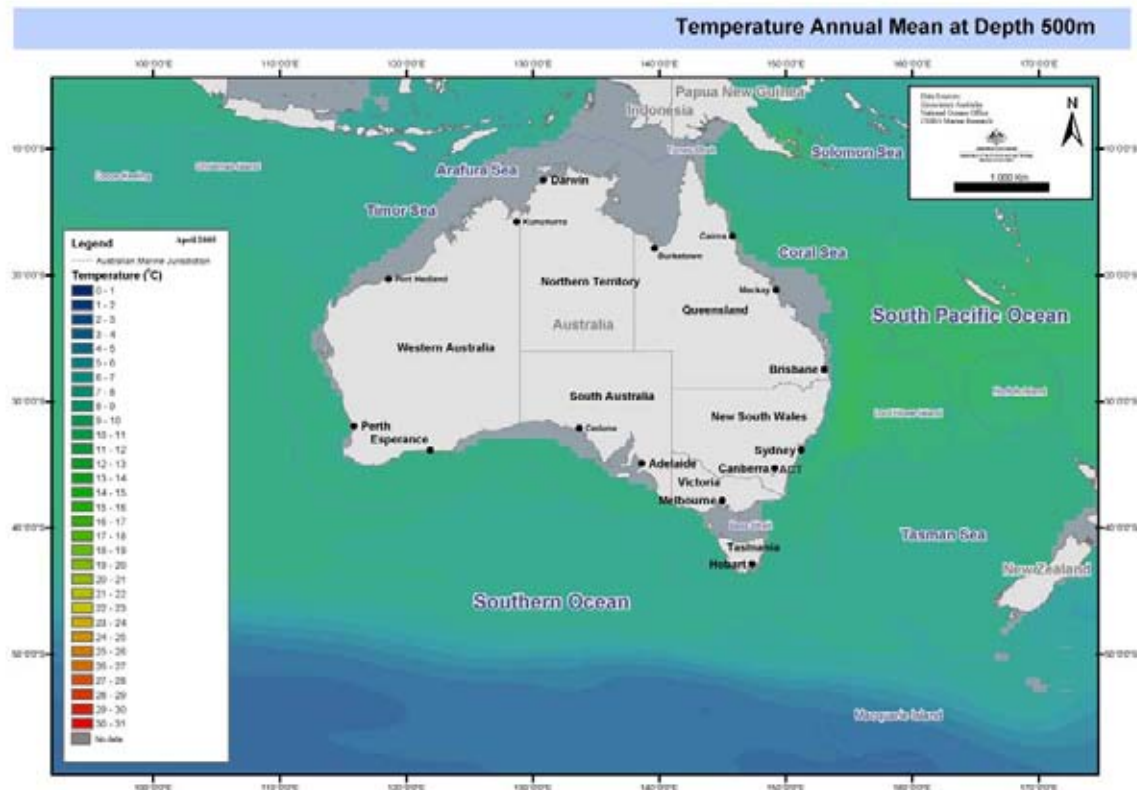


Figure 5.8 Temperature Annual Mean at (a) the surface, (b) 150 m, (c) 500 m, (d) 1000 m and (e) 2000 m.
Derived from CARS.

c



d

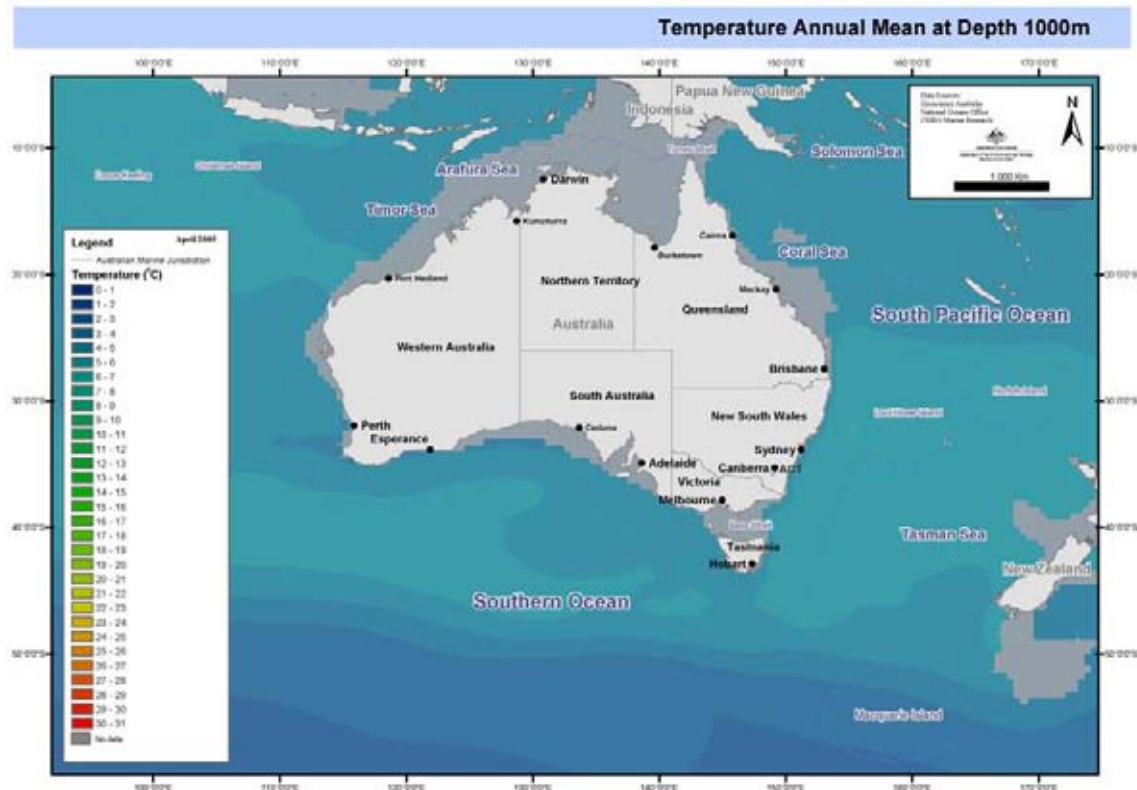


Figure 5.8 Temperature Annual Mean at (a) the surface, (b) 150 m, (c) 500 m, (d) 1000 m and (e) 2000 m. Derived from CARS.(cont)

e

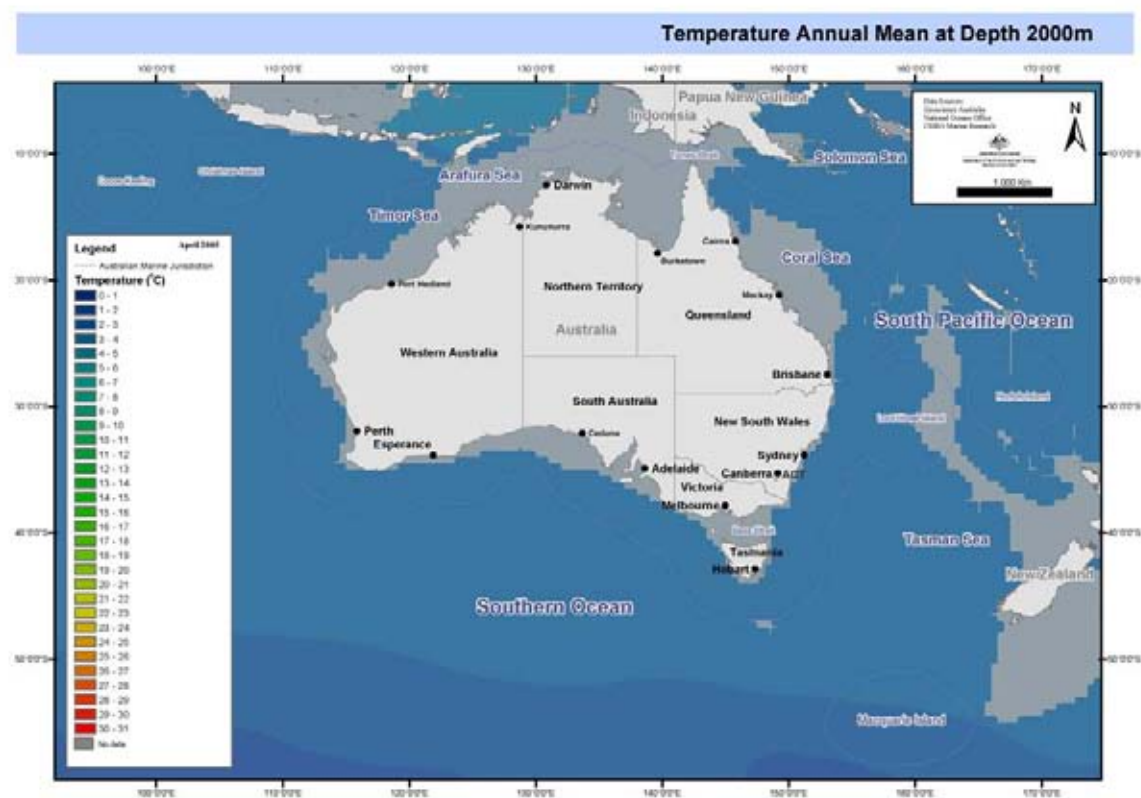


Figure 5.8 Temperature Annual Mean at (a) the surface, (b) 150 m, (c) 500 m, (d) 1000 m and (e) 2000 m.
Derived from CARS (cont).

5.3 Sea-surface Temperature

Sea-surface temperature (SST) is produced from data collected by the U.S. National Oceanographic and Atmospheric Administration (NOAA) satellites. These data provide high resolution spatial and temporal information at the sea surface, as can be seen in the image of the East Australian Current and associated eddies shown in Figure 5.9, which has a resolution of about 1 km, and contains a rich set of features in addition to the broad patterns of latitudinal variability seen in the CARS data. The temporal and enhanced spatial resolution offers a better dataset to discriminate the bioregionalisation units at Level 3 and finer scale, as evident in Figures 5.9 and 5.10.

Methods

Sea-surface temperature data, in DISIMP images, from NOAA Advanced Very High Resolution Radiometer (AVHRR) data received at the Australian Stations ACRES (Alice Springs), WASTAC (Perth), Australian Institute of Marine Science (Townsville), CSIRO Marine Laboratories (Hobart), CSIRO Atmospheric Research (Melbourne) and Bureau of Meteorology (Darwin). Potentially overlapping data from each station were consolidated (“stitched”) into a single, Australia-wide image per satellite overpass by the CSIRO/Earth Observation Centre, from various NOAA satellites with both day and night passes. Data span from October 1993 to June 2003. SST is calculated using the NLSST (non-linear SST) algorithm or the split window (McMillin) algorithm. The images cover the Australian continent and surrounding oceans.

Raw data originate from the AVHRR sensor on various NOAA polar-orbiting satellites, received at various stations around Australia and consolidated (“stitched”) by the CSIRO Earth Observation Centre. The stitching removes redundancy and minimises data corruption. Processing from the stitched archive to produce SST is carried out in the CMR Remote Sensing Facility in Hobart, using either the split window algorithm of McMillin for NOAA9 and NOAA12 satellites or the NLSST (NOAA non-linear SST) algorithm for the other satellites.

Roger Scott (CSIRO Marine Research) calculated means and variances from the DISIMP files (1993-2003) provided by the Remote Sensing Facility in Hobart.

Parameter accuracy

Nominally +/-0 1 deg, depends on cloud density and the prevalence of other atmospheric interference. Values are calibrated as bulk temperatures, but no adjustments for diurnal cycling of, for example, near-surface stratification, are made.

Completeness

Almost all the full-resolution NOAA AVHRR data that have been archived in Australia have been included, so there are very few gaps in time.

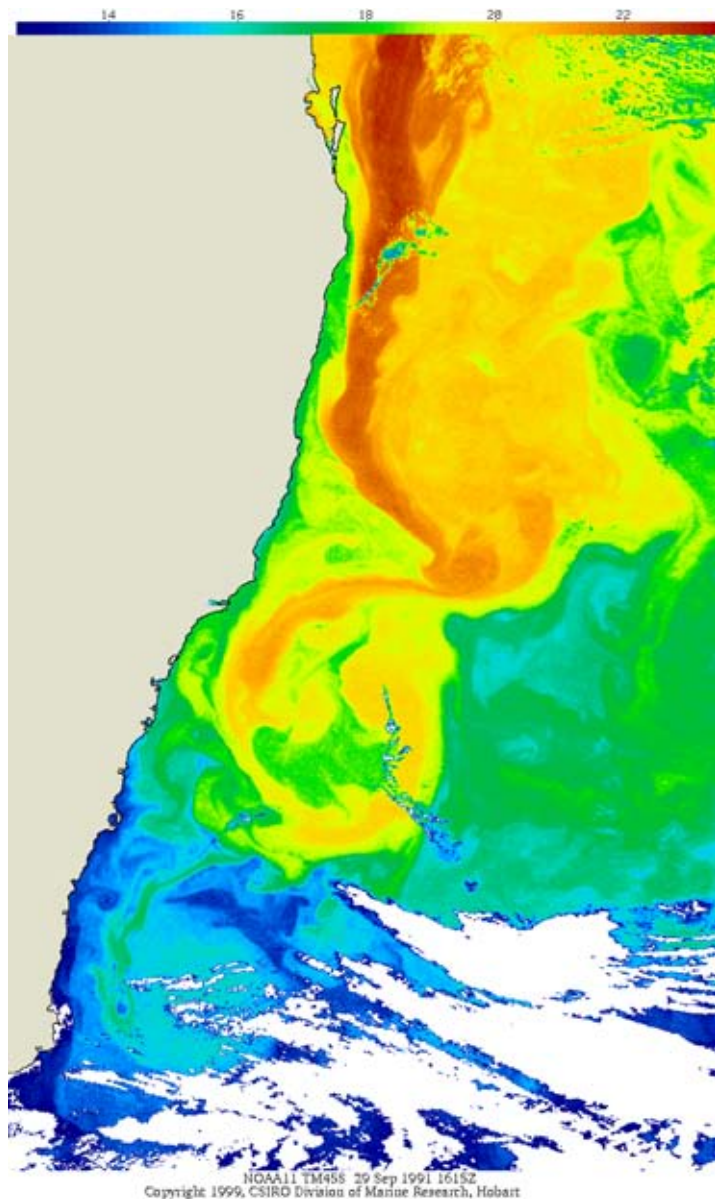


Figure 5.9 SST image of the East Australian Current and associated eddies.

Description

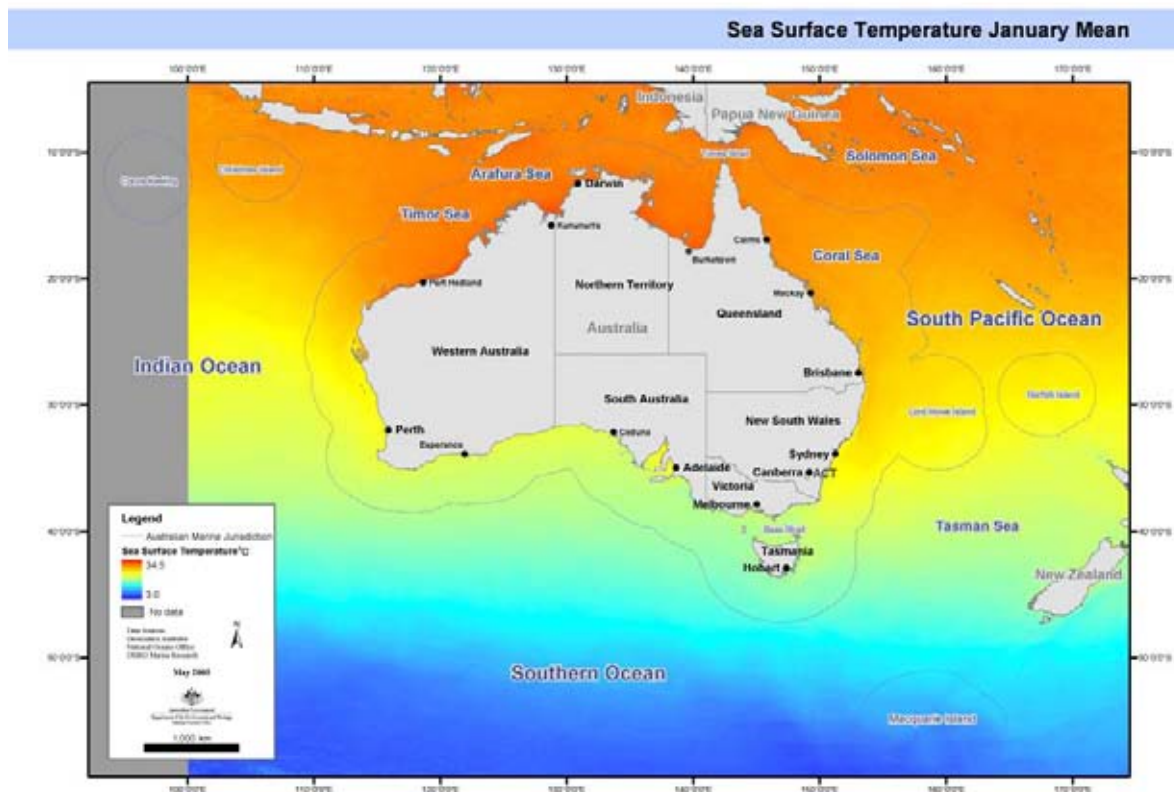
Maps of monthly-mean temperature are presented in Figure 5.10 (a-d) for January, April, July and October. The general pattern in these representative seasonal maps is dominated by the overall mean pattern (Figure 5.8) showing latitudinal temperature variation from the warm tropics to the cold Southern Ocean waters. Seasonal deviations from this pattern are most apparent at regional scales in winter (July map; Figure 5.10c) and along the coastal margins.

The winter map (Figure 5.10c) shows a general cooling off in the South Pacific Ocean but the central eastern sector of the Indian Ocean shows a slight warming. The relative warmth of the Leeuwin Current is evident from the warmer stream of current flowing at the edge of the continental shelf in southern Australia in July. A tongue of warm water also appears to flow south from about the mid-central coast of Western Australia in April. Northward “contractions” of the East Australian Current are most marked in July when the tongue of warm water, evident in the January and April maps, diminishes. Embayments and large shallow areas along the coast display the largest seasonal changes and this is evident for example in Shark Bay in Western Australia, the gulfs of Spencer and St Vincent in South Australia, the Gulf of Carpentaria in Queensland and Bass Strait.

The influence of warm waters around Tasmania from the extension of the East Australian Current is evident in the July and October maps. These show the waters of the subantarctic noticeably curving around Tasmania.

Variance of seasonal temperature (Figure 5.11 a-d) shows a general pattern consisting of high variances in the tropics, the Southern Ocean and boundary current regions of the East Australian Current and the Leeuwin Current. High variances in the tropics are most likely a result of cloud contamination. Similarly, the regular curved lines in the Southern Ocean appear to be artefacts from electronic noise in the satellite scans. Nevertheless enhanced variability is observed in the East Australian Current region which peaks in January. The extension of the East Australian Current off south-east Tasmania is also evident from increased variability in that region particularly in April. Other areas of high variance occur in south-west Australia in association with the Leeuwin Current, and across the Southern Ocean particularly in October. These interpretations of the variance maps must be tempered by possible contamination of images by cloud effects.

a



b

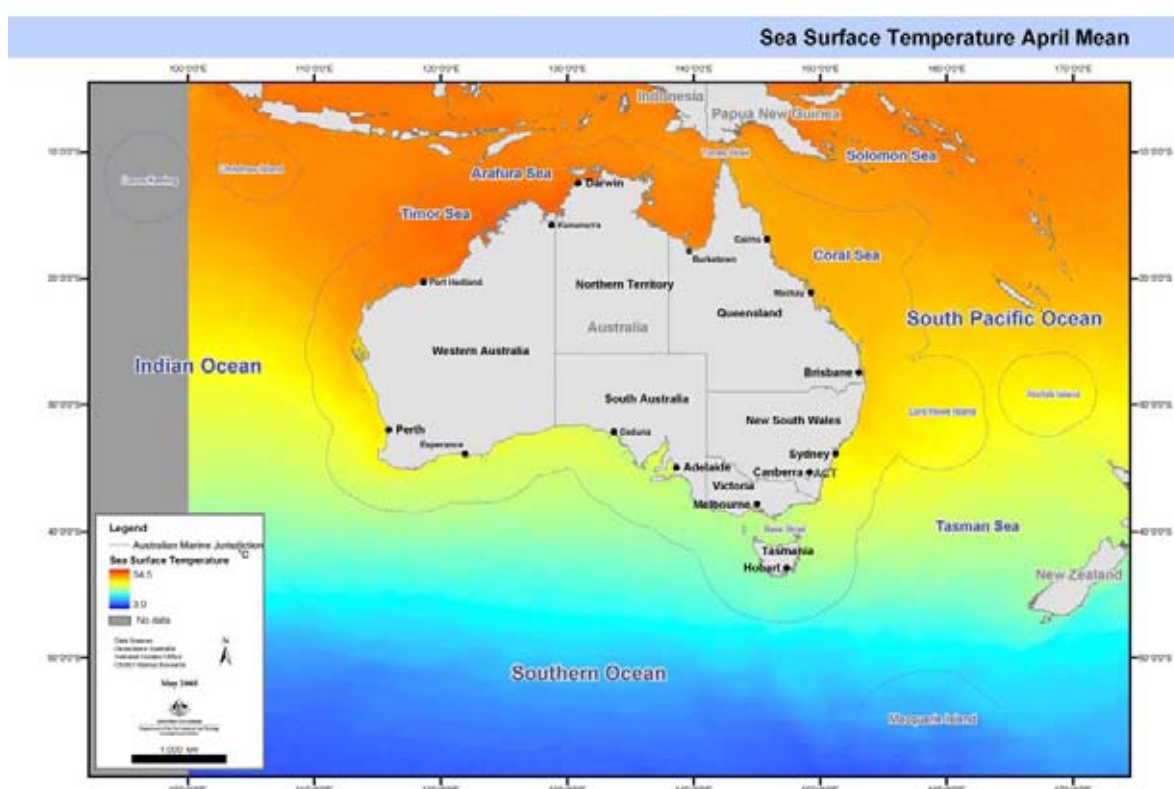
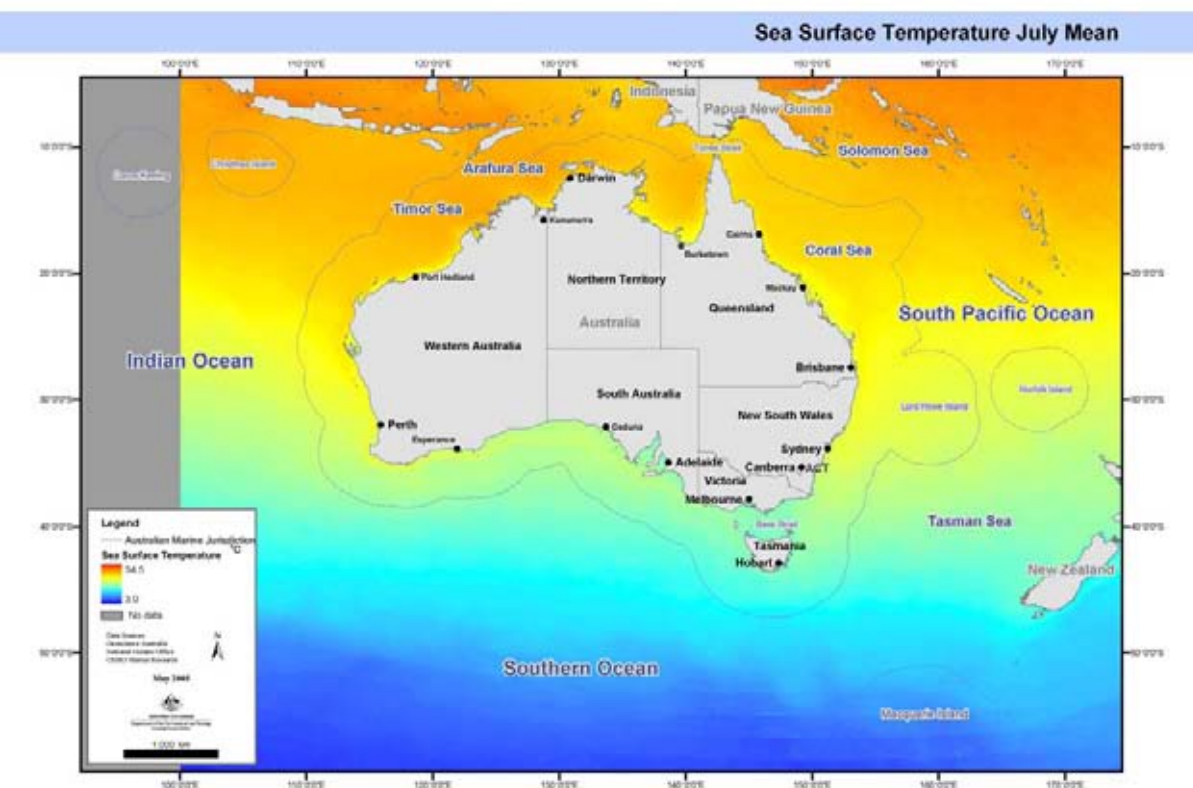


**Figure 5.10 Sea-surface Temperature Monthly Means for (a) January, (b) April, (c) July and (d) October
(means calculated over years 1993–2003).**

c



d

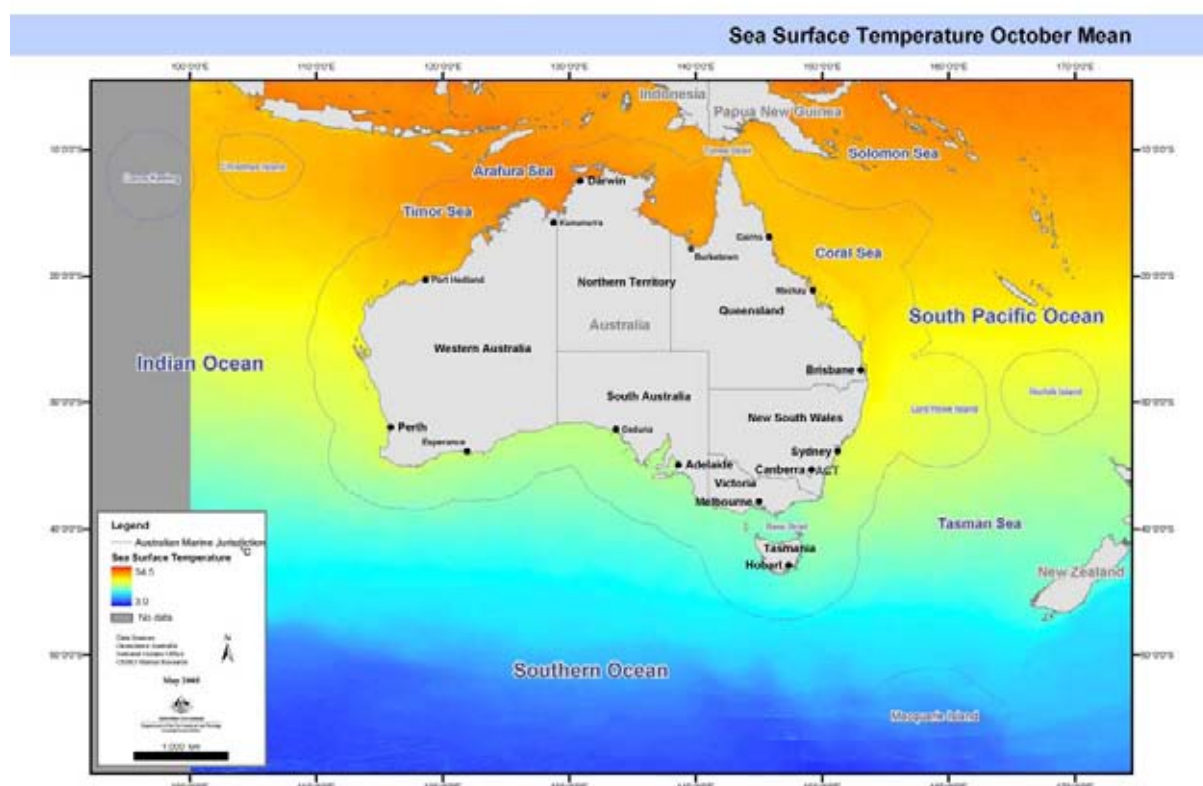
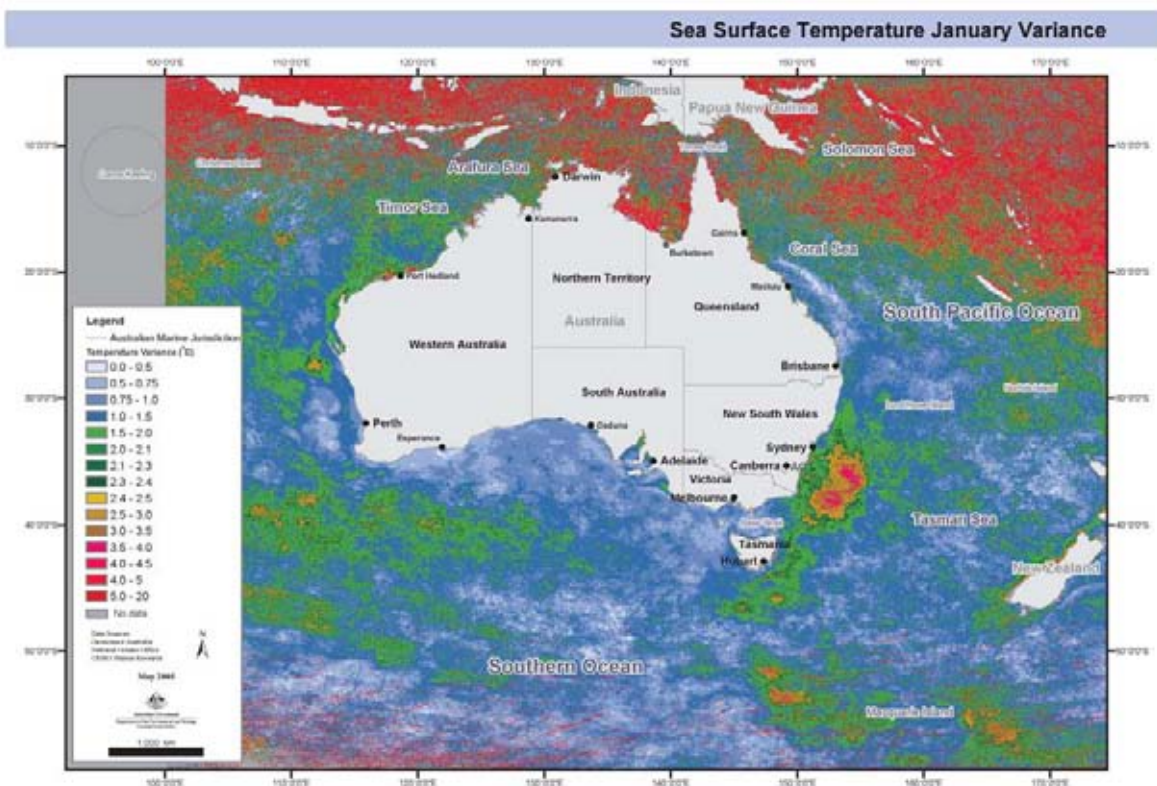


Figure 5.10 (cont.) Sea-surface Temperature Monthly Means for (a) January, (b) April, (c) July and (d) October (means calculated over years 1993–2003).

a



b

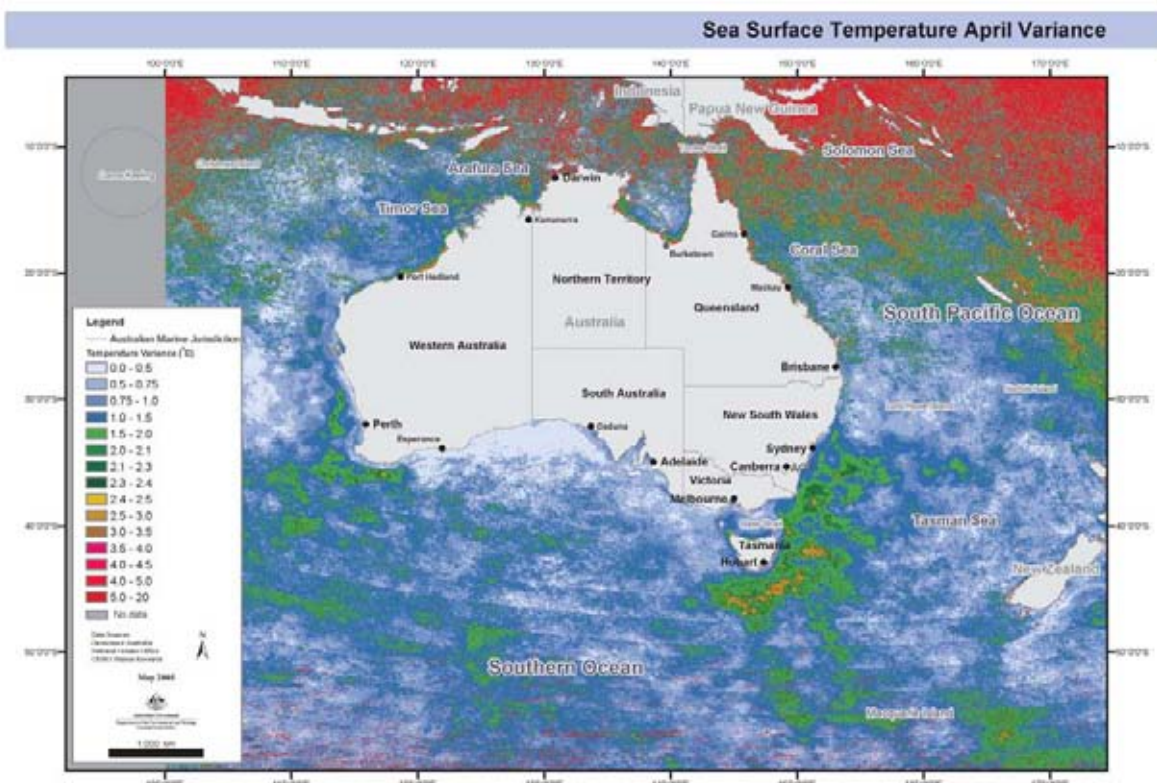
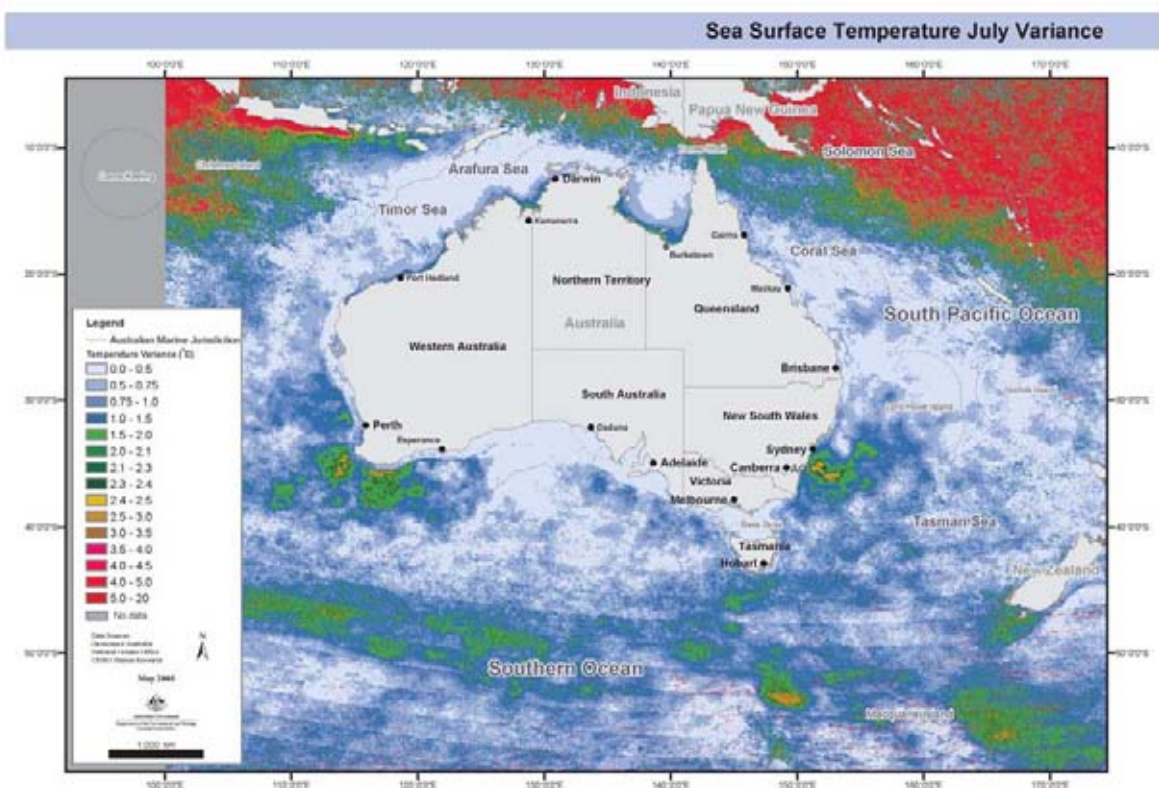


Figure 5.11 Sea-surface Temperature Monthly Means for (a) January, (b) April, (c) July and (d) October (variances calculated over years 1993–2003).

c



d

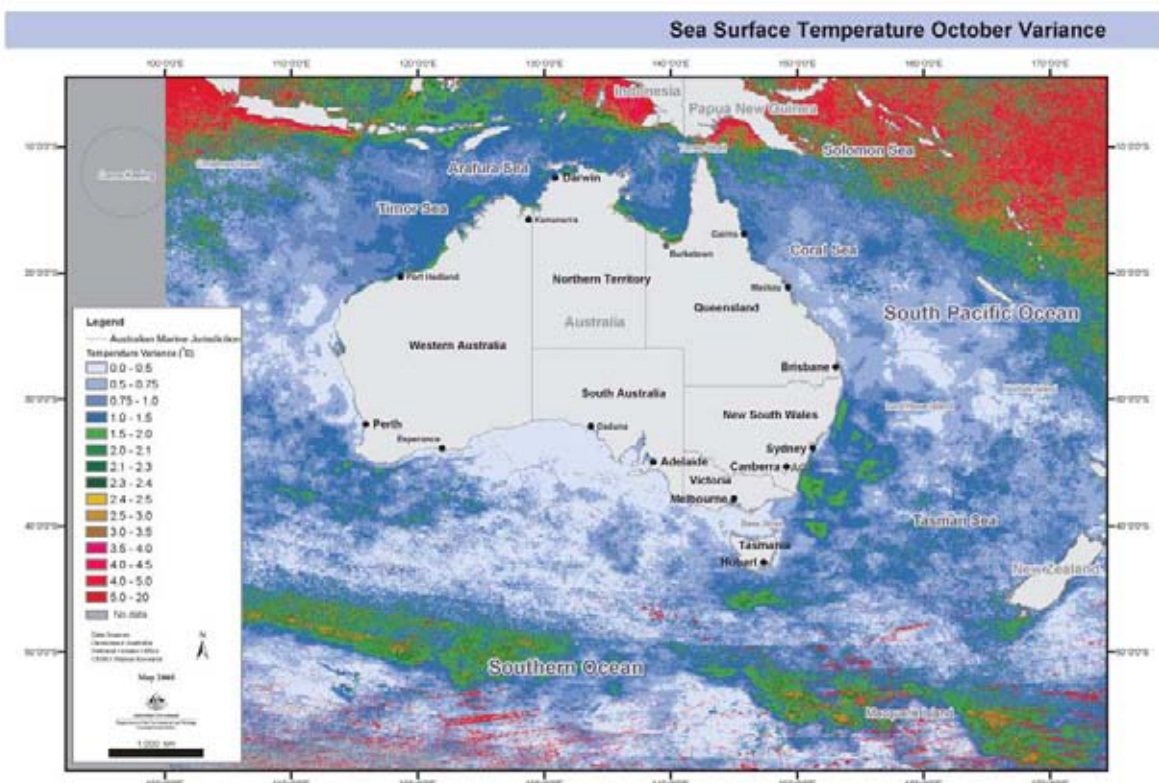


Figure 5.11 (cont.) Sea-surface Temperature Monthly Means for (a) January, (b) April, (c) July and (d) October (variances calculated over years 1993–2003).

5.4 Eddies and Fields based on SST

The remote sensing data on sea-surface temperature (SST) was analysed through a pattern recognition methodology developed by Vincent Lyne. This involved computing distributional properties of the localised variance in order to determine the most probable location of eddies. This “probability distribution”, along with gradient analysis of the filtered remote sensing data, was used to classify the image into a number of classes such as eddies, mixed eddy waters, major fronts and general background waters. Figures 5.11, 5.12, 5.13 and 5.14 show eddies, mixed eddy waters, major fronts and general background waters as Classes 1 through 4.

Feature classes determined from sea-surface temperature (SST) were used as input to the “Level 3” pelagic integrated analyses. A key component of these analyses were “SST classes”, which quantified variability/homogeneity fields in the SST.

The strategy in computing the classes was to classify the observed histogram of SST spatial gradients. The intention was to classify (spatial) fields based on the shape/form of the histogram so that the relative distinctiveness of fields was a function of the frequency (in space) with which they occurred.

The procedure used in deriving the classes was as follows: individual SST images were median-filtered with a 13 pixel by 13 pixel spatial filter in order to reduce the noise inherent in the images. The filter size was determined by exploratory analyses, which was a compromise chosen to reduce noise and to minimise the loss of gradient information to be used in the classifications. Pixel values in the SST image range between 0 and 255; the median was applied only to pixels that were greater than 0 and less than 250 – values outside these limits were due to land or cloud effects. Standard deviations were computed at each location of the median-filtered image using a spatial window of 25 x 25 pixels. An overall median of the standard deviation, denoted Std^m , was also computed. Key classes were identified as follows:

CLASS	DESCRIPTION
0	$\text{Std} < 0$ and $\text{Std} > 20$. Almost completely homogeneous (land)
1	$\text{Std} > 0$ and $\text{Std} < 0.55*\text{Std}^m$. Low heterogeneity (lower than that in eddy cores)
2	$\text{Std} \geq 0.55*\text{Std}^m$ and $\text{Std} < 1.55*\text{Std}^m$. <i>Medium heterogeneity (as in eddy cores)</i>
3	$\text{Std} \geq 0.55*\text{Std}^m$ and $\text{Std} < 20$. High heterogeneity (as in fronts and eddy edges)
4	Class 3 but also with high gradients (not useful class)

Note: Std denotes the standard deviation at a location determined from procedure (2). Class 4 was computed to capture very high gradient regions but this class was not used in the analyses and is not discussed further.

Class 1: This class is meant to identify fields of relatively homogenous temperature. Thus these areas have relatively stable temperatures and are characteristic of “core” water masses. The main regional distributions of this class occur off the north-west coast of Australia; the Great Australia Bight and a companion offshore area to the south-west; Bass Strait; the Gulf of Carpentaria; offshore of the Great Barrier Reef; and the extensive area offshore of the northern portion of eastern Australia.

Class 2: To a large extent, this field complements the Class 1 field but appears more pervasive than the former. This is to be expected, as this field characterises the peak in the histogram distribution of SST standard deviation. The textured nature of the field reflects the occurrence of numerous fronts embedded within this field.

Class 3: This field characterises the high gradient/variability region and typically occurs between the Class 1 and 2 fields. The field is most extensive in the Southern Ocean region and reflects the highly

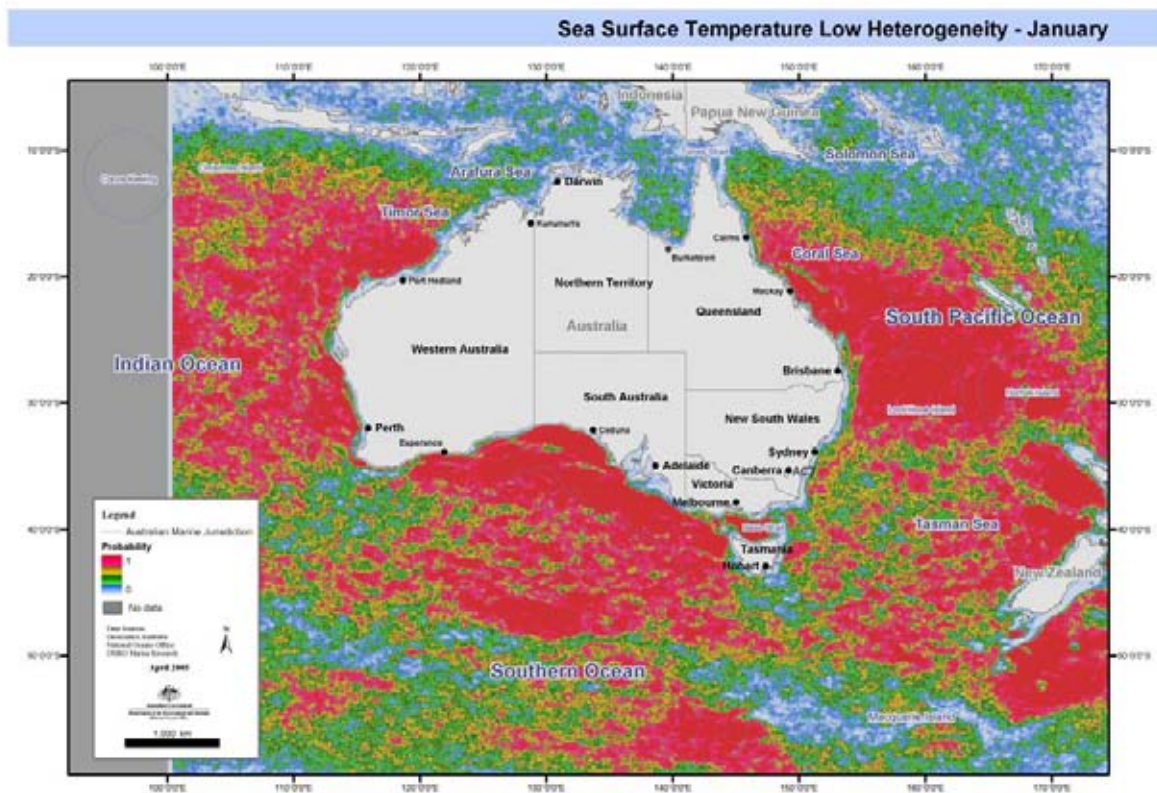
energetic nature of the mixing associated with the major Southern Ocean frontal systems and the underlying influence of bottom topography. Two other major areas occur off south-eastern Australia and south-west Australia. The East Australian Current eddy field is responsible for the former, while the latter is associated with the Leeuwin Current and its instabilities. The Leeuwin Current itself is clearly demarcated as a thin jet in the south-west of Australia, which disappears just west of the Great Australia Bight, although elements of this current reappear to the east and off western Tasmania (as the Zeehan Current). The shelf-break region of eastern Australia is also characterised as being of high variability and again may reflect the interaction of the East Australian Current and its eddies with the shelf/slope.

Data provided

- Sea-surface temperature monthly means
- Sea-surface temperature monthly variance
- Sea-surface temperature total mean
- Sea-surface temperature total variance
- Eddies and fields based on sea-surface temperature.

For a full list of products see Appendix A.

a



b

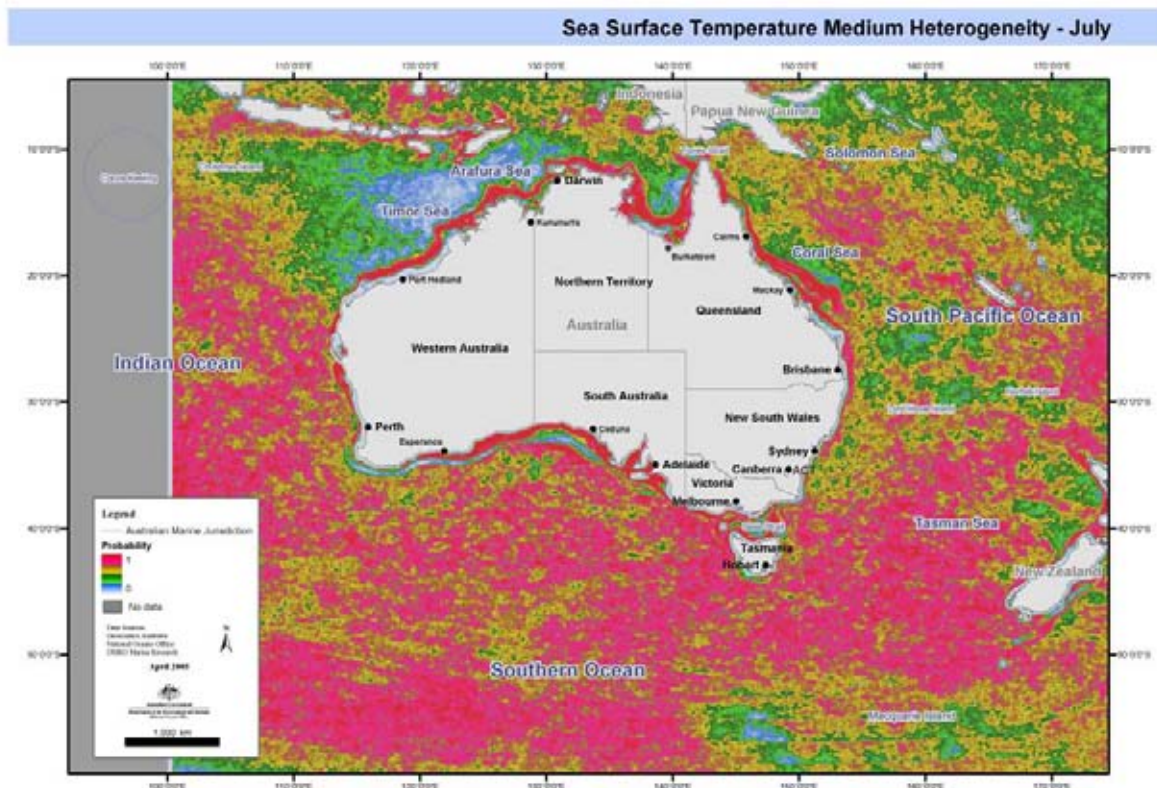
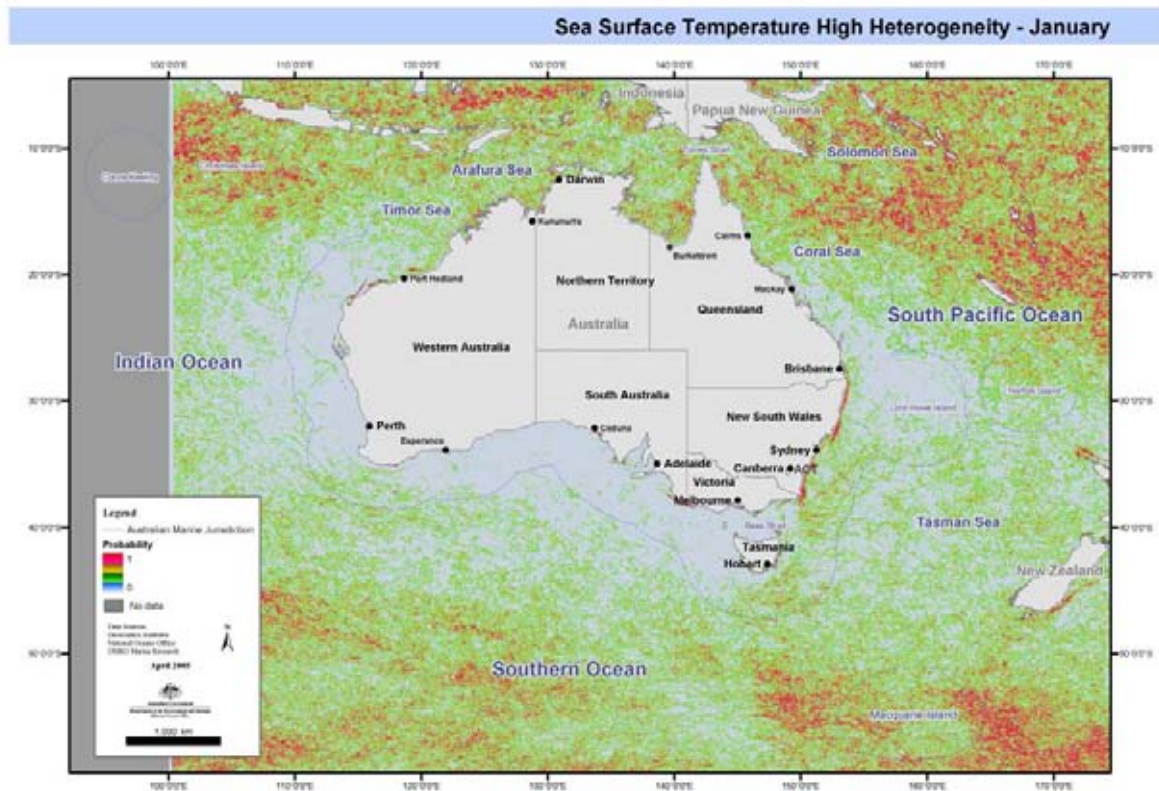


Figure 5.12 Eddies and fields based on sea-surface Temperature in January. (a) low heterogeneity, (b) medium heterogeneity, (c) high heterogeneity, (d) high heterogeneity and high gradients.

c



d

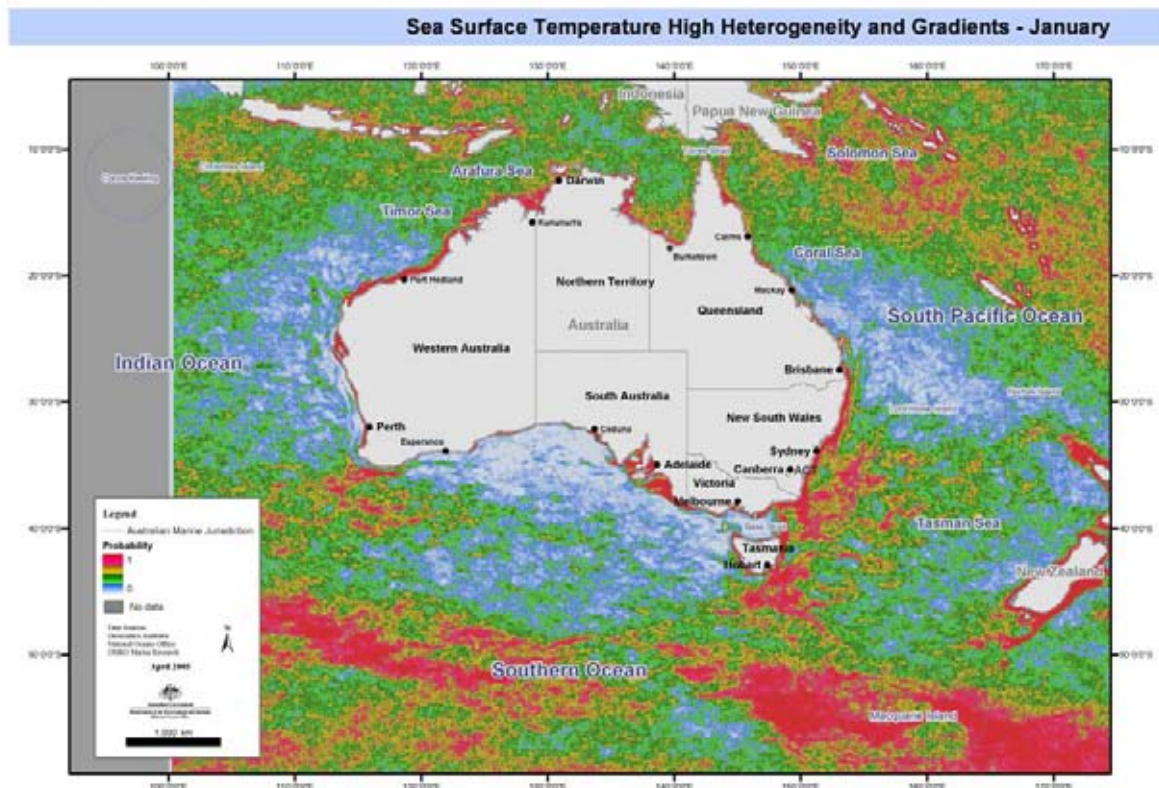
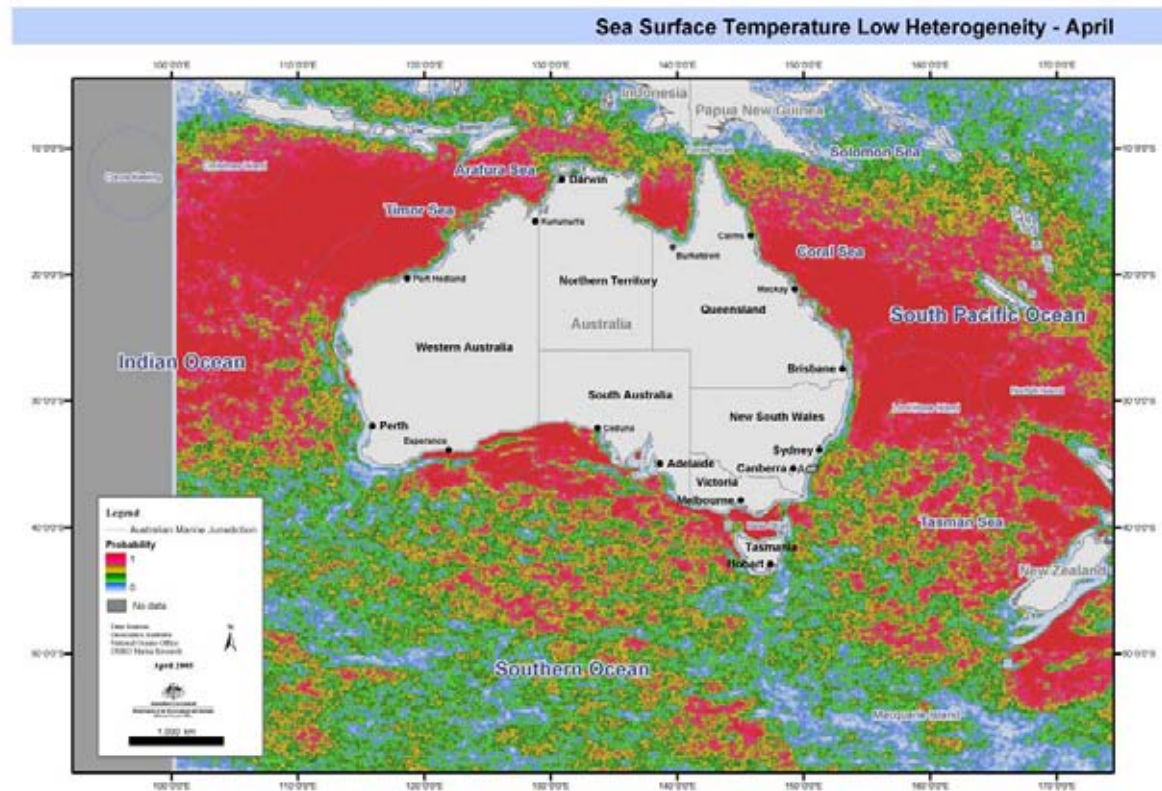


Figure 5.12 Eddies and fields based on sea-surface temperature in January. (a) low heterogeneity, (b) medium heterogeneity, (c) high heterogeneity, (d) high heterogeneity and high gradients (cont)

a



b

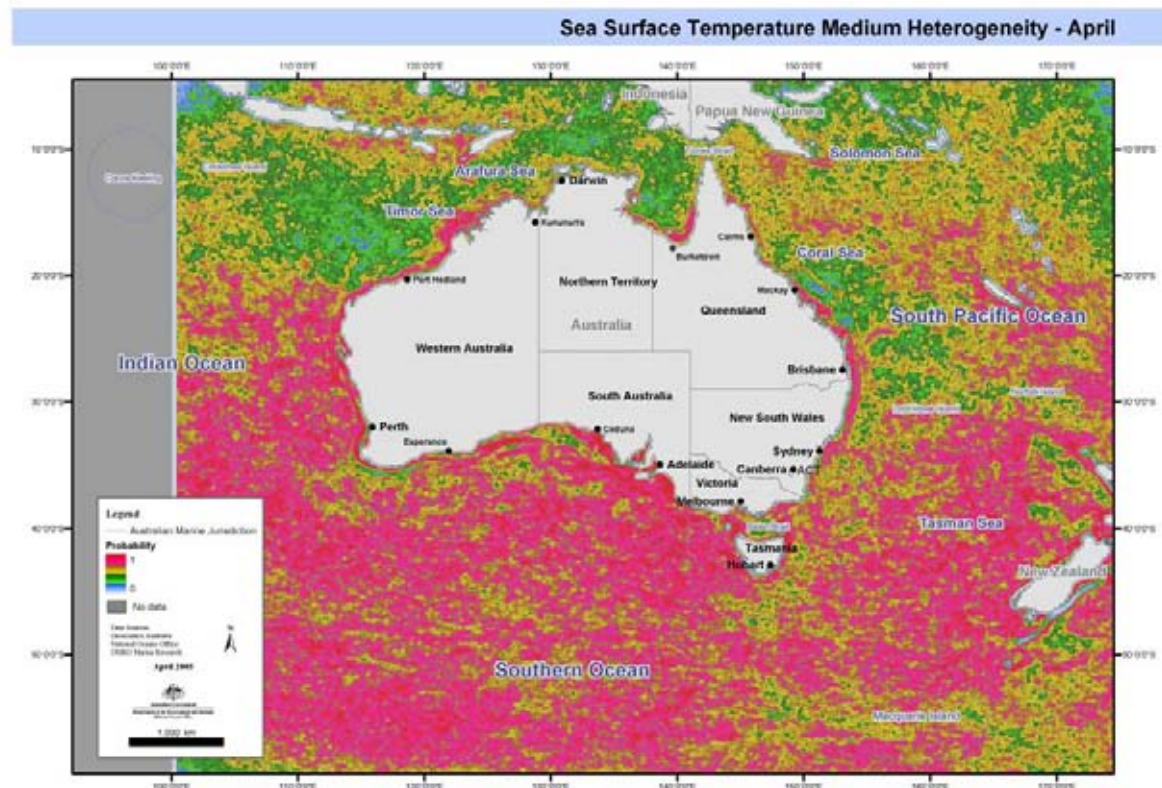
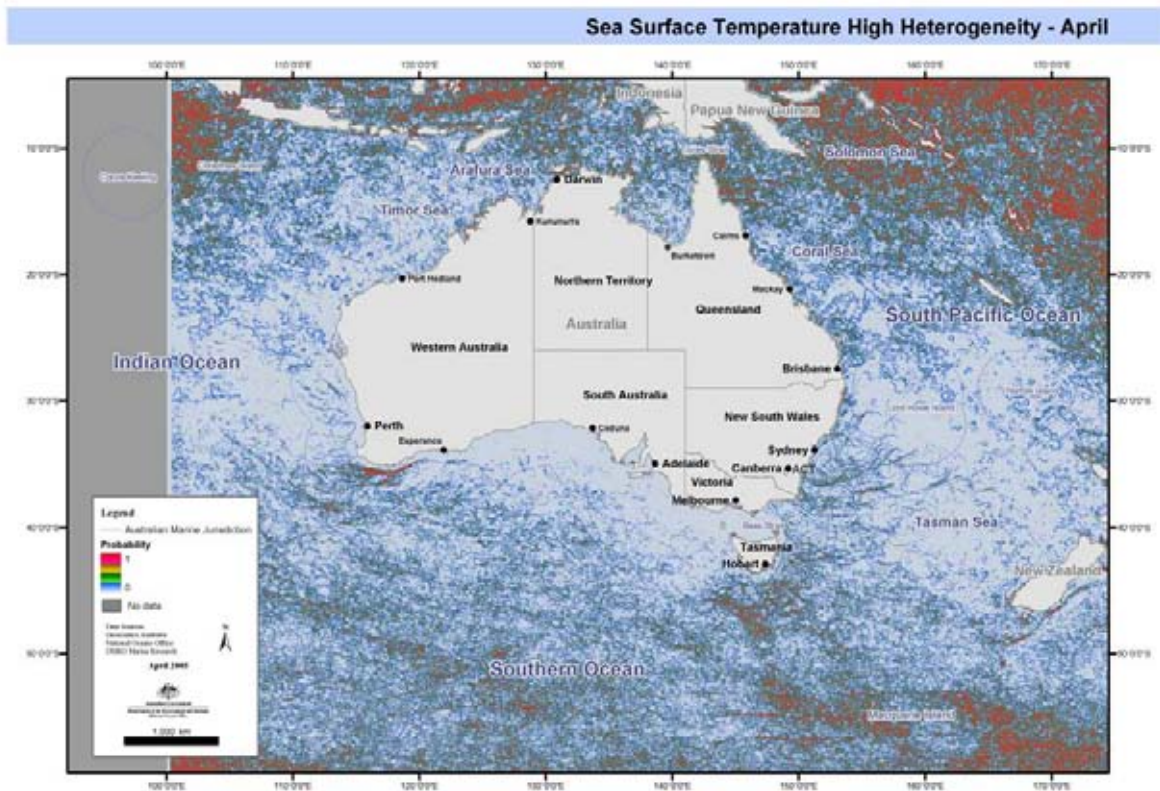


Figure 5.12 Eddies and fields based on sea-surface temperature in April. (a) low heterogeneity, (b) medium heterogeneity, (c) high heterogeneity, (d) high heterogeneity and high gradients (cont).

c



d

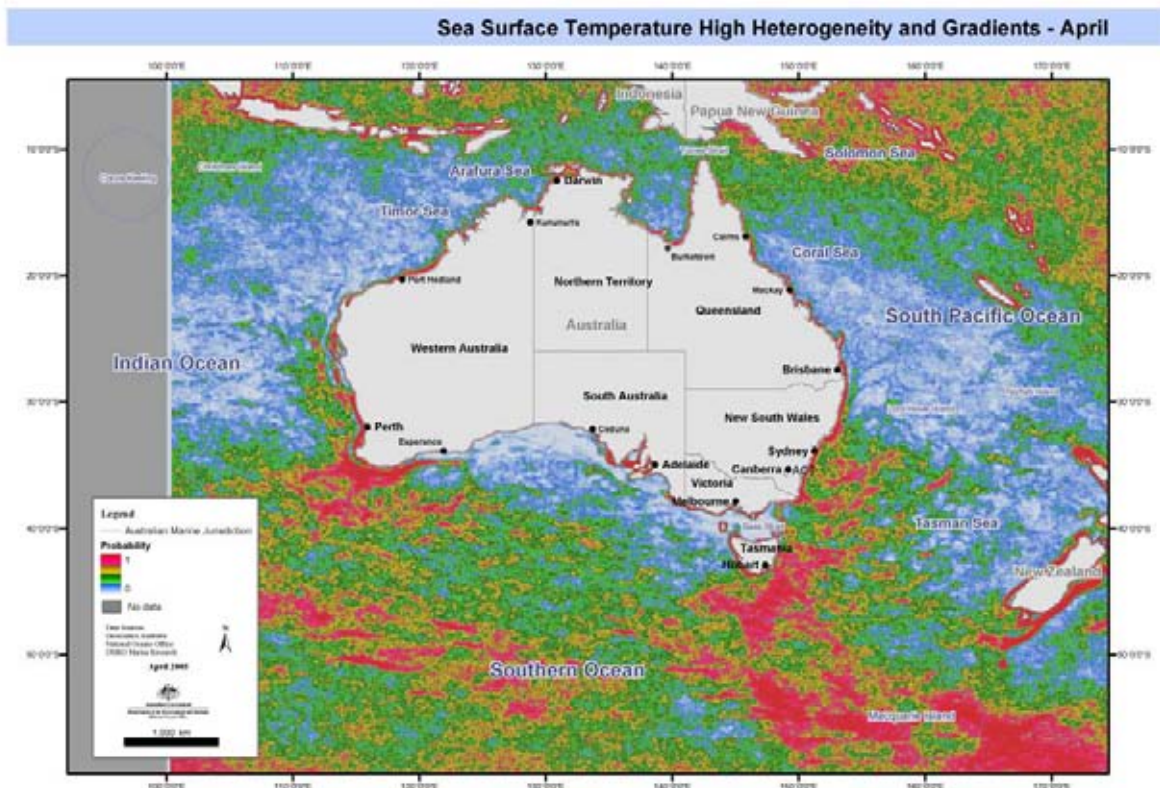
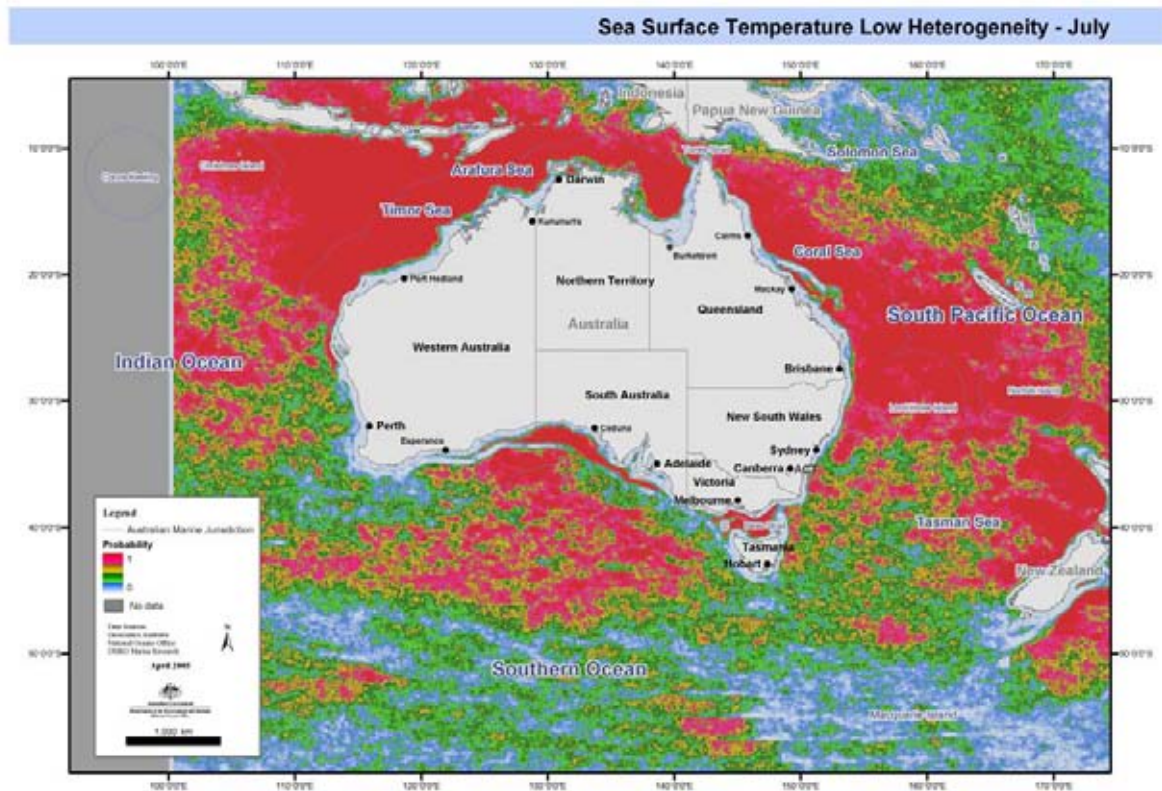


Figure 5.12 Eddies and fields based on sea-surface temperature in April. (a) low heterogeneity, (b) medium heterogeneity, (c) high heterogeneity, (d) high heterogeneity and high gradients (cont).

a



b

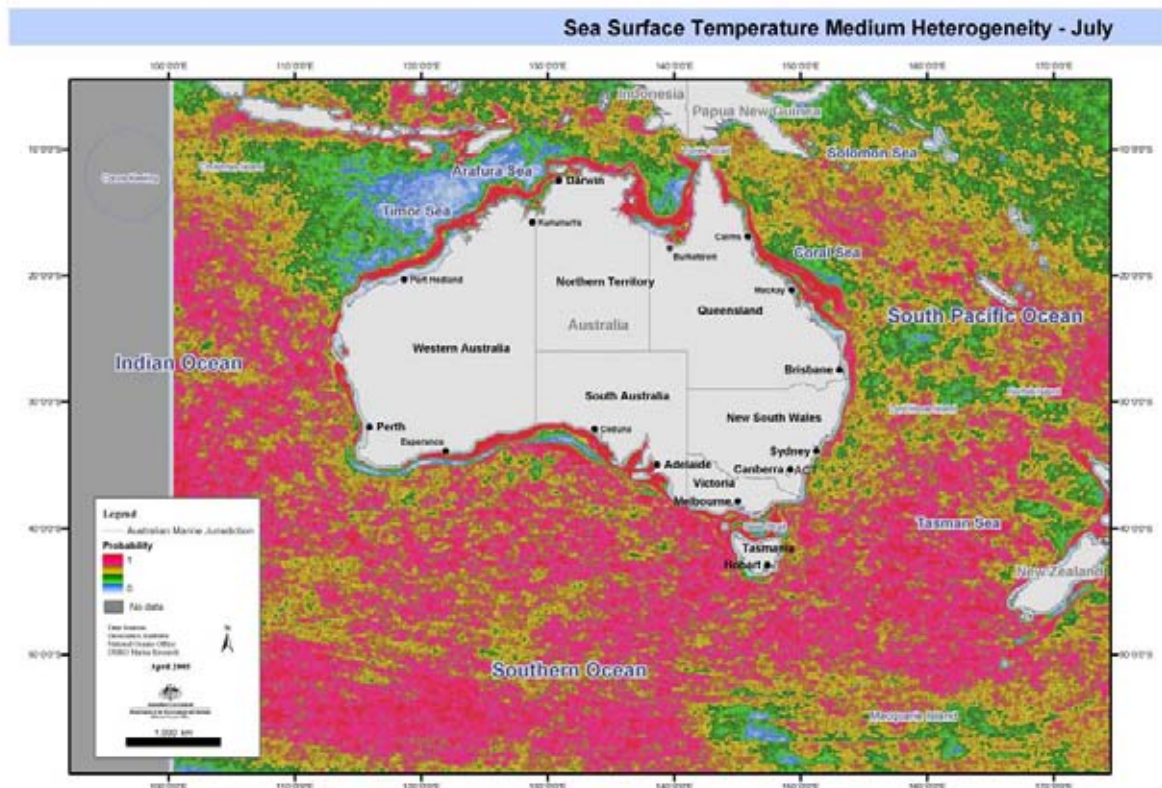
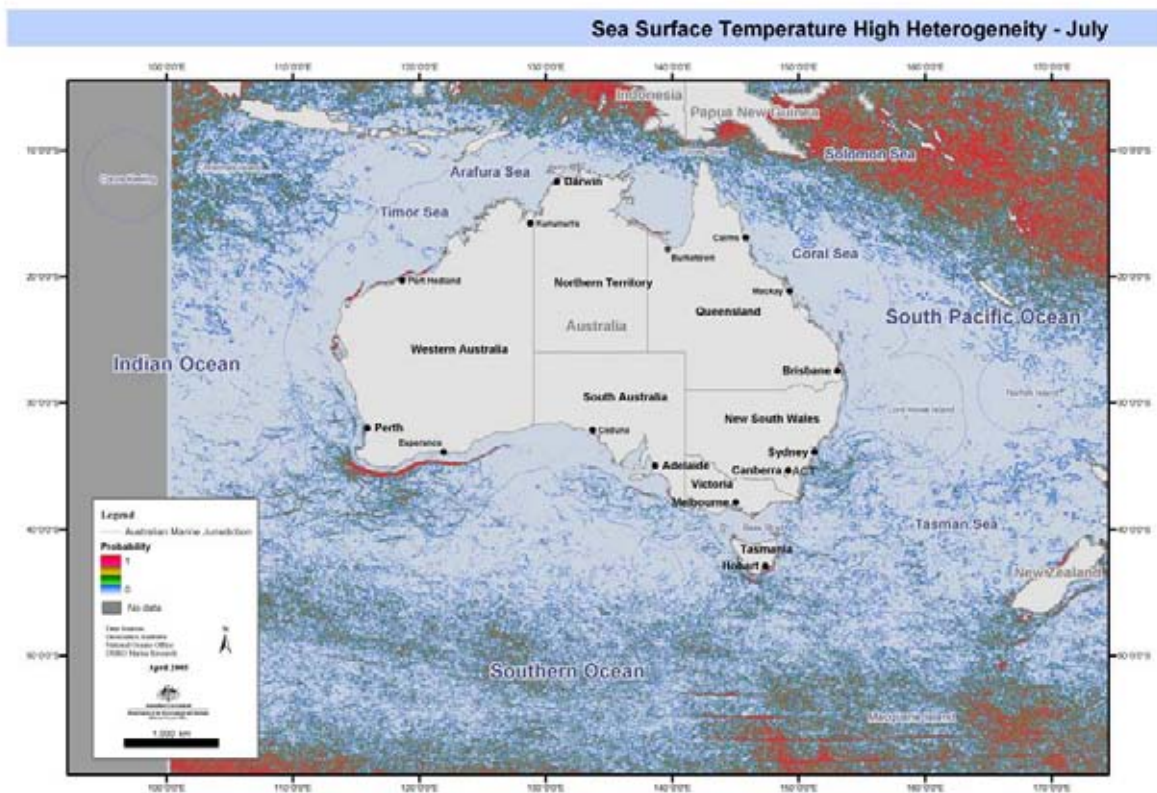


Figure 5.13 Eddies and fields based on sea-surface temperature in July. (a) low heterogeneity, (b) medium heterogeneity, (c) high heterogeneity, (d) high heterogeneity and high gradients

c



d

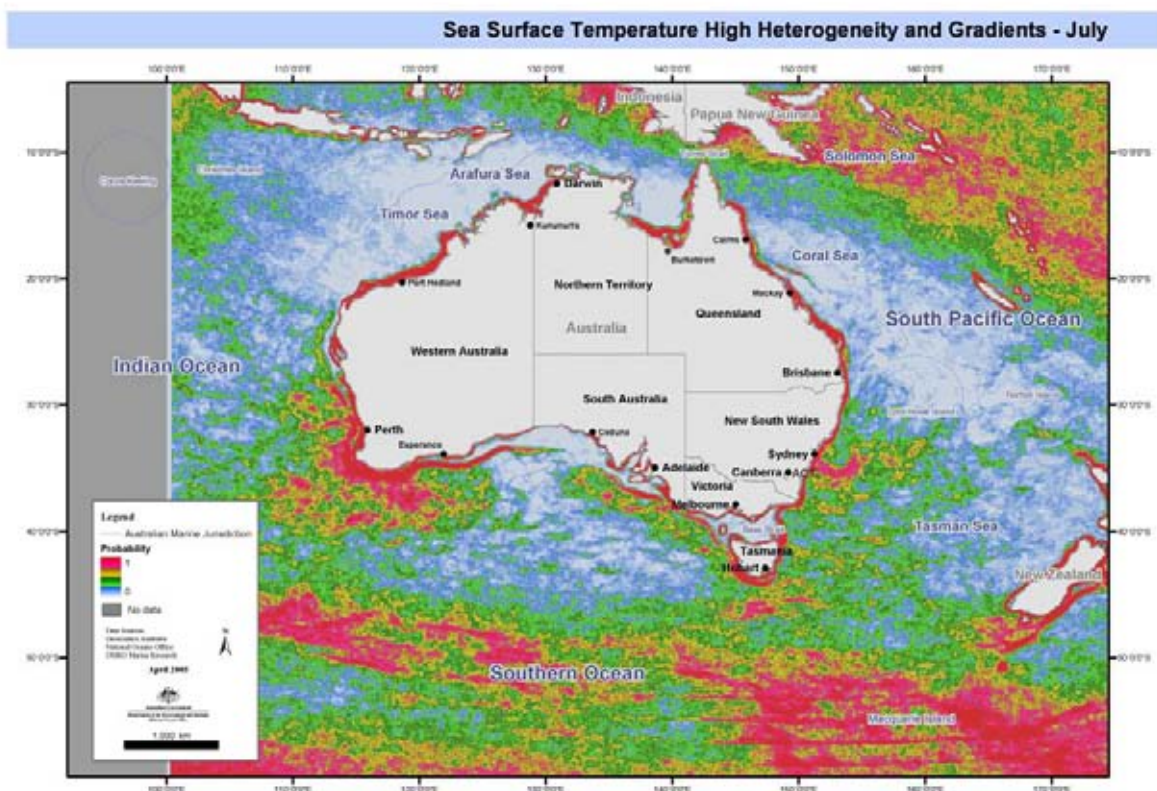
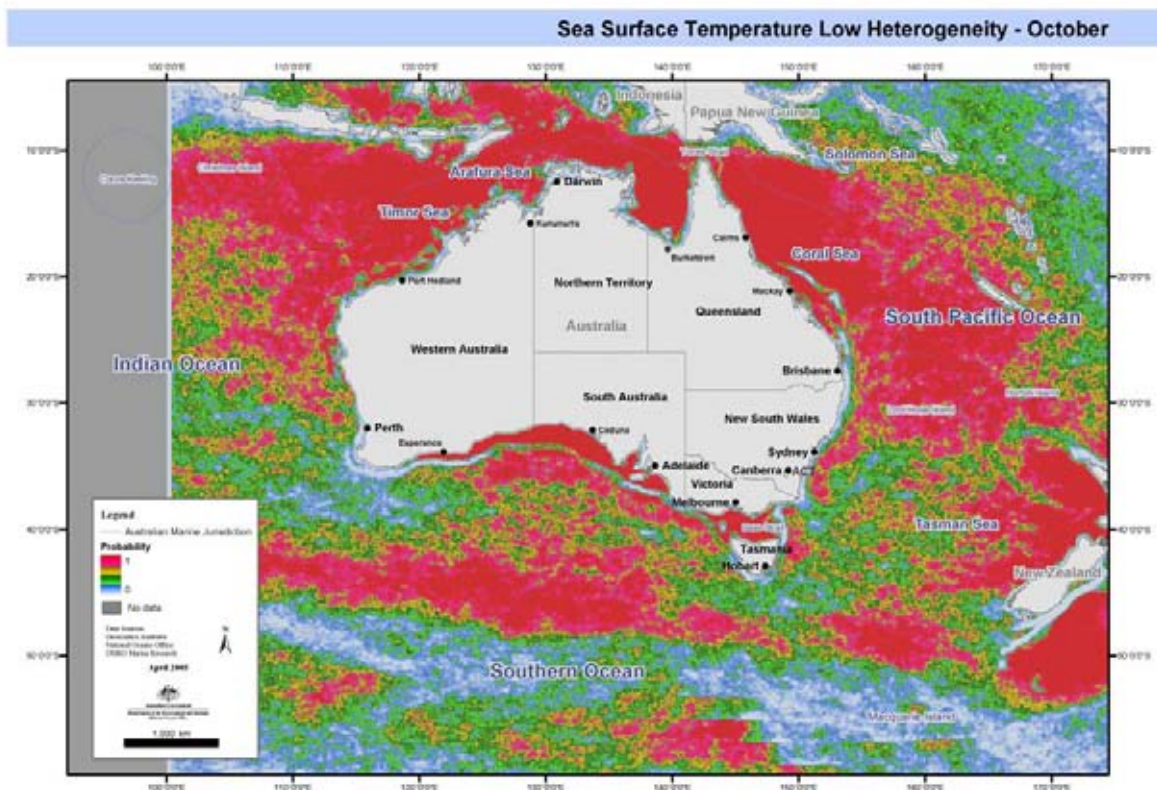


Figure 5.13 Eddies and fields based on sea-surface temperature in July. (a) low heterogeneity, (b) medium heterogeneity, (c) high heterogeneity, (d) high heterogeneity and high gradients (cont.).

a



b

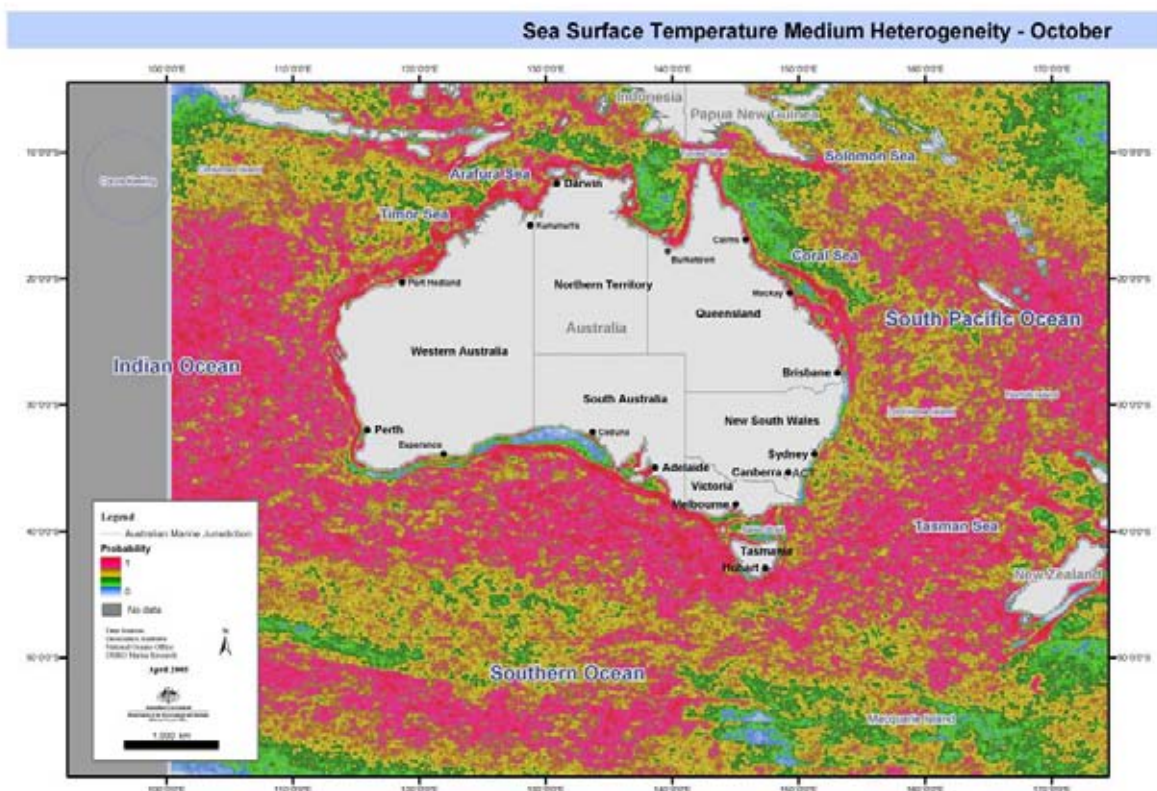
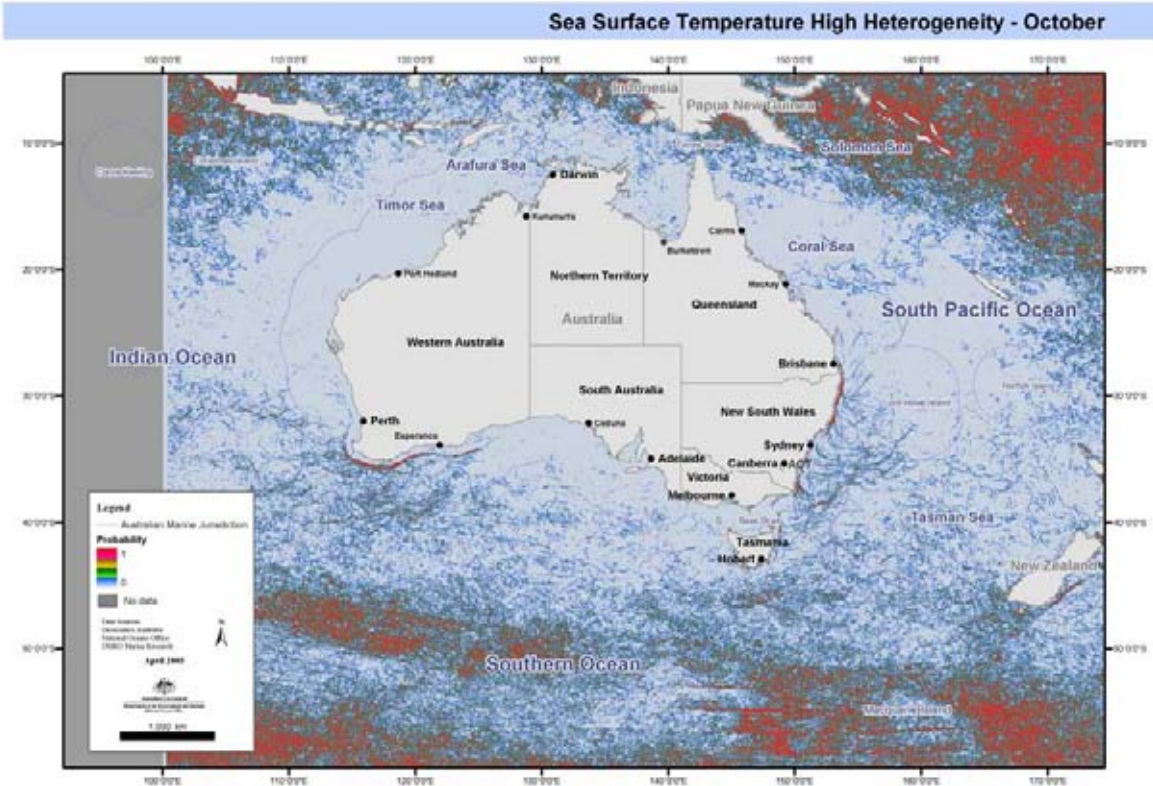


Figure 5.14 Eddies and fields based on sea- surface temperature in October. (a) low heterogeneity, (b) medium heterogeneity, (c) high heterogeneity, (d) high heterogeneity and high gradients.

c



d

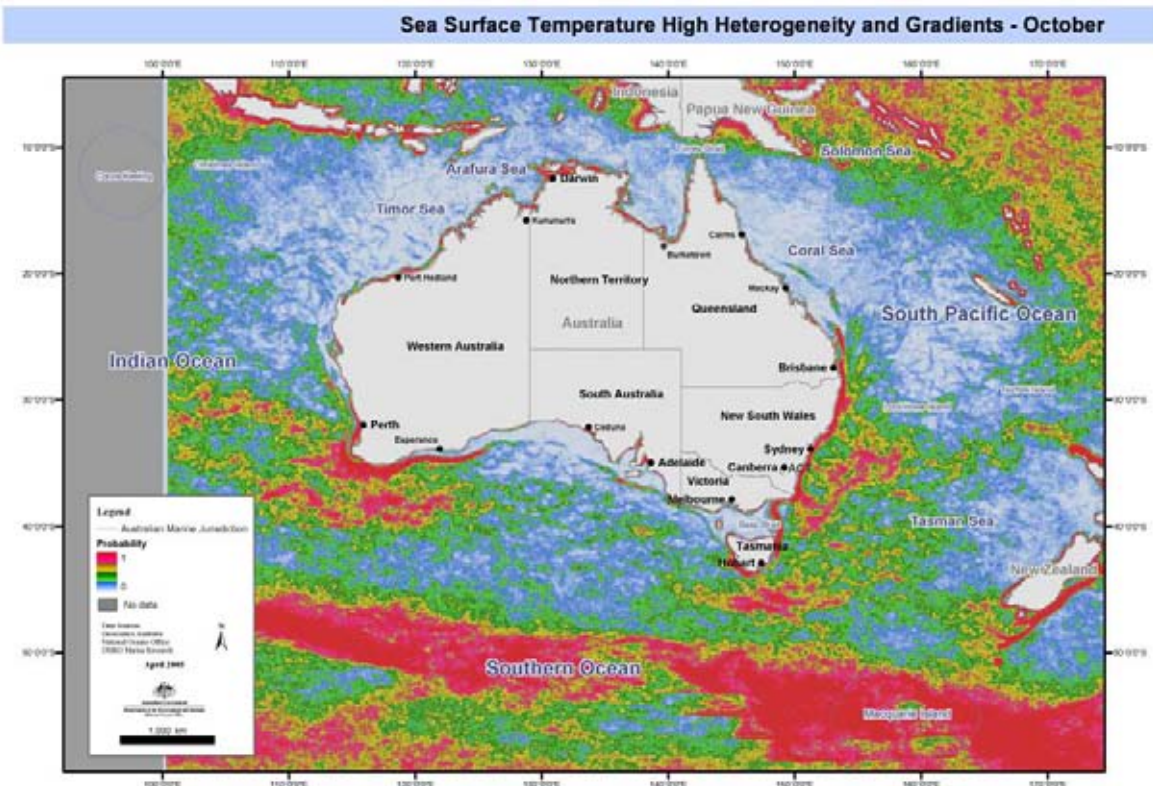


Figure 5.14 Eddies and fields based on sea-surface temperature in October. (a) low heterogeneity, (b) medium heterogeneity, (c) high heterogeneity, (d) high heterogeneity and high gradients(cont).

5.5 Sea-surface Steric Height

Steric height refers to the pressure associated with a column of water. Horizontal variations of this (due to horizontal variations in temperature and salinity) are mapped to determine what is called the steric topography and its corresponding geostrophic flow field in the ocean. The steric height, which is measured in steric metres, is defined as

$$D(p_1, p_2) = \frac{1}{g} \int_{p_1}^{p_2} \delta(T, S, p) dp$$

where, p_1 and p_2 are two reference pressure levels,

δ the specific volume anomaly,

T the temperature,

S the salinity,

P the pressure, and

g acceleration due to gravity.

Ideally, p_1 is set at a deep level in the ocean where the motion of water masses is relatively lower than that at p_2 . Steric height of sea surface referenced to 2000 m, is computed from the CARS2000 seasonal temperature and salinity fields (see Figure 5.15). This provides an integrated measure over the depth of the water column of the combined effects of temperature and salinity changes. Large signatures of surface steric-height exist in steric features such as eddies, so that while sea-surface height contains information about broad-scale patterns, it is susceptible to sampling problems from smaller-scale steric features.

Methods

Steric height of sea surface referenced to 2000 m, was computed from CARS2000. The three-dimensional seasonal temperature and salinity fields were calculated.

Logical consistency:

Points were generated by locally weighted filtering of measurements over a large domain, so there is a high degree of coherence and consistency between adjacent gridded values.

Positional accuracy:

Grid spacing is much finer than the length scales of mapping/interpolation, so there is no issue with positional accuracy.

Parameter accuracy:

CARS2000 temperature and salinity certainties are carried through the steric-height anomaly calculation into the height fields. Geostrophic currents uncertainties arise, as the currents are derived linearly from the pairwise difference of adjacent height estimates.

Limitations

The dataset was not defined for depths less than 400 m.

Completeness

Complete

Additional metadata:

CARS2000

http://www.marine.csiro.au/marq/edd_search.Browse_Citation?txtSession=5960

Description

The seasonal maps of surface steric height show that the ocean region has a topography – the spatial variations in the vertically ocean density over the region produce variations in surface height of more than 2 metres. The gradients of steric height provide a measure of the ocean current field. The maps show a broad gradient of steric height from north to south in both the east and west of Australia. This arises from the basinwide pattern produced by the large-scale circulation in the Pacific and Indian Oceans.

In the Indian Ocean the meridional gradient drives an eastward geostrophic flow onto the west coast of Australia between NW Cape and Cape Leeuwin. At the coast the height gradient is aligned along the boundary in the poleward direction. A poleward current forms, the Leeuwin Current, which flows along the continental slope directly into the prevailing equatorward winds. The maps show that the Leeuwin Current is strongest in autumn to winter, when the alongshore gradient is strongest and the winds are weakest.

In the Pacific Ocean, at the eastern Australian boundary the main feature is an intense alongshore steric height gradient. This is associated with the East Australian Current (EAC), the major western boundary current of the South Pacific. Figure 5.15 suggests that the EAC arises suddenly just to the south of the GBR. In fact, it is fed from a westward flow that enters the region between New Caledonia and Vanuatu within the 200-800-m depth range. The surface flow proceeds southwards until it separates from the coast between 32°S and 40°S as a series of eastward meanders. The north-south gradient between New Zealand and New Caledonia indicates that there is a broad region of eastward flow modulated by the complex topography in the region.

Immediately south of Australia the surface height gradients are much smaller indicating that the large-scale surface flow is far weaker than in the other regions. Further south (40-45°S) the maps show the intense zonal gradient associated with the Antarctic Circumpolar Current.

Data Provided

- Sea-surface steric height monthly means

5.6 Sea-surface Height Variability

This field reflects the spatial patterns showing regions of high and low variability in sea-surface height. High variability is likely in areas of high energetics such as eddy fields, frontal areas and boundary currents. As such, this variable is likely to be of value at Levels 3 and below.

Methods

Annual and monthly estimates of the standard deviations of sea-surface height (units in metres) were estimated on a 0.2 x 0.2 degree grid for the region 90°E - 180°E, 0°S - 60°S. Similar considerations apply as for monthly sea-surface height variability, but we can expect the annual field to be a smoother version of the monthly fields (compare Figure 5.16 and Figure 5.17). Longitude and latitude of grid points are also provided in the file. Land and shelf locations, where an estimate could not be made, are indicated in the standard deviation maps as NaNs (produced by Madeleine Cahill CSIRO Marine Research).

The data used in making the estimates are the gridded maps of height for 1993–2001 based on gauge and altimeter observations. The altimeters were Topex/Poseidon, Jason-1, ERS-1, and ERS-2.

Hindcast height maps are described in BLUELink hindcast.

Scientific limitations:

The gridded fields are created by optimal interpolation and the grid scale is smaller than the largest gaps between satellite tracks, so fine-scale (50 km) height gradients in the ocean are often missed.

Technical limitations:

For most of the time, data were available from only two satellites, and at times from only one.

The method of optimal interpolation has been verified against surface drifting buoys and is qualitatively verified with SST observations.

Description

Figures 5.16a-d are derived from the satellite altimeter. The main regions of high variability occur off the east coast, a zonal band from 40-55°S, and a more seasonally variable pattern off the western coast of Australia. These features all reflect the influence of major current systems and the eddy fields generated by them. The triangular structure in the Tasman Sea is an expression of the EAC eddies. The eddies form within the Tasman abyssal basin, a deep region located between the eastern boundary, Lord Howe Rise in the east and closed off in the north. There are also signs of reduced eddy activity further south, to the east of Tasmania showing evidence of the EAC proceeding southward around the poleward tip of Tasmania.

The southern zonal band of variability is associated with the ACC. It follows a meandering southeast trajectory which is strongly influenced by topography. The variability arises both from eddies as well as the latitudinal variations of the ACC frontal region.

Off western Australian there is a more spatially varying, seasonal pattern of variability. The Leeuwin Current system is rather vigorous and regularly generated mesoscale eddies.

Data Provided

- Sea-surface height monthly variance
- Sea-surface height annual variance

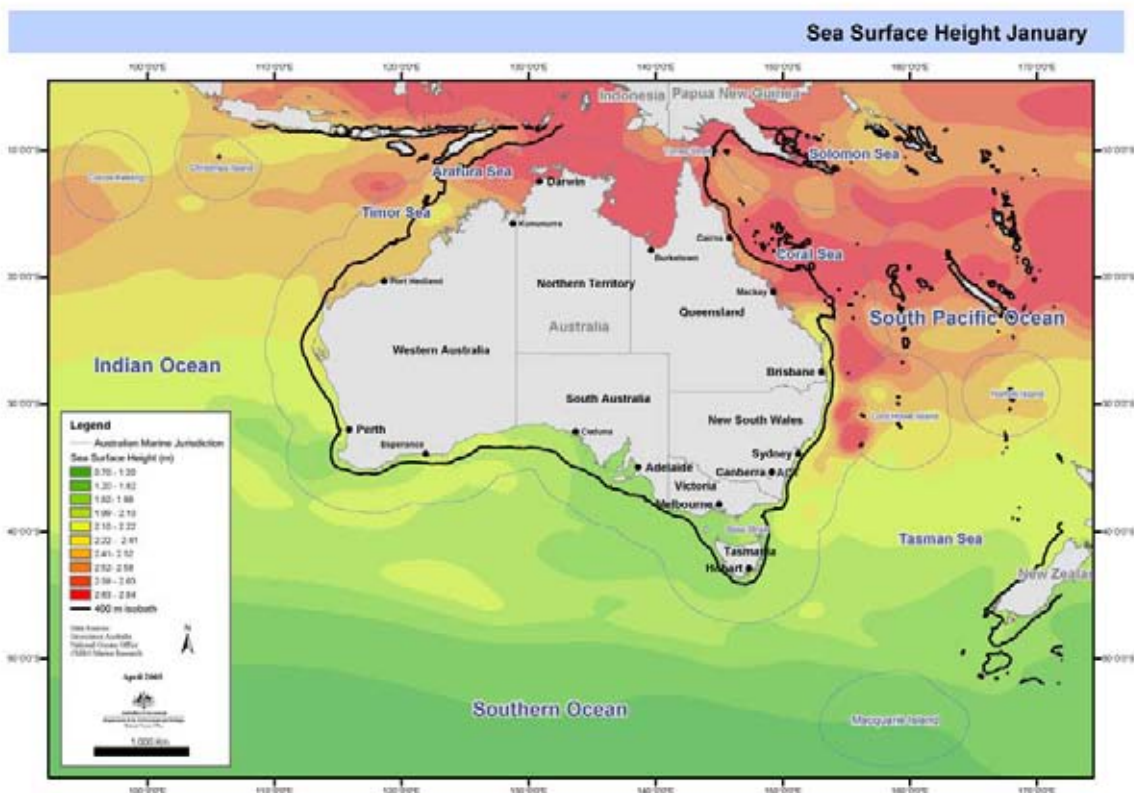
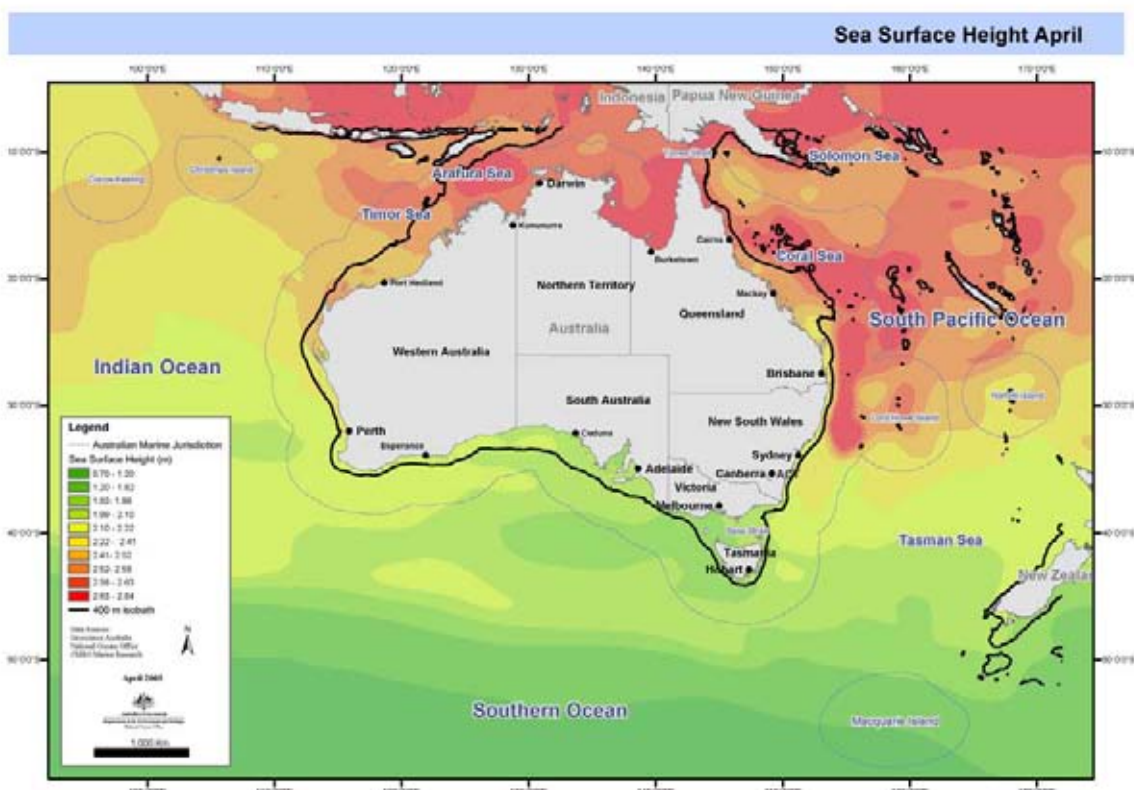
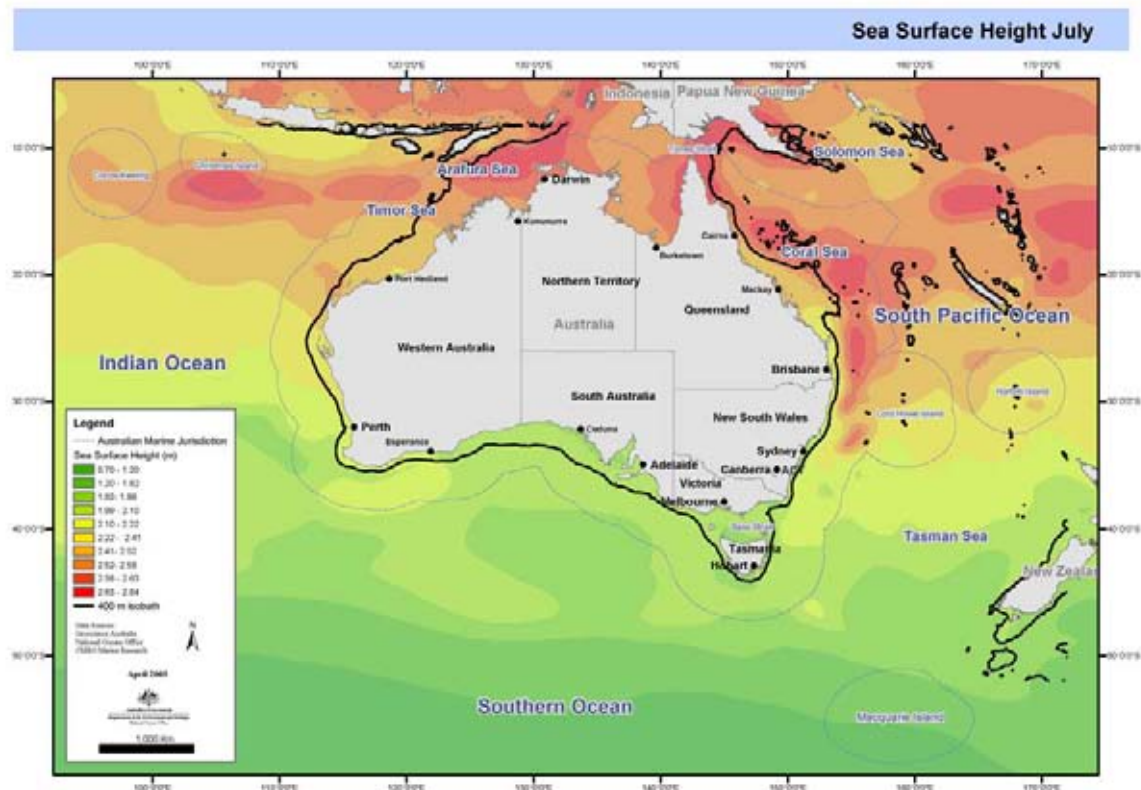
a**b**

Figure 5.15 Sea-surface steric height for (a) January, (b) April, (c) July and (d) October. Data not defined at depths shallower than 400 m. The 400 m contour is shown.

c



d

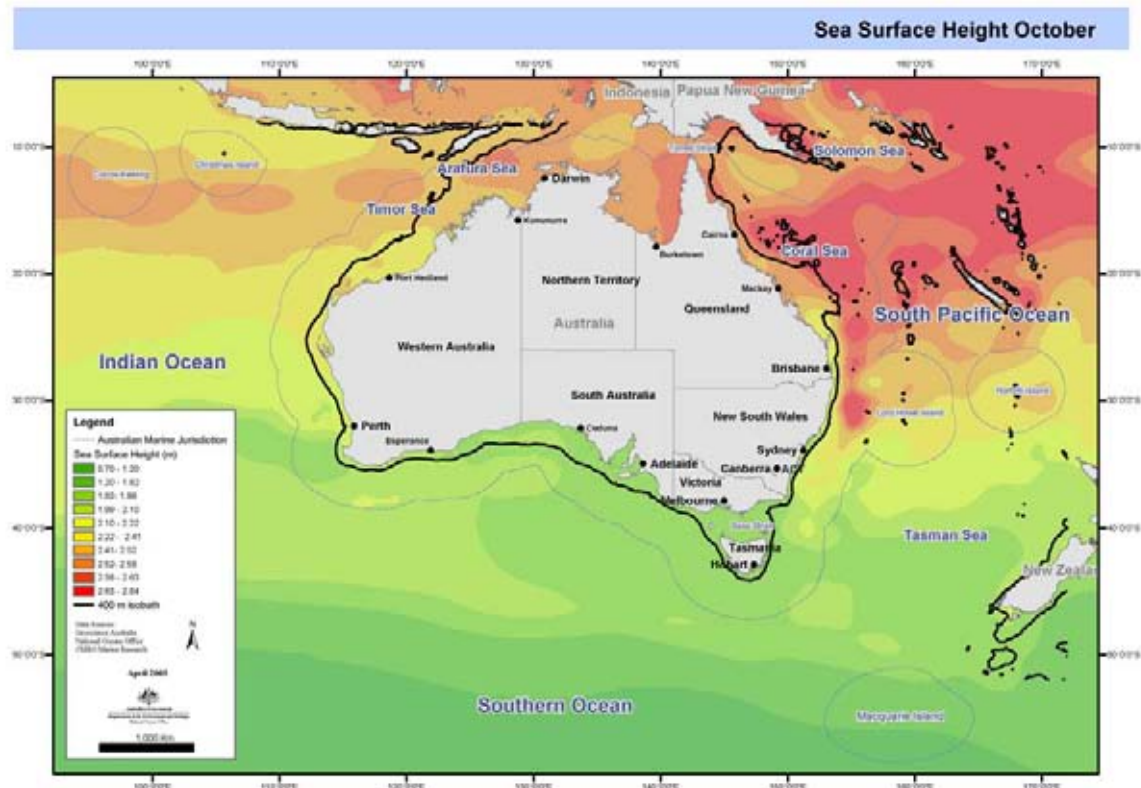
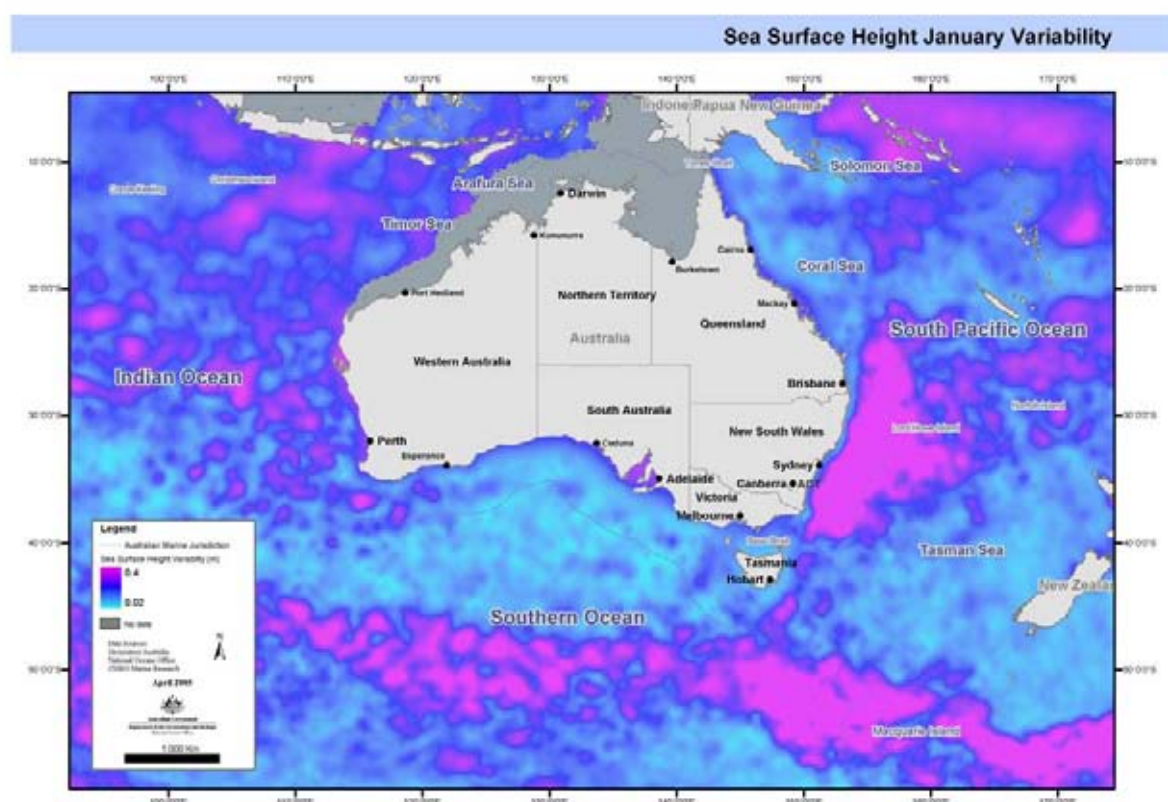


Figure 5.15 Sea-surface steric height for (a) January, (b) April, (c) July and (d) October. Data not defined at depths shallower than 400 m. The 400 m contour is shown (cont).

a



b

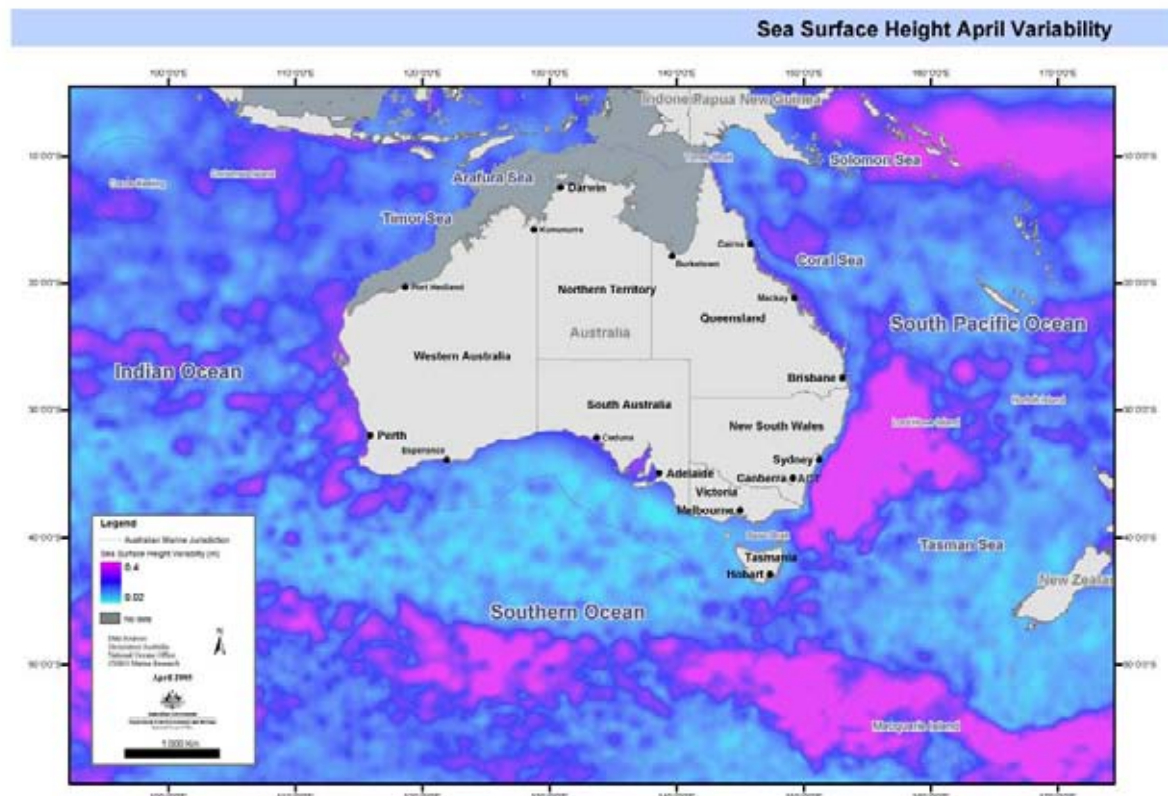
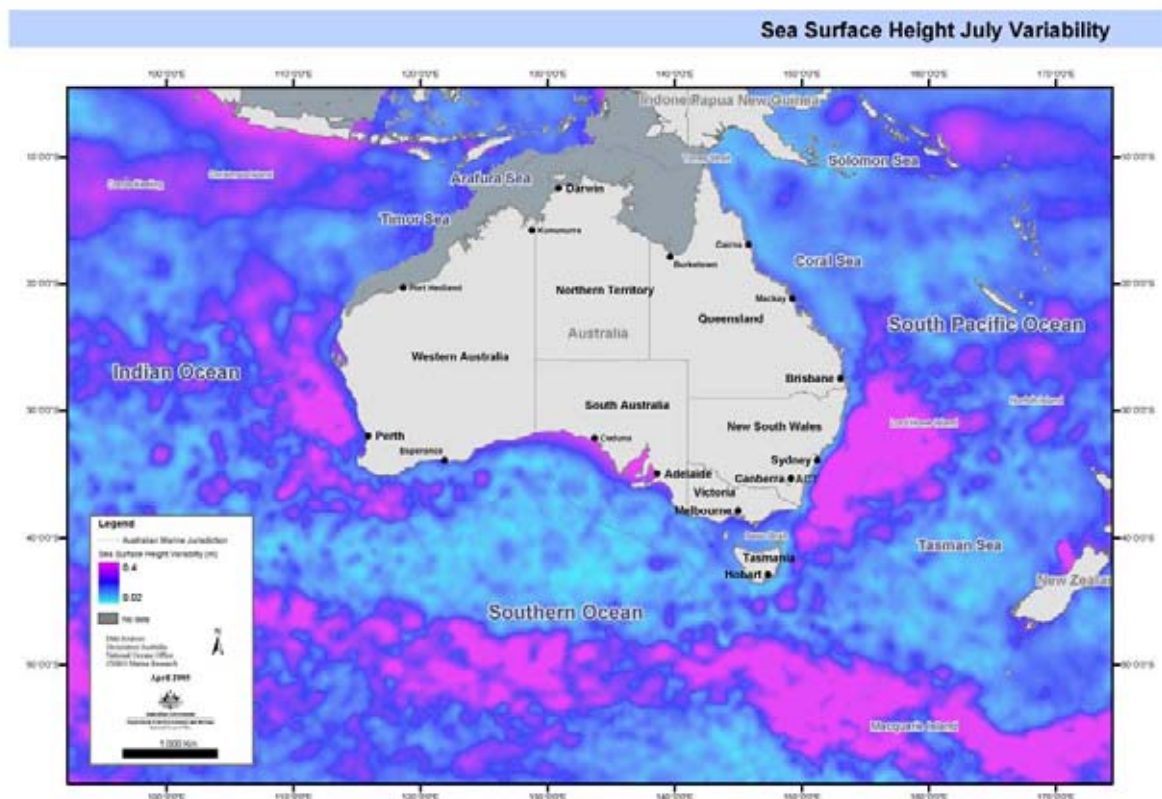


Figure 5.16 Sea-surface height monthly variability for (a) January, (b) April, (c) July and (d) October. Calculated from altimeter data (Topex/Poseidon, Jason-1, ERS-1, and ERS-2).

c



d

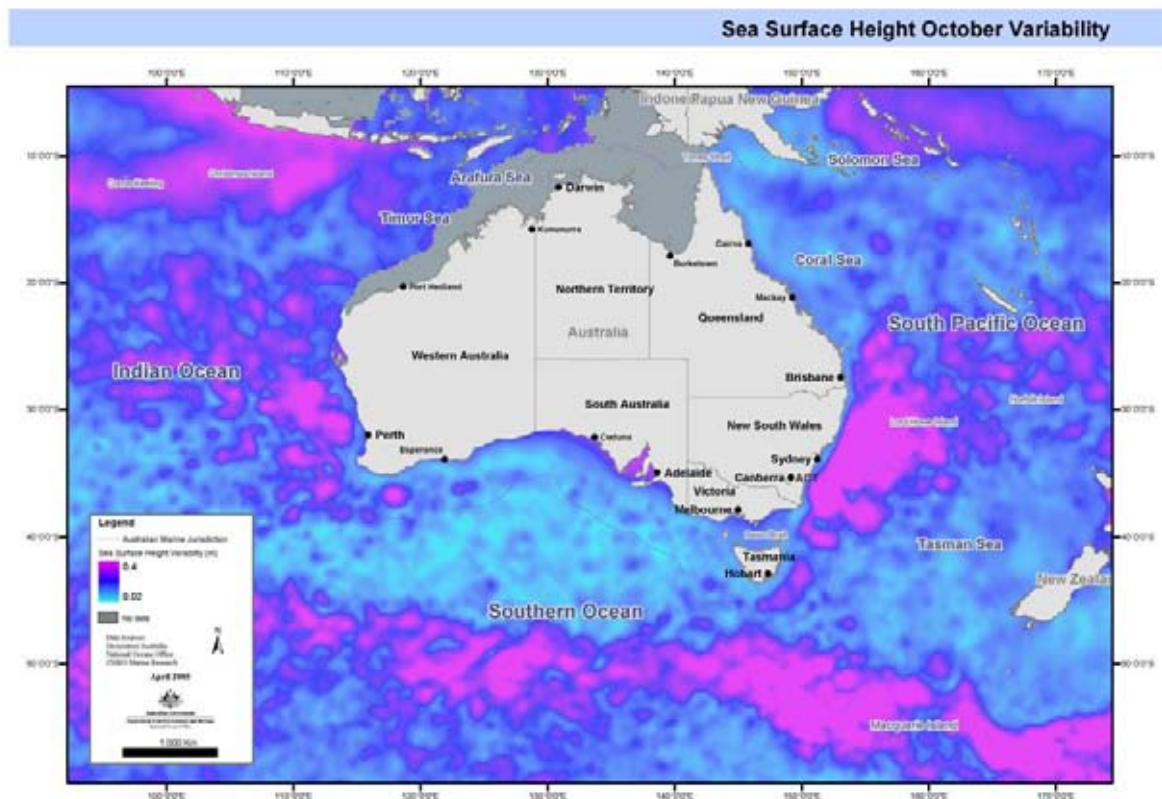


Figure 5.16 Sea-surface height monthly variability for (a) January, (b) April, (c) July and (d) October. Calculated from altimeter data (Topex/Poseidon, Jason-1, ERS-1, and ERS-2). (cont.)

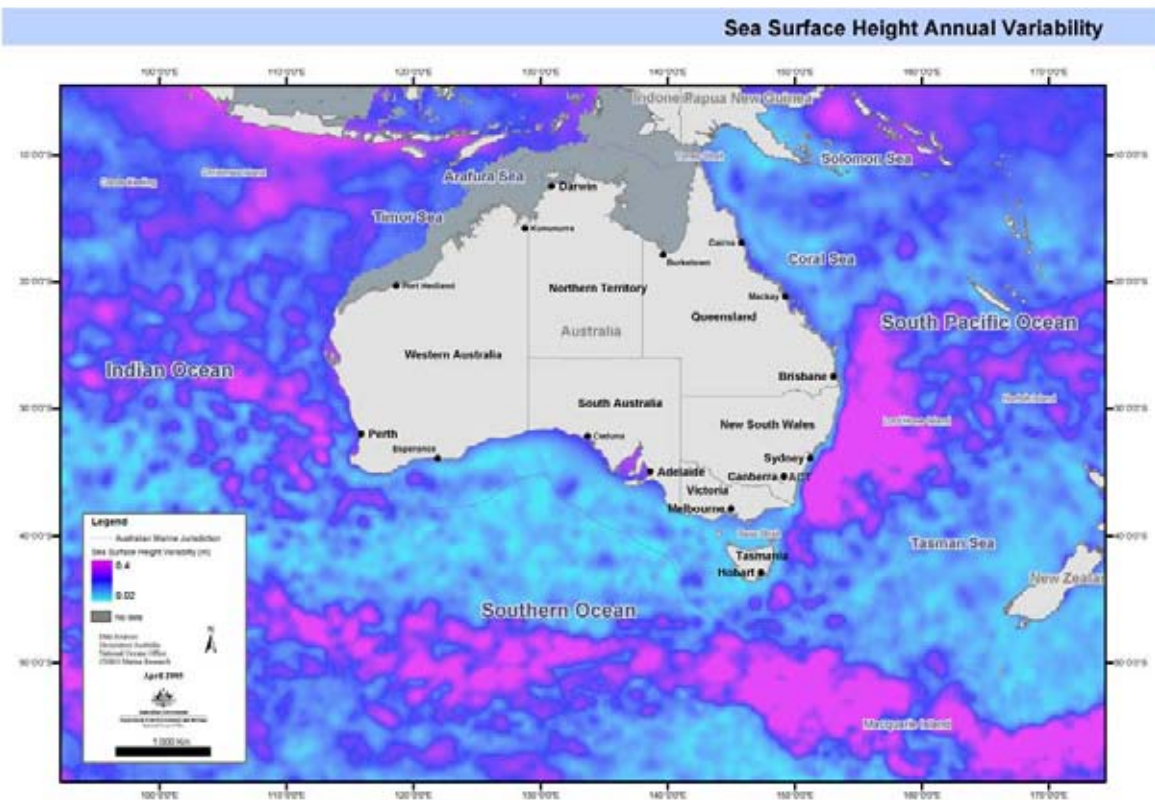


Figure 5.17 Sea-surface height annual variability. Calculated from altimeter data (Topex/Poseidon, Jason-1, ERS-1, and ERS-2).

5.7 Geostrophic Currents

Two fields were computed: surface currents and subsurface currents:

Methods

The currents are computed directly from steric-height fields, with Lagerloef equatorial (Lagerloef et al 1999) treatment. Monthly values are derived from annual and semi-annual temperature and salinity cycles. The cell size is 0.1°.

Logical consistency

The points are generated by locally weighted filtering of measurements over a large domain, so there is a high degree of coherence and consistency between adjacent gridded values.

Positional accuracy

The grid spacing is much finer than the length scales of mapping/interpolation, so there is no issue with positional accuracy.

Parameter accuracy

CARS2000 temperature and salinity uncertainties are carried through the steric height anomaly calculation into the height fields. Geostrophic current uncertainties arise as the currents are derived linearly from the pairwise differences in adjacent height estimates.

Limitations

The dataset is not defined for regions less than 400 m depth.

Completeness:

The dataset is complete.

Additional metadata:

CARS2000

http://www.marine.csiro.au/marq/edd_search.Browse_Citation?txtSession=5960

Description

- *Surface Currents*

This field is computed from sea-surface steric height, so in essence the patterns should reflect those of sea-surface height, but highlighting features such as fronts, boundary currents and eddy fields (Figure 5.18). We expect these data to be of value at Level 3 or lower scale.

Regional current systems have a major impact on seas in the Australian marine jurisdiction (Condie and Harris 2005). The Leeuwin Current flows southward down the west coast of Australia. Although weak in the summer, it intensifies in the autumn to flow around the southward corner of the Australian continent and continues eastward across the Great Australian Bight (Ridgway and Condie 2004).

The East Australian Current (EAC) is the main western boundary current in the south-east Pacific. The current is fed from the east by the South Equatorial Current (Ridgway & Dunn 2003), which splits into northward and southward components; the southward flow forms the east Australian Current. This current flows south, forming a series of anticyclonic eddies that extend as far south as Tasmania during the summer. The EAC separates from the upper slope at around 33°S to form the southern boundary of the South Pacific subtropical gyre (Condie and Harris 2005). Appendix D lists the principal oceanographic currents in the Australian Marine Jurisdiction.

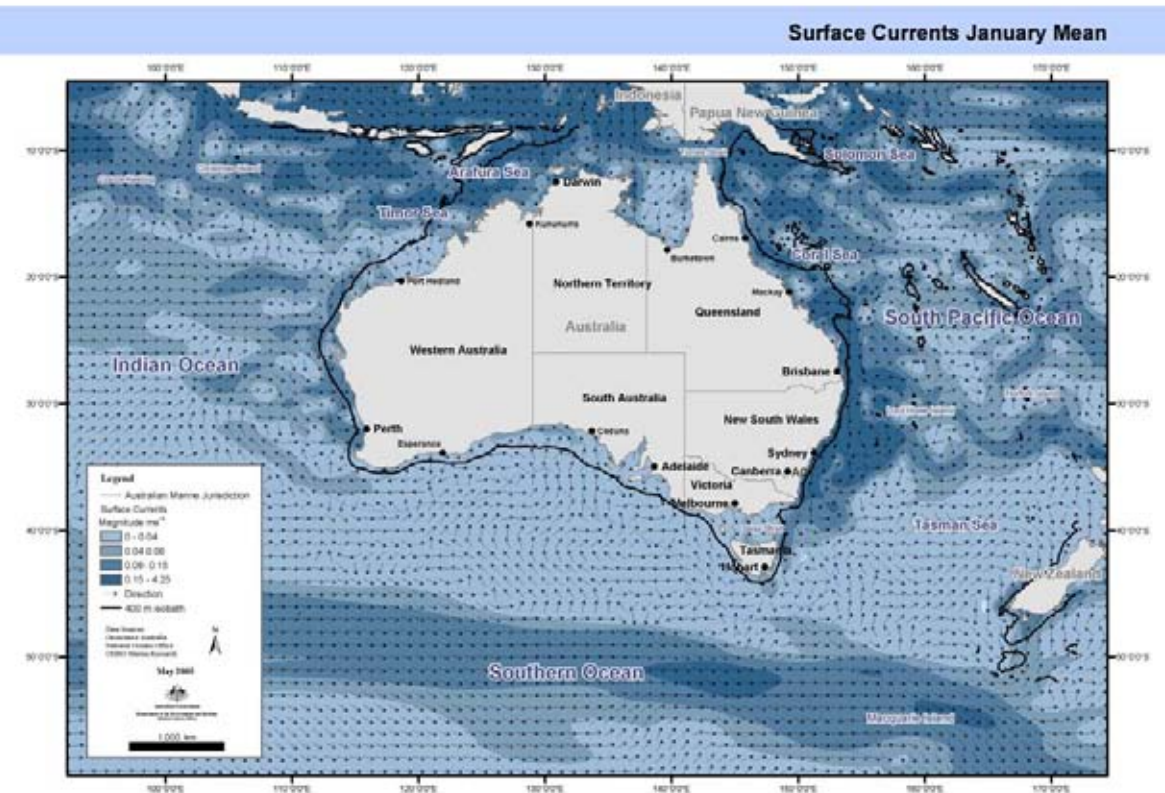
- *Subsurface Currents*

This field is computed from steric-height fields and highlights subsurface fronts, currents and eddies. These data will be of value at level 3 or lower.

Data Provided

- Geostrophic subsurface currents monthly means
- Geostrophic surface currents monthly means

a



b

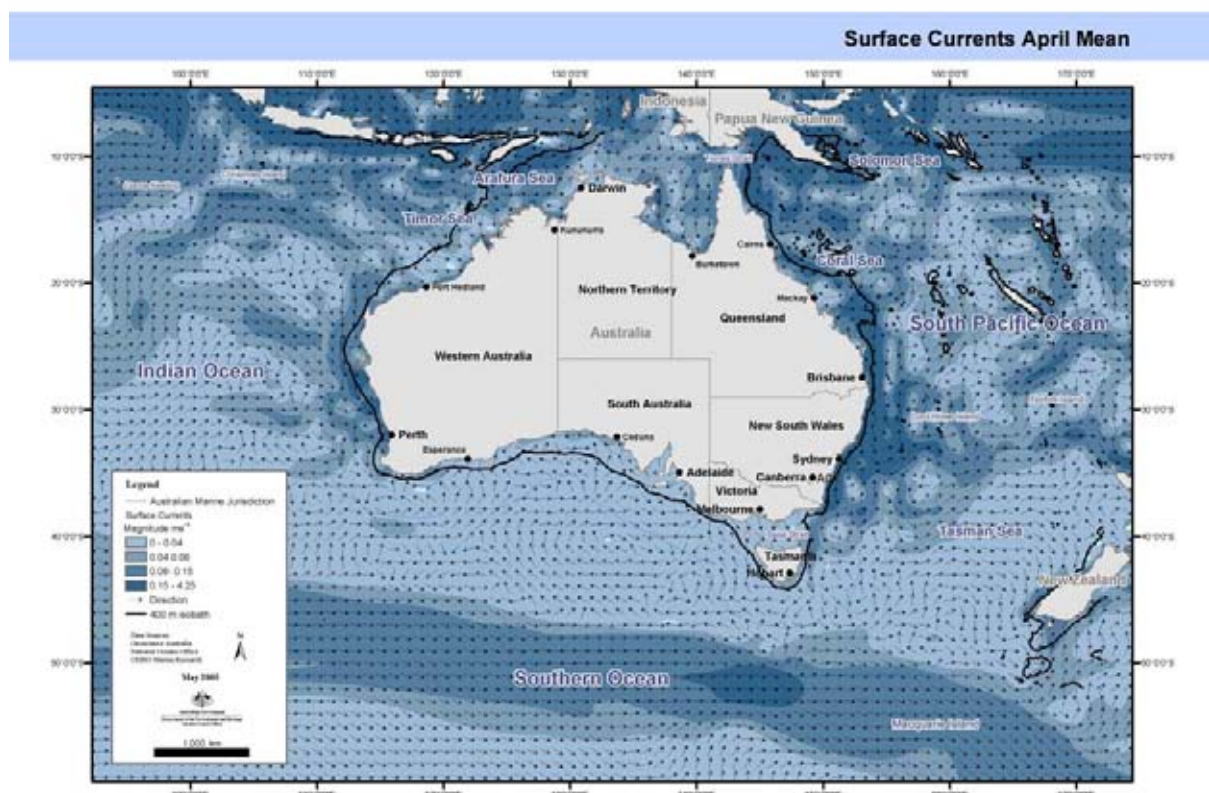
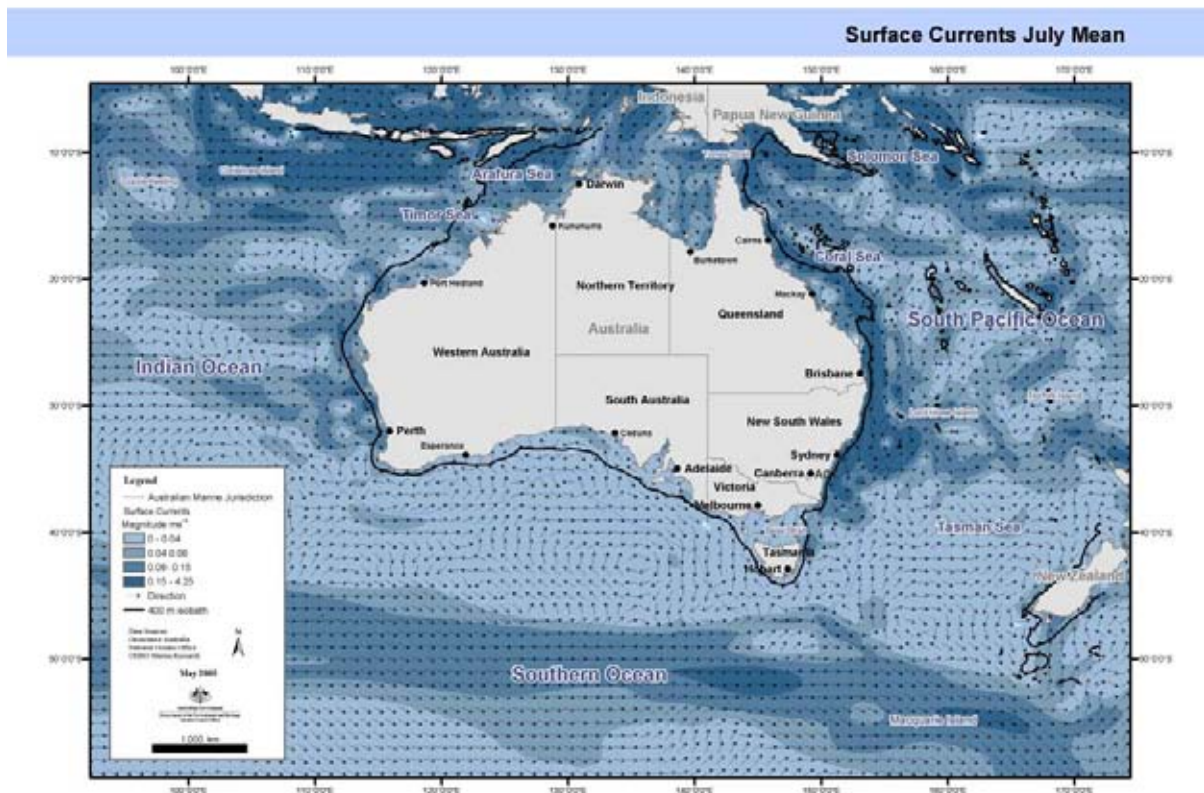


Figure 5.18 Geostrophic surface currents for (a) January, (b) April, (c) July and (d) October.

c



d

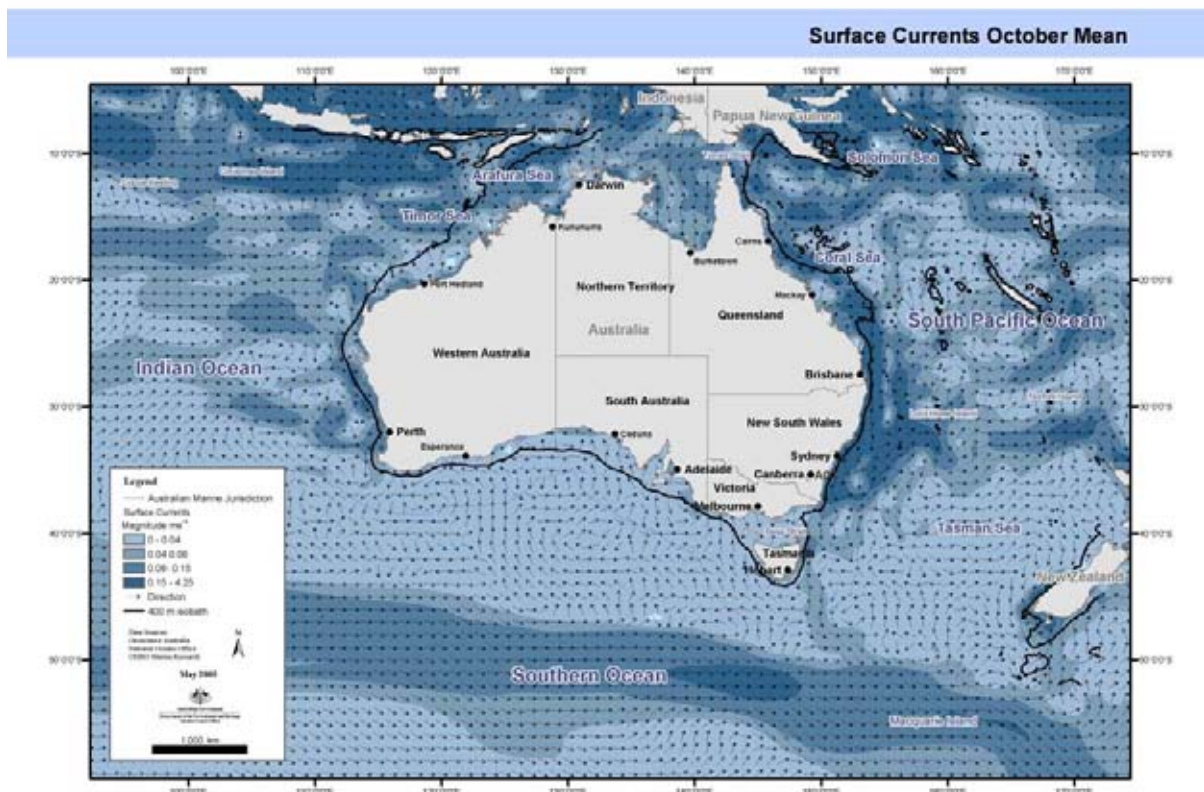


Figure 5.18 Geostrophic surface currents for (a) January, (b) April, (c) July and (d) October (cont.).

5.8 Mixed-layer Depth

Wind-stress, wave-breaking, and cooling on the surface of the ocean result in a well-mixed surface layer with relatively uniform temperature and salinity. The temperature, salinity and depth of the mixed layer vary from day to day and from season to season in response to:

- heat and freshwater flux through the surface
- mechanical stirring by winds and breaking waves that tend to destratify and mix the surface-layer waters with denser waters below.

The depth of the mixed layer has a critical influence on primary productivity, by governing both light availability and the supply of nutrients from deeper water (Gran and Braarud 1935, Riley 1942, Sverdrup 1953). The depth was estimated with a difference criterion, which Brainerd and Gregg (1995) found to be more stable than gradient criteria. The mixed-layer depth was defined as the minimum depth at which either of the following criteria was satisfied:

$$T < T(10 \text{ m}) - 0.04^\circ\text{C} \quad (1)$$

$$S > S(10 \text{ m}) - 0.03 \text{ PSU} \quad (2)$$

Equations (1) and (2) were used by Condie and Dunn (2004) after examining a large number of mixed layer depth estimates based on a range of criteria.

The value of mixed-layer depth as a regionalisation variable is difficult to assess. It contains large-scale climatic influences through the dependence on wind, solar forcing and evaporative exchange, while at the same time it is influenced by local water properties such as density stratification (Figure 5.19). Given its temporal dependence on water properties and climatic forcing, sampling issues are likely to arise. Our assessment is that these data, with appropriate processing, are of use at broad scales (Level 1/2), but sampling problems are likely to arise at smaller scales.

Methods

Mixed layer depth was calculated from the oceanographic temperature and salinity cast data used to generate CARS2000. It was defined to be the minimum (shallower) depth of depths z_t and z_s , where z_t and z_s are the shallowest depths such that

$$\text{abs}(T(z_t) - T(10 \text{ m})) \geq 0.4^\circ\text{C} \text{ and}$$

$$\text{abs}(S(z_s) - S(10 \text{ m})) \geq 0.03 \text{ PSU}.$$

These values were then mapped onto a regular 0.5 degree grid using a Loess filter, as used in CARS2000, simultaneously fitting quadratic spatial functions and annual harmonics. These fields were then linearly interpolated to the required 1/10th degree spatial resolution. The provided “annual amplitude” is simply the magnitude of the fitted annual sinusoid.

Logical consistency:

The points were generated by locally weighted filtering of measurements over a large domain, so there is a high degree of coherence and consistency between adjacent gridded values.

Positional accuracy:

The grid spacing is much finer than the length scales of mapping/interpolation, so there is no issue with positional accuracy.

Parameter accuracy:

Mixed-layer depth is an ill-defined and inaccurately measured quantity which has high variability over a broad range of temporal and spatial scales. It has been broadly estimated from temperature and salinity data that are too sparse in space and time to allow accurate mapping of its spatial and temporal patterns. The cast data are also often too sparse in the vertical dimension for even individual measurement to be accurate. It is not possible to quantify the accuracy of the mapped fields; they should be used as a broad guide only. Fine-scale structure within the fields should be regarded with suspicion.

Completeness:

Complete

Additional metadata:

CARS2000 http://www.marine.csiro.au/marq/edd_search.Browse_Citation?txtSession=5960

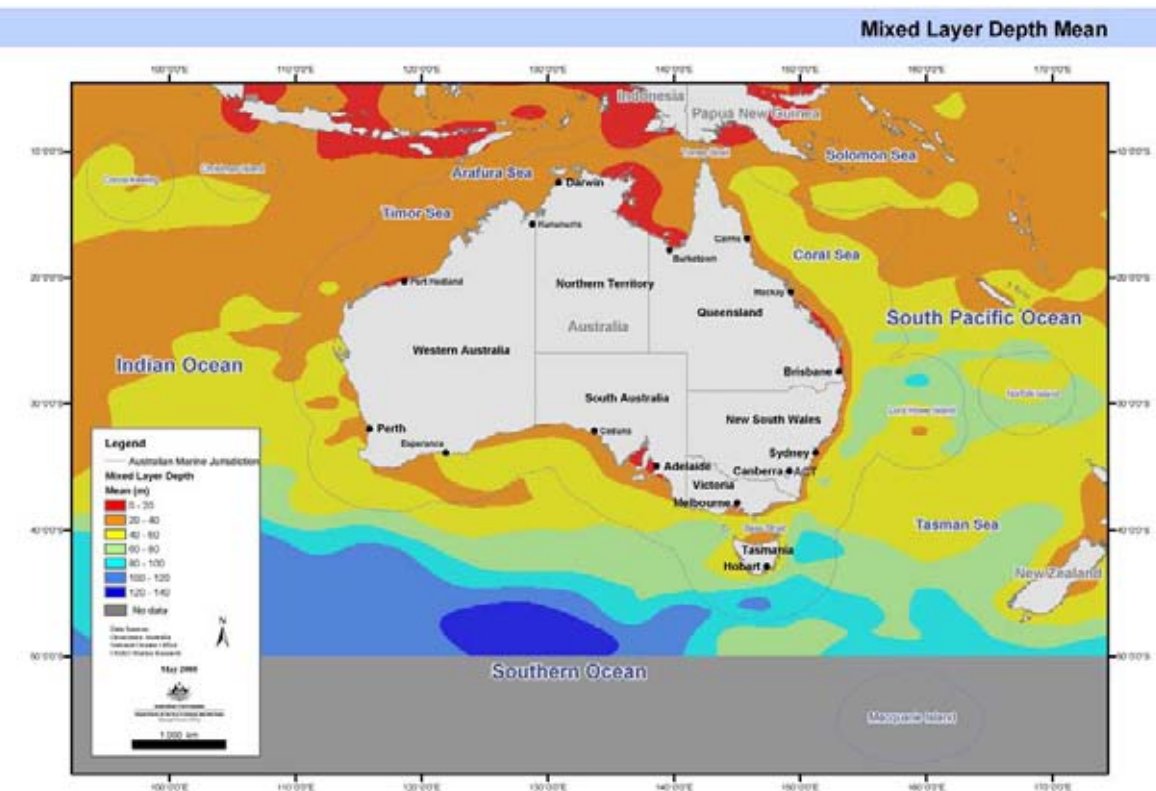
Description

The pattern seen in Figure 5.19a is for mixed-layer depth to increase from tropical to subantarctic waters. They are shallow (< 50 m) throughout the Indonesian Archipelago, increasing gradually through subtropical waters and then steeply across the Subtropical Front. During summer, mixed-layer depths were between 10 and 50 m throughout most of the subtropics, increasing to around 80 m at mid-latitudes. These mix down during autumn and winter under the influence of enhanced winds and surface-heat loss. Mixed-layer depths larger than 200 m occur over much of the Southern Ocean throughout winter and spring. Relatively deep mixed-layers (100 to 150 m) are also evident in the interior of the wintertime subtropical gyre off eastern Australia, contracting to around 70 m over spring (Figure 5.19a). Residuals in the tropics are generally comparable to the seasonal fields, but small in amplitude. However, larger amplitudes (Figure 5.19b) in the western equatorial Pacific again reflect significant interannual variability. Amplitudes are also large along the path of the East Australian Current due to unresolved eddy variability, and in regions south of the Subtropical Front where data densities are extremely low.

Data Provided

- Mixed-layer depth annual mean
- Mixed-layer depth annual amplitude

a



b

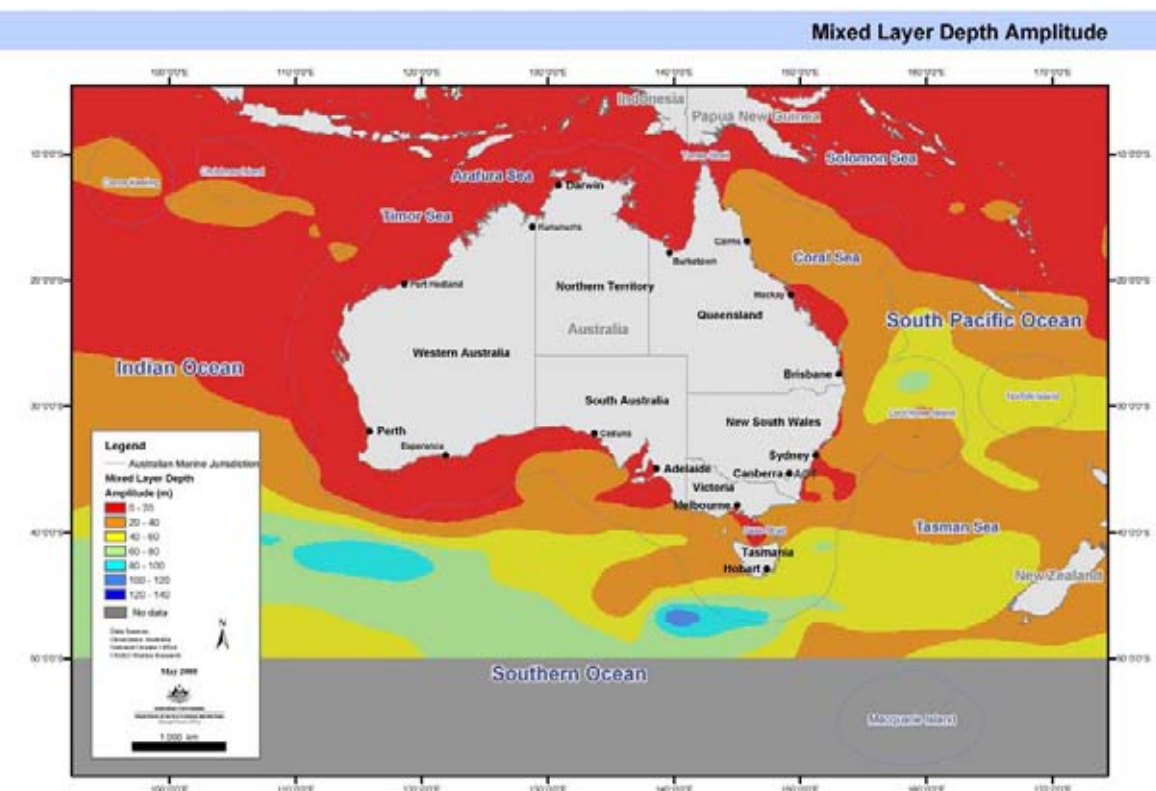


Figure 5.19 Mixed Layer (a) mean depth and (b) annual amplitude

5.9 Wind Stress

Wind-induced currents are among the strongest currents in the oceanic surface layer. Winds drive ocean currents by transferring momentum to this layer. The important quantity in this process is the wind stress, which is a quadratic function of wind speed. Wind stress—the shear stress of the wind on the sea surface—can be calculated from

$$T = \rho C_D U_{10}^2$$

where $\rho = 1.3 \text{ kg/m}^3$ (the density of air),

U_{10} is wind speed at 10 metres, and

C_D is the drag coefficient.

Methods

The data used in this project were produced by the NCEP/NCAR reanalysis project (Kalnay et al 1996). While the pattern is climatic in nature and hence of value at the broad scale (Level 1/2), wind stress is highly seasonal and also highly variable on timescales of days, weeks or even hours (Figure 5.20). Over the long timescales of the NCEP/NCAR reanalysis, we can expect patterns to be less prone to temporal and spatial sampling problems: hence our assessment is that these data are of use at the broad scale (Level 1/2).

NCEP and NCAR are cooperating in a project (denoted “Reanalysis”) to produce a 40-year record of global analyses of atmospheric fields in support of the needs of the research and climate monitoring communities. This effort involves the recovery of land surface, ship, rawinsonde, pibal, aircraft, satellite and other data, and then quality controlling and assimilating these data with a data assimilation system, which is kept unchanged over the reanalysis period 1957 through 1996. This eliminates perceiving climate jumps that are actually associated with changes in the data-assimilation system.

Wind-stress dataset covers the period 1965 to 1997 and contains the fields

- zonal wind stress
- meridional wind stress

Vector magnitude and direction were calculated from these fields.

Description

The overall regional distribution of seasonal wind stress (Figure 5.20 a-d) shows highest wind stresses in the Southern Ocean during the transitional months of April and October representing autumn and spring respectively. Southern Ocean wind stresses are persistent westerlies to south-westerlies. In the tropics, south-easterlies predominate for most of the year except for a reversal in January that is most noticeable in the Indian Ocean sector. A band of enhanced south-easterly wind stresses occur in the Indian Ocean between approximately 10°S and 25°S with peak stresses in July. This band is part of a regional circulation which links up with the Southern Ocean westerlies. The southerly component of this circulation which blows off the coast of Western Australia has peak wind stresses in January when the winds in the North West Shelf area of Western Australia reverse from south-easterly to westerlies. During this period, winds along the southern half of the coast of Western Australia and the Great Australian Bight also experience higher wind stresses. In the northern part of the Tasman Sea, winds vary from easterlies in January to westerlies in October while in the southern part westerlies persist for most of the year. Enhanced stresses in the East Australian Current region occur in July (winter) when the winds are predominantly south-westerlies. The northern part of the Pacific Ocean

that includes the Solomon Sea and Coral Sea experiences north-westerly winds in January which revert to south-easterlies in July and October; peak stresses in this region occur in July.

Data provided

- Wind-stress monthly means

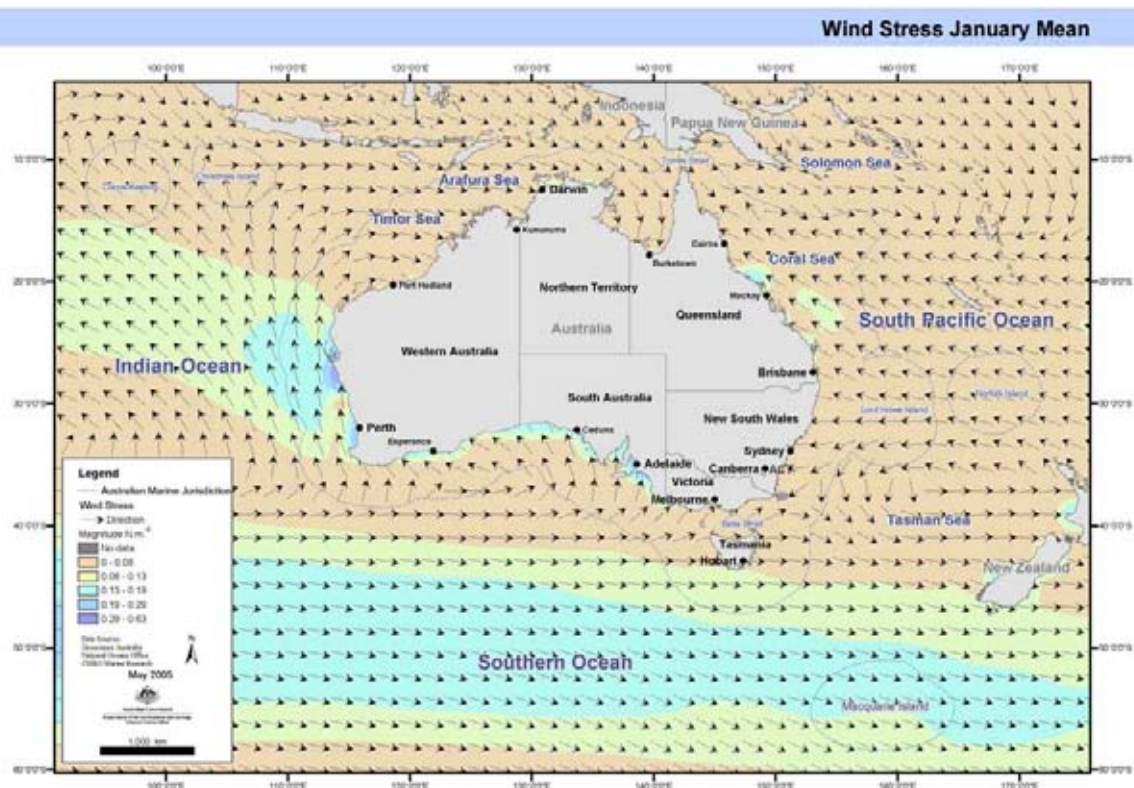
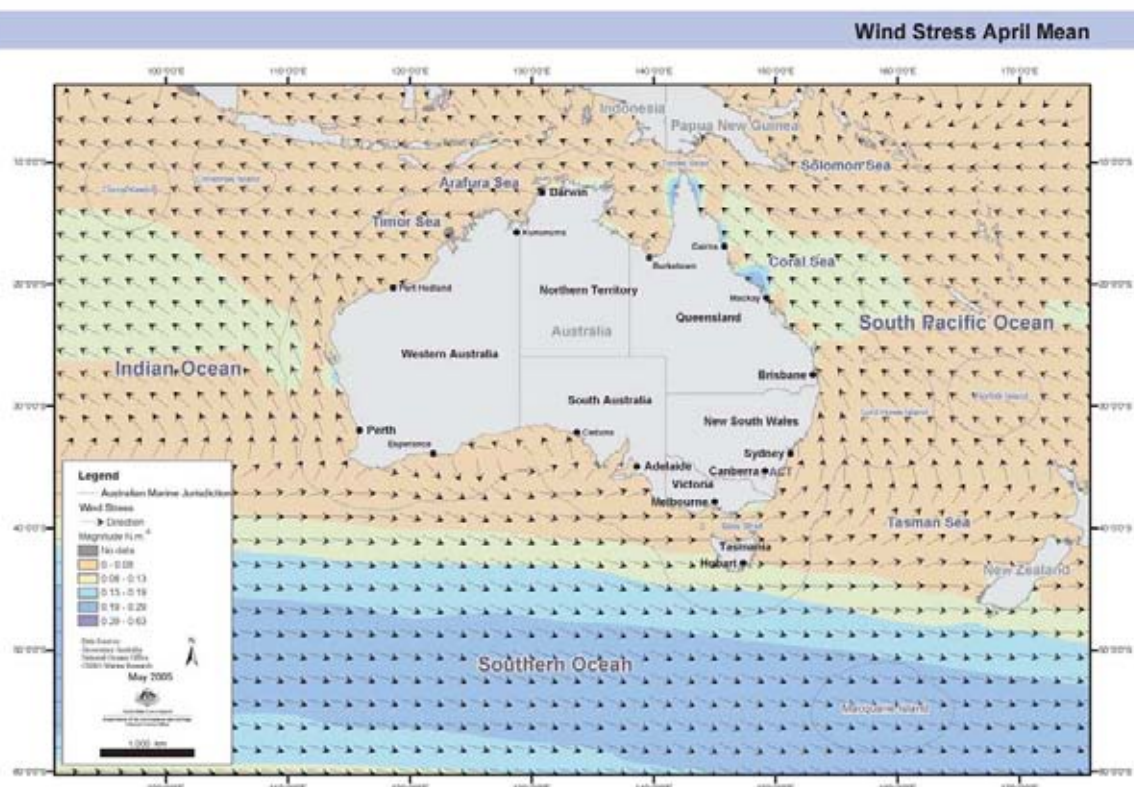
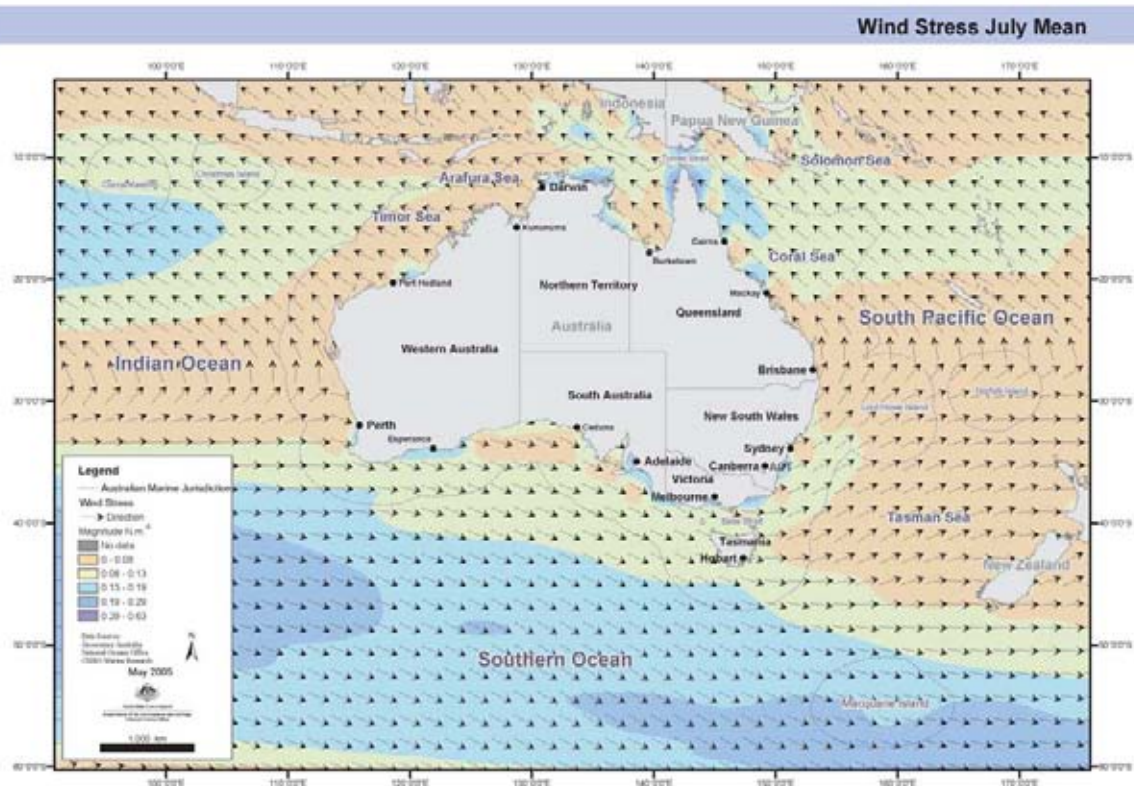
a**b**

Figure 5.20 Wind stress (a) January, (b) April, (c) July and (d) October (NCEP NCAR reanalysis project).

c



d

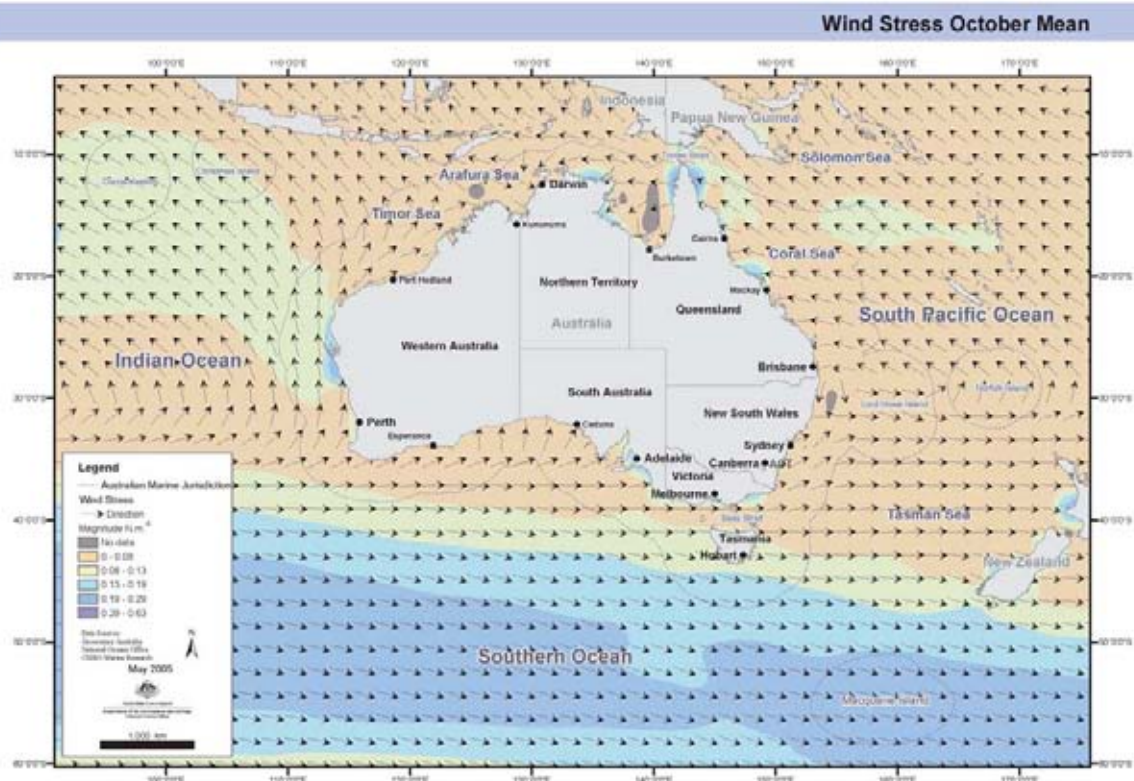


Figure 5.20 Wind stress (a) January, (b) April, (c) July and (d) October (NCEP NCAR reanalysis project) (cont.).

5.10 Wind-stress Curl

Methods

Steady winds blowing on the sea surface produce an Ekman drift layer that transports water to the left of wind stress in the southern hemisphere. Spatial variability of the wind can lead to upwelling and downwelling, which enhances mixing in the ocean. Upwelling is particularly important in some regions, as it enhances biological productivity. The magnitude of the Ekman layer transport M_e is given by

$$|M_e| = \left| \frac{\tau}{f} \right|$$

where M_e is the wind-generated mass transport per unit width integrated over the depth of the Ekman layer with dimensions of $\text{kg.m}^{-1}\text{s}^{-1}$;
 τ is the wind stress; and
 f is the Coriolis parameter given by

$$f = \frac{4\pi \sin \Omega}{T_d}$$

where Ω is the latitude, and
 T_d is the rotation of the earth in seconds.

Most of the ocean is characterised by convergent Ekman transport or by downwelling with some regions of upwelling. The relationship between Ekman pumping and the wind-stress curl provides information about upwelling and downwelling.

$$\text{Curl} \left(\frac{\tau}{f} \right) = \frac{\partial \frac{\tau_y}{f}}{\partial x} - \frac{\partial \frac{\tau_x}{f}}{\partial y}$$

Given the broad scale nature of the field, it is likely to be relevant at bioregionalisation levels 1 and 2.

Description

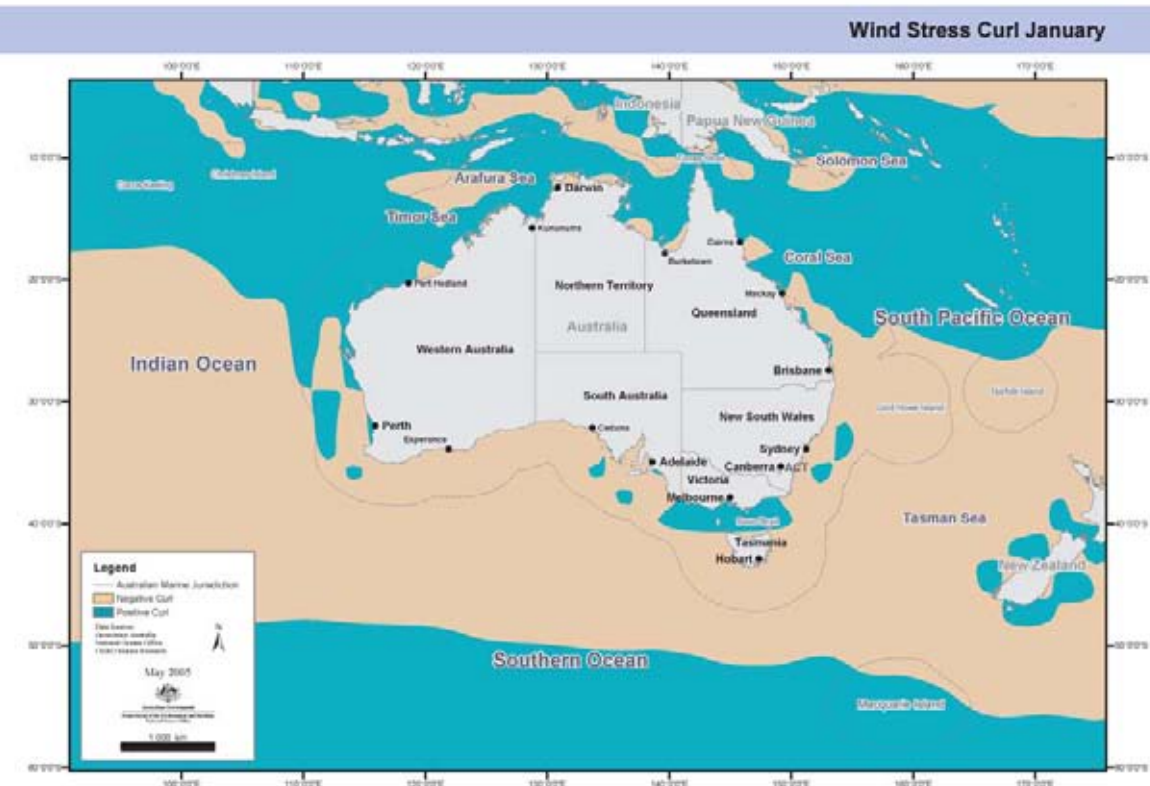
Figure 5.21 shows curl (τ/f) for January, February, July and October. Overall, the pattern of wind stress curl is positive (upwellings) in the tropics and the Southern Ocean. The Southern Ocean pattern is most persistent and shows upwelling favourable winds south of the peak in the westerly wind stresses; in this region, the southward decrease in wind stresses induces upwellings, and the reverse occurs north of this region. In the tropics, clockwise wind stress circulations cause upwellings which is most extensive in January and July. In the Tasman Sea, wind stress curl is mostly downwelling favourable except for July when it reverses to upwelling favourable. July is also the period when much of the coast from central west Australia to New South Wales is under upwelling favourable winds.

Regions of negative curl are regions where the potential of the wind field can induce downwelling; they are represented by most of the ocean's surface. Regions of positive curl are regions where the wind induces upwellings, although this does not necessarily mean that upwelling or downwelling actually occurs, as there may be other dominant forces present.

Data Provided

- Monthly wind stress curl

a



b

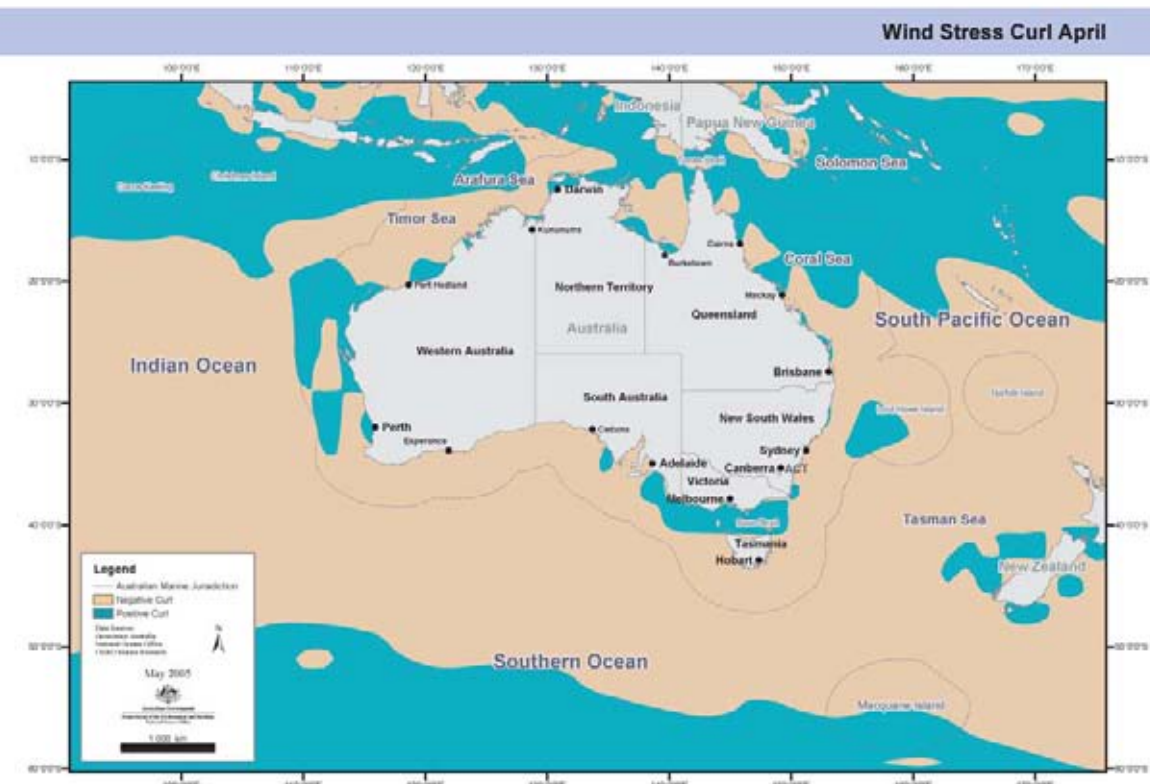
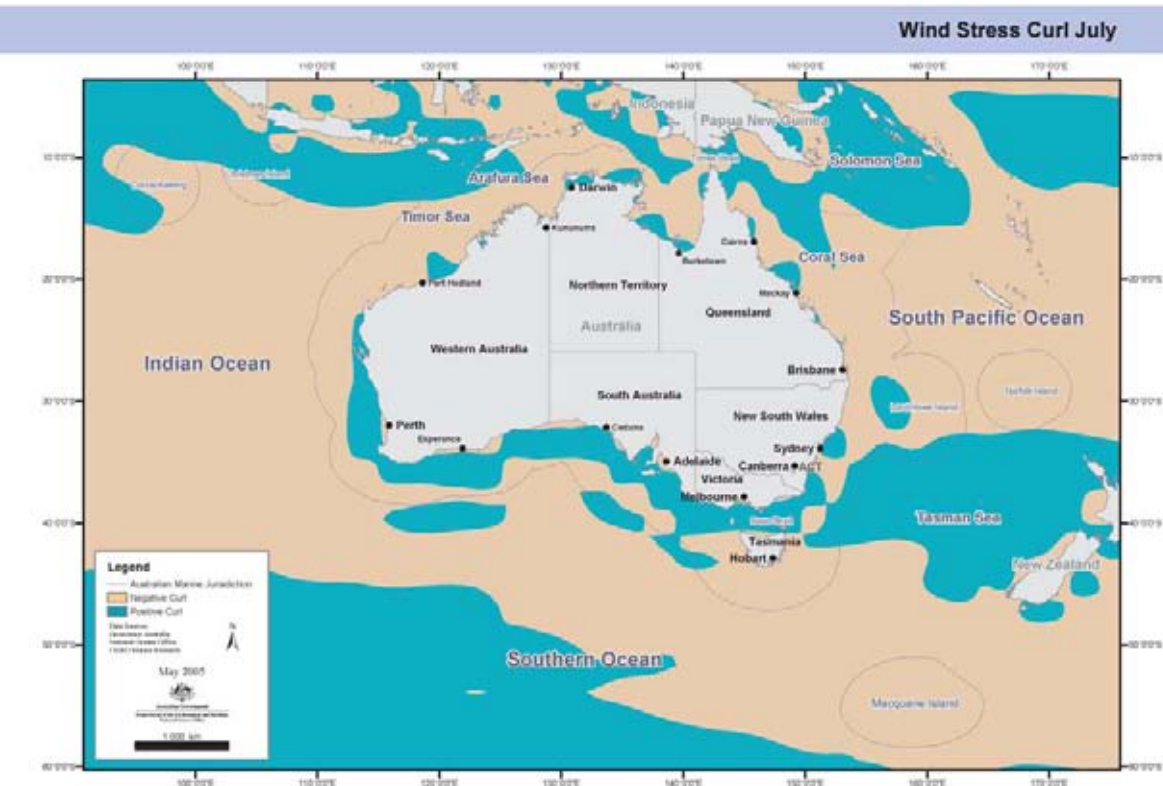


Figure 5.21 Wind-stress curl (a) January, (b) April, (c) July and (d) October (NCEP NCAR reanalysis project).

c



d

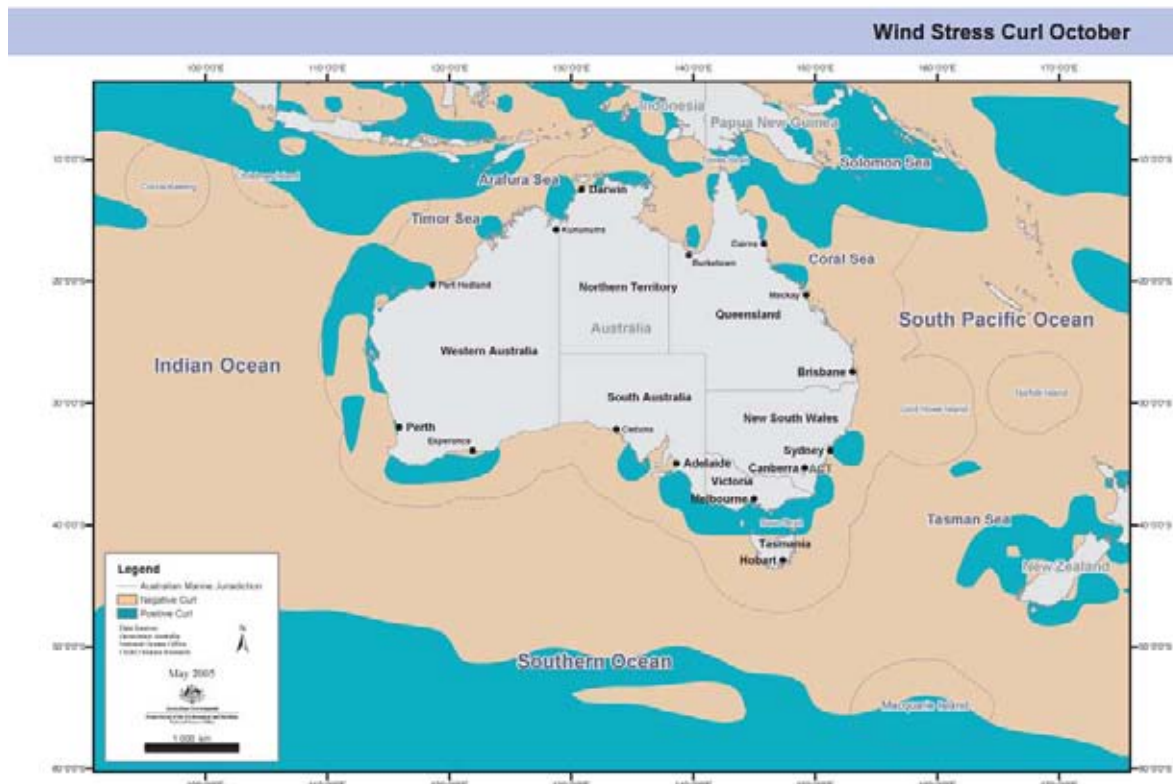


Figure 5.21. Wind stress curl (a) January, (b) April, (c) July and (d) October (NCEP NCAR reanalysis project) (cont.).

5.11 Surface Waves

Methods

The wave data estimates from surface wind speed, generated by the Australian Bureau of Meteorology's regional atmospheric model, provided input to the Wave Model, WAM (Hasselman et al 1988; Komen et al 1994), to yield estimates of mean wave height and period. The data are six-hourly predictions of significant wave height (SWH), period and mean wave direction, gridded at 0.1° spatial resolution, for the period March 1997 to February 2000, inclusive. The WAM model is run operationally at many forecasting centres around the world, including a version at the Australian Bureau of Meteorology. When compared to observations of SWH from wave-rider buoys around the Australian coast, the root mean square error of forecast SWH is approximately 0.5 m.

This high-resolution wave model (0.1°) was nested within a regional wave model (1°), which spans the oceans around Australia, ranging from latitudes 60°S to 12°N and longitudes 69°E to 180°E. The spectral resolution was the same for both models. The regional wave model (1°) provided the boundary conditions for input to the high-resolution wave model (0.1°). This regional wave model, in turn, was nested within a global model (for details see Porter-Smith et al 2004).

Arc info grids were generated from the model outputs (0.1° grids).

Description

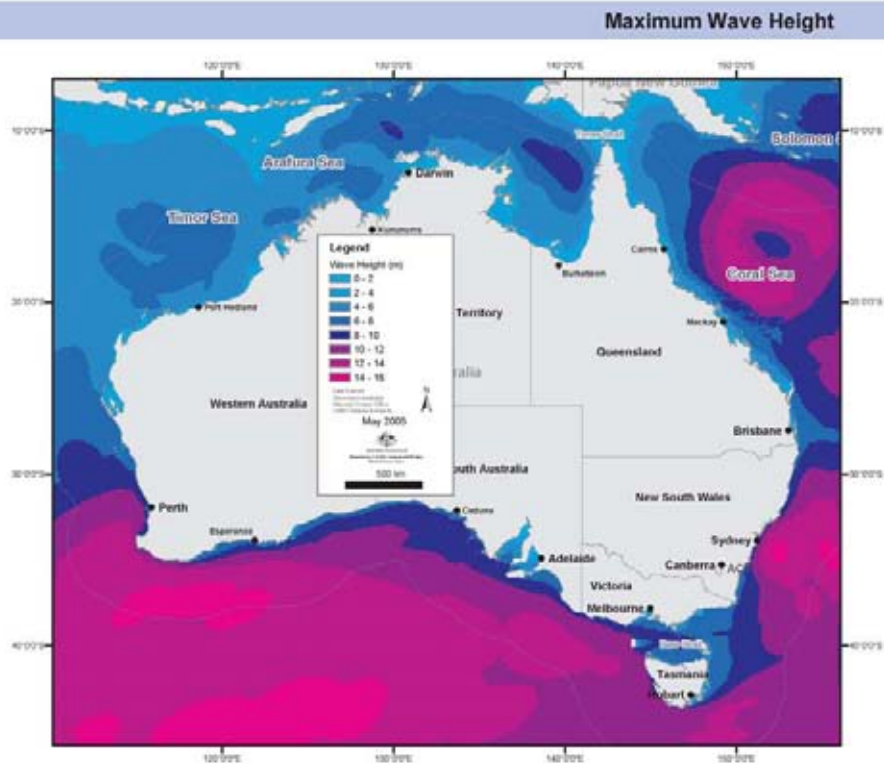
Annual mean wave height is greater in southern waters than in northern waters (Figure 5.22b). The largest and longest-period waves occur off the west coast of Western Australia, in the Great Australian Bight and off western Tasmania (see Figures 5.22a and 5.23a). Low mean heights and smaller periods occur off the North West Shelf, the Arafura Sea and in the Gulf of Carpentaria (see Figures 5.22a and 5.23a). The patterns of waves estimates produced by the model are generally consistent with previous wave studies (Porter-Smith et al 2004).

Data Provided

Six-hourly predictions of

- significant wave height
- wave period
- wave direction
- annual maximum wave height
- annual mean wave height

a



b

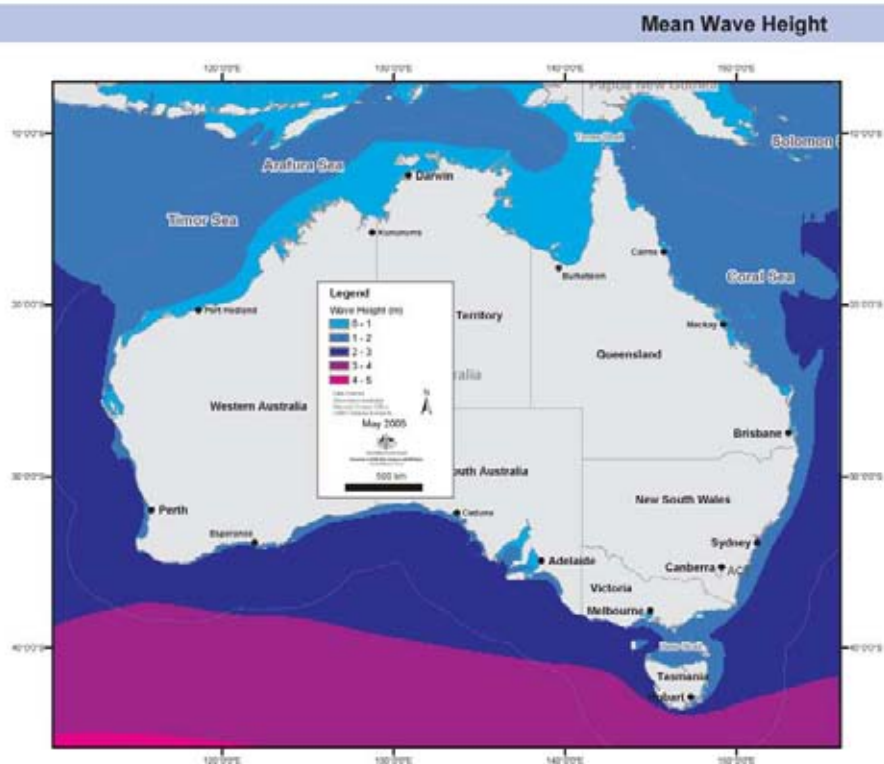
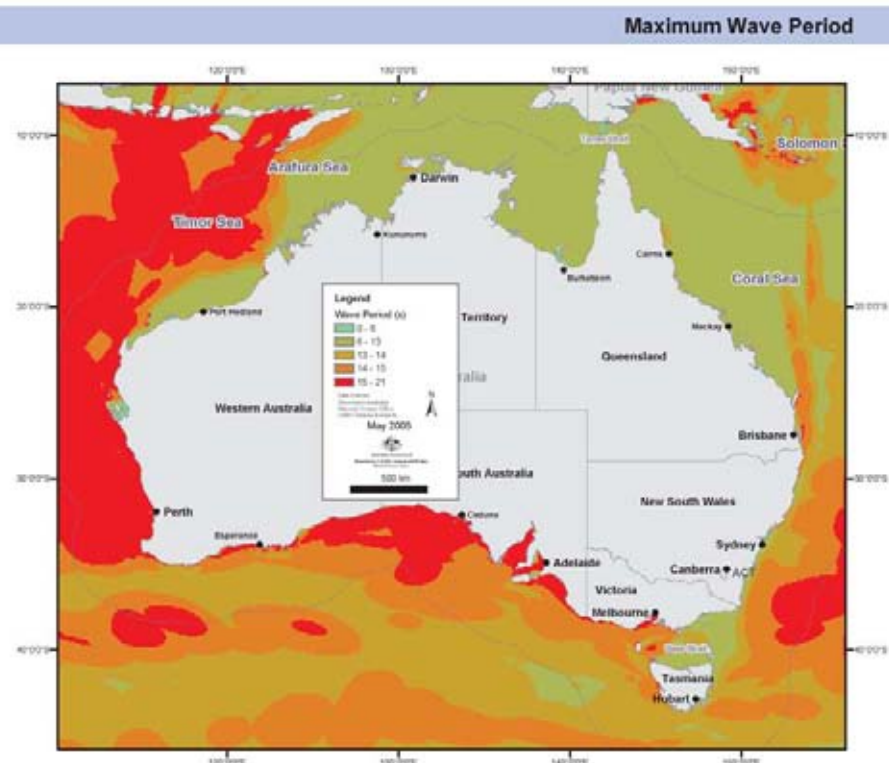


Figure 5.22 Wave height for the Australian Region (a) Maximum wave height, (b) Mean wave height.

a



b

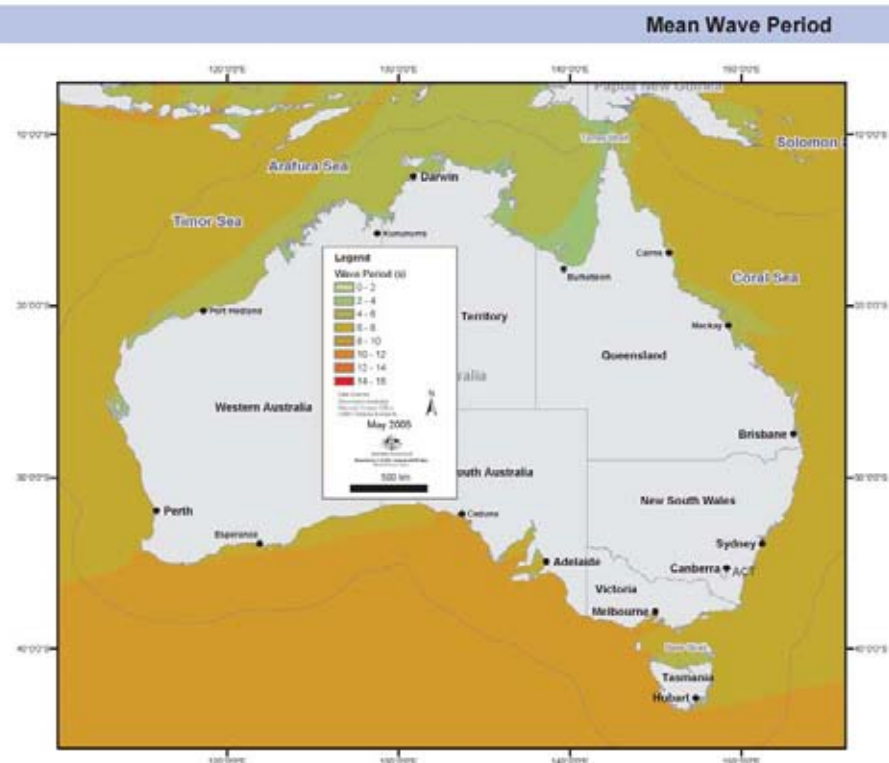


Figure 5.23 Wave period for the Australian Region (a) Maximum wave period, (b) Mean wave period.

5.12 Tides

Methods

The tide data were generated from a tide model for the Australian shelf that was set up for the region 0°S to 45°S and 109°E to 160°E (Porter-Smith et al 2004). The spatial resolution of the model output is 0.067° in both latitude and longitude and the temporal resolution is half a lunar cycle (Egbert et al 1994; Anderson et al 1995; Porter-Smith et al 2004).

Description

The model outputs show the strongest tidal currents occurring on the macrotidal shelf areas. The highest maximum tidal currents are at Collier Bay, King Sound, Torres Strait and Broad Sound (Figure 5.24a and 5.24b).

Tidal currents are also moderately strong in some mesotidal and microtidal gulfs, and shelf seaways: Spencer Gulf, Gulf of Carpentaria, Gulf of St Vincent, Bass Strait and Torres Strait (Harris 1994). Amphidromic points in the Gulf of Carpentaria, Joseph Bonaparte Gulf and Bass Strait (Harris 1994) are locations of tidal current maximum (see Figure 5.24a).

Arc info grids were generated from the model outputs (0.1° grids).

Data Provided

- Half-lunar cycle
- Maximum tidal current
- Mean tidal current

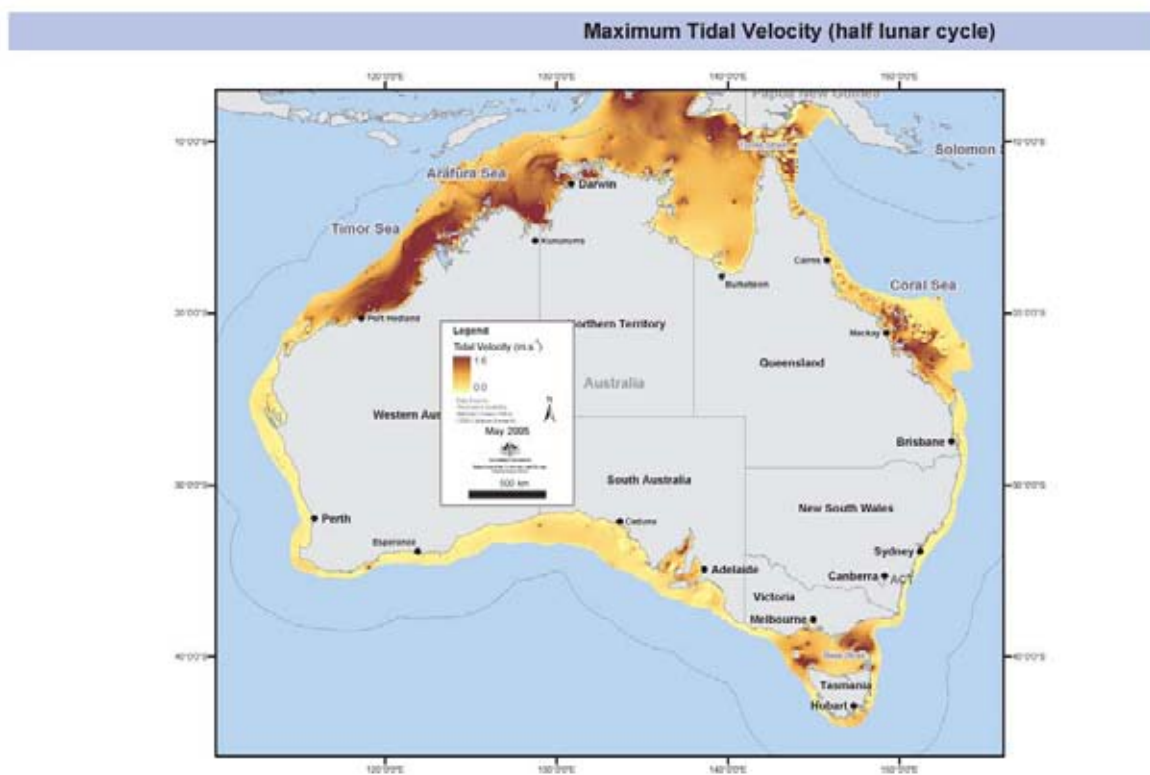
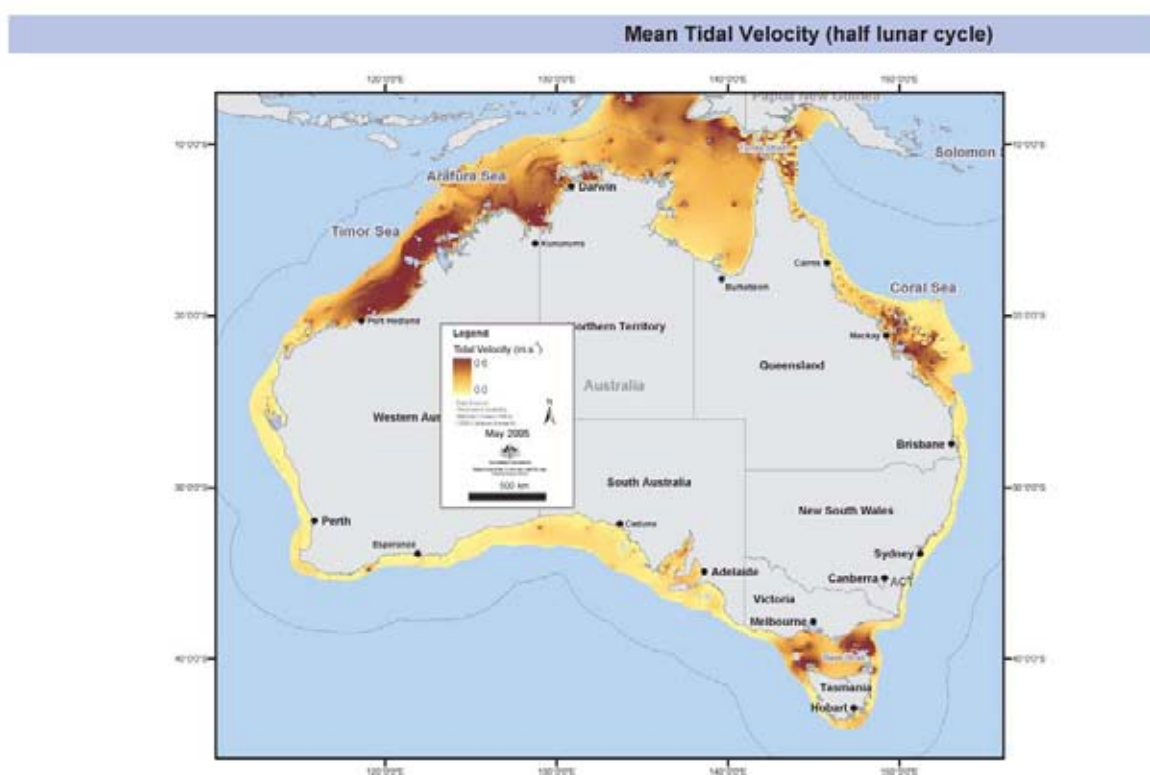
a**b**

Figure 5.24 Tidal Velocities in the Australian Region (a) Maximum tidal velocity, (b) Mean tidal velocity.

5.13 Photosynthetically Active Radiation

Photosynthetically Active radiation (PAR) is defined as the light energy required for photosynthesis at wavelengths between 400 and 700 nm. The amount of PAR on a square metre of ocean surface is determined by the elevation of the sun above the horizon, cloud cover, and atmospheric transmittance of light from the sun. The elevation of the sun varies with latitude and month. The sun's altitude above the horizon at noon on specified dates and latitudes (Table 5.2) is highest in December and lowest in June. Information in Tables 5.2 and 5.3 is available at http://aa.usno.navy.mil/data/docs/RS_OneYear.html.

Table 5.2 Solar zenith angle (degrees) at noon on specified dates and latitudes.

Latitude	21 Dec	21 Mar	21 Jun	21 Sep
Equator	66.5	90	66.5	90
10°S	76.5	80	56.5	80
20°S	86.5	70	46.5	70
30°S	83.5	60	36.5	60
40°S	73.5	50	26.5	50
50°S	63.5	40	16.5	40
60°S	53.5	30	6.5	30

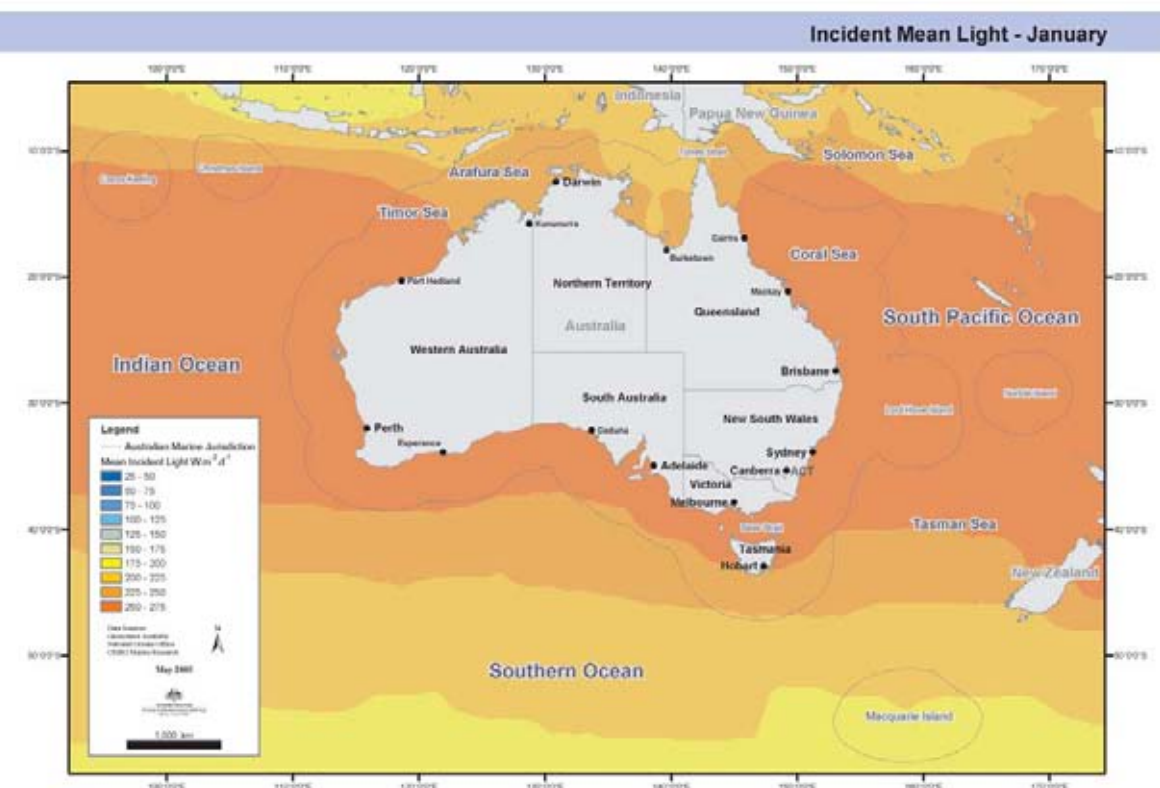
Day length is defined as the period between sunrise and sunset. Day lengths at 10 degree increments in latitude are given in Table 5.3. Day length plus sun altitudes determine the daily amount of PAR per unit area, and availability for photosynthesis and primary production at depth.

Table 5.3 Day lengths in 10 degree latitude bands, rounded to the nearest 15 minutes.

Latitude	January	April	July	October
Equator	12:00	12:00	12:00	12:00
10°S	12:45	12:00	11:30	12:15
20°S	13:15	11:45	11:00	12:30
30°S	14:00	11:30	10:15	12:30
40°S	15:00	11:30	9:30	12:45
50°S	16:15	11:15	8:15	13:00
60°S	18:30	10:45	6:15	13:30

These two tables explain much of the latitudinal variation in PAR seen in Figure 5.25, which gives mean incident light adjusted for cloud in January, April, July and October. The longitudinal unevenness in mean incident light is due to differences in cloud cover across the large area included. The reduction in PAR, and the conspicuous latitudinal banding in mean PAR (particularly south of 20°S), are due primarily to changes in solar elevation. PAR is reduced in the Southern Ocean south of 40°S due to heavy and persistent cloud in the Roaring 40's and Furious 50's all year round. The effects of persistent cloudiness in the Southern Ocean is best seen on the chlorophyll composite maps, where black spaces indicate no ocean colour data were received during the time period (typically 1 month) over which the data are averaged. The effects of cloud mean that PAR measured on board research vessels can range from 17% above (on exceptionally clear days) to 62% below (on very cloudy days) the climatological mean PAR that these images are based on in the Southern Ocean (Griffiths, unpublished data).

a



b

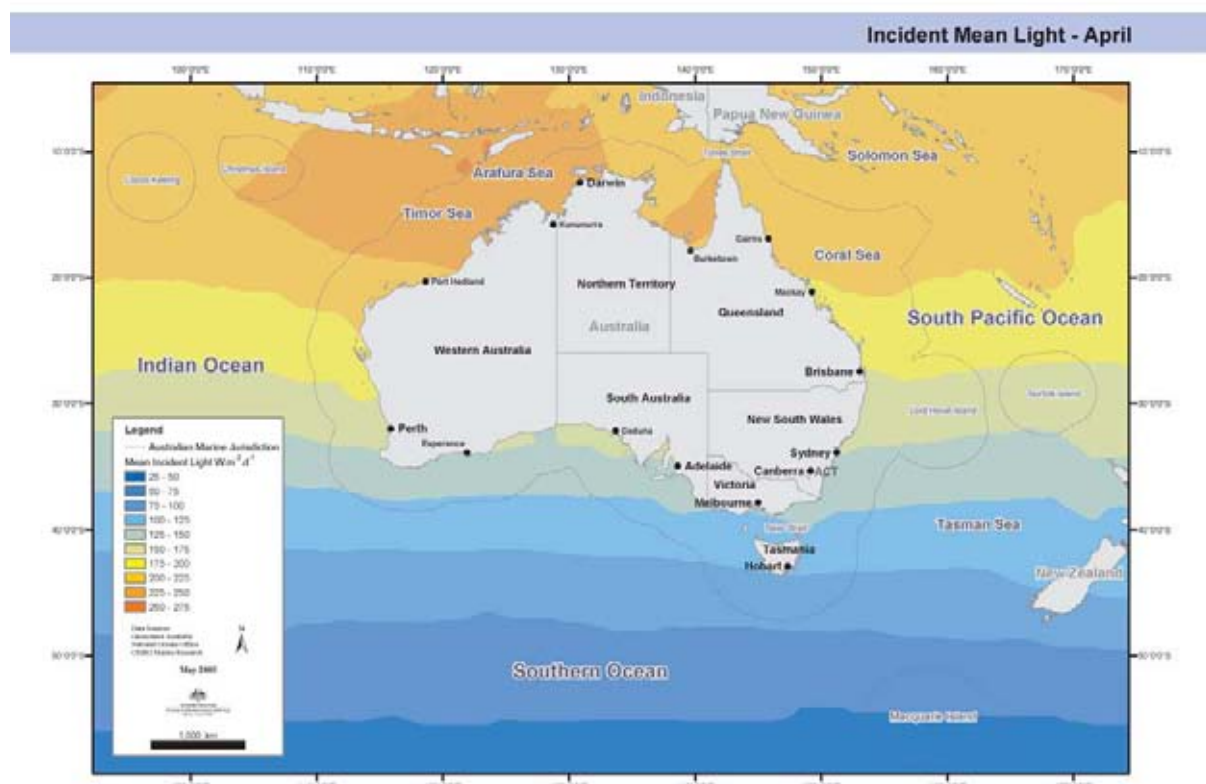
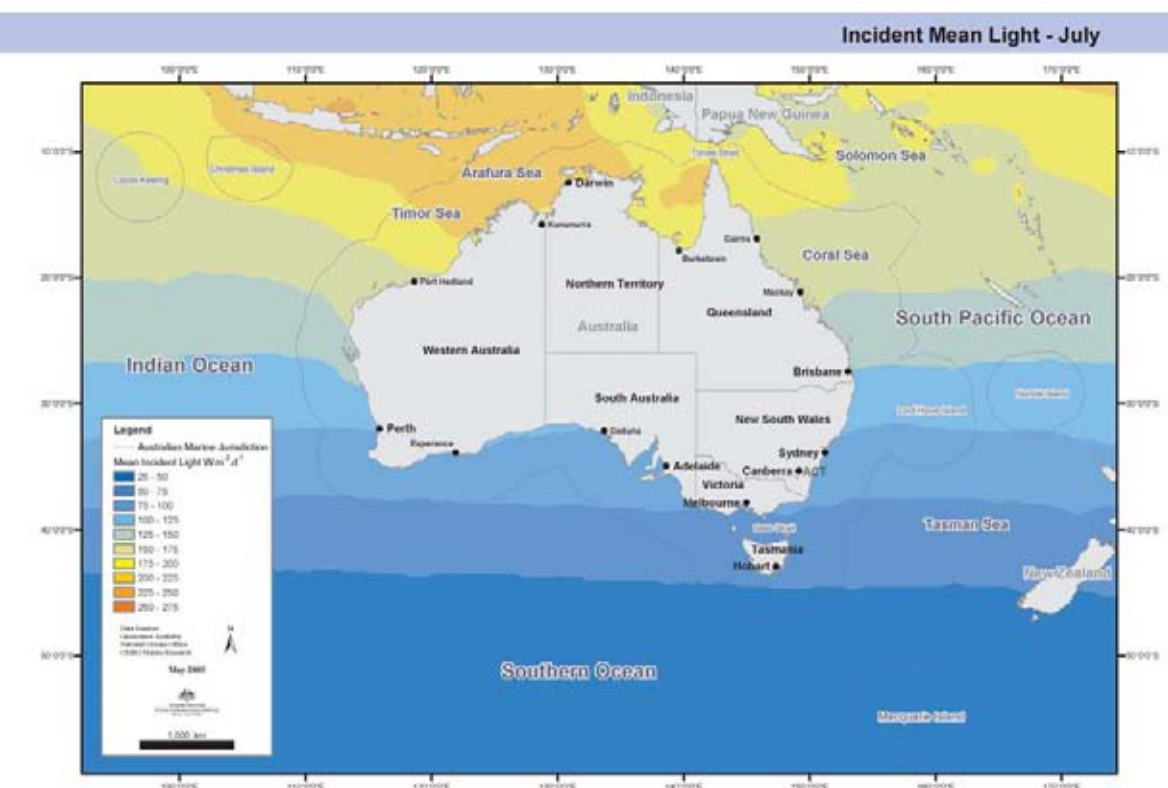


Figure 5.25 Photosynthetically Active Radiation for (a) January, (b) April, (c) July and (d) October.

c



d

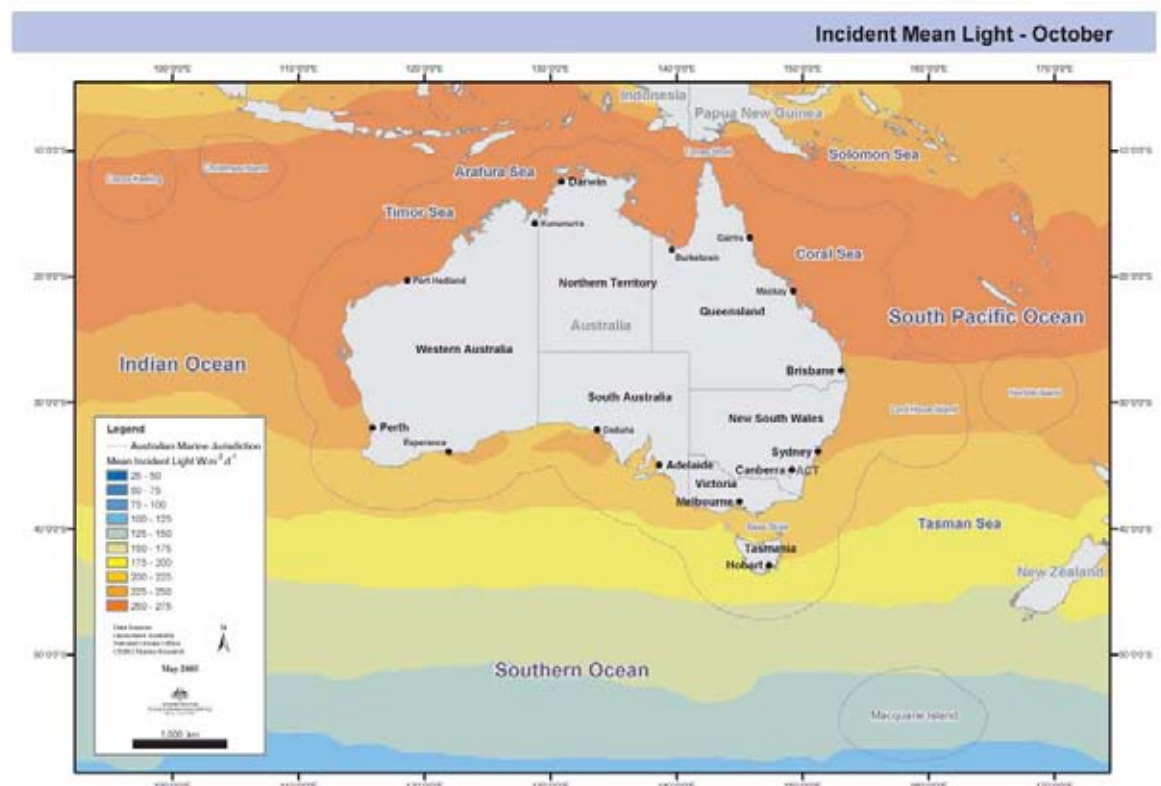


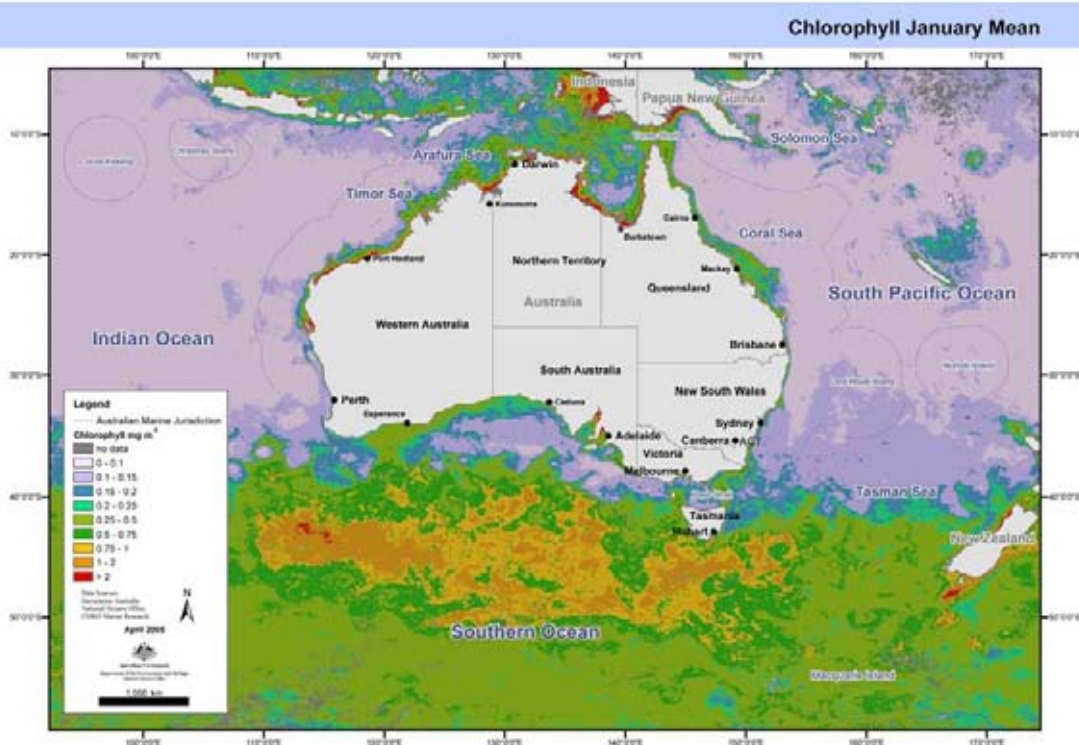
Figure 5.25 Photosynthetically Active Radiation for (a) January, (b) April, (c) July and (d) October. (cont.)

5.14 Chlorophyll-a from the MODIS Aqua Ocean Colour Satellite

The data used to prepare the chlorophyll maps were the Level 3, 4.88 km resolution, monthly mean chlorophylls obtained from the MODIS satellite. The data are stored at NASA/GSFC in the USA. A user manual for the MODIS data is available at <http://modis-ocean.gsfc.nasa.gov/userguide.html> and the data would have been transferred from /imgjj/sensor/modis/NASA_data/l3/daac.gsfc/aasia/MO. These data products are flagged for: 0 = good, 1 = questionable, 2 = cloudy and 3 = bad other than cloud. The data were filtered, and levels 0 and 1 data were kept in the dataset used here. The images are monthly means; grey areas on the images indicate areas where no acceptable ocean-colour data were received during that month. The satellite detection limit for chlorophyll in these datasets is 0.01 mg Chl-a m⁻³. The black areas on the images are caused by clouds, especially in the Southern Ocean south of 40°S. The monthly averaging also means that fine mesoscale and regional-scale structures seen on single scene images are lost, and only broad patterns remain.

Four months (January, April, July and October) were chosen to illustrate the patterns in chlorophyll distribution and the ranges seen by the satellites (Figure 5.26). The chlorophyll data used here were calculated for Case 1 waters: these are the clear oceanic waters, away from the interference of coastal and riverine sediments, coloured dissolved organic matter or Gelbstoff and interference due to reflectance from the bottom. Suspended sediment can be a problem in the Spencer Gulf, the Gulf of Carpentaria, Joseph Bonaparte Gulf, and along the west coast of Papua New Guinea and Irian Jaya. Bottom reflectance may be a problem along the coastal margin of the North West Shelf (including Shark Bay) and perhaps near-shore regions in the Great Australian Bight, especially in winter. Chlorophyll results, especially high chlorophylls from these inshore waters, must be treated with some degree of scepticism. CDOM may be interfering with estimates of chlorophyll in surface waters on the west coast of Tasmania and the west coast of Papua New Guinea and Irian Jaya.

a



b

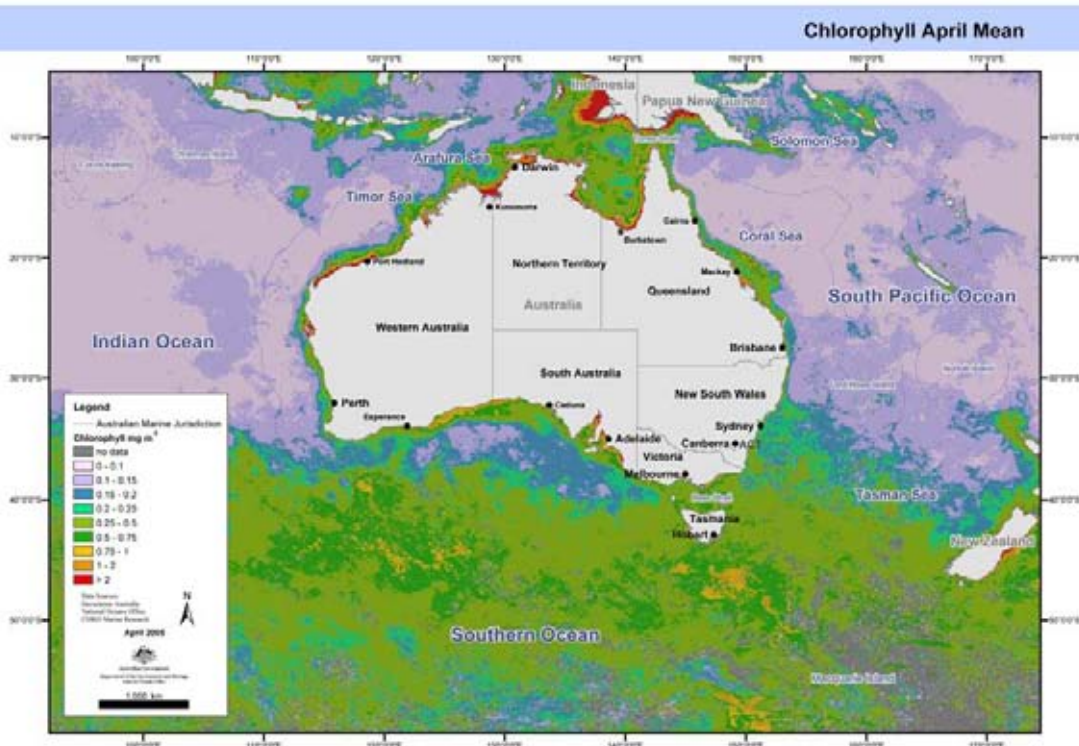
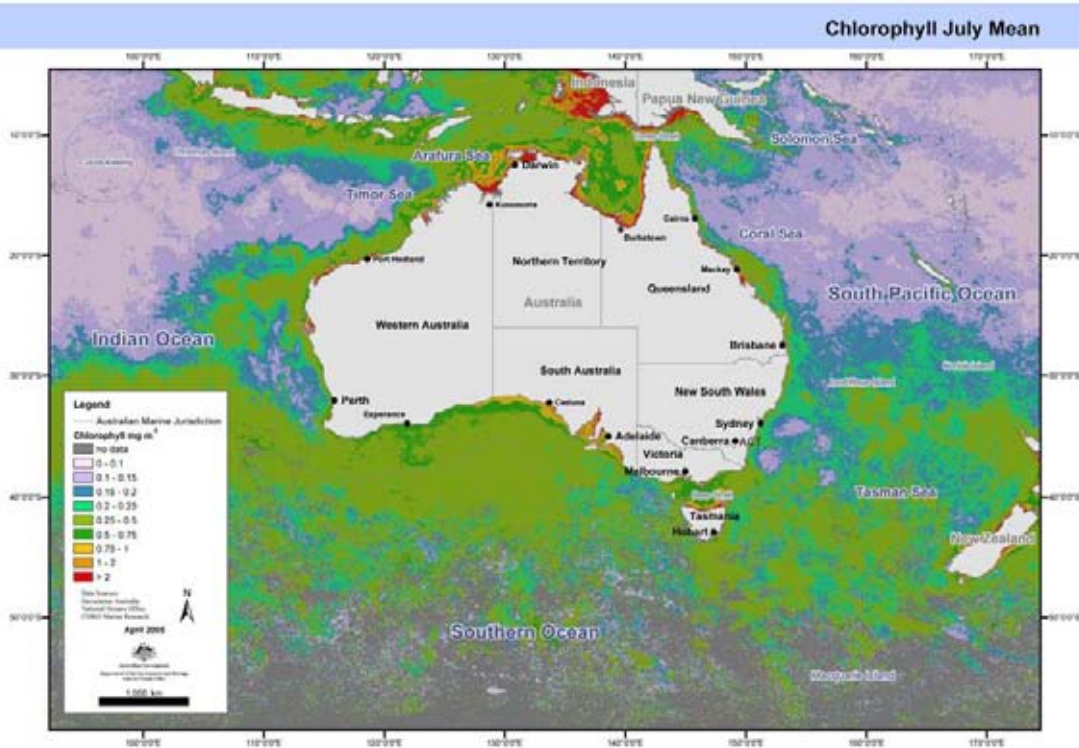


Figure 5.26 Monthly mean Chlorophyll for (a) January, (b) April, (c) July and (d) October.

c



d

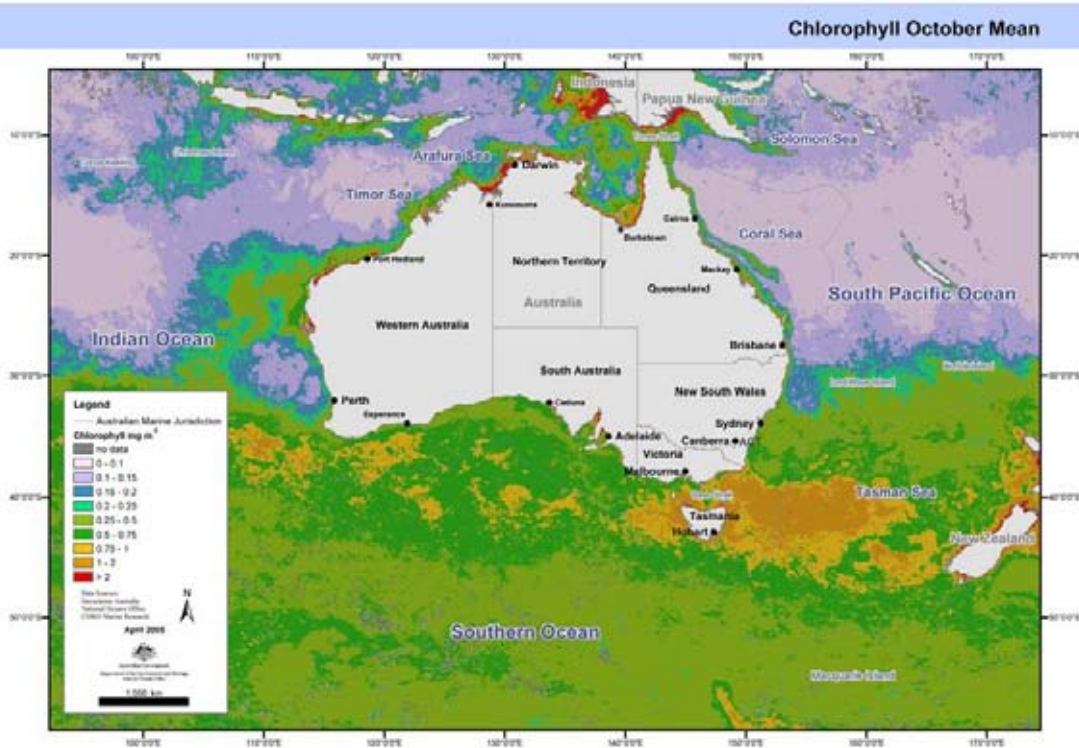


Figure 5.26 Monthly mean Chlorophyll for (a) January, (b) April, (c) July and (d) October (cont.).

The other major drawback with chlorophyll estimates from ocean-colour satellites is that the estimate is for surface chlorophyll only. The signal received by the satellite is generated from chlorophyll contained in one extinction depth, typically <25 m, and in high chlorophyll regions, often much shallower than this. The models developed to estimate total chlorophyll in the water column from surface chlorophyll have had varying degrees of success, depending on how good the ground-truth data are in different regions. In the Southern Ocean south of Tasmania, for example, Griffiths and Matear (2004) found that the column chlorophyll estimates used in the Behrenfeld–Falkowski primary production model are about a factor of 2 lower than the measured column chlorophyll. The estimates of surface chlorophyll in our region have also been found to be too high at very low chlorophyll levels, but too low at high chlorophyll levels. Hanson (2004) has shown the phytoplankton biomass within the Leeuwin Current is largely confined to the base of the mixed layer in a deep chlorophyll maximum. This mirrors the situation seen in the Timor, Arafura and Coral seas. The satellite chlorophyll distributions are the only way, however, to get broad coverage of the huge Australian exclusive economic zone (EEZ), and work is actively proceeding on obtaining more ground-truth data to improve the accuracy of the column estimates, and hence of the modelled primary-production estimates. Seasonal and regional algorithms will eventually be developed to provide better estimates of the total amount and distribution of chlorophyll in the water column and of primary production from ocean colour satellites. At present we simply do not know enough about the vertical distribution of chlorophyll or the seasonal patterns of chlorophyll in the water column in waters around Australia.

In January, the two dominant features on the image are the very high and extensive chlorophyll region ($0.75 - 1 \text{ mg m}^{-3}$) in the Subantarctic Zone south of Australia, and the very low chlorophyll regions north of 35°S extending to the equator (Figure 5.26a). Some mesoscale dynamics are highlighted in the patterns in chlorophyll, including a link from the coastal region near Esperance to the offshore, high-chlorophyll waters. This same pattern is often seen in thermal images, as warmer shelf waters wrap around mesoscale eddies in the Subtropical Convergence. Some of the complex mesoscale structure on the northern edge of the STC is seen between 38°S and 40°S . The regions north of $35^\circ - 40^\circ\text{S}$ all show extremely low chlorophylls, due principally to low nutrients in the mixed layer, and the presence of deep chlorophyll maxima at depths between 70 and 150 m. These deep chlorophyll maxima are typically not productive, because photosynthesis at these depths is often severely light-limited. There do appear to be some continuing, moderately high, concentrations of chlorophyll along the outer edge of the Great Barrier Reef, and possibly in the Arafura Sea and north and south of Joseph Bonaparte Gulf. The high apparent chlorophyll close inshore between Cape York and the North West Shelf and along the Papua New Guinea and Irian Jaya coasts is probably due to a combination of suspended sediment and bottom reflection interfering with the estimates (as this is the wet season in Australia's monsoonal tropics).

The blooms in the Southern Ocean in April (Figure 5.26b) are rapidly reducing under the twin influences of decreasing PAR and nutrients. The band of higher chlorophyll is starting to move north, towards the winter position described earlier. The increase in chlorophyll on the shelf in the Bight is moving eastwards, possibly being at least partly driven by the Leeuwin current as it follows the shelf eastwards. There seasonal increase along the North West Shelf is beginning, starting in the northern region. The Tropical and Subtropical Indian Ocean region and the Coral Sea are still in the deeply mixed, nutrient-limited, low-chlorophyll condition. There is a marked increase in the Arafura Sea region, and in near-shore regions of the Gulf of Carpentaria. The very high apparent chlorophylls off the western coast of Irian Jaya are almost certainly due to a combination of suspended sediment and high concentrations of coloured dissolved organic matter from the lowland swamps and large rivers in this area. April is the end of the wet season in Indonesia, and the dry season continues until October. The high chlorophyll at the outer edge of the Great Barrier Reef, and slight enrichment south of the reef along the Queensland coast probably results from wind-driven upwelling at the reef. There is a regular increase in chlorophyll in autumn and/winter along the west Australian coast. Neither the cause of this increase nor the mechanism that moves the increased chlorophyll south is clear. The Leeuwin Current would be responsible for advecting the high chlorophyll-containing water seen on the shelf and upper slope offshore.

In July, chlorophylls are increasing in the Arafura Sea region, along the southern side of the Indonesian archipelago and along the North West Shelf region of Western Australia and extending offshore from North West Cape (Figure 5.26c). The broad area of high chlorophyll ($0.5\text{--}0.75 \text{ mg m}^{-3}$) south of Java and the Indonesia archipelago is due to wind-induced upwelling. Over much of the remaining areas north of 30°S , chlorophylls are low ($<0.20 \text{ mg m}^{-3}$). The images show very high chlorophyll off the west coast of Irian Jaya and Papua New Guinea, due to suspended sediment being carried into the ocean by the rivers in the area, and high CDOM draining from the extensive swampy lowlands along this coast. This image shows a thin band of apparent high chlorophyll close inshore extending from Cape York to Joseph Bonaparte Gulf. This is probably not chlorophyll, but suspended sediments or interference due to bottom reflection in these Case 2 waters. There is a region of high chlorophyll in and near the southern end of the Great Barrier Reef, offshore from Mackay in July. Much of the Southern Ocean (south of 45°S) is covered in cloud, severely limiting the data available. The broad area extending from about 30°S in the Subtropical Convergence region west of Western Australia through the Great Australian Bight, past Tasmania and across to New Zealand is showing the normal winter chlorophyll concentrations ($<0.5 \text{ mg Chl-}a \text{ m}^{-3}$).

In October (Figure 5.26d), there is some evidence of raised chlorophyll along the outer edge of the Great Barrier Reef, and some patches of high chlorophyll remain north of the Gulf of Carpentaria and eastern Arafura Sea. The chlorophyll concentration in waters along the North West Shelf region has dropped, but the enrichment off North West Cape is still very evident. The broad area of very low chlorophyll *a* in the Indian Ocean and in the Timor Sea north of 30°S , and in the Coral Sea, is probably due to nutrient exhaustion in the euphotic zone, and there is probably a chlorophyll maximum at the thermocline or nutricline that is too deep to be detected by the satellite. The spring phytoplankton bloom is well underway in a band of about 10 degrees of latitude in the Subtropical Convergence region south of Western Australia, in the Great Australian Bight and the Tasman Sea, where surface chlorophylls exceed $1 \text{ mg Chl-}a \text{ m}^{-3}$ between about 40°S and 45°S . This latitudinal band of high chlorophyll in the Indian Ocean, and Tasman Sea, started moving south in late August, continuing until February in the Tasman Sea, but until March or April in the Indian Ocean. The increase in chlorophyll to $0.5 \text{ mg Chl-}a \text{ m}^{-3}$ in Polar and Antarctic waters is most probably caused by the formation of the seasonal, shallow mixed-layer and increasing PAR.

The broad patterns are for high chlorophylls in winter in the tropical regions, and in summer in the regions south of Australia. The patterns are a continuum, and very dynamic in movie loops of the weekly images. The different regions are connected, and the whole system is driven by a combination of basin- and regional-scale physics, with PAR as the ultimate controller of phytoplankton growth.

5.15 Seasonal and Interannual Variations in Surface Chlorophyll from SeaWiFS Ocean-colour Satellite

A movie linking the weekly composited (Level 3, 9 km mean) surface chlorophyll maps from the SeaWiFS ocean-colour satellite has been constructed and delivered to the National Oceans Office (see Appendix A). This movie, covering the period between September 1997 and March 2000, was included to show the dynamic nature of chlorophyll distributions and the latitudinal, seasonal and interannual abundance patterns in the waters around Australia. It allows a separation of two broad regions north and south of about 20°S, where the dynamics and timing of chlorophyll increases and decreases change. The weekly compositing technique leaves some of the mesoscale and regional-scale distribution patterns that are removed by the monthly compositing scheme used in Figure 5.26. An understanding of the regional scale variability is vital to an understanding of faunal boundaries used to separate the higher level regions described in Lyne and Hayes (2005).

The seasonal patterns of surface chlorophyll in the southern Coral and northern Tasman Seas show surface chlorophylls are highest in winter (May–October), but drop rapidly to quite low levels from November to April. In March, high chlorophylls are concentrated in the Subtropical Convergence region near 40°S. By June there is a distinct band of higher chlorophyll about 10 degrees of latitude wide. The northern edge of this band moves north to between 20°–25°S by August, with the southern edge somewhat north of 40°S. By early October, the southern edge of the band is south of 40°S, while the northern edge has moved to around 30°S. By December, the northern edge has moved to around 35°S – 40°S. The southern boundary crosses the Subtropical Convergence into the Subantarctic Zone and then starts to retreat northwards again in February–March. The general picture is of a band of chlorophyll moving south and north, probably in response to nutrient availability and the development of seasonally shallow mixed-layers. Nitrate is most probably limiting phytoplankton biomass (measured as chlorophyll) and primary production in the southern Coral Sea and Tasman Sea, and nitrate and especially silicate in the Subtropical Convergence and Subantarctic Zone. Iron contributes to constraining phytoplankton biomass in the Subantarctic Zone; its role in the Tasman and Coral Seas has not yet been investigated. Both the Coral and Tasman Seas typically have deep chlorophyll maxima near the nutricline (CSIRO Division of Fisheries and Oceanography 1963) when very little chlorophyll or phytoplankton biomass is seen on ocean-colour images. These deep chlorophyll maxima may be quite productive, particularly if they are relatively shallow (in the 1–10% of surface-light zone—otherwise the primary production would be very light-limited).

The spring bloom in the Horseshoe region at the eastern end of Bass Strait was weaker but longer (between September and November in 1998), than the intense and short bloom in September/early October in 1999. Warm-core eddies shed by the East Australian Current are clearly visible as areas of very low chlorophyll off the southern coast of New South Wales and their movements can be traced by following the low-chlorophyll patterns. Increased chlorophyll associated with the shelf-break upwelling being driven seasonally by the Leeuwin Current can be traced from North West Cape south to Cape Leeuwin, and into the Great Australian Bight. It serves to emphasise that the seasonal chlorophyll distribution patterns may be somewhat independent of the physical oceanographic water-mass boundaries, particularly during the spring bloom in the Coral and Tasman Seas, and across the Subtropical Convergence.

South of Australia, there is continuity in the chlorophyll patterns from the Indian Ocean through to the Tasman Sea. The latitudinal change of the banding from west to east is due to the current patterns and bottom topography.

The fronts in the Southern Ocean are important biogeographical boundaries and define the limits of

distinct biological communities. For example, throughout the year the Antarctic Zone is rich in major nutrients such as silicate, nitrate, and phosphate, allowing diatoms to dominate the phytoplankton community until silicate and iron become limiting. *Phaeocystis* and nanoflagellates then dominate the community. In contrast, Subantarctic Zone waters are low in silicate year-round and are dominated by diatoms in spring, but nanoplankton, ciliates and coccolithophorids in summer and autumn. Primary production throughout the Southern Ocean is probably limited, at least in part, by a lack of trace nutrients such as iron, but has different proximate controls in each water mass. In the Subantarctic Zone, silicate limits diatom growth, but nitrate and light limit the mixed summer community. In the Polar Zone, light, silicate and iron seem to be the main factors limiting the more extensive growth of diatoms. Deep chlorophyll maxima are seen in both water masses, but especially just south of the northern branch of the Polar Front. These deep chlorophyll maxima may be productive between depths of 60 and 90 m or so, but when they occur at depths below 100 m they are typically extremely light-limited and non-productive. In the Permanently Open Ocean Zone between about 58°S and 61°S (along 140°E), light and temperature, and potentially grazing, may be limiting the standing stock of phytoplankton. In the Sea Ice Zone, light is the main control of primary production. Where shallow mixed-layers form, there may be quite large phytoplankton blooms, providing there is sufficient iron for diatoms to utilise the silicate. These blooms will persist only as long as the shallow mixed-layers, formed by fresh water from melting sea ice, persist. Blooms do not always, at least in the Australian sector of the Antarctic, follow the melting ice-edge.

North of 20°S, there are small but significant differences in the timing and magnitude of the chlorophyll patterns of the Timor and Coral Seas. In the Coral Sea, chlorophyll increases from April to August when the south-east trade winds are blowing strongly, with very low chlorophylls in surface waters between September and-March. There is evidence of some interannual variation in the timing of these patterns. Much of the increase appears to originate near Papua New Guinea, and moves west and south from the northern section of the Coral Sea. There appear to be pulses of surface water with higher chlorophyll concentrations coming through the Louisiade Archipelago, often in November and December that penetrate into the Coral Sea. During the low surface-chlorophyll periods, there is probably a deep chlorophyll maximum at the pycnocline that, depending on depth and light, may be fairly productive.

In the Timor Sea, the increase in chlorophyll is initially most noticeable along the North West Shelf and south of the Indonesian Archipelago from about May. There is a progression of increasing chlorophyll south-west along the North West Shelf from Joseph Bonaparte Gulf to North West Cape between May and July, and there appears to be a connection between this coastal enrichment and the increase in surface chlorophyll offshore from North West Cape. The increase in chlorophyll along the coast of Western Australia is associated with this pattern and with the development of the Leeuwin Current. The increase on the shelf may actually be caused by upwelling driven by several small-scale, shelf currents (Ningaloo and Capes Currents; Hanson et al submitted, 2004) particularly in the Gascoyne region of this coast. The increase in chlorophyll is particularly visible from March to May, when the current is pushing strongly southwards along the west Australian coast. After May, there is a generalised increase in surface chlorophyll further offshore, matching the onshore increase. This typically persists until October or early November when it decreases along the shelf. November through March is a time of very low surface chlorophylls, but there is evidence of subsurface chlorophyll maxima near the nutricline both on the shelf and offshore.

Along the Indonesian Archipelago, there are streamers of high chlorophyll that move south and west in the Timor Sea, and extend as far west as 90°E. Chlorophyll increases in surface waters of the Timor Sea in July–August, apparently originating on the coast of both Indonesia and Australia and moving south and north to cover the surface waters. By November, there is a marked decline in surface chlorophyll in the centre of the Timor Sea. This condition persists until about April.

Inshore, regular summer upwellings occur off the Eyre Peninsula, Kangaroo Island, the Bonney Coast (Robe to Portland) and eastern Victoria (Lakes Entrance to Mallacoota). The most prominent of these is along the Bonney Coast, where classical upwelling plumes of low-temperature surface water, and

increased chlorophyll biomass, are regularly observed. These regions of enhanced chlorophyll biomass will persist for short periods until the upwelled nutrients are exhausted, after upwelling ceases. The enhanced production and biomass can be advected away from the upwelling site by surface currents, spreading the effects of the upwelling well beyond the point source. Surface swarms of krill (*Nyctiphanes australis*) develop in response to the enhanced productivity induced by the upwelling, especially off the Bonney Coast and Kangaroo Island. Further east, the pattern of high chlorophyll in winter and low in summer persists through Portland in Victoria. There are seasonally predictable phytoplankton blooms (in September) along the shelf break at the eastern end of Bass Strait. The occasional short-lived (days to weeks) chlorophyll patches in the Point Hicks–Cape Howe region that probably result from upwelling in this region due to combinations of favourable winds, tides and currents. The constant tidal motions in Bass Strait, combined with its relative shallowness, result in increased standing stocks of chlorophyll in the strait, which are exported eastwards. This almost constant transport of phytoplankton would contribute to the rich fisheries in the area.

The seasonal pattern of chlorophyll biomass in the Great Australian Bight region is relatively simple. From November through April, chlorophyll north of the Subtropical Convergence, and off the shelf, is quite low. From April, a band of higher chlorophyll moves northwards to the shelf, with an extension from the shelf southwards. This raised chlorophyll in the head of the bight persists until late spring, when the high-chlorophyll band moves south towards the Subtropical Convergence. As noted above, there is evidence of occasional upwelling in the Recherche Archipelago through to near Eyre, especially in March-April.

5.16 Primary Production Estimates from the MODIS AQUA Ocean Colour Satellite and the Behrenfeld–Falkowski Vertical Generalised Production Model

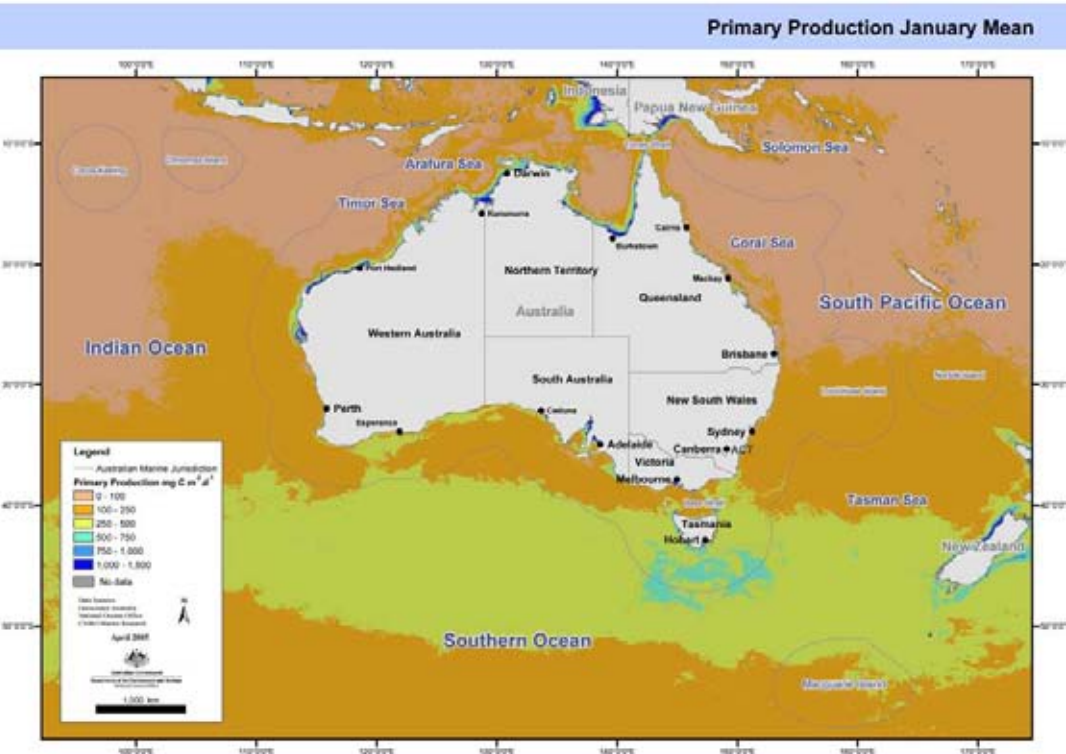
The core equation describing the relationship between surface chlorophyll sensed by ocean-colour satellites and depth-integrated primary production is

$$PP_{eu} = 0.66125 * P_{opt}^B * (E_o / (E_o + 4.1)) * C_{SAT} * Z_{eu} * D_{irr}$$

where: PP_{eu} is the daily carbon fixation from the surface to the bottom of the euphotic zone (Z_{eu}),
 P_{opt}^B is the optimal rate of carbon fixation in the water column, (a complex function of temperature),
 E_o is the sea-surface daily Photosynthetically Active Radiation (PAR),
 Z_{eu} is the depth of the euphotic zone defined as the penetration depth of 1% of surface irradiance, calculated from C_{SAT} ,
 C_{SAT} is the surface-chlorophyll concentration as derived from satellite measurements of water leaving radiance,
 D_{irr} is the daily photoperiod calculated for the middle of the month for each pixel.

The Behrenfeld–Falkowski Vertical Generalised Production Model (VGPM) calculations of primary production are based on monthly average C_{SAT} estimates. Details of the model are given in Behrenfeld and Falkowski (1997).

a



b

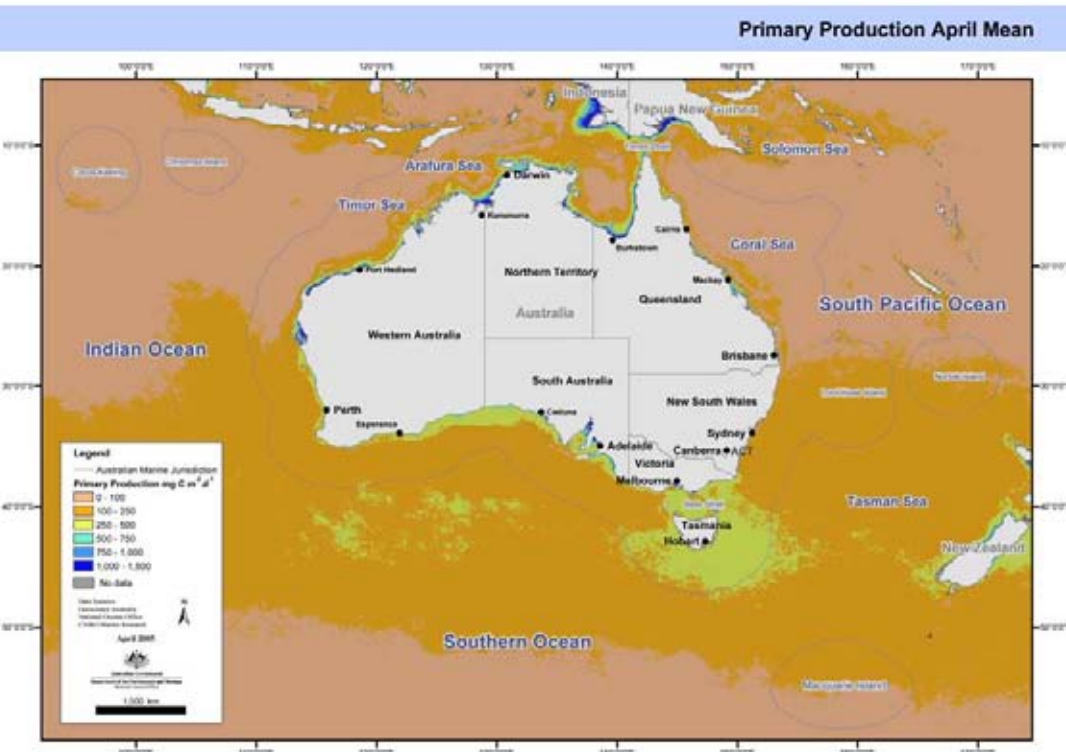
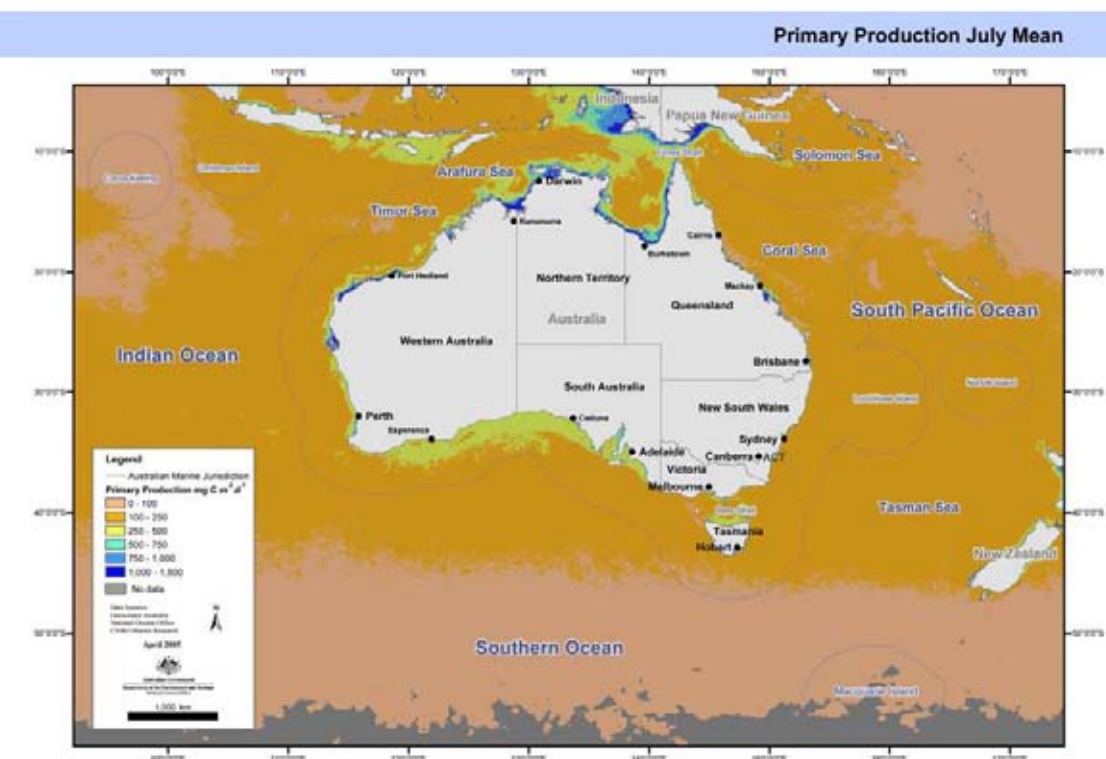


Figure 5.27 Monthly means for primary production for (a) January, (b) April, (c) July and (d) October.

c



d

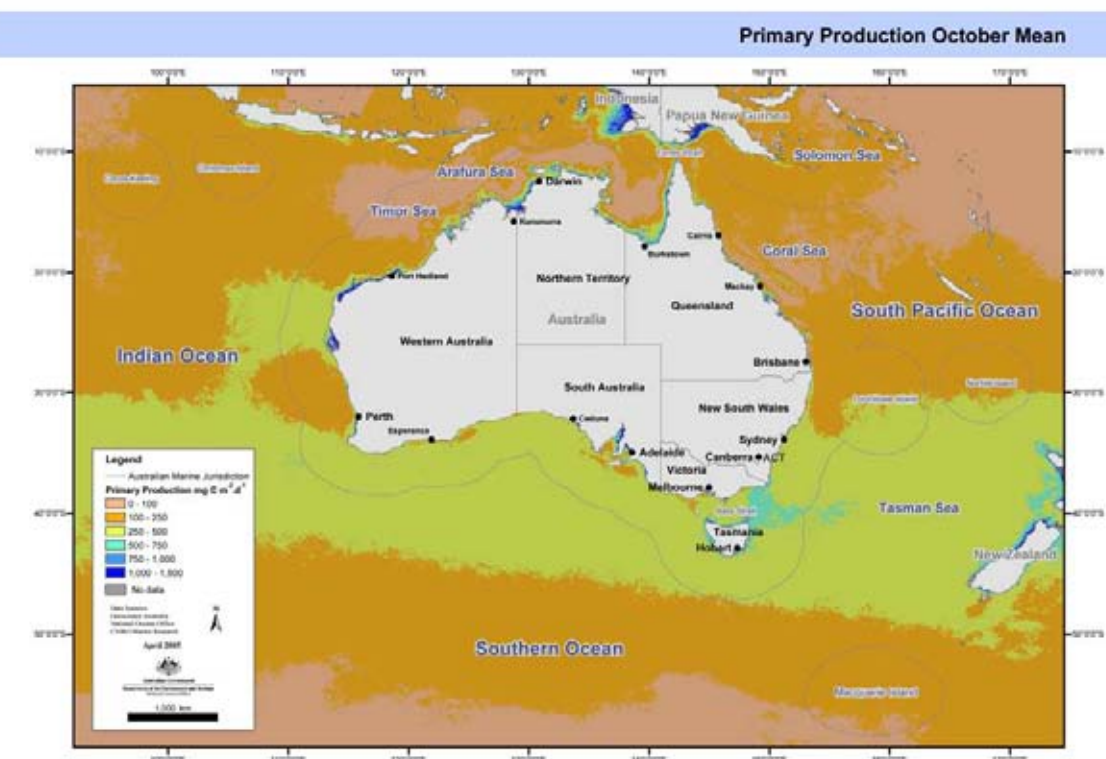


Figure 5.27 Monthly means for primary production for (a) January, (b) April, (c) July and (d) October. (cont).

In the band of extremely low production ($<100 \text{ mg C m}^{-2} \text{ d}^{-1}$) extending from the centre in January (Figure 5.27a) there is a band of moderate production ($250\text{--}500 \text{ mg C m}^{-2} \text{ d}^{-1}$) between 40°S and $50^{\circ}\text{S}\text{--}53^{\circ}\text{S}$. A low-production band to the north of this region extends south to about 40°S . This seasonal movement is repeatable, and quite dramatic when seen in movie loops of the weekly estimates of chlorophyll distribution and primary production. The primary driver for this is probably the pattern in seasonal PAR, which reaches a maximum at the end of December when the sun is highest. The other dramatic change is the very low primary production ($<100 \text{ mg C m}^{-2} \text{ d}^{-1}$) in waters north of 30°S . This is most probably due to nutrient exhaustion in the depths that the satellite can “see” to, and the formation of deep chlorophyll maxima near the thermocline or nutricline well below the depths that can be registered by the sensors on the satellite. Production is low, even in the chlorophyll maximum, because PAR is typically $<10\%$, and often $<1\%$ of surface irradiance values. The Arafura Sea region is an exception to this tropical band of extremely low production, which is possibly connected to wind mixing during the wet season of the relatively shallow waters in this region.

The band of extremely low productivity persists to April (Figure 5.27b) in waters north of 30°S , with little change in the pattern. In April, productivity south of 40°S is declining, and the latitudinal band is starting to move north as PAR decreases in autumn. The higher production around Tasmania is probably due to the interaction and interleaving of the East Australian Current extending south along Tasmania’s east coast and interacting with the Subtropical Convergence and Subantarctic waters south of Tasmania. In the Great Australian Bight, production is beginning to increase on the shelf.

In July, a combination of low sun elevation, heavy cloud cover, and of deep mixed-layers and low chlorophyll concentrations south of 40°S , means light is controlling primary production in the Southern Ocean (Figure 5.27c). Between 20°S and 40°S , the primary production is in the $100\text{--}250 \text{ mg C m}^{-2} \text{ d}^{-1}$ range, which is due to low standing stocks of chlorophyll, and possibly some light limitation. Nutrients in the water masses between these latitudes are starting to increase with the winter cooling and deepening of the mixed layer. There is moderate ($250\text{--}500 \text{ mg C m}^{-2} \text{ d}^{-1}$) production along the shelf and shelf break in the Great Australian Bight, and along the North West Shelf region of Western Australia. The increases are probably connected with increases of nutrients in the euphotic zone due to mesoscale processes associated with the Leeuwin Current in the Bight, and tidal mixing along the North West Shelf. The increased production south of Indonesia is connected with seasonal upwelling along this coast (the “Java Upwelling”), bringing cool, nutrient-rich water into the euphotic zone. The broad areas of extremely low production around the Cocos(Keeling) Islands and in the South Pacific east of New Caledonia are due to nutrient limitation of phytoplankton growth in the upper water column.

In October, the spring phytoplankton bloom is underway, especially in the Tasman Sea and Great Australian Bight regions (Figure 5.27d). There is a region of slightly elevated primary production near North West Cape off the west Australian coast. An extension of the very low production zone from east of New Caledonia to the Queensland coast is probably associated with the inflow of high-salinity, warm, nutrient-poor water from the central South Pacific. The band of extremely low production ($<100 \text{ mg C m}^{-2} \text{ d}^{-1}$) extending from the centre of the Gulf of Carpentaria through the Arafura Sea to the centre of the Timor Sea is due to low surface chlorophyll caused by low nutrient availability. There is enrichment off North West Cape from the high-chlorophyll water that moves south-east along the North West Shelf, where it splits; some flows down the Western Australia coast, and some moves offshore. A broad band of moderate production ($250\text{--}500 \text{ mg C m}^{-2} \text{ d}^{-1}$) is seen extending from about 30°S to 40°S in the west, to 50°S in the east. This is due to a combination of the development of shallow, seasonal mixed-layers that allow phytoplankton to accumulate in near-surface water, and high light intensities in the euphotic zone as the sun elevation increases towards the mid-summer maximum. The high production area ($500\text{--}750 \text{ mg C m}^{-2} \text{ d}^{-1}$) east of Bass Strait is a regular occurrence; it is due to nutrient enrichment caused by the complex mesoscale physics in this region.

It must be emphasised that the patterns of primary production are dynamic, as are the chlorophyll patterns, and there is a constant movement from week to week in the large domains, plus a great deal

of mesoscale and regional-scale patterning. There is a seasonal, north–south progression of increasing productivity and chlorophyll moving southwards from about 20°S in July/August to 55°S in January/February, and then a retreat northwards until July. North of 30°S, the pattern is for low production in July and October to be replaced by very low production from January through to May, and then returning to the July picture.

Primary Production Historical Data

Primary production was estimated from the uptake of radioactive carbon during a series of 27 research voyages on the naval frigates *Diamantina* and *Gascoyne* between 1959 and 1965. A variety of *in situ* and simulated *in situ* incubation techniques was used to produce the datasets. A variety of samplers was also used to sample zooplankton. The data have been extracted from the CSIRO Division of Fisheries and Oceanography Oceanographical Cruise Reports and collated into an Excel spreadsheet. The greatest difficulty with this dataset is that continual improvements or changes were made in the methods, as the science behind primary production work was evolving rapidly. The column integrated production data should be quite comparable between methods. It covers an area from roughly 10°N to 50°S, and 90°E to 180°E (Figure 5.28).

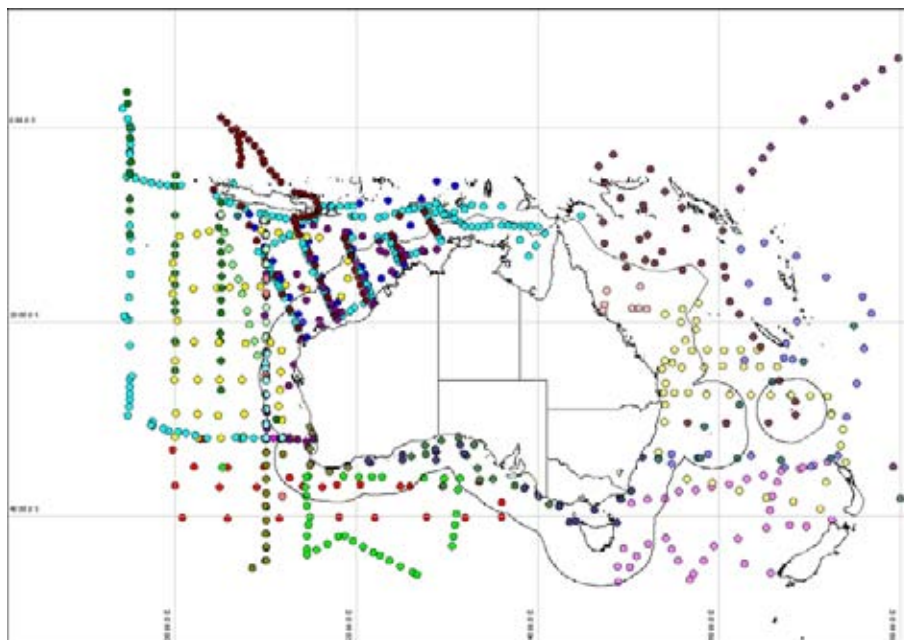


Figure 5.28 Areal coverage of 27 research voyages measuring primary production in Australian waters between 1959 and 1965.

Each dot represents a sampling station, colours represent different surveys.

Mapping

For seasonal mapping of the data, we separated the tropical north from the temperate south, using 20°S latitude based on the patterns described in sections 5.2 to 5.4. Using historical datasets, we distinguished four seasons (Table 5.3). These four seasons emphasise the difference in patterns from ship-based measurements with incomplete annual coverage and the patterns revealed by satellite oceanography.

Table 5.3 Definition of seasons for mapping

North (Latitude < 20° S)			
Low chlorophyll	Transition 1	High chlorophyll	Transition 2
Dec. to Apr.	May/June	July/Aug	Sept. to Nov.
South (Latitude > 20° S)			
Summer	Autumn	Winter	Spring
Dec. to Feb.	Mar. to May	June to Aug.	Sept. to Nov.

Six surveys, two by the *Gascoyne* (G 4/62; G 1/63) and four by the *Diamantina* (DM 1/63, DM 2/63, DM 3/63) surveyed the 110°E latitude line travelling north, resampling the same stations on the return voyage. For mapping the overlying stations the samples from the return voyage were moved by 5° to the 105° E longitude line.

Primary production data were recorded as integrated values over the depth ranges to 25, 50, 75, 100 and 150 m. We mapped only the primary production integrated over the top 100 m depth. Several methods of incubation were used over the years; only incubation by constant artificial light was mapped.

The primary production recorded over all surveys (Figure 5.29) shows to the east of Australia an overall higher productivity in the Tasman Sea region, than in the southern Coral Sea. In the north-east high variability can be detected, possibly because there were many more surveys covering all seasons in that region. In this representation all seasons were combined.

Sample coverage by season is patchy, especially for the south (Figures 5.30, 5.31). Nonetheless, these historical data-sets help interpret and check new data collected remotely by the MODIS satellite (Figures 5.26 and 5.27). The patterns in primary production calculated from ocean-colour satellite data and primary production models are broadly quantitatively similar, but do differ in fine detail. There is an urgent need to conduct more ground truth comparisons between measured primary production and primary production estimated from remote sensing data, in all areas north of the Subtropical Convergence in the Australian EEZ.

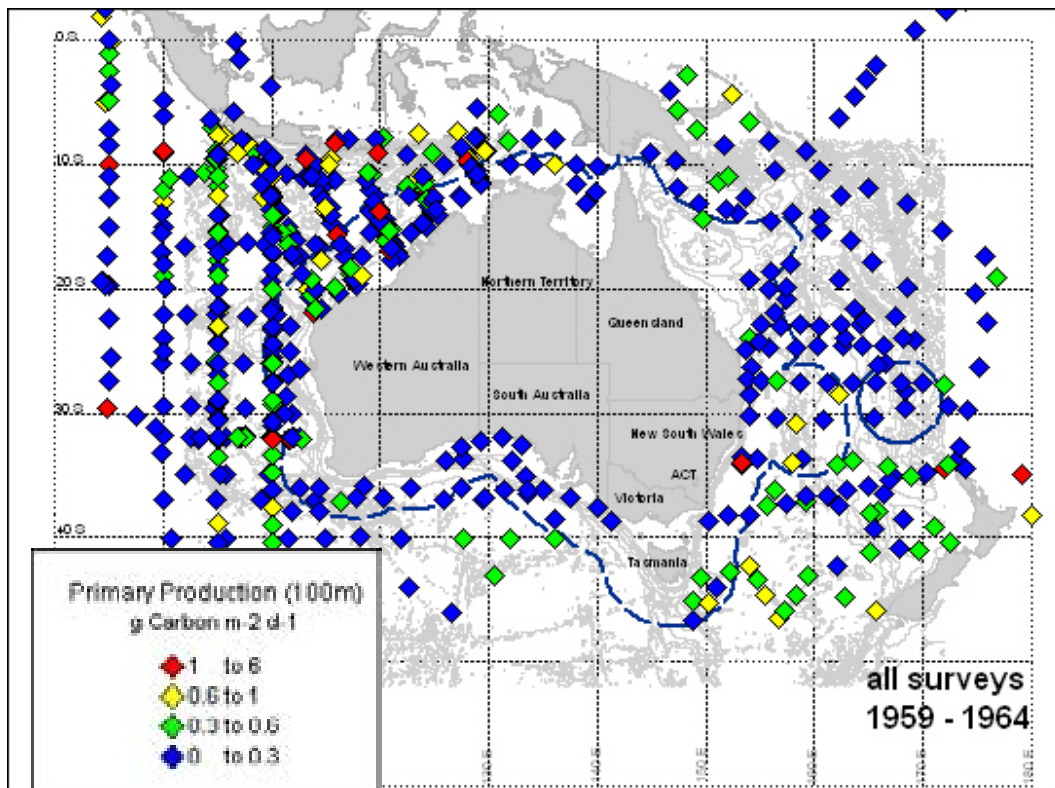


Figure 5.29 Primary productivity (grams C $\text{m}^{-2} \text{ d}^{-1}$) from 1959 to 1964.
(Samples from return trips along the 110°E latitude line were shifted to 105°E.)

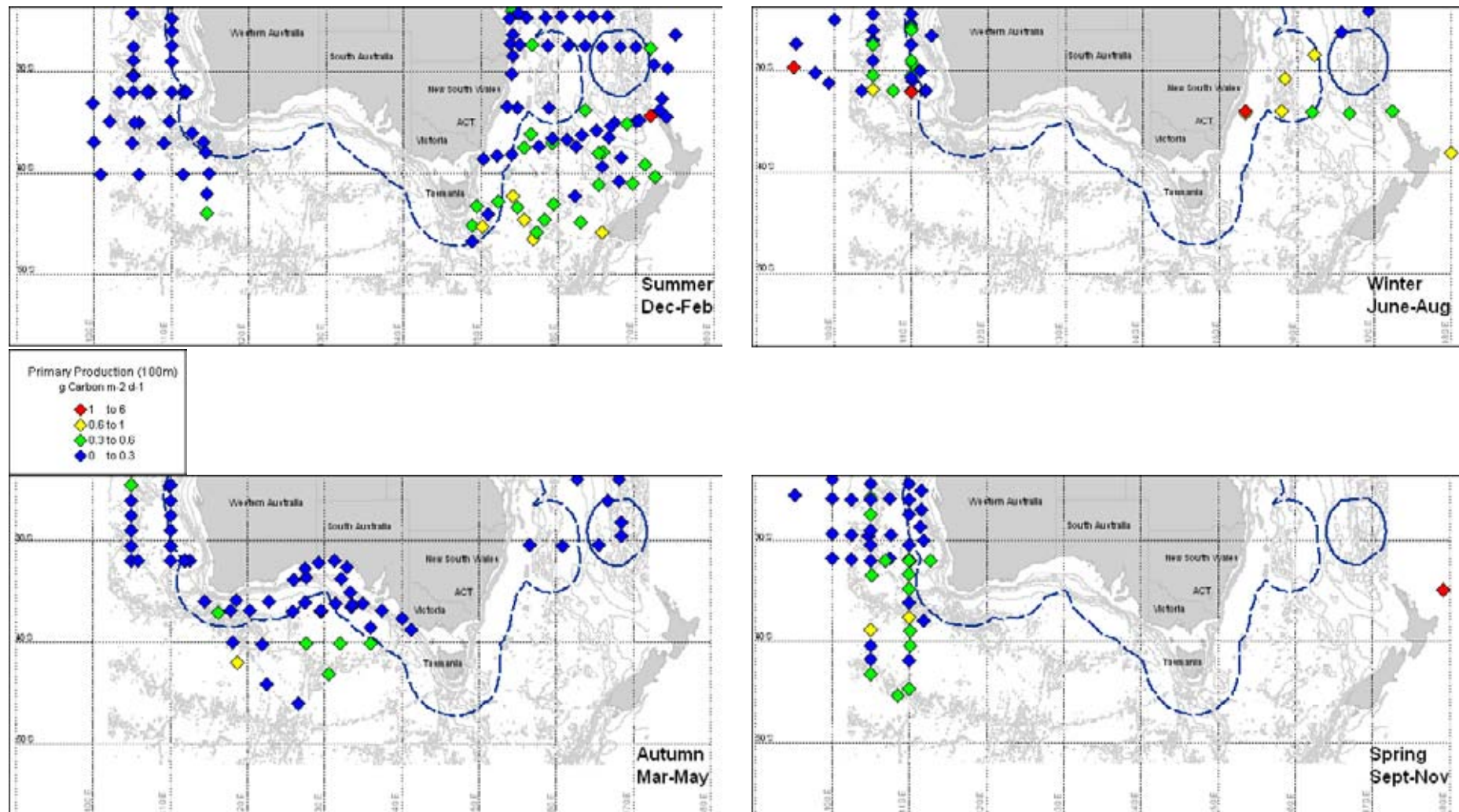


Figure 5.30 Primary productivity in southern Australian waters by southern season
(Samples from return trips along the 110°E latitude line were shifted to 105°E.)

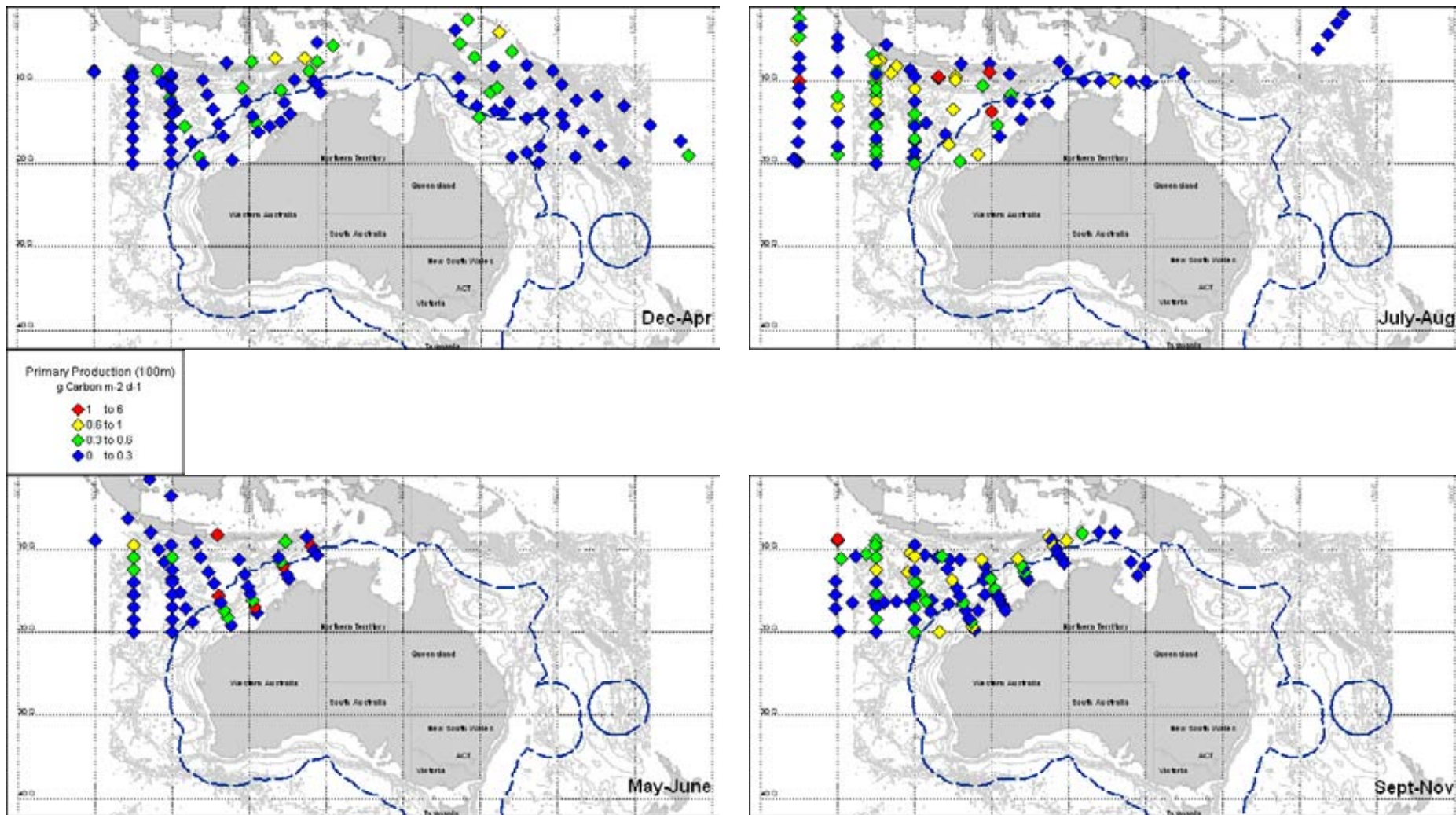


Figure 5.31 Primary productivity in northern Australian waters by northern season
(Samples from return-trips along the 110°E latitude line were shifted to 105°E.)

5.17 Zooplankton Biomass – Historical Data

Zooplankton biomass was sampled along with primary production on many of the surveys between 1959 and 1964. Four categories were consistently distinguished: zooplankton, large organisms, predominantly gelatinous organisms, and pyrosomes. Figure 5.32 shows the regional distribution of all samples taken in oblique hauls from 200 m to the surface with Clarke–Bumpus gear, indicating the biomass sampled (size of Pie-chart) and its breakdown into the four categories. Again, the area west of Australia was much more intensively surveyed. In this representation all seasons were combined. Four methods of sampling zooplankton were used: oblique hauls, integrating zooplankton from 200 m depth to the surface; horizontal hauls at depths up to 75 m; horizontal surface hauls with Clarke–Bumpus gear; and vertical hauls from 200 m depth to the surface with the Indian Ocean Standard Net. The last was used for seasonal sampling along the 110°E longitude line. Only data collected in the Clarke–Bumpus oblique hauls and the Indian Ocean standard net were mapped. Where stations were sampled in duplicate, we used the average biomass.

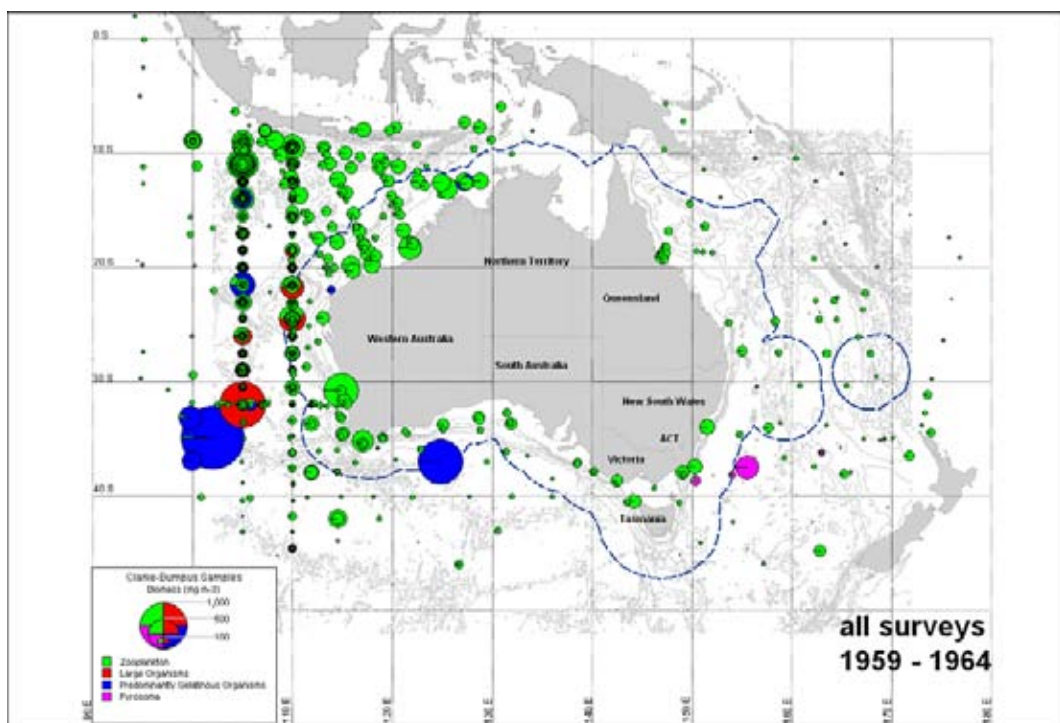


Figure 5.32 Zooplankton biomass ($\text{mg wet weight m}^{-3}$) by category
Clark–Bumpus sampler, 1959–1964 (samples from return-trips along the 110°E latitude line were shifted to 105°E).

Zooplankton biomass in the southern region was highest in winter (Figure 5.33). Gelatinous organisms appear to be highly clumped in their distribution: four samples—three in summer and one in autumn—caught large masses of these. In the northern region only the Timor Sea was sampled for zooplankton biomass (Figure 5.34). The figures do not show any clear peak season. Seasonal records of zooplankton biomass were collected along the 110°E latitude line with the Indian Ocean Standard Net (Figures 5.35, 5.36). These data were mapped by surveys from January to October. Tranter and Kerr (1969) concluded zooplankton biomass was highest in September and March, and lowest in December and June. They found biomass was relatively uniform over a wide central region (16–

27°S). Tranter (1977) found six plankton geocenoses (two tropical, two subtropical and two tropical/subtropical mixtures) from analysing copepod samples along the 110°E line. The tropical geocenoses were associated with the Java Dome, a south-east monsoonal upwelling system near the Indonesian coast. This is a region identified from the ocean-colour satellites as being extremely rich. The subtropical geocenoses corresponded with the higher salinity, cooler waters found typically south of about 20°S in the west-wind drift transition zone. Tranter (1977) considers this to be a unique area, because of its characteristic turbulence and deep mixed-layer. The tropical/subtropical geocenoses were seasonal phases, and corresponded to the central water mass in the Timor Sea, and the west-wind drift transition zone. This is the region that shows the greatest variation in chlorophyll patterns, and also the westward drift of patches of high chlorophyll, on ocean-colour images. There are no corresponding analyses of zooplankton biomass or species distributions in Australian waters in the early historical data.

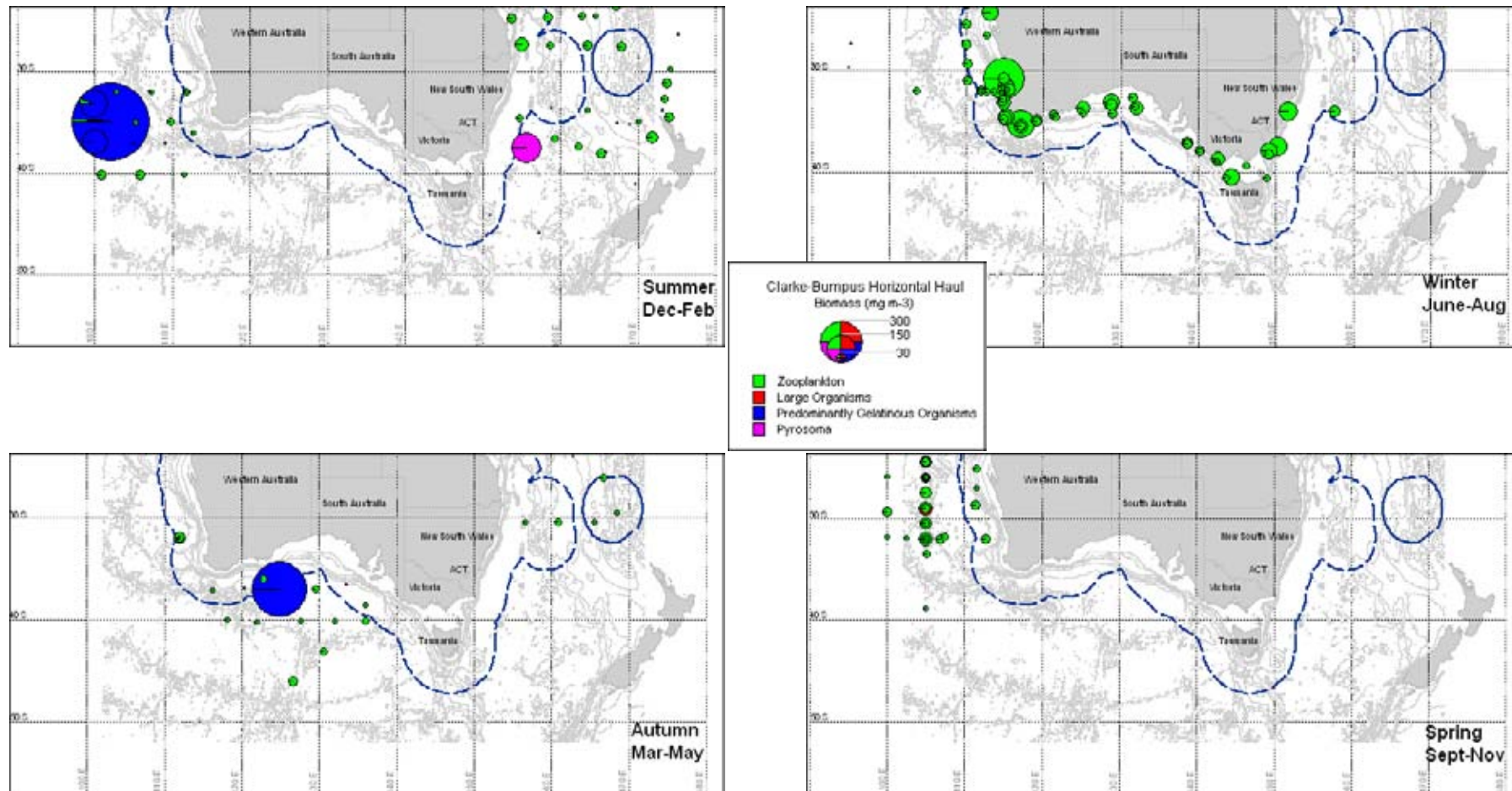


Figure 5.33 Zooplankton biomass ($\text{mg wet weight m}^{-3}$) in southern Australian waters by southern season.
Clark Bumpus oblique hauls (samples from return-trips along the 110°E latitude line were shifted to 105° E)

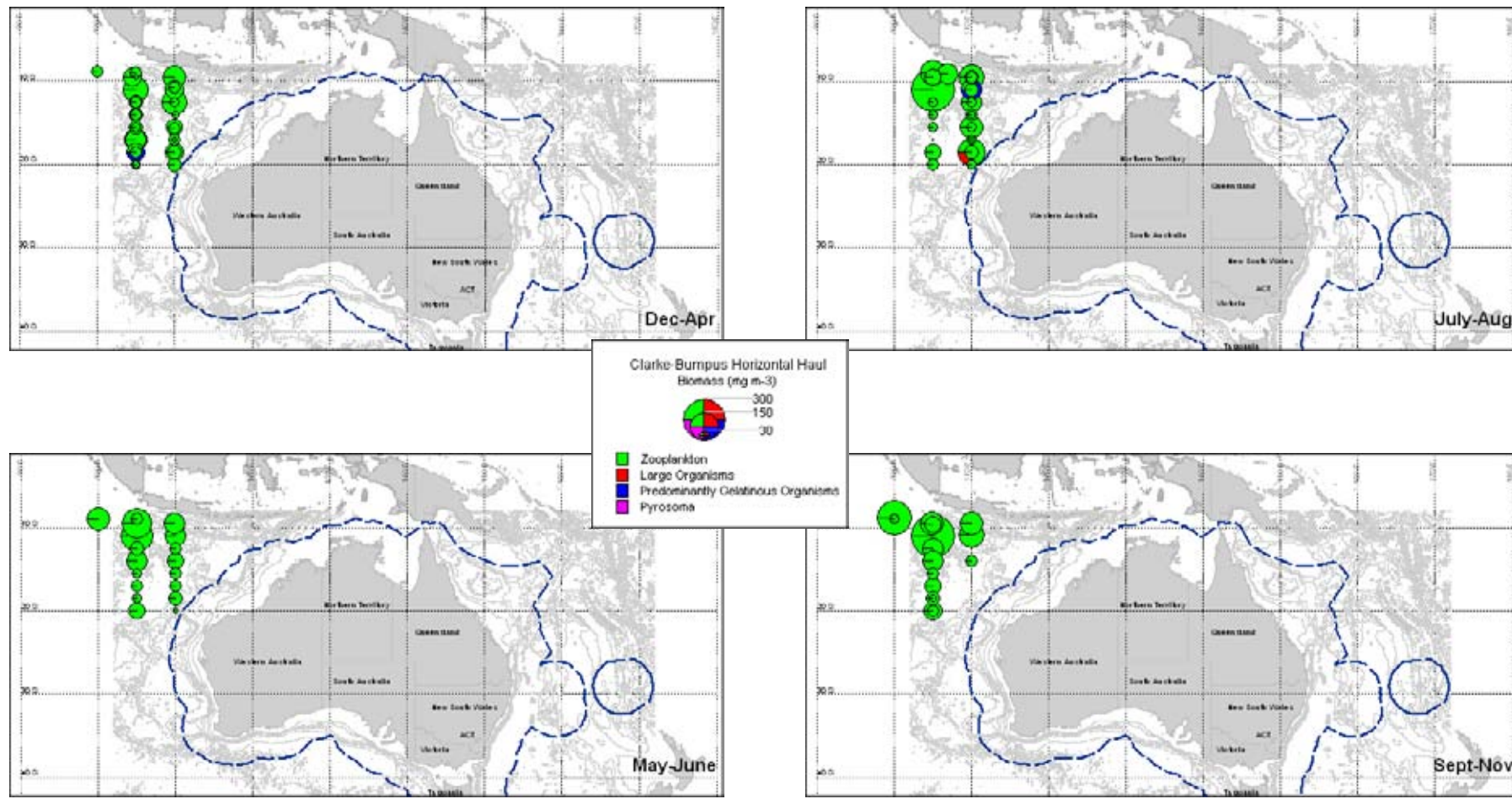


Figure 5.34 Zooplankton biomass ($\text{mg wet weight m}^{-3}$) in the Timor triangle by northern season.
Clark Bumpus oblique hauls (samples from return-trips along the 110°E latitude line were shifted to 105°E).

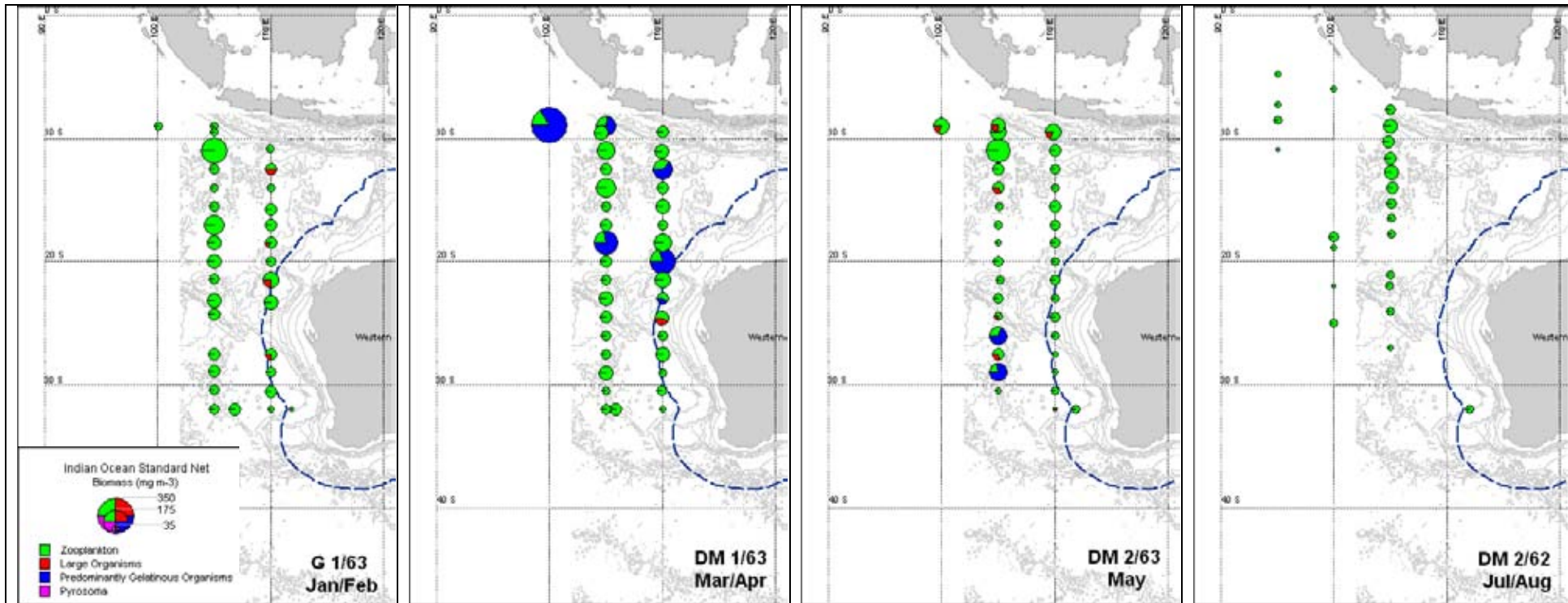


Figure 5.35 Zooplankton biomass seasonality (Jan. to Aug.) along 110° E.
Indian Ocean Standard Net (samples from return trips along the 110° E latitude line were shifted to 105° E).

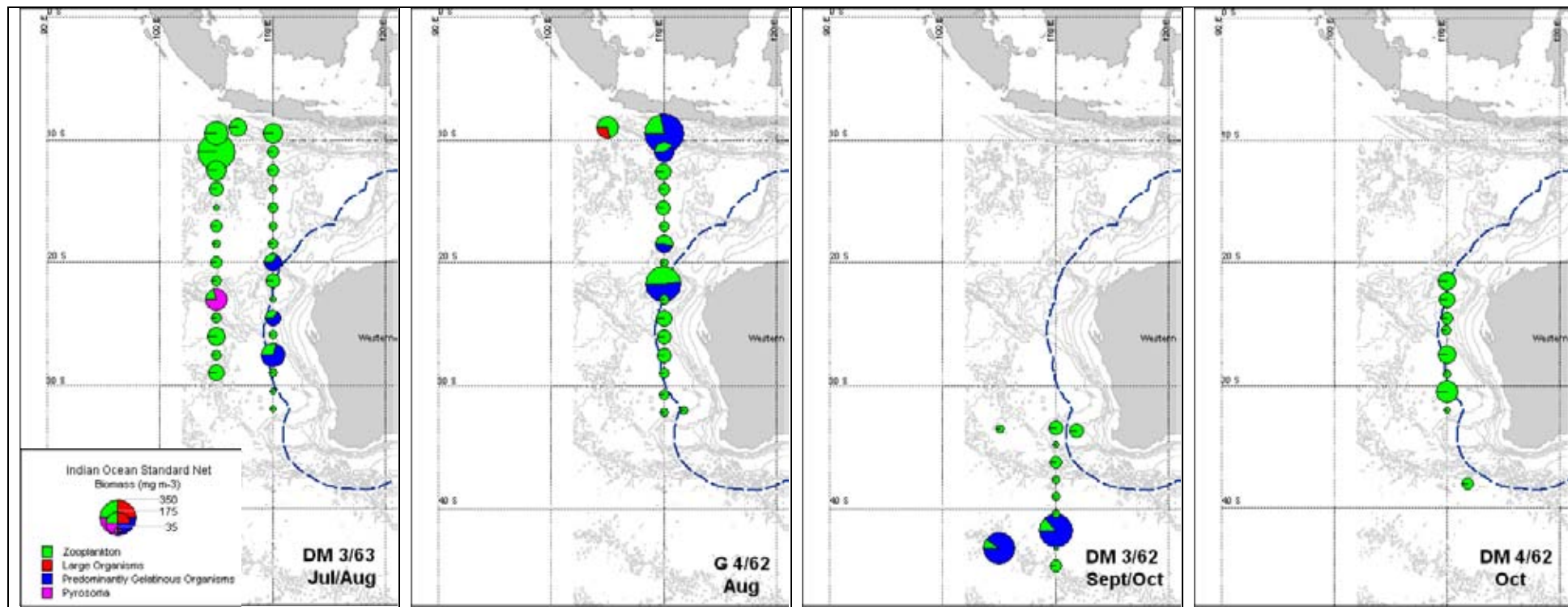


Figure 5.36 Zooplankton biomass seasonality (July to Oct.) along 110° E.
Indian Ocean Standard Net (samples from return trips along the 110° E latitude line were shifted to 105° E).

Summary

The historical data collected and described here form, despite the patchiness of sample distribution, a fairly comprehensive dataset of primary productivity and zooplankton biomass in Australian waters (Figures 5.33 – 5.36). These data not only give a historical reference point to compare new data against, but they can also be used to check patterns observed with remote sensing tools.

However, the historical datasets that have been accessible for this study do not have the temporal or spatial continuity to allow bioregions to be determined. The ocean-colour satellite observations, and estimates of primary production derived from these, give unparalleled views of the dynamics and interconnectivity of the phytoplankton processes around Australia.

The satellite observations reveal that the oceans around Australia, on the basis of the timing, duration, extent and magnitude of changes in chlorophyll *a* can be divided into three main regions: the ocean areas north of about 20°S; the ocean areas south of about 20°S; and coastal and shelf waters. In the northern area, three major basins can be distinguished: the Timor, Arafura and Coral sea. The Gulf of Carpentaria can be considered a subregion of the Arafura Sea. These basins differ in the timing of the seasonal increase and decrease in surface chlorophyll *a*, and the primary production estimates derived from these estimates. South of 20°S, the subtropical regions east (Tasman Sea) and west (South Indian Ocean) of Australia down to the Subtropical Convergence form two related, but geographically separate, regions. These regions are linked by the waters influenced by the Leeuwin Current between the southern coast of Australia and the Subtropical Convergence. South of the Convergence, the Subantarctic and Polar waters form a continuous band through the Australian EEZ, and show the strong seasonal patterns expected in temperate and cooler waters. Further studies combining *in situ* and satellite observations are needed if finer bioregional patterns are to be distinguished.

The other main result revealed by the satellite data is the interconnectivity of the regions: the patterns of seasonal changes are related to ocean circulation, and any one region cannot be treated independently from the oceanic and seasonal processes in adjacent regions. This is particularly evident in the spring increase that starts in the north near 25°S in the Tasman Sea in subtropical waters and spreads south to the Polar waters between 53° and 56°S. It retreats again during winter. It is also seen in the river-like movement of higher chlorophylls that start close to the Joseph Bonaparte Gulf, spreading south-west along the North West Shelf, and splitting into an offshore component at North West Cape and a coastal, southward component extending along the Western Australian coast into the Great Australian Bight. These patterns and regions are repeatable over time and space, but there are interannual variations in both the timing and magnitude of the patterns seen. These variations will have the greatest impact on short-term events such as successful or unsuccessful fish recruitment. Any attempt at bioregionalisation must take into account this interconnectivity of the regions.

6 Marine Phytoplankton Perspective on Australian Pelagic Bioregionalisation

6.1 Background

Significant early investigations of the taxonomy and distribution of marine microalgae in Australian seas were made in the Great Barrier Reef region (Marshall 1933), the Java Sea (Allen & Cupp 1935), Sydney coastal waters (Dakin & Colefax 1933, 1940) and the Australia-wide surveys of netphytoplankton (Wood 1954). The first effort to produce an Australian map of marine phytoplankton provinces (based on dinoflagellate associations) was by Wood (1954). Although hampered by limited taxonomic discrimination, this work is impressive in its sample coverage and produced the first conclusive biological evidence for the existence of what is now called the Leeuwin Current. A subsequent bioregionalisation effort by Markina (1972) was limited to net phytoplankton on the west coast of Australia.

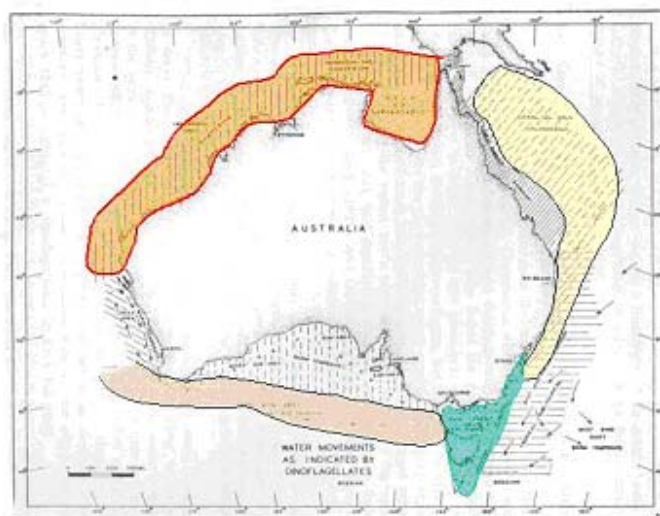


Figure 6.1 An early effort towards pelagic bioregionalisation by Wood (1954) based on dinoflagellate communities.

In the period 1978 to 1984, under the auspices of a series of CSIRO Division of Fisheries & Oceanography cruises, significant advances were made in plankton collection methods (finer-mesh plankton nets, water-bottle sampling, more delicate preservatives, enrichment cultures, satellite oceanography) and notably the use of electron microscopy for species identification considerably improved our knowledge of marine microalgal species communities in the Australian region. Classic studies were published on New South Wales coastal waters (Hallegraeff & Reid 1986, Hallegraeff & Jeffrey 1993), East Australian Current eddies (Jeffrey & Hallegraeff 1980, 1987), the Coral Sea (Revelante & Gilmartin 1982, Revelante *et al.* 1982) and the North West Shelf and Gulf of Carpentaria (Hallegraeff & Jeffrey 1984, Rothlisberg *et al.* 1994).

A new recognition from the modern work was the importance of delicate nanoplankton flagellates (2–20 µm size) and minute coccoid picoplankton (0.2–2 µm size). Despite their size, they can

account for up to 90% of total phytoplankton chlorophyll biomass, except during episodic large blooms of diatoms or dinoflagellates (Hallegraeff 1981). Few of these species would have been recognised had the older harsh preservatives or coarse ($>20\text{ }\mu\text{m}$ mesh) plankton nets been used. As elsewhere in the world, Australian nanoplankton is primarily composed of haptophytes (notably *Chrysochromulina* spp. and calcareous coccolithophorids), prasinophytes and small unarmoured dinoflagellates, chrysophytes, cryptomonads and small diatoms (e.g. *Minidiscus*, *Nitzschia*, *Thalassiosira*), while picoplankton is composed of prokaryote cyanobacteria (e.g. *Synechococcus*) and prochlorophytes (e.g. *Prochlorococcus*) (Hallegraeff 1983, Jeffrey & Hallegraeff 1987, LeRoi & Hallegraeff 2004, Moestrup 1979).

Surprisingly, the nanoplankton communities of Australian tropical and temperate, inshore and offshore waters appeared remarkably similar. In contrast, the netphytoplankton diatoms and dinoflagellates (20 to 200 μm size) could be differentiated into a temperate neritic community of coastal waters of New South Wales, Victoria and Tasmania, a tropical neritic community confined to the Gulf of Carpentaria and North-west Australia, and a tropical oceanic community in the offshore waters of the Coral Sea and Indian Ocean. Tropical netphytoplankton diatoms (*Bacteriastrum*, *Planktoniella*) and dinoflagellates (*Histioneis*, *Ornithocercus*) are characterised by ornate morphologies with hair- or wing-like extensions as well as the incidence of many symbiotic associations (e.g. dinophysoid dinoflagellates with cyanobacterial exosymbionts, symbiotic dinoflagellate zooxanthellae with tropical zooplankton). Occasionally, typical warm-water species are found in subtropical or temperate waters. This results from tropical waters penetrating southwards in the Leeuwin Current as it extends from the Indian Ocean through the Great Australian Bight to the west coast of Tasmania, and the East Australian Current stretching from the Coral Sea down to the east coast of Tasmania (Jeffrey & Hallegraeff 1990, Hallegraeff 1995).

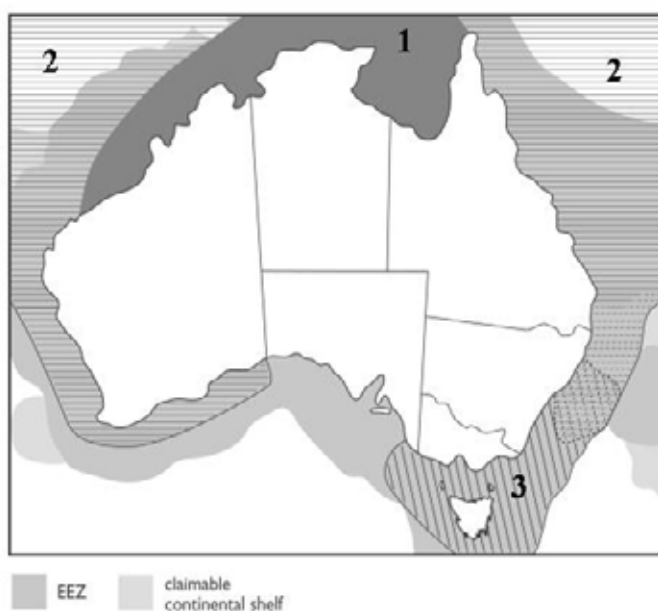


Figure 6.2 Three main phytoplankton bioregions recognised by Jeffrey & Hallegraeff (1990): 1. tropical neritic; 2. tropical oceanic; 3. temperate neritic.

New phytoplankton species data that have become available since 1990 include further Gulf of Carpentaria work by Rothlisberg *et al.* (1994) and Burford *et al.* (1995), Burford & Rothlisberg (1999); Great Barrier Reef surveys by Furnas & Mitchell (1996, 1999); New South Wales coastal studies by Ajani *et al.* (2001) and Lee *et al.* (2001); University of Western Australia eddy cruises by Waite and others (Waite 2004, unpublished); South Australian Shellfish Quality Assurance

Program algal surveys by Wilkinson (2004); Bass Strait phytoplankton surveys by University of Melbourne students (Blasé, Hill, McFadden, unpublished); and extensive Tasmanian surveys by Hallegraeff and students (Hallegraeff & Westwood 1995; Hallegraeff 2002). Dinoflagellate cyst surveys of all the main Australian ports between 1990 and 2004 (McMinn 1990, Bolch & Hallegraeff 1990, unpublished) have further confirmed the phytoplankton biogeographic boundaries described here. These mostly qualitative phytoplankton species data have been supplemented by SeaWiFS synoptic surveys of surface phytoplankton chlorophyll surveys (available since 1997). It is emphasised, however, that the relationship between surface chlorophyll and total water column chlorophyll varies significantly, depending on the season and region. The present work seeks to update the early phytoplankton bioregions as delineated by Jeffrey & Hallegraeff (1990), taking into account additional phytoplankton data collected from 1990 to 2004.

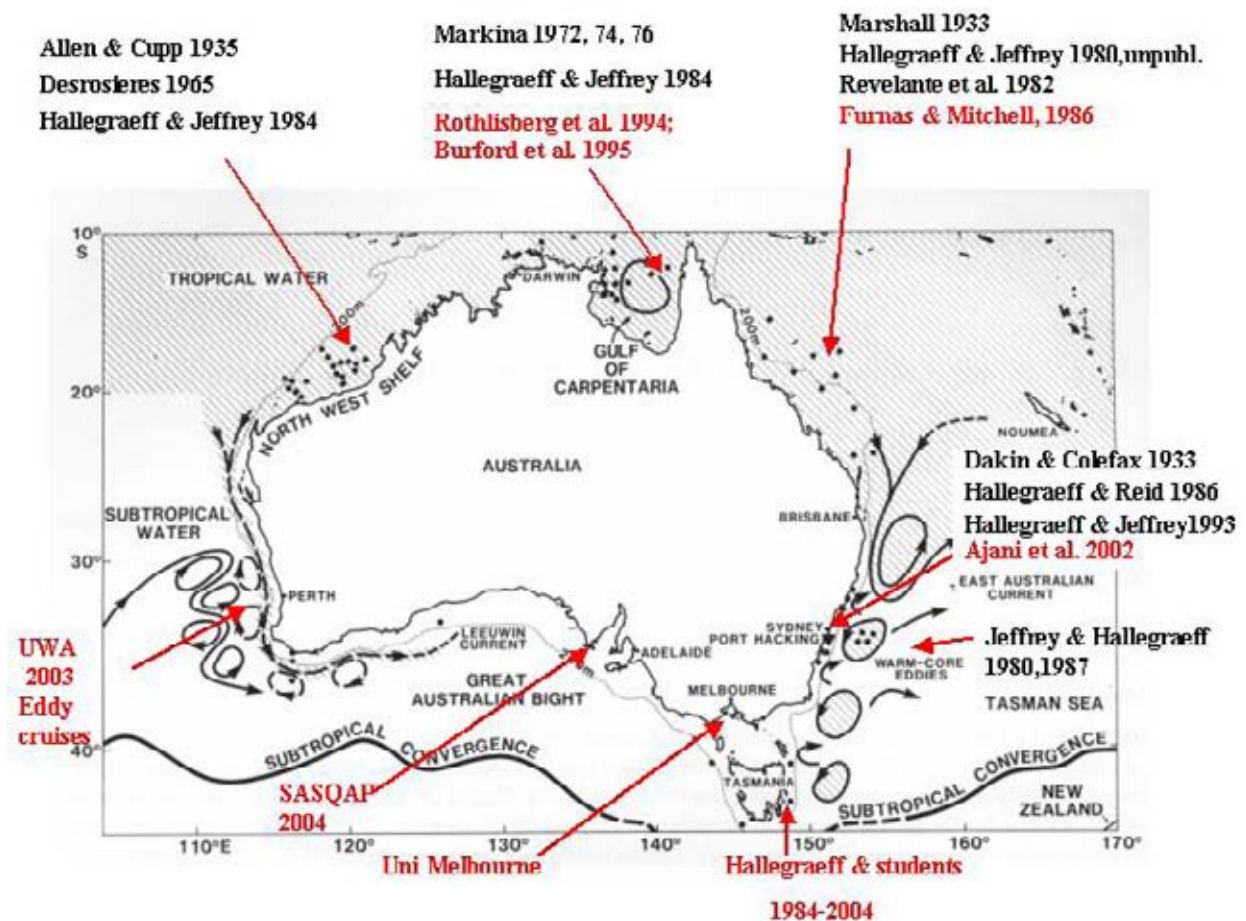


Figure 6.3 The phytoplankton dataset available for the present work.
Data in red have become available since Jeffrey & Hallegraeff (1990). Note the absence of phytoplankton information for the region between Cape Leeuwin and Adelaide.

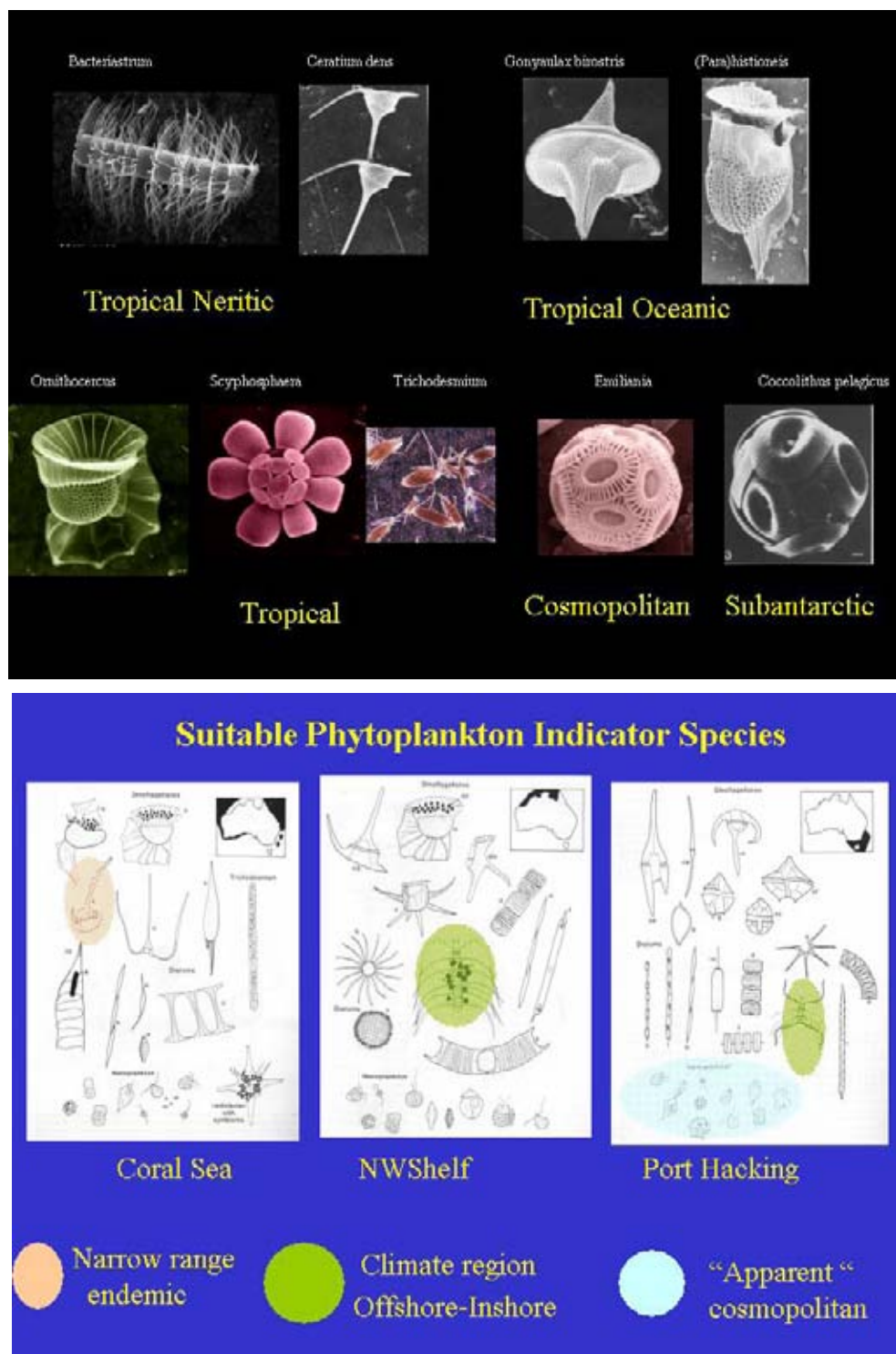


Figure 6.4 Examples of key phytoplankton indicator species used to discriminate between tropical and temperate, neritic and oceanic, cosmopolitan and subantarctic communities.

Typical Coral Sea taxa illustrated on the box on the left include Ceratium, Ornithocercus, Histioneis, Podolampas, Climacodium, Pseudo-nitzschia, Rhizosolenia clevei, Richelia; Typical NW Shelf taxa illustrated in the middle box include Ceratocorys, Ceratium dens, Dinophysis miles, Ornithocercus, Synechocystis consortia, Chaetoceros coarctatus, Vorticella, Detonula, Eucampia, (Pseudo)-nitzschia, Rhizosolenia, Thalassiosira; typical Port Hacking taxa are illustrated in the right box and include Ceratium, Prorocentrum, Gonyaulax, Protoperidinium, Scrippsiella, Skeletonema, Leptocylindrus, Pseudo-nitzschia, Ditylum, Thalassiosira, Asterionellopsis, Chaetoceros, Rhizosolenia, Eucampia.

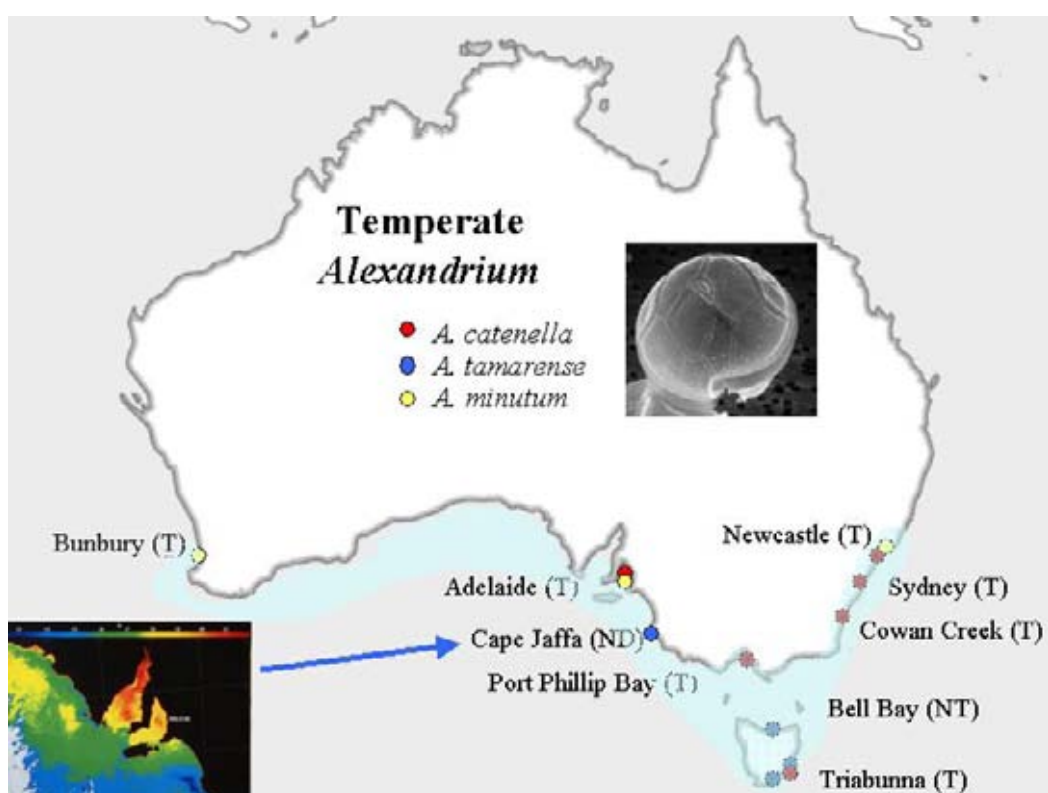
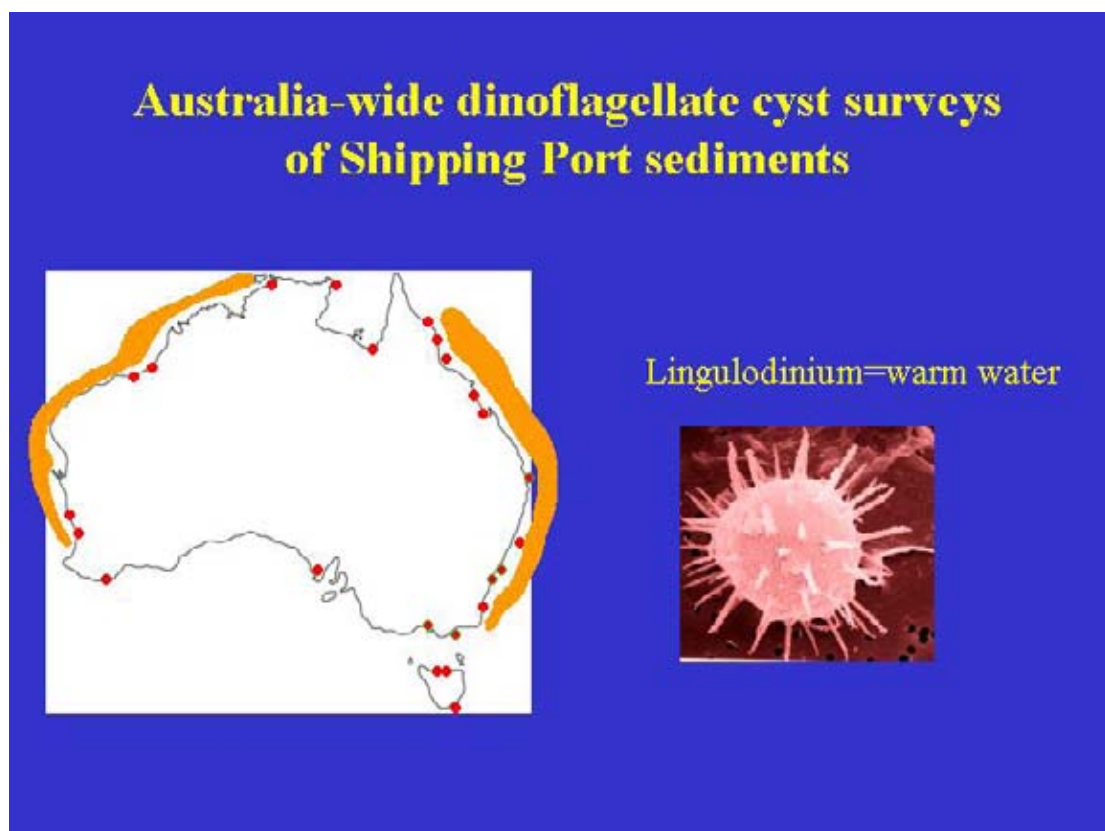


Figure 6.5 The results of comprehensive Australia-wide cyst surveys support the biogeographic boundary between warm-water species (e.g. dinoflagellate cyst type *Lingulodinium* (in orange; top figure) and temperate species (toxic *Alexandrium* dinoflagellates (in blue, bottom figure).

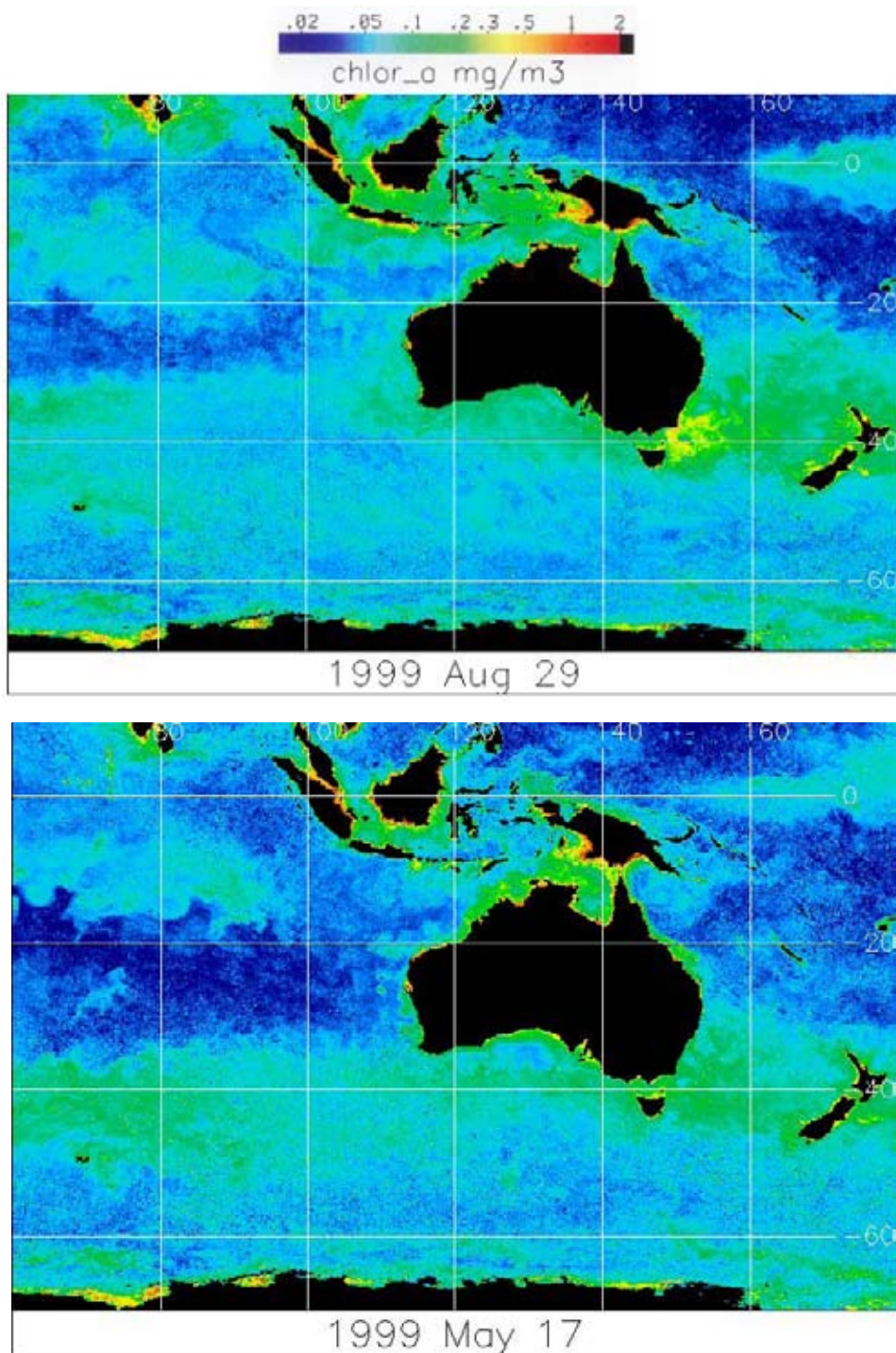


Figure 6.6 Examples of typical SeaWiFS images of surface phytoplankton chlorophyll showing significant spring bloom activity in the south in the Sydney–Tasmania region in the top map (August 1999), and nutrient-enrichment phenomena on the North West Shelf/Gulf of Carpentaria in the bottom map (May 1999). Data courtesy CSIRO.

6.2 Characterisation of Australian Marine Phytoplankton Provinces

1 Tropical Indian Ocean Shelf Province

The phytoplankton of the shelf waters of north-west Australia, the Gulf of Carpentaria, Arafura Sea and Timor Sea is basically a diatom flora, distinctly different from the oceanic, predominantly dinoflagellate, flora of the Coral Sea and Indian Ocean. Large, morphologically elaborate, tropical netphytoplankton diatoms include *Bacteriastrum*, *Chaetoceros*, *Coscinodiscus*, *Pseudo-nitzschia*, *Rhizosolenia*, *Thalassiosira*, *Thalassionema* and *Thalassiothrix*, with the tropical dinoflagellates *Ornithocercus* and the endemic *Ceratium dens* also common. Water-column chlorophyll values in both North West Shelf and Gulf waters range from 10 to 55 mg/m². The three biomes specified below are discriminated on the basis of subtle differences in species dominance, as well as patterns of phytoplankton chlorophyll biomass.

1a North West Shelf

Nutrients are supplied to the North West Shelf through a combination of barotropic and internal tidal motions, summertime wind-driven upwelling, and episodic cyclone events (Holloway *et al.* 1985). Nitrate is rapidly consumed and is usually depleted in depths less than 50 m. Phytoplankton tends to concentrate below the thermocline or in the bottom mixed-layer, but primary production rates are high even in shallow water because of the rapid recycling of nutrients (Ayukai & Miller 1998, Furnas & Mitchell 1999).

1b Arafura Sea / Gulf of Carpentaria

The Arafura Sea and Gulf of Carpentaria form a large, shallow, semi-enclosed basin bounded by Australia and New Guinea. The monsoon produces substantial riverine inputs of freshwater and sediments into the gulf. The phytoplankton community in the Gulf of Carpentaria consists mainly of large diatoms, cyanobacteria (*Trichodesmium*), and nanoplankton. Within the turbid coastal zone, primary production rates are high and usually light-limited (Rothlisberg *et al.* 1994), but these rates have been reported to increase by 70% when stratification develops during summer (Burford and Rothlisberg 1999). Wintertime enhancement of the phytoplankton chlorophyll biomass by a factor of two to three has also been observed.

1c Central Gulf of Carpentaria

The turbid coastal zone in the Gulf of Carpentaria is characterised by enhanced silicate levels, but relatively low nitrate and phosphate (Burford *et al.* 1995). As such it contrasts with the Central Gulf where during summertime stratification nutrients tend to accumulate in the lower water column. Discrete subsurface blooms of small *Thalassiosira* diatoms characterize this zone.

2 Tropical Oceanic Province

2a Tropical Eastern Indian Ocean

There are two main water masses that occupy the eastern Indian Ocean. The first is Indonesian Throughflow Water, which derives from Pacific Ocean Central Water. It is formed during transit through the Indonesian archipelago, where high precipitation lowers the salinity. The water enters the Indian Ocean between Timor and the North West Shelf and through the various passages between the islands east of Bali. It spreads across the central Indian Ocean as a zonal low-nutrient, low-salinity tongue. The interface between the jet-like flow of Indonesian Throughflow Water and the eastward penetration of the South Indian Central Water produces a massive frontal region between 10 and 15°S. The second is the subtropical water mass South Indian Central Water, formed and subducted in the Subtropical Convergence from the western Indian Ocean into the Great Australian Bight. The phytoplankton of this oligotrophic zone is characterised by tropical dinoflagellates, many of which are also found in the offshore Coral Sea.

2b The Leeuwin Current

The west Australian coastline is the geographical analogue of the eastern boundary current regions of the Atlantic and Pacific oceans. The Leeuwin Current is fed by nutrient-poor Indonesian Throughflow Water and inflow from the west effectively suppresses any upwelling of nutrients, generally resulting in oligotrophic conditions. Nutrient levels in the undercurrent are somewhat higher, being derived from South Indian Central Water. Surface chlorophyll levels are generally low in the Leeuwin Current, although they increase in winter when exchange with more productive shelf waters increases as the current strengthens. While there is a general decline in surface chlorophyll as summer approaches and the current weakens, there is evidence of a persistent subsurface chlorophyll maxima near the nutricline both on the shelf and offshore. The Leeuwin Current and its associated eddy field can carry tropical planktonic organisms (e.g. the coccolithophorid *Scyphosphaera*, cyanobacterium *Trichodesmium*) many hundreds of kilometres, as far as Tasmania. The wintertime eastward extension of the Leeuwin Current coincides with enhanced chlorophyll in the Great Australian Bight, where summer brings a general decline in chlorophyll. Limited phytoplankton species data from off Western Australia suggest that the different species composition on the continental shelf may be different to that in the Leeuwin Current itself (Hanson 2004).

2c Tropical Southwest Pacific

Coral Sea phytoplankton communities include diatoms, cyanobacteria, and a great diversity of tropical dinoflagellates (Jeffrey & Hallegraeff 1990). Cell concentrations are generally very low and nanoplankton and picoplankton form a high percentage of total chlorophyll (70–95%), consistent with the oligotrophic nature of the environment. Ocean-colour imagery suggests higher chlorophylls are present in the Coral Sea region from April to August when the south-east trade winds are blowing. While surface values generally remain low for the remainder of the year, deep chlorophyll maxima within the seasonal pycnocline (down to 150 m depth) are probably present throughout the year.

2-D The East Australian Current system

The East Australian Current advects mainly oligotrophic Coral Sea water along the east coast. At prominent coastal features (Cape Byron, Smoky Point) the current moves away from the coast, driving upwelling, which draws nutrient-rich water from a depth of 200 m or more. However, while the current may drive nutrient-rich water onto the shelf, upwelling-favourable winds (northerly) are needed to bring that water to the surface. The eddies themselves are also important

for nutrient cycling and biological productivity. In a phytoplankton study of eddy F (Nov–Dec 1978), higher diatom biomass was found at the centre, a dominance shift from *Pseudo-nitzschia* (centre) to *Proboscia* (edge), and the concentration of dinoflagellates decreased at the eddy centre (Jeffrey & Hallegraeff 1980). In contrast, in eddy Mario (April–May 1981) the centre and western margin were enriched with *Pseudo-nitzschia* and *Proboscia*, with tropical flora (*Trichodesmium*, *Scyphosphaera*, *Richelia*) flooded throughout the eddy system (Jeffrey & Hallegraeff 1987).

3 Great Barrier Reef Lagoon

The Great Barrier Reef system is made up of almost 3000 individual coral reefs extending 2600 km along Australia's east coast from the Tropic of Capricorn in the south to the coast of Papua New Guinea in the north. Tides are the dominant motions. Nearshore, riverine inputs can significantly affect salinity levels and suspended sediment loads. While nutrients levels are usually relatively low in the lagoon, there are episodic influxes through near-bottom intrusions associated with upwelling along the outer shelf (Furnas & Mitchell 1996). The Great Barrier Reef supports a diverse phytoplankton community (Revelante & Gilmartin 1982). The outer-shelf is dominated by nanoplankton and picoplankton, with larger diatoms becoming more prominent during intrusion events from offshore. Dinoflagellates appear to outcompete diatoms on the mid-shelf, but this reverses on the inner-shelf, where sediment-laden river plumes are present (Revelante *et al.* 1982). The Great Barrier Reef lagoon itself is dominated by fast-growing nanoplankton diatoms.

4 Temperate neritic province of New South Wales, Tasmania, Victoria, South Australia

New South Wales

The New South Wales shelf experiences species successions from small diatoms to large dinoflagellates over spring and summer (Hallegraeff & Jeffrey 1993). However, when upwelling associated with the East Australian Current carries nutrient-rich water into the euphotic zone, short-lived (days to weeks) diatom blooms can result; they may be critically important for larval recruitment of both pelagic and benthic species.

Bass Strait

Nutrient levels in central Bass Strait are low throughout the year, but increase substantially along the eastern edge during winter when the cold-water front is present. There are seasonally predictable phytoplankton blooms (in September) along the shelf break at the eastern end of Bass Strait. There are also occasional short-lived (days to weeks) chlorophyll patches in the Point Hicks–Cape Howe region that probably result from upwelling in this region associated with favorable combinations of winds, tides and currents. Constant tidal motions in the relatively shallow environment of Bass Strait result in increased standing stocks of chlorophyll that are exported eastwards (Gibbs *et al.* 1991).

Tasmania

The well-studied phytoplankton communities of Tasmanian waters (Hallegraeff & Westwood 1995) show broad similarities with those of Sydney coastal waters. Episodic diatom blooms of *Pseudonitzschia* appear to be driven by seasonal intrusions of nitrate-rich shelf water.. Dinoflagellates dominance in Tasmanian estuaries (*Ceratium*, *Dinophysis*, *Gymnodinium*) may be related to humic substances from land runoff limiting light penetration and influencing micronutrient chemistry. Blooms in late summer / autumn of the introduced toxic dinoflagellate *Gymnodinium catenatum* (since 1980) show no correlation with macronutrients (nitrate, phosphate) but instead appear to be related to rainfall events and periods of low windstress. Episodic incursions of cold-water Subantarctic (diatom *Chaetoceros criophilum*, dinoflagellate

Dinophysis truncata) and warm-water East Australian Current species (diatom Bacteriastrum furcatum) have also been reported, with the red tide dinoflagellate Noctiluca (since 1994) appearing to be a recent recent extension from New South Wales.

Southern Australia

Regular summer upwelling occurs off the Eyre Peninsula, Kangaroo Island, the Bonney Coast (Robe to Portland) and eastern Victoria. The most prominent events occur along the Bonney Coast, where classical upwelling plumes of low-temperature surface water and increased chlorophyll biomass are regularly observed. Nitrate levels have been observed to increase by factors of 30 to 70 during upwelling events on the Bonney Coast (Lewis 1981).

5 Transitional Zone

A highly variable oceanic transition zone, distinct from inshore phytoplankton communities and embedded tropical flora, is bordered to the South by a phytoplankton-rich Subantarctic phytoplankton province.

6 Subantarctic

The region polewards of the Australian mainland north of the Antarctic Circumpolar Current provides a major pathway for the exchange of mass and heat between the Pacific and Indian Ocean basins. It encompasses the Subtropical Front, which follows a nearly zonal path along 40°S before looping poleward around the southern tip of Tasmania. Cold-water indicator species include the coccolithophorid *Coccolithus pelagicus* and the diatom *Fragilaropsis curta*, which occasionally appear on Tasmania's west coast (Hiramatsu & De Deckker 1996, Findlay & Flores 2000, Scott & Marchant 2005).

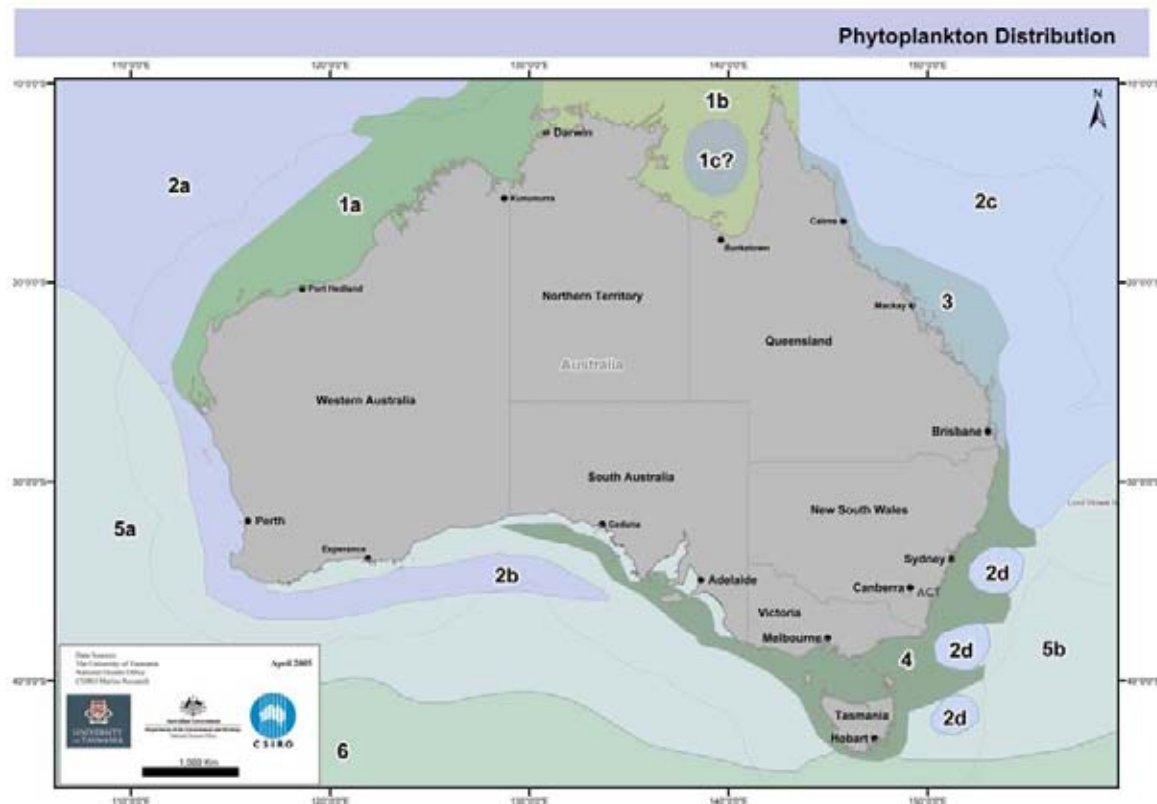


Figure 6.7 Phytoplankton provinces in Australia

(1) comprising the shelf waters of north-west Australia, the Gulf of Carpentaria, Arafura Sea and Timor Sea is basically a tropical diatom flora (keystone species are *Bacteriastrum*, *Chaetoceros*, *Coscinodiscus*, *Rhizosolenia*, *halassionema*, *Thalassiothrix*). Subtle differences in species dominance and phytoplankton chlorophyll biomass are discriminants of the biomes 1 a, b, c. The floristically largely distinct shallow waters of the Great Barrier Reef lagoon (3) are dominated by fast-growing nanoplankton diatoms. These tropical neritic communities are distinct from the tropical oceanic, predominantly dinoflagellate flora (*Gonyaulax birostris*, *Histioneis*, *Ornithocercus*) of the Indian Ocean (2a) and Coral Sea (2c), which are carried southwards by the Leeuwin Current (2b) and East Australian Current (2-D), respectively. The productive temperate neritic province (4) comprising coastal waters of New South Wales, Tasmania, Victoria, and South Australia exhibits predictable succession patterns of phytoplankton species from small diatoms (*Asterionellopsis*, *Pseudonitzschia*, *Skeletonema*, *Thalassiosira*) to large diatoms (*Detonula*, *Ditylum*, *Eucampia*) to larger dinoflagellates (*Ceratium*, *Protoperidinium*), in response to nutrient enrichments from current-induced upwellings. A highly variable oceanic transition zone (5), distinct from inshore phytoplankton communities (4) and embedded tropical flora (2b,d), is bordered to the south by a Subantarctic phytoplankton province (6), where the coccolithophorid *Coccolithus pelagicus* is an indicator organism.

7 Water Mass Formation and Subduction

7.1 Introduction

The tropics are usually thought of as invariably warm, so it is surprising that waters of very low temperature can also be found there. These cold waters originate from polar regions where surface waters are cooled, become denser, sink deep into the ocean and slowly make their way along the abyssal pathways to tropical areas. This circulation of cold, deep water to the tropics and warm waters to the poles results in exchanges of heat (energy) and water mass that has the effect of stabilising the properties of the oceans, atmosphere and land. In places, the cooling process is not intense enough for deep convection and waters of intermediate density are formed that flow along intermediate depths in the ocean.

The movement of water from the surface is called subduction. It is driven by wind stresses, and by mixing and convection. In certain places, the rotation of the earth combined with patterns of wind stresses causes upwellings or downwellings of water masses through the so-called Ekman pumping effect.

This section will describe the formation and subduction of Subantarctic Mode Water (SAMW), which is one of the major types of water mass found around the oceans of Australia. Figures 7.1 and 7.2 show that SAMW lies between the so-called Subtropical Lower Water (SLW) and Antarctic Intermediate Water (AIW). The surface signature of SAMW is found in the subantarctic waters to the south of Australia, where it is formed by winter cooling causing deep convection. The cooling is, however, not as intense as that at the poles, and so water of intermediate density is formed. It descends to over 600 m and subsequently flows towards the tropics, where it rises gently through the mediation of mixing, diffusive exchange processes and upwelling/downwelling to change its density. We attempt to follow the path of this water mass from its formation through to its spread to various parts of the oceans around Australia, and we describe how the character of the water mass changes as it interacts with surrounding waters and topographic influences.

7.2 Mode Waters

The SAMW is an example of a water body termed “Mode Water”. Mode waters have their properties set when intense heat/moisture exchange with the atmosphere results in deep and extensive surface mixing that may extend to 400 m depth or more in the subantarctic region. In the tropics, the greater stratification of waters and less exchange with the atmosphere result in mixed layers being generally shallower. Thus, much of the mode waters are formed in polar and subpolar regions. The formation of mode waters imparts them with characteristic values of temperature, salinity and dissolved oxygen. These properties remain unchanged or evolve slowly until the water mass is again involved in the formation of another mode water (which may have a different formation) or it reaches the surface.

The characteristic structure of these waters is illustrated in the salinity section through the top 2000 m of the water column shown in Figure 7.1 and in the full-depth section through the Lyne and Hayes' (2005) regionalisation (Figure 7.2).

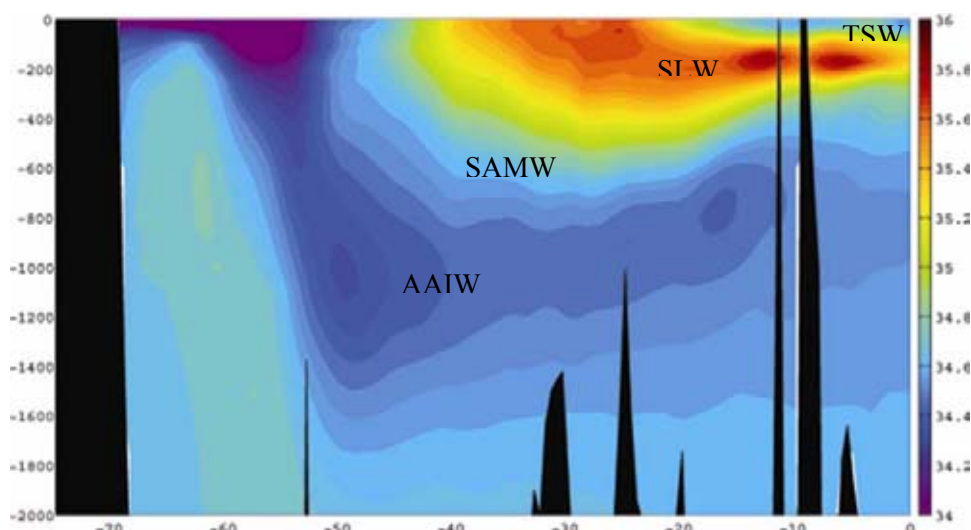


Figure 7.1 Section of salinity (in PSU units) along the 160°E section down to a depth of 2000 m based on the CARS. Major water masses are also indicated.

Subantarctic Mode Water (SAMW), Subtropical Lower Water (SLW), Antarctic Intermediate Water (AAIW)

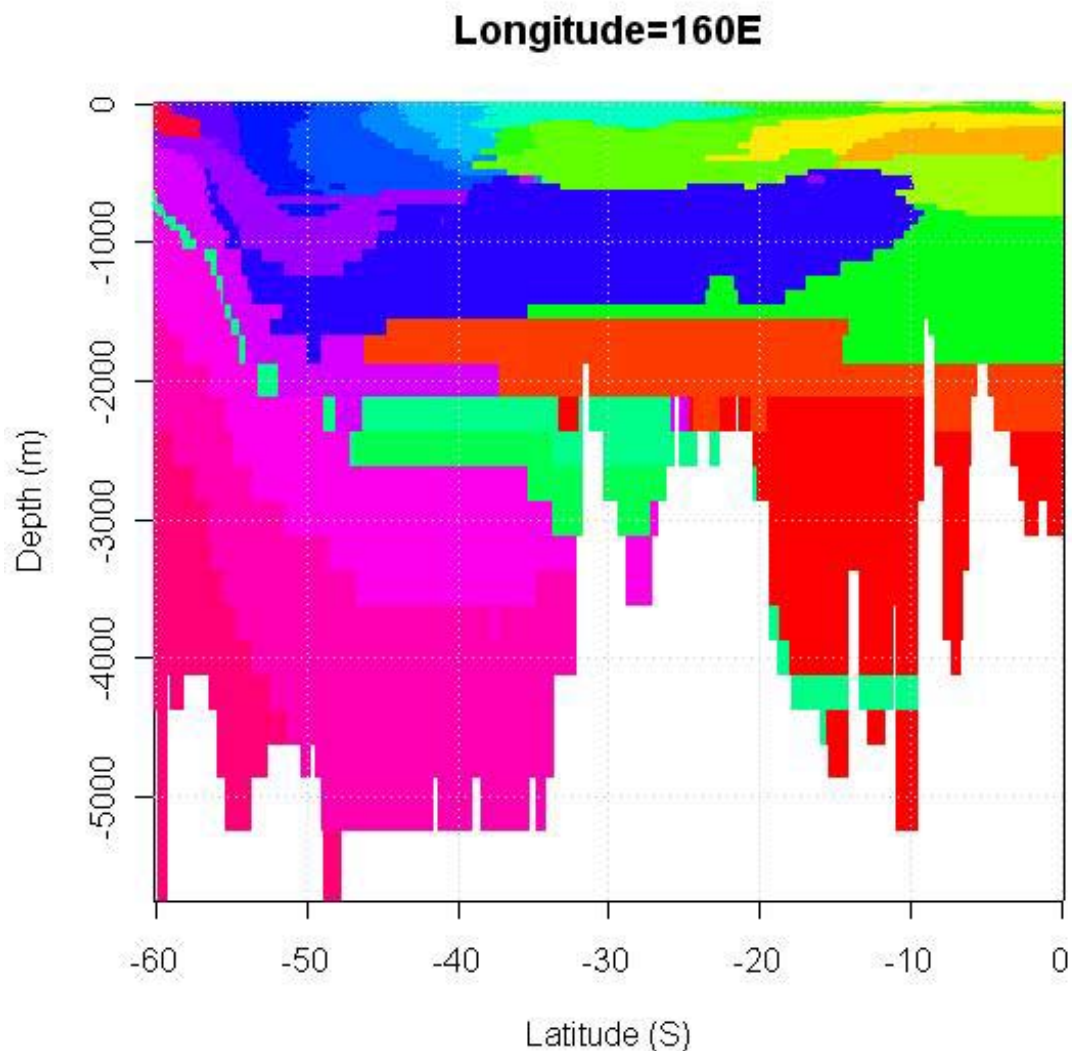


Figure 7.2 Longitude section along 160°E of the regionalisation of Lyne and Hayes (2005) showing the structuring by depth and longitude of the so-called Level 1b regionalisations.

Of particular note for this section is the intrusive dark blue region of the Antarctic Intermediate Water, which at this longitude is seen to extend north up to about 10°S. The green unit lying above the Antarctic Intermediate Water is the Subantarctic Mode Water (SAMW), but note that the Lyne and Hayes (2005) classification indicates that its character has changed from that in its formation region (see text).

7.3 Large-scale Setting: WOCE Section P11

We first describe the large-scale setting for the SAMW by referring to the detailed observations made during the World Ocean Circulation Experiment (WOCE) Section P11 voyage, which provided a meridional section along 155°E from Papua New Guinea to 43°S in the winter of 1993. We also draw upon the analyses of Sokolov & Rintoul (2000) in understanding the formation and evolution of this water mass. Section 7.5 has been extracted from their paper with permission from the authors and publishers (Sokolov & Rintoul 2000)⁴

The position of the track of WOCE P11 is shown in Figure 7.3. Vertical sections of water properties are shown in Figure 7.4. These sections show the distributions of temperature, salinity, Oxygen and neutral density along section P11.

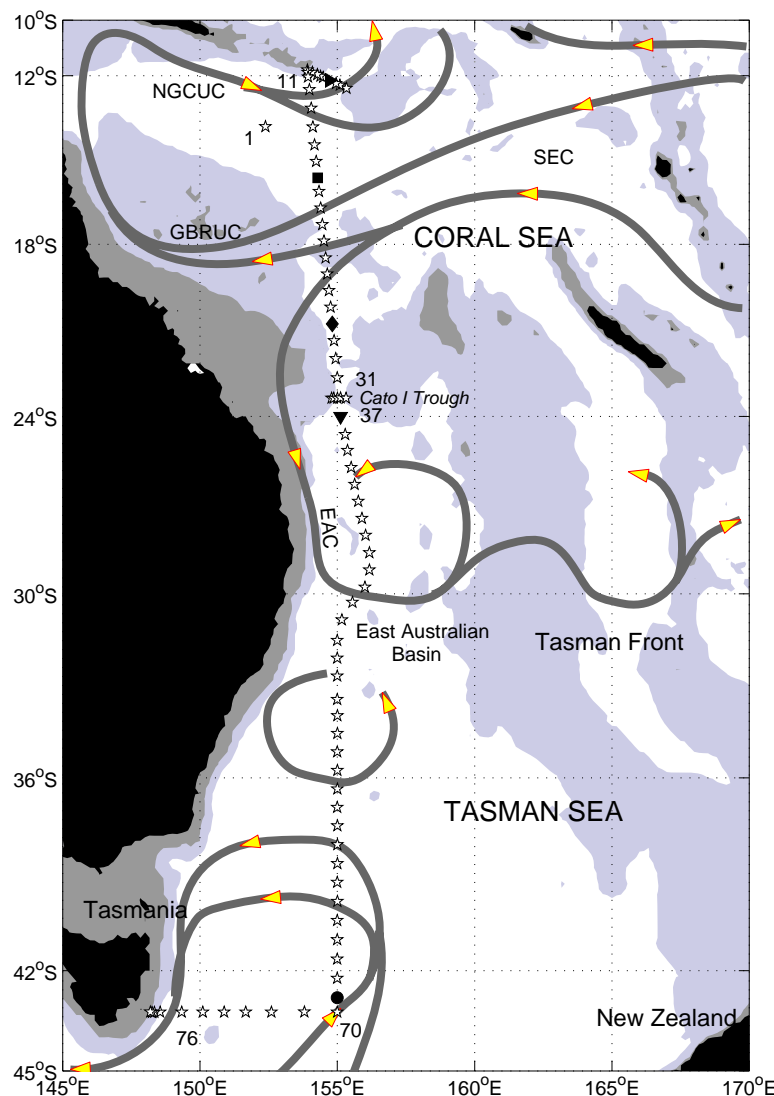


Figure 7.3 Position of the Track of *RV Franklin* 9306 (WOCE section P11).

⁴ ©Journal of Marine Research

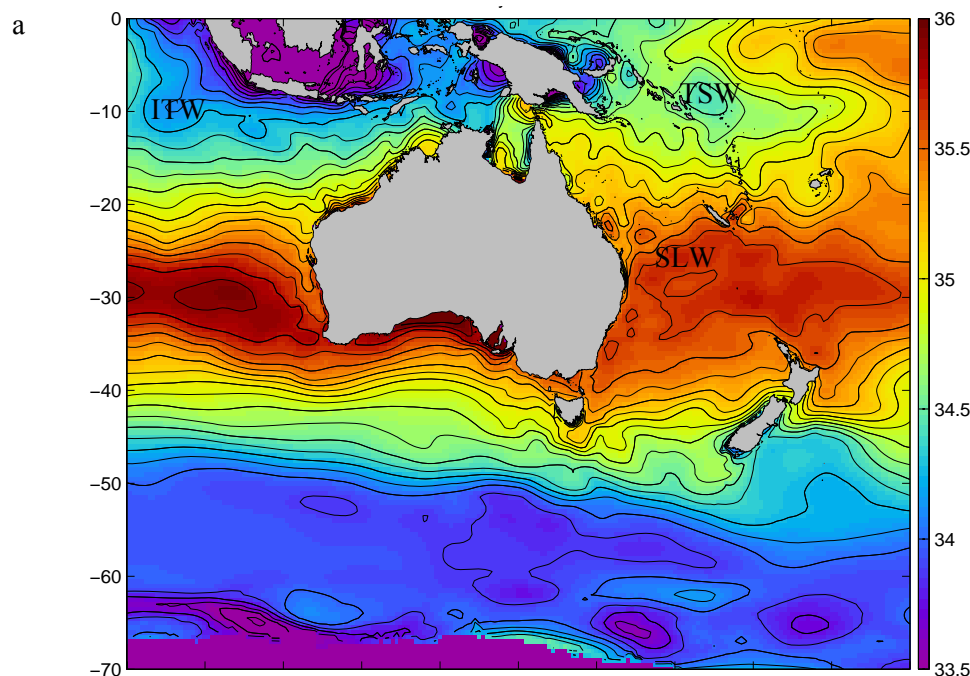
Light shading indicates depth shallower than 2500 m. Dark shading indicates depth shallower than 250 m. Arrows indicate major circulation features of the south-west Pacific (Sokolov & Rintoul 2000)
©Journal of Marine Research.

7.4 Water Masses of the South-west Pacific

The near-surface layers east of Australia and north of the Subtropical Front consist of relatively warm, fresh Tropical Surface Water (TSW) and more saline Subtropical Lower Water (SLW). At greater depth, thermocline waters are renewed by Subantarctic Mode Water (SAMW) above low-salinity Antarctic Intermediate Water (AIW), as both water masses spread from the Southern Ocean into the South Pacific Subtropical Gyre.

Tropical Surface Water (TSW) originates at the surface in the western equatorial Pacific where heavy precipitation forms a thin surface layer (depth ~ 100 m, $T \sim 25^\circ\text{C}$, $S < 35.1$) and spreads both south and east (low-salinity tongue in Figures 7.6 and 7.7).

Subtropical Lower Water (SLW) forms in the central Pacific and initially spreads westward below the Tropical Surface Water and across the northern flank of Fiji and New Caledonia as part of the subtropical gyre. In this region it is characterised by low oxygen, low nutrients, and a pronounced salinity maximum at 150 m penetrating into the Coral Sea around 14°S (Figure 7.4). It reaches the surface in the central Tasman Sea ($\sim 25^\circ\text{S}$), where it is modified by precipitation and heat losses to the atmosphere (Figure 7.5). This exposure to the atmosphere means that the southern component of the Subtropical Lower Water is not only cooler and fresher, but also higher in oxygen than its northern counterpart.



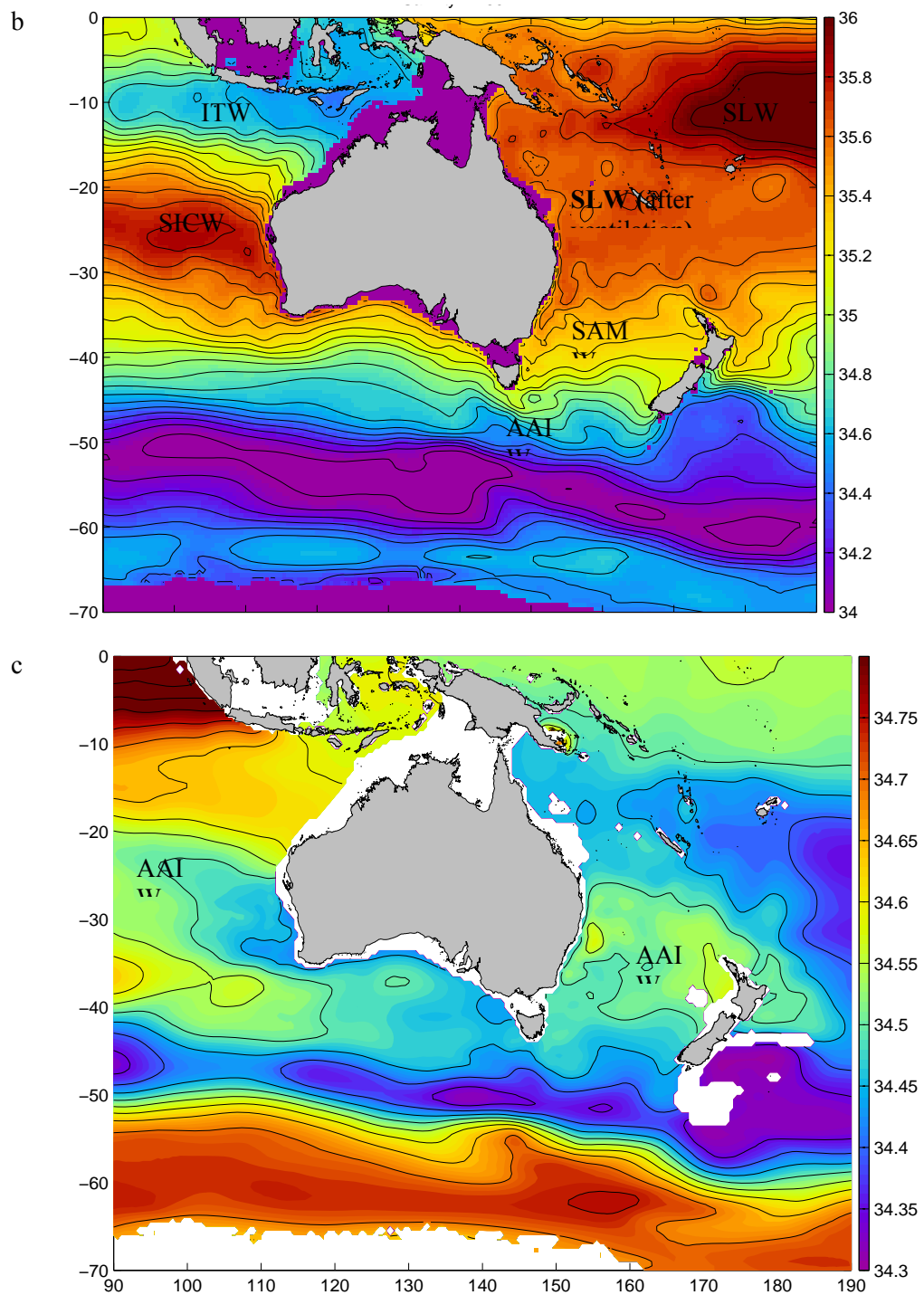


Figure 7.4 Salinity at the (a) surface, (b) 150 m, and (c) 800 m, based CARS. Major water masses are also indicated (definitions in Appendix C).

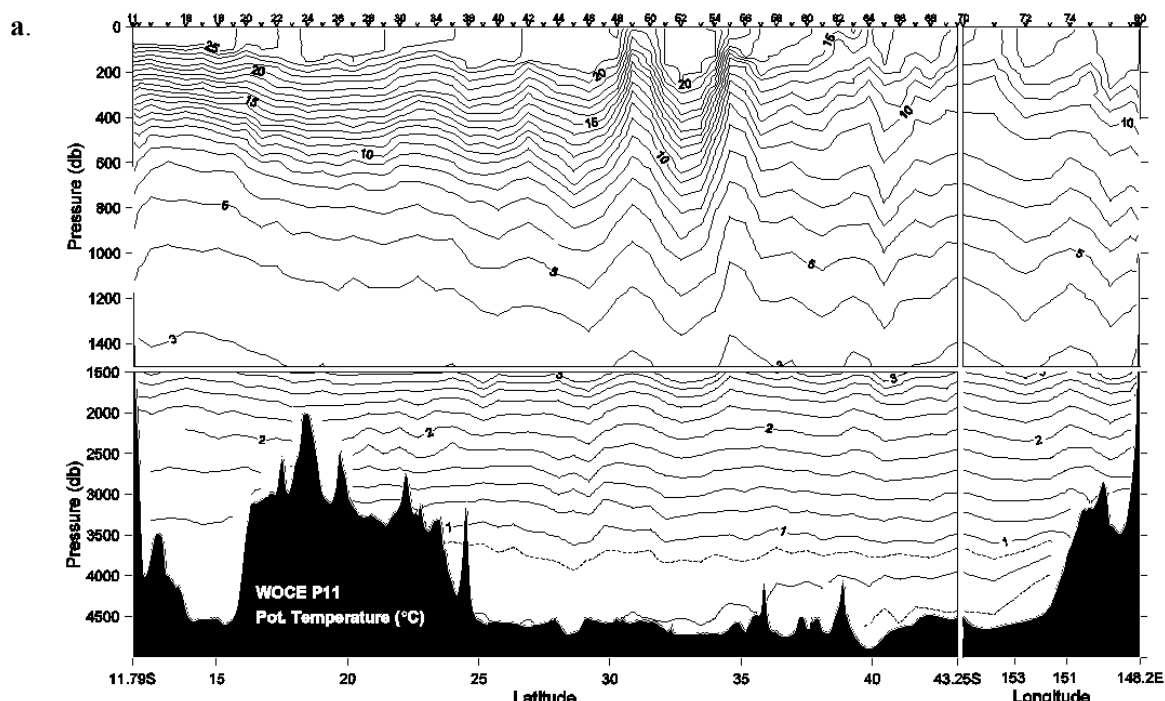
Subantarctic Mode Water (SAMW) forms by deep winter convection between the Subtropical Front and the Subantarctic Front. It retains its characteristics of high oxygen content within a thick layer of constant density as it spreads equatorward in the subtropical gyres centered at around 600 m depth (Figure 7.5). A warm, salty variety is confined to the Tasman Sea and east of New Zealand, while a cooler, fresher and denser variety is circulated within the subtropical gyre and enters the Coral Sea north of Vanuatu.

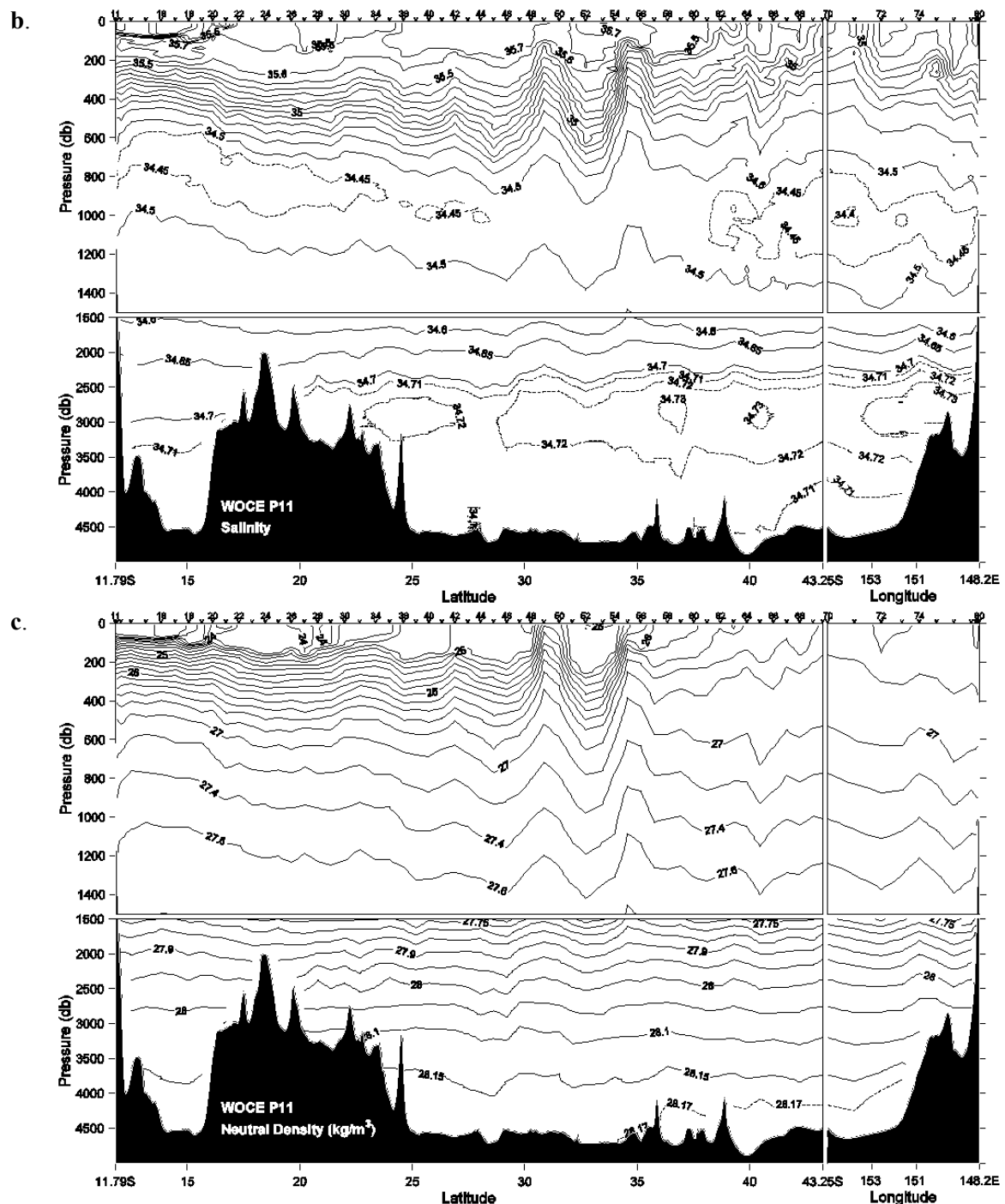
Antarctic Intermediate Water (AIW) occurs as a distinctive salinity minimum with only moderate oxygen content suggesting that the water mass has been isolated from the surface for an extended period. It arrives from the east as two distinct varieties, the first spreading into the southern Tasman Sea and the second entering the Coral Sea with similar salinities but relatively higher temperatures (Figure 7.1, Figure 7.3).

The distribution of these water masses produce two major frontal regions:

- The Tasman Front stretches almost zonally across the Tasman Sea at approximately 35°S, marking the boundary between warmer Coral Sea water and cooler Tasman Sea water. However, the change in water-mass properties is usually small; its real significance is that it marks the path of the separated East Australian Current.
- The Subtropical Front or Subtropical Convergence is the interface between subantarctic and subtropical water masses. Between Tasmania and New Zealand it lies around 40°S. It is a dynamically active zone, with active exchange across the boundary and large seasonal variability in surface chlorophyll levels.

Depending on the intensity of air/sea interactions, the properties of the water masses and their transport through the oceans, a variety of mode waters are formed, interleaving and flowing along various paths in the oceans. The flow paths in turn are influenced by water properties through what is called geostrophy, which is related to pressure distributions imposed on water masses because of density variations through the water column; it is analogous in some sense to the more familiar Highs and Lows that affect our atmospheric weather patterns.





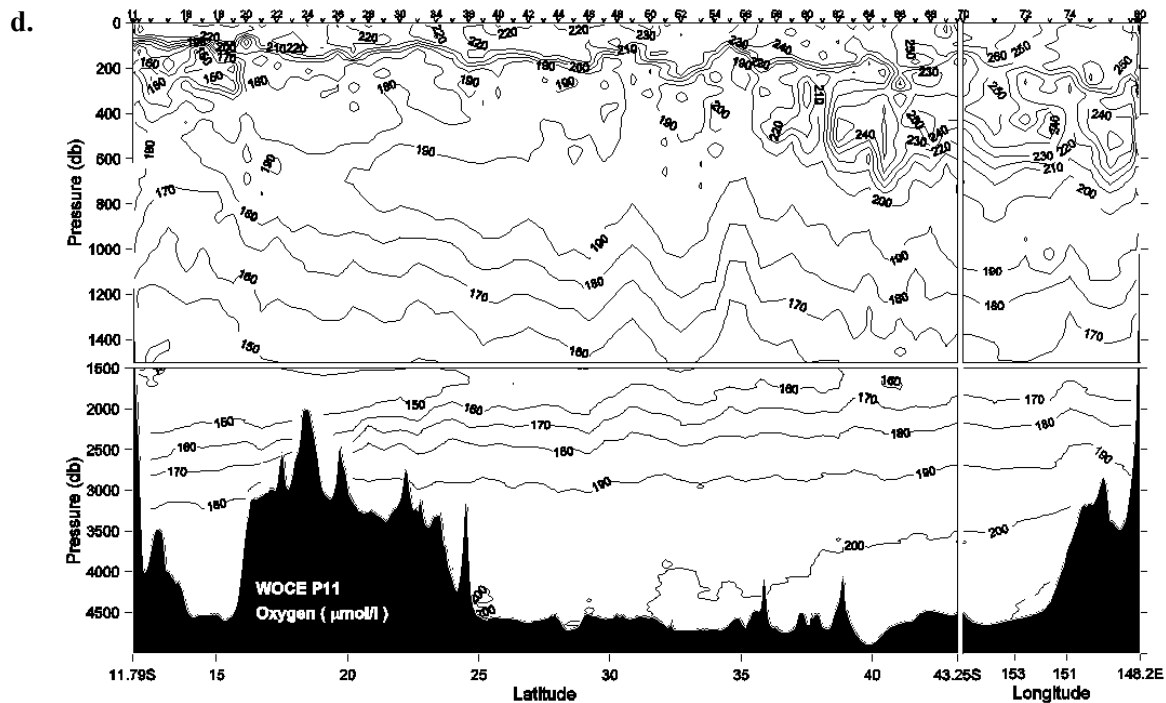


Figure 7.5 Vertical sections of water properties along WOCE section p11.

The section turns at 43S and runs west to the coast of Tasmania. (a) Potential temperature ($^{\circ}\text{C}$) distribution along WOCE section P11 (contour interval 1 $^{\circ}\text{C}$ above and 0.2 $^{\circ}\text{C}$ below 1500db); (b) Salinity distribution (contour interval 0.1 above and 0.05 below 1500db); (c) Neutral density (kg m^{-3}) (contour interval 0.1 above and 0.05 below 1500 db); (d) Oxygen ($\mu\text{mol/L}$) distribution (contour interval 10 $\mu\text{mol/L}$). (Sokolov & Rintoul 2000) ©Journal of Marine Research.

7.5 Subantarctic Mode Water (SAMW)

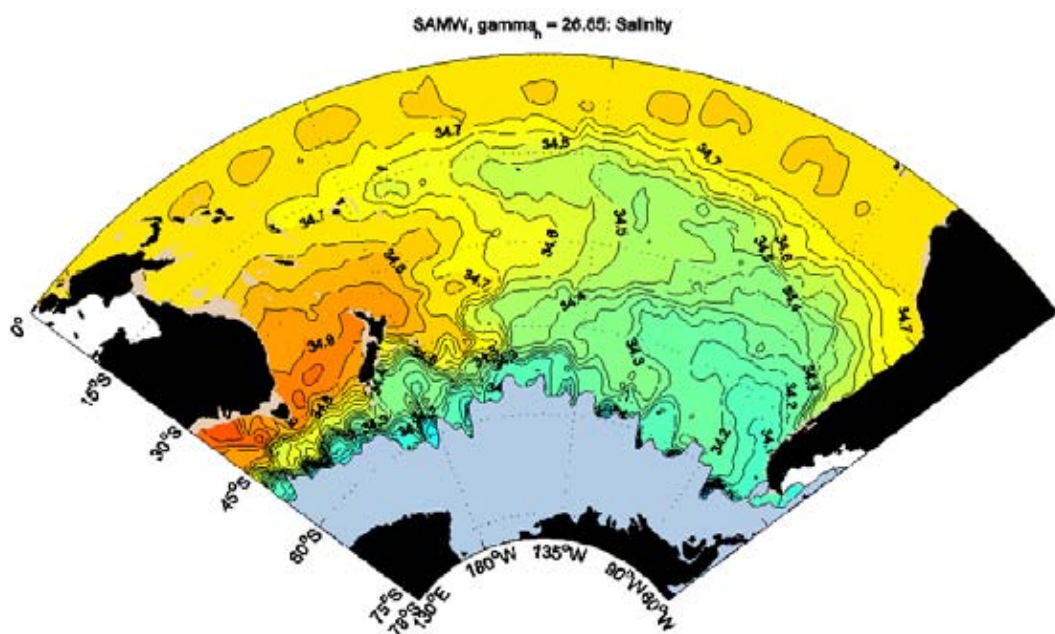
The Subantarctic Mode Water (SAMW) is formed by deep winter convection north of the Antarctic circumpolar current (ACC), between the Sub Tropical Front (STF) and the Sub Arctic Front (SAF) (McCartney 1977). The deep mixing that forms SAMW imprints this water mass with its characteristic properties: high oxygen and a thick pycnostad (density layer of low potential vorticity). From these water mass signatures, the SAMW can be traced from its formation region in the Southern Ocean as it spreads equator-ward in the subtropical gyres. Due to its high oxygen content, the SAMW plays an important role in ventilating the lower thermocline of the southern hemisphere subtropical gyres (McCartney 1982).

On P11 the SAMW forms a prominent pycnostad with densities between 26.8 and 27.0 south of 38°S (Figure 5d). The potential vorticity minimum, with values less than $5 \times 10^{-11} \text{ m}^{-1} \text{ sec}^{-1}$, is located between 200 and 600 m depth (Figure 5c) and coincides with a layer of high oxygen concentrations (Figure 5c). The SAMW does not outcrop on P11, so it must be advected from the formation region located further south. In late winter the SAMW produced south of Tasmania forms a 600-m thick thermostad with temperatures of 8.5 - 9.5°C, salinities of about 34.60 - 34.75, and neutral densities of 26.8-27.0 (Thompson & Edwards, 1981; Rintoul *et al.* 1997), similar in properties to the SAMW observed on P11.

The distribution of SAMW in the South Pacific has been discussed by several authors (see e.g., McCartney 1982; McCartney and Baringer 1993; Stramma *et al.* 1995; Bingham and Lukas 1995; Tsuchiya and Talley 1996; Rintoul *et al.* 1997). These studies generally confirm McCartney's (1982) suggestion that the SAMW formed in the Pacific spans a wide range of densities (from potential densities σ_0 of 26.9–27.0 in the west to 27.04–27.11 in the east), with the circulation of the lighter SAMW restricted to the south-west corner of the basin, while the denser SAMW is swept north-westward by the subtropical gyre circulation. The western varieties are much warmer and saltier (8.0 - 9.5°C and 34.60 - 34.75; Thompson & Edwards, 1981 Rintoul & Bullister 1998) than the eastern varieties (4.3 - 5.1°C, 34.20; McCartney & Baringer 1993). Modes with intermediate properties form in the subantarctic zone near New Zealand (Gordon 1975); however their circulation is restricted to the area west of the East Pacific Rise (McCartney & Baringer 1993).

Maps of properties on the SAMW isopycnal surfaces clearly show these patterns, with the warm, salty western varieties confined to the Tasman Sea and east of New Zealand, and a tongue of the cool, fresh SAMW formed in the south-eastern Pacific spreading north-westward with the subtropical gyre circulation (Figure 7.6 and Figure 7.7). The tongue of fresh and cool SAMW formed in the south-eastern Pacific bifurcates at 90°W: a northern branch carries predominantly denser varieties of SAMW around the subtropical gyre to enter the Coral Sea north of Vanuatu; and a southern branch carries somewhat lighter varieties westward south of 35°S. The southern branch does not appear on previously published maps based on more limited data (see e.g., Reid, 1965), although McCartney & Baringer (1993) inferred its existence from the fact that the lighter modes that spread north across the Scorpio section at 43°S did not appear on the 28°S section, and so must have recirculated to the west south of 28°S.

a



b

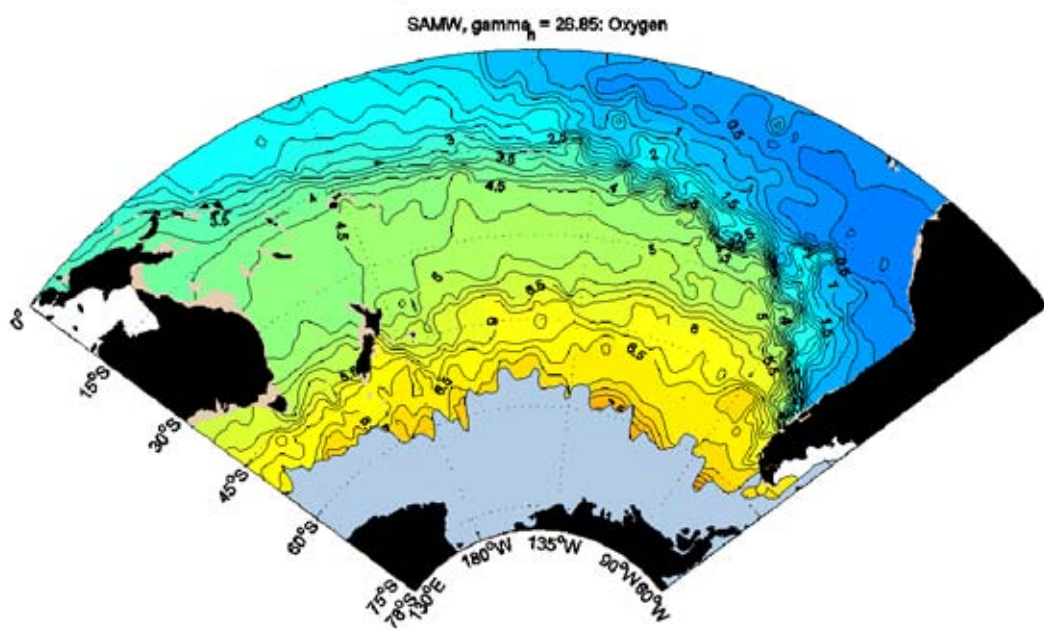


Figure 7.6 Water properties on the isopycnal corresponding to the Subantarctic Mode Water (SAMW) ($\gamma_n = 26.85$) (a) Salinity (shading indicates salinity lower than 34.7), (b) Oxygen (mL/L) (shading indicates oxygen higher than 4.5 mL/L) (Sokolov & Rintoul 2000) ©Journal of Marine Research.

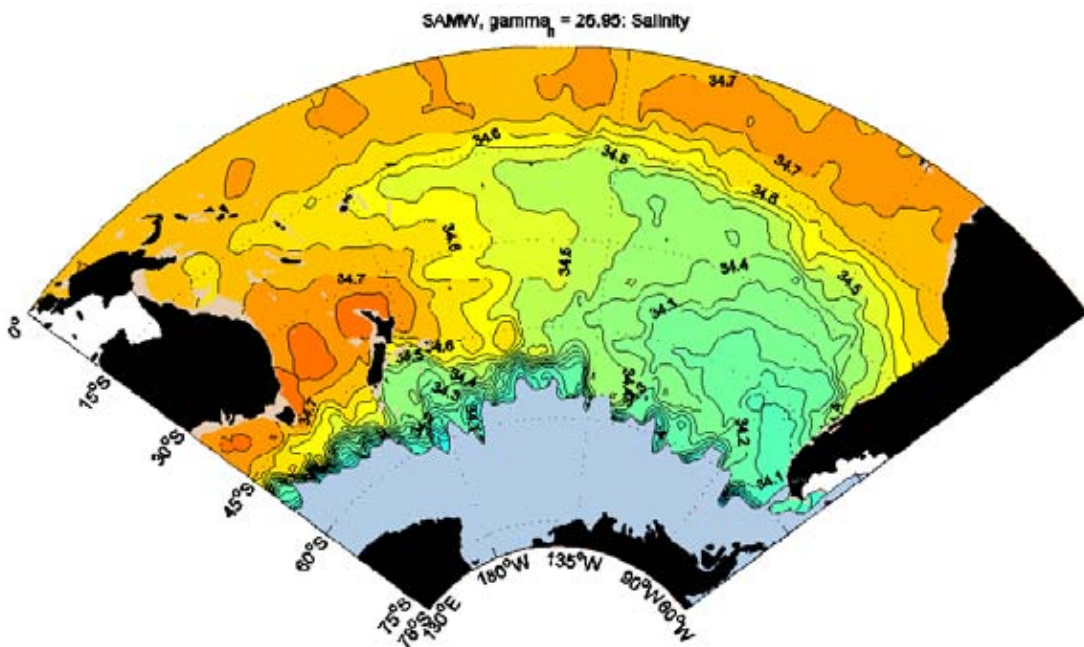


Figure 7.7 Salinity on the isopycnal corresponding to the Subantarctic Mode Water (SAMW) ($\gamma_n = 26.95$). Shading indicates salinity lower than 34.65 (Sokolov & Rintoul 2000) ©Journal of Marine Research.

The distribution of SAMW on P11 provides additional detail on the circulation patterns of the different varieties of SAMW in the south-west Pacific.

The SAMW pycnostad is prominent on the 43°S section, but it is not uniform along the section, reflecting flows entering and leaving the southern Tasman Sea (Figure 7.5). The pycnostad is thickest and highest in oxygen at station 71, where the geostrophic velocities show northward flow (see section 5), while the pycnostad is poorly developed and low in oxygen in the southward flow adjacent to the coast of Tasmania (inshore of station 78). Between stations 71 and 78, the SAMW is of intermediate "strength" and varies from station to station as the flow alternates from southward (carrying weak SAMW) to northward (carrying strong or recently formed SAMW).

SAMW entering the Tasman Sea from the south extends as far north as 36°S, where a strong front in all water properties is found between stations 56 and 57. To the south of the front, water on the neutral density surfaces 26.8 - 27.0 is higher in oxygen, saltier and warmer (Figure 7.8). The difference in water properties across the front is large: greater than 0.8°C in temperature, 0.24 in salinity and 60 µmol/L in oxygen (Figure 7.4). Nevertheless, some influence of the lighter SAMW entering from the south can be seen as far north as 28°S (e.g. the oxygen maximum and thicker layer of 26.7 to 26.9 water at station 45). Water from the south is entrained at the edge of anticyclonic East Australian Current (EAC) eddies, producing a "curtain" of higher oxygen water wrapped around the perimeter of the eddy. This description accords with the Lyne and Hayes (2005) classification, which identifies a number of different classes associated with the more classic description of a modal SAMW (see Figure 7.2).

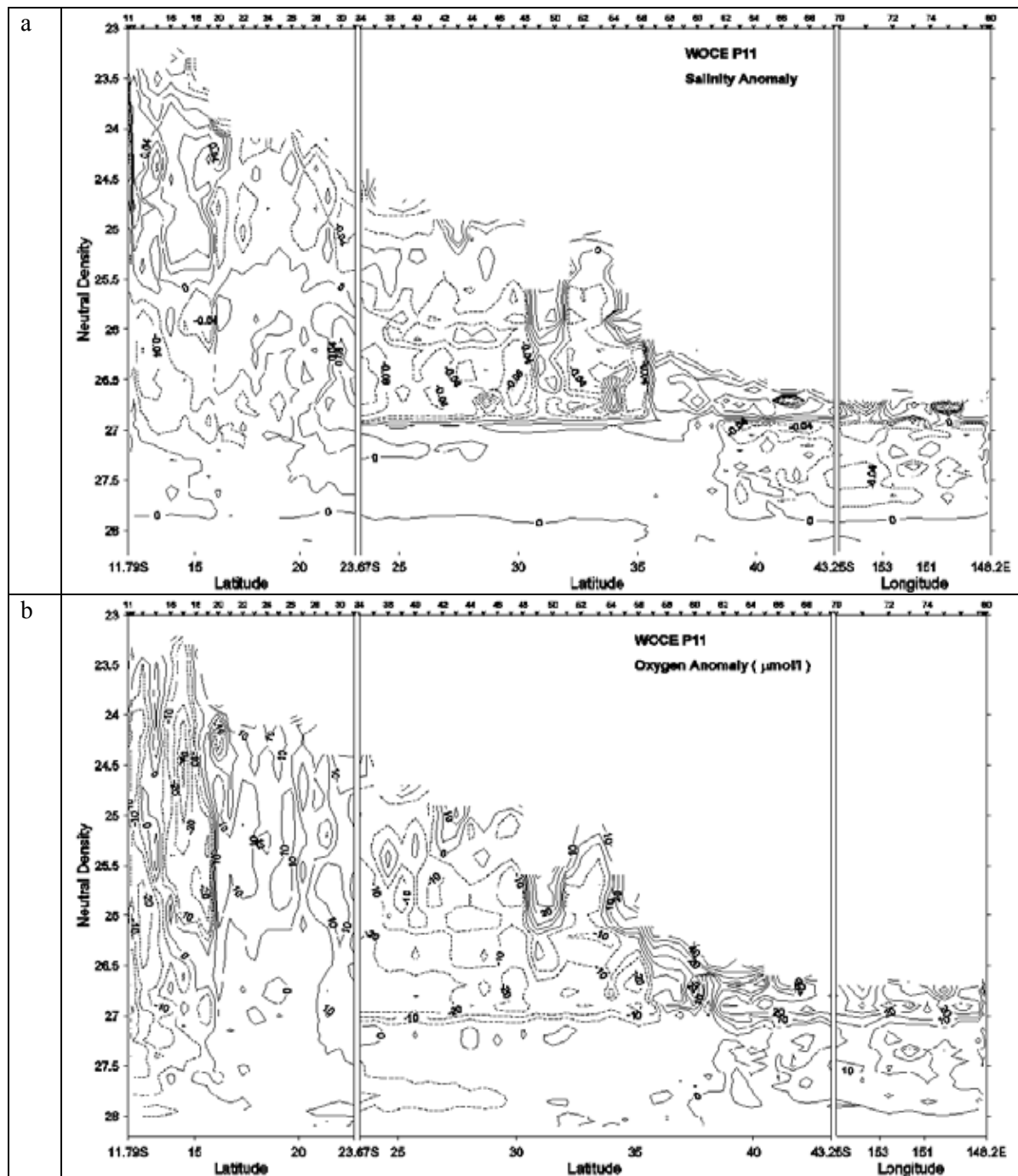


Figure 7.8 Water property anomalies along WOCE section P11 plotted in neutral density coordinates. Anomalies are defined relative to the mean profile for stations in the coral sea (left panel) and in the Tasman Sea (middle and right panels). Positive values are higher in salinity or oxygen than the mean profile. (a) Salinity anomaly, (b) oxygen anomaly (Sokolov & Rintoul 2000) ©Journal of Marine Research.

As discussed above, the denser SAMW formed in the south-eastern Pacific enters the Coral Sea north of Vanuatu and is carried westward across P11 by the SEC. At the oxygen maximum core level density of 27.15 (Figure 7.9), this water is fresher than 34.45 and cooler than 6.75°C, and it lies at a depth of 700 - 900 m. By the time the eastern SAMW has reached the Coral Sea, the initially high oxygen saturation has been decreased to 60 - 65% through mixing and oxygen consumption. Mixing during its transit of the South Pacific has also eroded the strong pycnostad characteristic of this water

type. After the South Equatorial Current (SEC) bifurcates at 18°S near the coast of Australia, part of the eastern SAMW flows cyclonically around the Gulf of Papua New Guinea (PNG), where it forms an oxygen maximum at a depth of about 600 m in the NGCUC at the northern end of P11, and then enters the Solomon Sea.

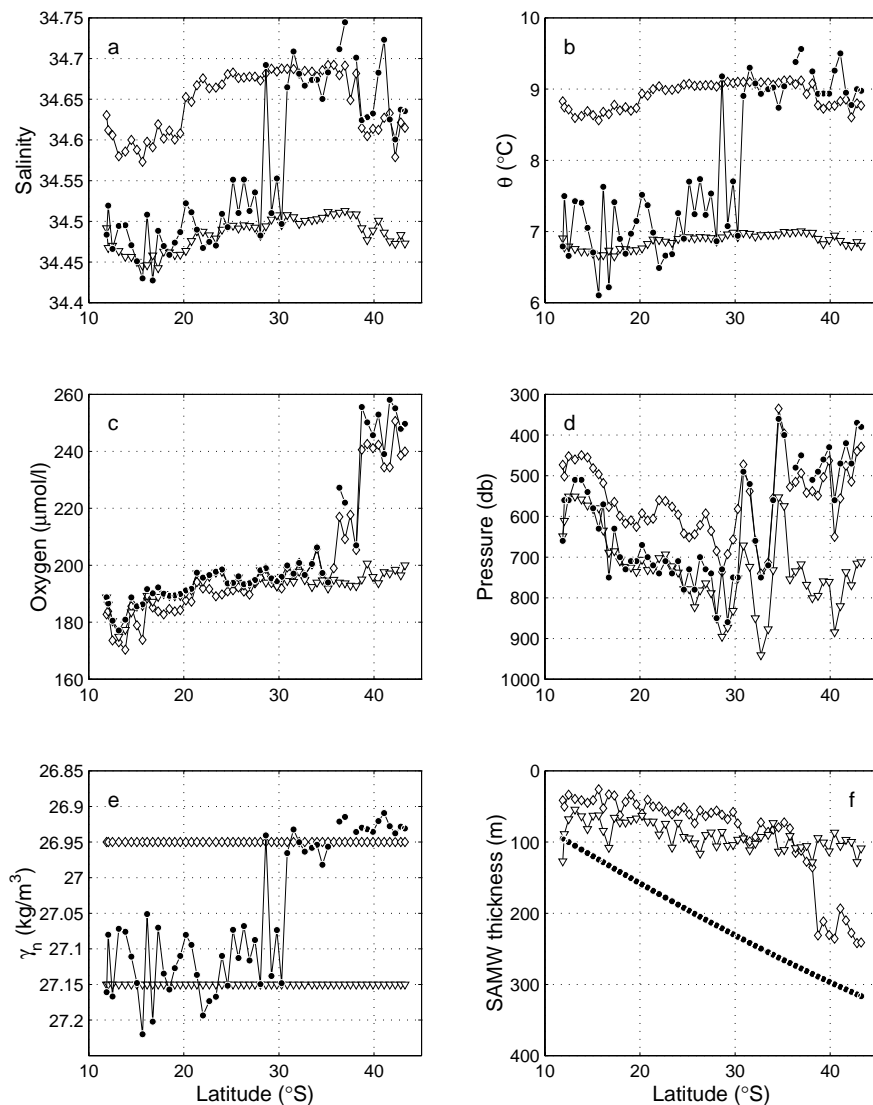


Figure 7.9 Properties of the Subantarctic Mode Water along P11.

The oxygen maximum core layer is indicated with solid circles, the $\gamma_n = 26.95$ surface with diamonds, and the $\gamma_n = 27.15$ surface with open triangles. (a) salinity, (b) potential temperature, (c) oxygen, (d) pressure, e. neutral density, f. thickness of the density layer defined by 26.95 ± 0.05 (triangles). In (f), the filled circles show the expected change in thickness due to change in Coriolis parameter for a layer translated over the latitude range of the P11 section while conserving its planetary vorticity. The $\gamma_n = 27.15$ mode is approximately 320 m thick near 43S in the southeast Pacific (Sokolov & Rintoul 2000) ©Journal of Marine Research.

The remainder of the SAMW carried westward in the South Equatorial Current turns southward after the bifurcation and feeds the East Australian Current. The eastern SAMW entering the Tasman Sea in the East Australian Current is characterised by oxygen maximum at a density of 27.15 and a depth of about 700 m. While changes in oxygen between the mode water entering the Coral Sea across P11 and the mode water transported to the south by the East Australian Current are small, the changes in temperature and salinity are more dramatic (Figure 7.9). Between the bifurcation point of the South Equatorial Current at 18°S and 22°S, where the East Australian Current crosses P11 from north-west

to south-east, the temperature increases from 6.75°C to 6.95°C, and the salinity from 34.45 to 34.49. Further south, between 22°S and 36°S, the properties along the 27.15 isopycnal are almost uniform, with a gradual salinity and temperature rise of about 0.02 and 0.1°C respectively. This distribution of properties suggests that fresh, cool eastern SAMW is carried into the Tasman Sea from the north by the East Australian Current, where vigorous stirring by the eddy field rapidly homogenizes the temperature and salinity along isopycnals. Around the perimeter of the anticyclonic eddy south of the East Australian Current, remnants of the SAMW entering from the south and east are superposed, forming a weak double oxygen maximum at 34°S and (even weaker) at 32°S.

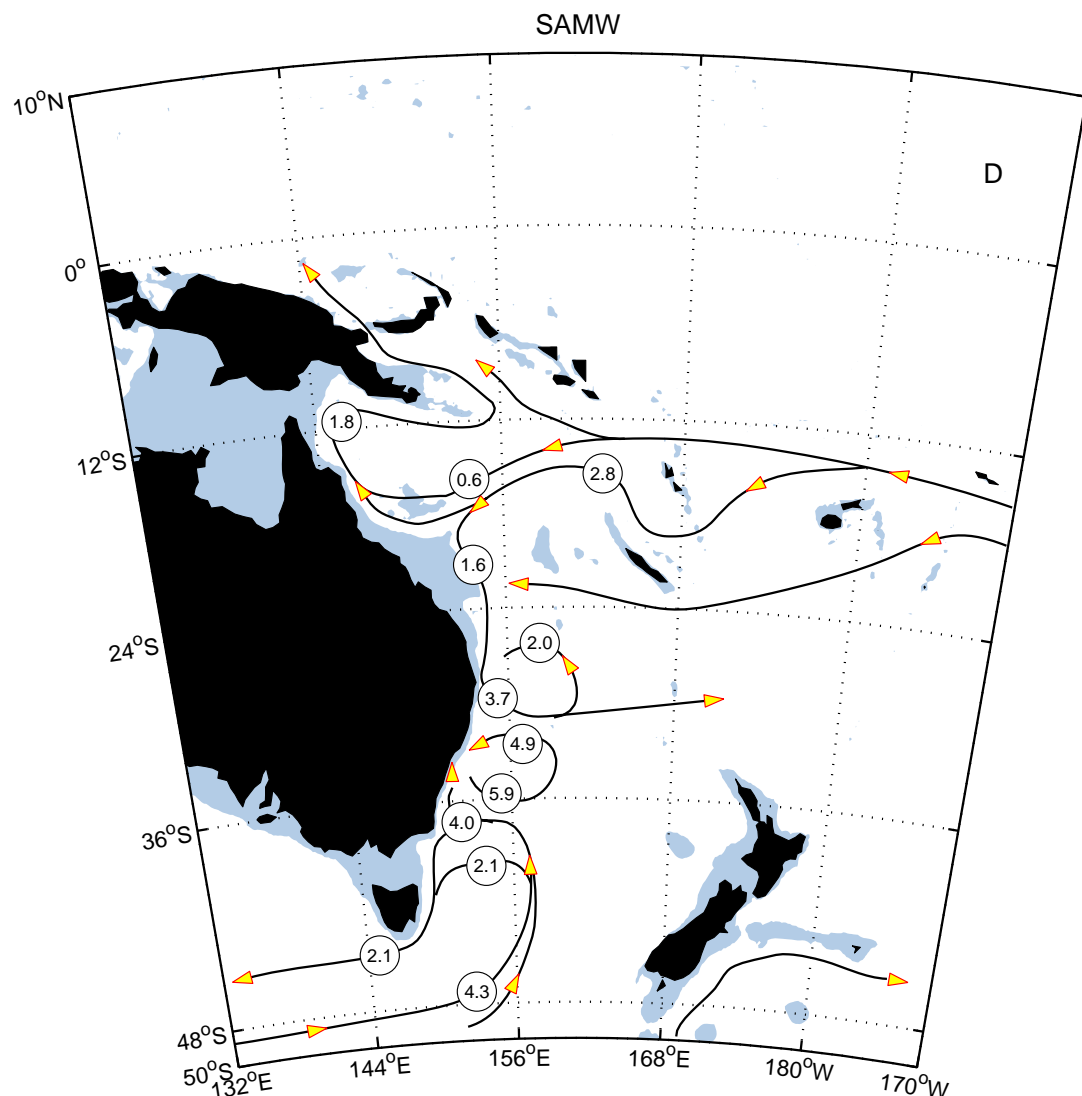


Figure 7.10 Circulation of SAMW. Paths of water masses are shown by solid lines with arrows, and transports are indicated in circles (Sv) (Sokolov & Rintoul 2000)©Journal of Marine Research.

7.6 Summary

The intent with this section was to describe the formation and subduction of one of the major water mass types found in the South Pacific Ocean – namely the Subantarctic Mode Water. The story of its formation and evolution is far from simple, and intertwined with the formation histories of a variety of other water masses with which it is associated. In addition, subtle spatio-temporal variations in air/sea exchange processes and circulation processes lead to various “flavours” of this mode water, which in turn may take diverging paths through the ocean due to variations in the depth at which they are formed and corresponding depth variations in the water currents. Nonetheless, the SAMW is a relatively well defined water mass with a high oxygen presence that is vital for the survival of a variety of marine fauna at depth. It demonstrates that subduction processes are critical in “ventilating” the deep ocean, which would otherwise be relegated to the erroneous common view of a dark and lifeless abyss.

8 The Dynamics of the East Australian Current and its Eddies

8.1 Introduction

This section describes the oceanographic and biological setting of the East Australian Current (EAC) and in particular the nature of physical and biological processes associated with various structural (spatial) components of the East Australian Current. It is presented here as a case study of one of the components of the regionalisation of the waters around Australia.

The large-scale setting that gives rise to the East Australian Current is first described. This provides an overview of the key physical driving forces, at ocean basin scales, which lead to the formation of the EAC. It also provides an understanding of how large-scale variability may affect this current. Since a preliminary regionalisation of the pelagic environment is available (see Lyne and Hayes, 2005), the large-scale context can now be described in terms of the results of that regionalisation – which is used where possible.

At regional scales, the EAC extends as the southern arm of a bifurcated current system that starts off Queensland and forms the distinctive core boundary current off New South Wales. It subsequently separates and veers north-eastward along the Tasman Front to the north-western tip of New Zealand. Characteristic spatial and dynamic components of the current system are described with reference to the results of the pelagic regionalisation and with descriptions, where possible, of the processes involved in generating, maintaining and modifying these regionalisation structures.

At feature scales of about the size of individual eddies, or smaller, the characterisation in terms of “energetics” is provided with reference to implications on mixing, nutrient upwellings, satellite-derived chlorophyll estimates, and biological information available from research voyages. The available data and analyses from biological studies focused on individual eddies and eddy features, are summarised to examine the link between physical processes and biological distributions.

8.2 Large-scale setting: Oceanographic context

(Much of the oceanographic descriptive material in this subsection was kindly provided by Ken Ridgway of CSIRO Marine Research)

The East Australian Current (EAC) is a vigorous and substantial southward current that flows down the shelf edge of the eastern coast of Australia. It is related to a group of major ocean currents- the Gulf Stream, Kuroshio, Agulhas Current and the Brazil Current. These are the so-called western boundary currents that transport tropical waters to cooler temperate regions. They all provide an intense poleward return flow at the western side of large-scale recirculation features or gyres that flow around the major ocean basins. These gyre systems are driven by solar heating, air-sea exchanges and global wind systems. Friction associated with the vigorous, narrow, western boundary currents provides a balance to the wind stresses imposed on the gyre. At the same time, the boundary current “closes” the water transports between the tropical and temperate arms of the gyre. The celebrated oceanographer Hank Stommel showed in an early paper that the effective latitudinal variation of the earth’s rotation normal to the surface of the ocean, known as the β (Beta) factor, drives the asymmetry in gyre circulation that is necessary for the existence of western boundary currents. Thus, while these current systems are narrow and swift, they span a substantial range of latitude and their characters also vary with latitude.

At a broad scale, the contributions to the EAC system stem from what Lyne and Hayes (2005) have regionalised as the Coral Sea region (Level 1b_17 in their terminology – see Figure 8.1) contains waters of the South Equatorial Current that impinge on the north-eastern coast of Australia. The southward arm of this split is seen to intrude south along the coast (The headwaters of the EAC also appear to draw in waters from the L2_20 unit, which is south of the South Equatorial Current (the southern boundary of which is demarcated by the southern boundary of the Level 1b_17 unit). This L2_20 zone is within the northern arm of the Coral Sea Circulation.

The core of the EAC current and recirculation is within the L2_22 unit in which in the Lyne and Hayes (2005) regionalisation also comprises the waters along the Tasman Front, whose southern boundary wraps around the north-western coast of New Zealand. The Lyne and Hayes (2005) regionalisation also demarcates distinctive waters to the north and south of the Tasman Front – L2_21 and L2_19 respectively.

The following sections in this report detail the main characteristics of these water masses and the processes involved in their formation and maintenance.

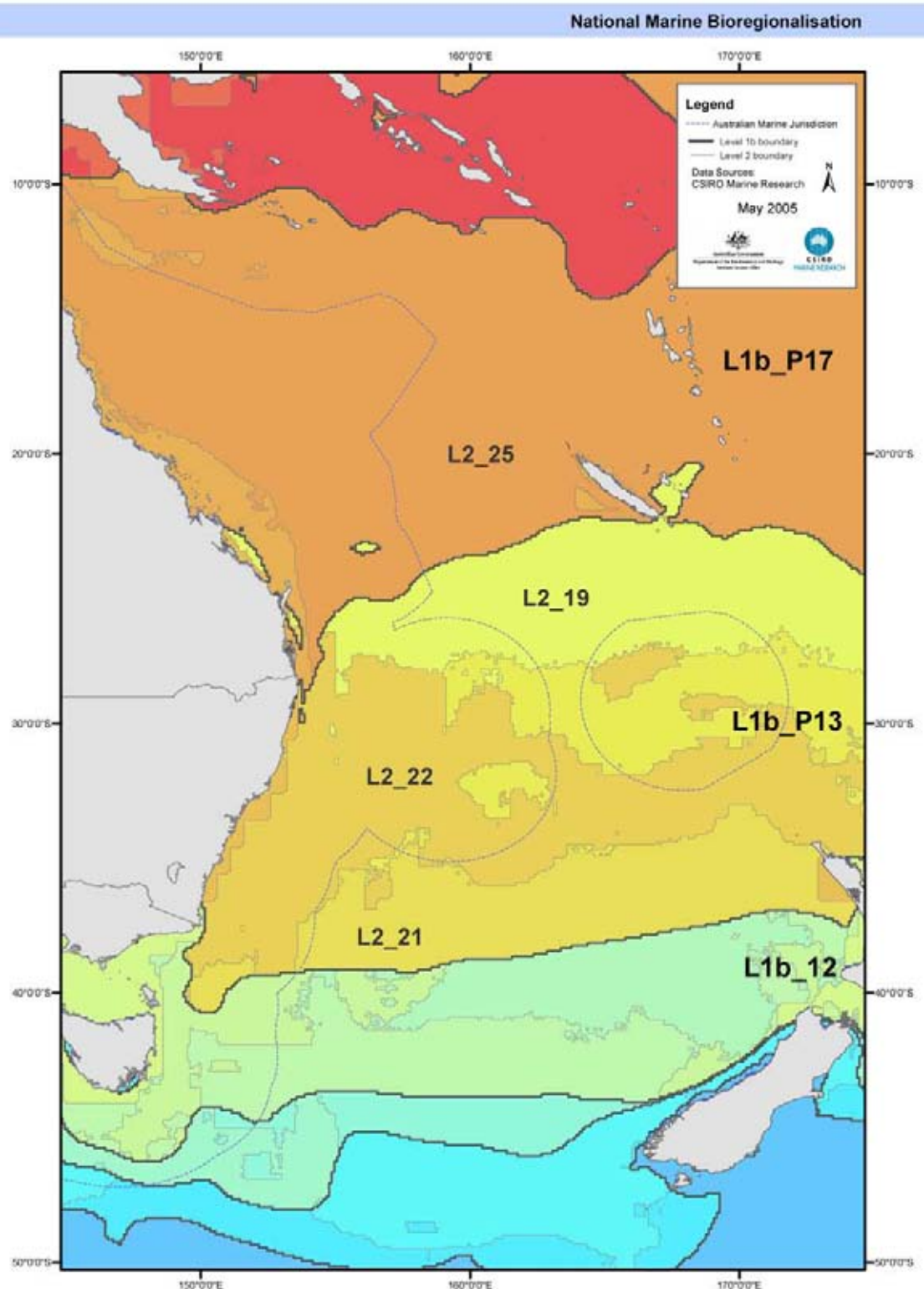


Figure 8.1 Map of the waters off eastern Australia showing surface regionalisations of water properties from Lyne and Hayes (2005).

The northern large-scale unit is the Level 1b_P17 region that contains the Coral Sea region and the South Equatorial Current system which bifurcates in the north-west corner of the image. The collection of regions marked with the L2 prefix is comprised of the Coral Sea Circulation region and includes the East Australian Current water masses (core is within L2_22 unit) which are described in the text. The Australian Marine Jurisdiction is also marked on the map.

8.3 Circulation patterns and processes

The circulation of the EAC system is affected by the complex topography in the region (Ridgway & Dunn 2003). The bathymetry is dominated by several ridges that radiate northward from the New Zealand land mass. A complicated pattern of island groups, reef systems and seamounts all influence the circulation at both large and small scales. In particular, the basin geometry of the region serves to contain the boundary current system, leading to extensive recirculation, mixing and hence relatively uniform ocean properties in the southern Coral Sea and northern Tasman Sea (collection of L2 prefix units in the EAC is fed by an inflow to the Coral Sea (southern part of Level 1b_17 and L2_21 units in provided by the westward flow of the gyre-scale tropical South Equatorial Current (SEC), which enters the region between the Solomon Islands and New Caledonia (200-800 m depth). This forms the northern arm of the anticlockwise flow of the South Pacific Subtropical Gyre which circulates around the Southern Pacific basin between South America and Australia. As it approaches the east Australian coast, the South Equatorial Current (EAC) is separated into a series of narrow jets by the complex island and reef systems in the South-west Pacific. At the Queensland coast the westward flow is split into northward and southward components. This separation point varies in time (during summer it moves to at least 14° in latitude) and also moves southward with increasing depth (from 15°S at the surface to 19°S at 500 m depth). This means that, over the first 300 - 400-km the northern boundary current is an undercurrent which then extends to the surface at ~ 15°S.

Beyond the northern end of the Great Barrier Reef (GBR) (15°S) the coastal boundary flow is steered in a clockwise trajectory around the shelf-edge connecting northern Queensland and the southern coast of Papua New Guinea (PNG). It then turns northwards around the south-eastern tip of Papua New Guinea to feed the New Guinea Coastal Undercurrent, which flows through Vitiaz Strait.

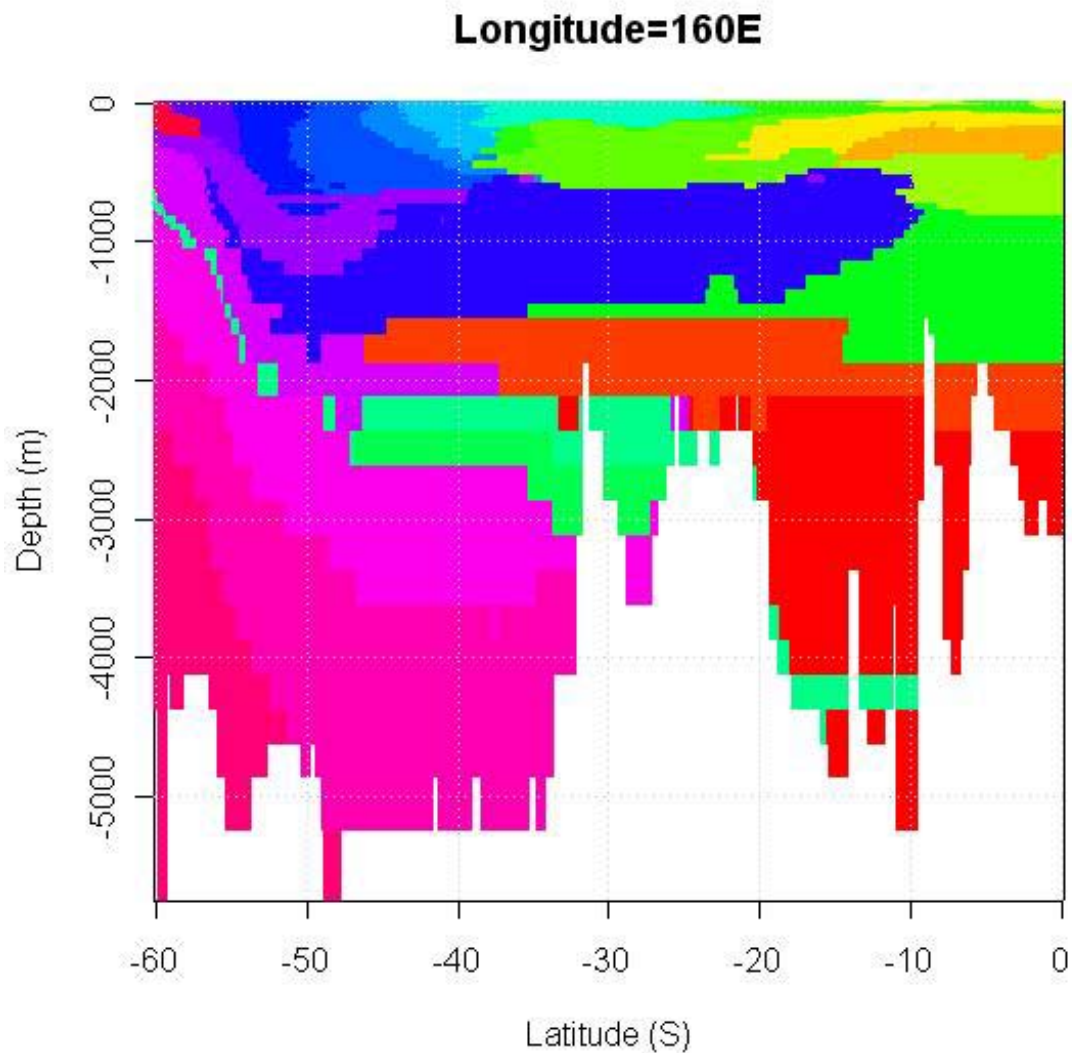


Figure 8.2 Longitude section along 160°E of the regionalisation of Lyne and Hayes (2005) showing the structuring by depth and longitude of the so-called Level 1b regionalisations.

Of particular note for this report are the waters of the East Australian Current region between 20°S and 40°S in the top 1000 m. The intrusive dark blue region is the Antarctic Intermediate Water, which at this longitude is seen to extend north to about 10°S. The light cyan surface unit located between 20 and 40°S are the waters of the collection of units marked with the L2 prefix in Figure 8.1, with the Level 1b_17 unit (light green surface layer) just to its north.

The southern branch of the current provides the source waters of the EAC. This current dominates the circulation of the region and transports a large volume of low-nutrient, warm, tropical water south down the Australian coast (just offshore of the shelf break) towards the temperate region. Because the Coral Sea waters are warm (~30°C) and have a low density, the Coral Sea is almost a metre higher than the Tasman Sea. This “pressure” difference is enough to drive the current southwards and enables it to reach such high current speeds.

Over the first 500 km this is a relatively shallow surface flow, but just south of the Great Barrier Reef it intensifies and deepens and reaches its maximum strength between 25 and 30°S. The longitudinal structure of the water masses by depth shown in Figure 8. shows a highly structured arrangement of layered water masses in the top 500 m north of about 45°S. South of about 38°S the layers “peel” off to surface, while north of about 20°S intrusive depth-stratified layers overlay each other. Between

these zones at approximately 20 - 38°S, is an extensive layered set of units underlain by the massive Antarctic Intermediate Water unit, whose upper depth at this longitude is at about 500 m. This unit between 20 - 38°S is the core of the EAC identified as L2_22 in the Lyne and Hayes (2005) classification (Figure 8.1).

Within the central part of the core EAC region (~25-30°S), the current at the surface averages ~ 1 m.s⁻¹, and transports up to 30 million cubic metres per second (about 150 times the average volume flow rate of the great Amazon River). Peak values may be more than twice this rate. The current strength weakens with depth, but its effects extend down several thousand metres. It has a distinct surface core of warm water with a trough-shaped (zonal) cross-section that is about 100 km wide and 100 m deep. The current is strongest in summer, peaking in February, and weakest (by as much as half the flow) in winter.

The upper layers of the EAC separate from the coast before reaching Sydney. A substantial portion recirculates within the abyssal basin adjacent to the coast (L2_22 unit in Figure 8.1) while the remainder meanders south and eastward across the Tasman Sea as a series of current jets. The main component of this eastward flow occurs between 33 and 35°S – the so-called Tasman Front (extension of L2-22 unit to the east). It follows a meandering path in the upper 500 m, as the Lord Howe Rise and Norfolk Ridge block deeper flows. A semi-permanent eddy is established over the Norfolk Basin which is one of a sequence of such features, all tied to bathymetric structure. A unique feature of the circulation is that the current reattaches to the continental slope to the north of New Zealand. This occurs some 2000 km after it separates from the Australian coast and is the only known example of such a phenomenon. The East Auckland Current flows around the north-east coast of New Zealand and provides the southern arm of the (South Pacific Subtropical) gyre flow.

Back at the Australian boundary a component of the EAC continues southward, with no topographic barriers to its path, it extends virtually throughout the water column. This portion of the EAC flow passes east of Tasmania and appears to turn westward around its southern tip.

8.4 East Australian Current Eddy Field and Energetics

At the southern boundary, the EAC is highly variable and is associated with a highly energetic eddy field as shown in the Lyne and Hayes (2005) characterisation of the energetics field (Figure 8.). The maximum surface-height variability (a measure of eddy and frontal activity) is also contained within the abyssal basin, between the steep continental wall in the west and the ocean ridge in the east. Individual eddies are 200-300 km in diameter and 2 to 3 eddies are generated annually, although their lifetimes often exceed a year. They follow complicated southward trajectories, but are generally constrained within the deep basin. The EAC flow varies seasonally – it is strongest in summer and the separation location also migrates up and down the coast with season. These features also vary over shorter periods and exhibit major differences from year to year.

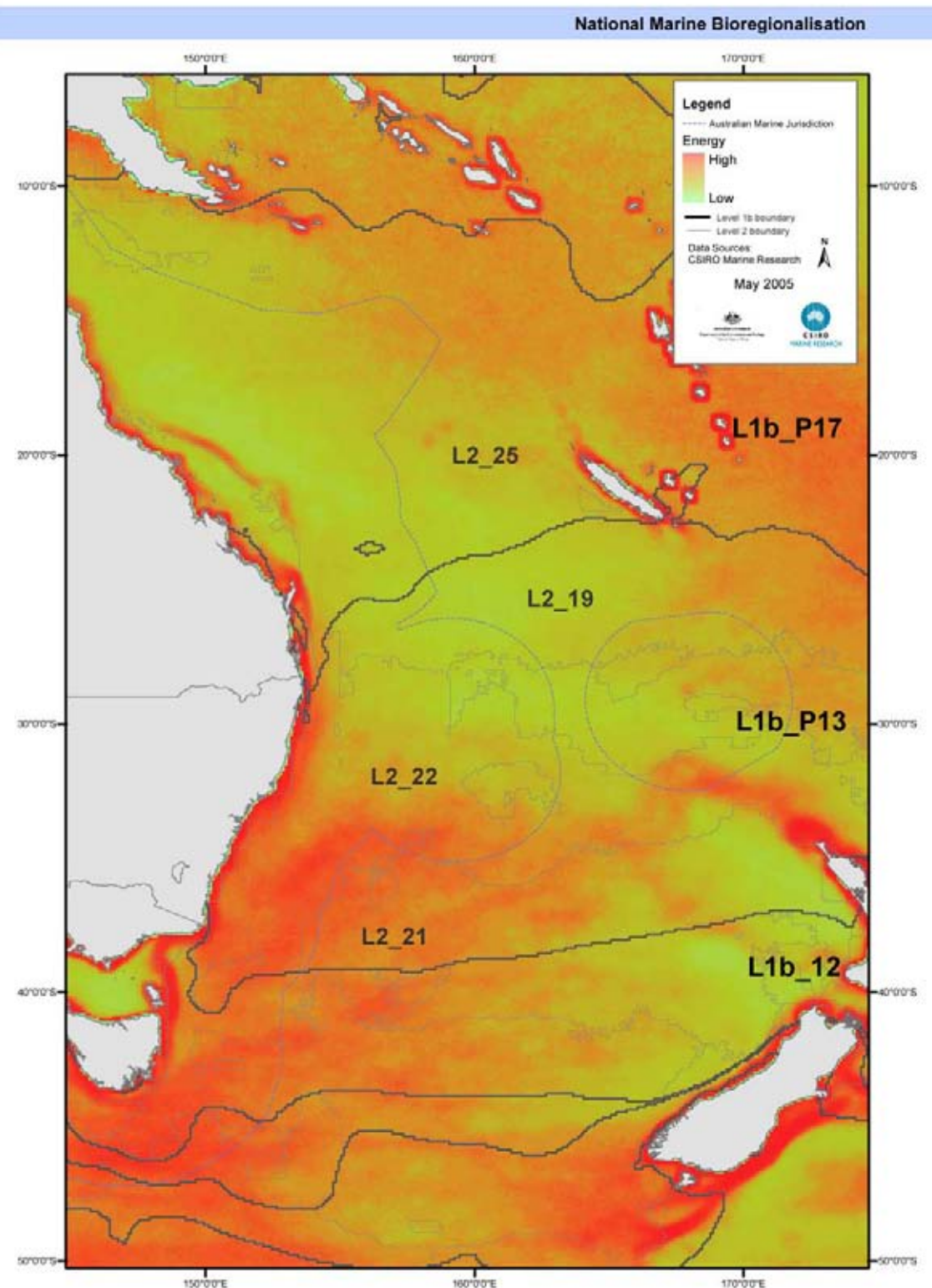


Figure 8.3 Map showing superposition of “energetics” field onto the regionalisation of Figure 8.1 (See Lyne and Hayes (2005) for a description of the derivation of the field). Higher energetics is displayed with denser shades of red. Of particular note with this image are the intense energetics all along the east coast of Australia and the offshore shelf-break region off the Great Barrier Reef. In the offshore region, high energetics are to be found in the recirculation region of the East Australian Current – primarily in the L2_22 and L2_19 units of Figure 8.1. Note also the Tasman Front, which originates in the west as a very broad mixing region and narrows down to the eastern boundary off the north-west coast of New Zealand.

The pattern of variability exhibits a level of intensity of similar magnitude, although smaller spatial extent, to that in other major western boundary currents, such as the Gulf Stream and the Kuroshio. However, in contrast to these other systems, where eddies generally result from instabilities created after the currents have separated from the coast, the EAC eddies appear to develop while the mean flow is attached to the coastal boundary well before the separation at 32°S, and are aligned meridionally.

South of the separation point, the energetics field (Figure 8.3) shows the core of the current as a low-energetics region. This is clearly not so, but is a consequence of the Lyne and Hayes (2005) energetics field being derived from analyses of temperature variability as observed in satellite sea-surface temperature fields. What it implies is that the core of the current is relatively stable (spatially), and also relatively stable in temperature – relative to the variability seen in the eddy fields. Either side of the core has areas of high energetics with the offshore (eastern) field of high energetics being very broad in extent. Ridgway and Dunn (2003) show that the core of the EAC (L2_22 unit in Figure 8.1) contains vigorous recirculations and the energetics field also shows the offshore extent of this field as a region of high energetics/variability.

8.5 Features of the EAC and the biological context

The separation of the current is important for some fish populations. For example the gemfish run and spawning are believed to be linked to it. In fact the location and timing of gemfish aggregations appear to be determined by the oscillations of the EAC. Other species such as tuna appear to favour the frontal region – either on the subtropical (yellowfin tuna) or subantarctic side (southern bluefin tuna).

The main biological influence of the eddies is to increase the vertical mixing within the upper ocean in the western Tasman Sea, in effect extending the effective mixed-layer depth and thus suppressing the winter phytoplankton and zooplankton populations through limiting light conditions. These conditions result in spring and autumn blooms of chlorophyll-*a*. In addition, upwelling associated with eddies supplies more nutrients to the surface layer, once the bloom has begun, delaying the exhaustion of nutrients and prolonging the duration of the blooms.

The EAC and its eddies frequently move onto the continental shelf and close inshore and influence the local circulation patterns. At prominent coastal features (Cape Byron, Smoky Point), the EAC moves away from the coast, driving upwelling which, draws nutrient-rich water from a depth of 200 m or more.

8.6 Overview of impacts of eddies and the East Australian Current on bioregionalisation processes in the Tasman Sea

A successful marine bioregionalisation depends on understanding the zoogeography of the species and communities in a region, and the role that currents and other oceanographic features (such as eddies) play in the distribution of these species and communities. The warm-core eddies shed by the East Australian Current affect the biology in the Tasman Sea in a number of different ways. During a study of the EAC, which ran from 1977 to 1983, CSIRO Marine Research posed these questions:

1. When an eddy is formed and separated, does it carry with it the water properties and the associated biology that are characteristic of the parent water body and the frontal region that defines the “edge” of the EAC current system?
2. Does the biology differ between the core, the margin and the outside of the eddy, and if so, are these differences maintained?
3. What are the relevant characteristic structures of the eddy field in relation to biological productivity, composition and distribution?
4. What is the latitudinal variability of biology in relation to the corresponding variability in the eddy field and interactions with the surrounding Tasman Sea waters?
5. How do the biological communities trapped inside an eddy when it forms evolve as eddies age?
6. What are the results of “close encounters” with the continental slope and shelf edge, both to the eddy and to the shelf and slope?

To answer these questions, we will review the processes of eddy formation and disappearance, examine the zoogeography of selected micronekton in the Coral and Tasman seas, and review how these groups of organisms behaved in relation to the questions posed above. Sampling took place in and around warm-core eddies F (1978) and J (1979 and 1980) off the New South Wales coast, and during two cruises (in 1982 and 1983) that with the aim of determining the zoogeographic distribution of myctophid fishes and mesopelagic crustaceans in the Coral and Tasman seas. The micronekton was chosen for this purpose largely because these animals are found in the upper 500 m of the water column at night. Typically, these mesopelagic taxa are small crustaceans, fish and cephalopods that can swim, and are in the size range of 2–20 cm. There is a diversity of species, with a variety of swimming abilities and durations of life stages, which makes them ideal for following changes in eddy structure through time.

Micronekton can be divided into groups based on their vertical distribution and migration patterns (Table 8.1).

Table 8.1: Micronekton groups and the depths at which they have been found during the day and night.

Group	Daytime depth (range)	Night-time depth (range)
Epipelagic	0-200 m	0-200 m
Mesopelagic migrant	200-500 m	0-200 m
Mesopelagic non-migrant	200-500 m	200-500 m
Bathypelagic migrant to surface layer	> 500 m	0-200 m
Bathypelagic migrant to intermediate layer	> 500 m	200-500 m
Bathypelagic migrant to both surface and intermediate layers	>500 m	0-500 m

The crustacean families commonly found in the epipelagic layer include the copepods, euphausiids and amphipods, as well as the larval stages of many different families. Mesopelagic and bathypelagic crustaceans that may migrate into the epipelagic layer at night include some euphausiids, amphipods, sergestid and penaeid prawns, and carid shrimps and some Mysidacea. The squid families found in the epipelagic layer are usually from the Onychoteuthidae and Cranchidae, while the mesopelagic and bathypelagic families include the Cranchidae, Chiroteuthidae, Mastigoteuthidae, Histio teuthidea and Enoploteuthidea. The epipelagic fishes during the day are larvae of a number of different families, but at night the fauna is dominated by fish from the families Myctophidae, Gonostomatidae, Sternopychidae and Phosichthyidae. Species belonging to the Melamphaidae, Myctophidae, Chauliodidae, Gonostomatidae, and Percichthyidae are found in the 200-500 m depth range at night.

8.7 Eddy formation and disappearance

One of the major problems in working in the Coral and Tasman Seas is that on the basis of temperature vs. salinity plots, all regions appear to be derived from the same water mass. However, there are clear differences in temperature and salinity with depth at the different sites. The main differences between the warm-core eddies from the derived Coral Sea, and shed by the East Australian Current and the surrounding Tasman Sea water are in the vertical distributions of temperature, salinity and mixed-layer depths. Plots of temperature or salinity (Griffiths & Brandt 1983a, 1983b, Griffiths & Wadley 1986) show that the water inside an eddy is typically warmer (2–7°C) depending on depth), and saltier (0.1–0.5 psu) than outside the eddy. The main difference between the inside of an eddy and the surrounding water is the presence of a deep surface mixed-layer, or thermostad, inside the eddy that gives a distinctive subsurface signature for subsequent identification. This isothermal and isohaline signature layer can reach to nearly 400 m at the end of winter, but may be capped by a warmer layer caused by solar heating. This insulates the signature layer from further changes (Cresswell 1983). For this reason, Griffiths and Wadley (1986) consider the sites represent separate domains within a single water mass. Dodimead et al (1963) define domains as regions within a water mass that have consistent structure and oceanographic behaviour, caused by environmental events such as seasonal heating and cooling, wind mixing, evaporation, precipitation, advection and diffusion.

Eddies are areas of high geopotential, in this case released by the East Australian Current (EAC), that rotate anticyclonically. Much of what follows is from Cresswell (1983); Nilsson et al, (1977); and Nilsson and Cresswell (1980). In the EAC, north of about 33°S, areas of high geopotential drift south and are quasi-permanently connected to the EAC. Warm core eddies (WCE) are formed from the pinching off of the southern edge of one of these regions of high geopotential that had moved southwards along the New South Wales coast, but had then retracted to the north. The pinched-off region of high geopotential reaches from the surface to the bottom, resembling a pillar of water rotating anticyclonically. Fauna inside a geopotential high are “captured” when the eddy pinches off, and are carried by the eddy as it moves.

South of about 33°S, where the EAC commonly leaves the Australian coast, the anticyclonic eddies show no systematic movement, and are generally not connected to the surface warm core constituting the EAC. Occasional reconnections to the EAC can occur, resulting in surface water advecting around and over an eddy in filaments typically <100 m thick, but sometimes 170 m.

The relatively warmer waters inside a newly formed warm-core eddy means that the surface of an eddy is higher than the cooler, denser Tasman Sea water surrounding it making it difficult for this water to flow onto the eddy at the surface. This mechanism helps warm-core eddies retain their physical and biological environments; it also distinguishes their physical and biological evolution from that of the cold-core eddies off the east coast of America.

During the warm-core eddy study off Australia, three regions were routinely identified on the basis of the temperature at 250 m (T_{250}). The boundary around an eddy was defined as lying between T_{250} of 14°C and 16°C; this marked the region of the strongest surface currents around the eddy. Regions where the T_{250} was $> 16^\circ\text{C}$ were regarded as inside the eddy, and regions with a $T_{250} < 14^\circ\text{C}$ were regarded as being outside the eddy. These naming conventions were used by all the authors reporting results during the eddy study.

Cresswell (personal communication) speculates that warm-core eddies have life-times of two or more years and suggests the dissipation of an eddy is a gradual process. Successive winters will cool the eddy core, altering the signature layer, and cause a decrease in the dynamic height as the density of water inside the eddy increases. This, plus friction, will reduce the energy in the eddy, and make it

more likely to be over-run by filaments of Tasman Sea water, hastening the loss of identity. Warm-core eddies also lose mass and volume as submesoscale eddies are spun off the core and meander off into the Tasman Sea. Gradually, the eddy loses its identity and is absorbed into the surrounding Tasman Sea.

It is likely that an eddy's lifetime is greater than that of many of the species trapped inside the eddy when it is formed. Communities inside the eddy evolve as some species can reproduce inside the eddy more successfully than others and immigrants may penetrate the front around the eddy, probably as a consequence of vertical migration. Eventually, as the eddy loses its identity, the northern species would die out in the changed environment of the Tasman Sea.

The main biological influence of the eddies is to increase the vertical mixing within the upper ocean in the western Tasman Sea, in effect deepening the effective depth of the mixed-layer and thus light-limiting the growth of the winter phytoplankton. These conditions result in spring and autumn blooms of chlorophyll-*a*. In addition, upwelling associated with the frontal region around eddies may supply more nutrients to the surface layer, initiating increases in phytoplankton biomass and possibly prolonging its duration of the.

The EAC and its eddies frequently move onto the continental shelf and close inshore, influencing the local circulation patterns. At prominent coastal features (Cape Byron, Smoky Point) the EAC moves away from the coast, driving upwelling that draws nutrient-rich water from a depth of 200 m or more.

8.8 Natural History of Eddies F and J.

History of Eddy F

The two best-studied eddies were Eddies F and J (Figure 8.4).

Eddy F formed by the subdivision of a larger eddy D some time between May and December 1978. Eddy (D) formed from the EAC in February 1978. A signature layer of 17.5–17.7°C extending to a depth of about 290 m formed over winter 1978. By December 1978, when the biological samples were taken, a warm summer cap (18.0–18.2°C, 60–65 m deep) had formed over the eddy. Eddy F moved southwards between September and December 1979 to about 36°30'S, where it remained stationary until February 1979. It was not followed after February 1979.

The waters inside Eddy F were warmer and saltier than the surrounding Tasman Sea water, and the eddy edge stations were closer in temperature and salinity properties to the Tasman Sea than the eddy interior. Fluorescence patterns in and around Eddy F, and the eddy's structure, were detailed in reports by Tranter et al (1979a, b; 1980a, b). There were differences in phytoplankton levels (Tranter et al 1980c) and species composition (Jeffrey and Hallegraaff 1980); nutrient cycling (Scott 1978), and copepod species distributions (Tranter et al 1983).

The mesopelagic fauna of Eddy F was sampled between 28 November and 12 December 1978, between 35.45°S and 36.8°S between 150.5°E and 152.8°E. A commercial Engel midwater trawl with a 10 mm stretch-mesh liner was used to collect the samples from depths of about 50, 150, and 250 m. The Engel trawl had a mouth area of about 600 m², but much of the net was made up of meshes that were very much larger than the organisms we were interested in. The distributions of the fish (Brandt 1981), mesopelagic crustaceans (Griffiths & Brandt 1983) and cephalopods (Brandt 1983b) are the basis of this review.

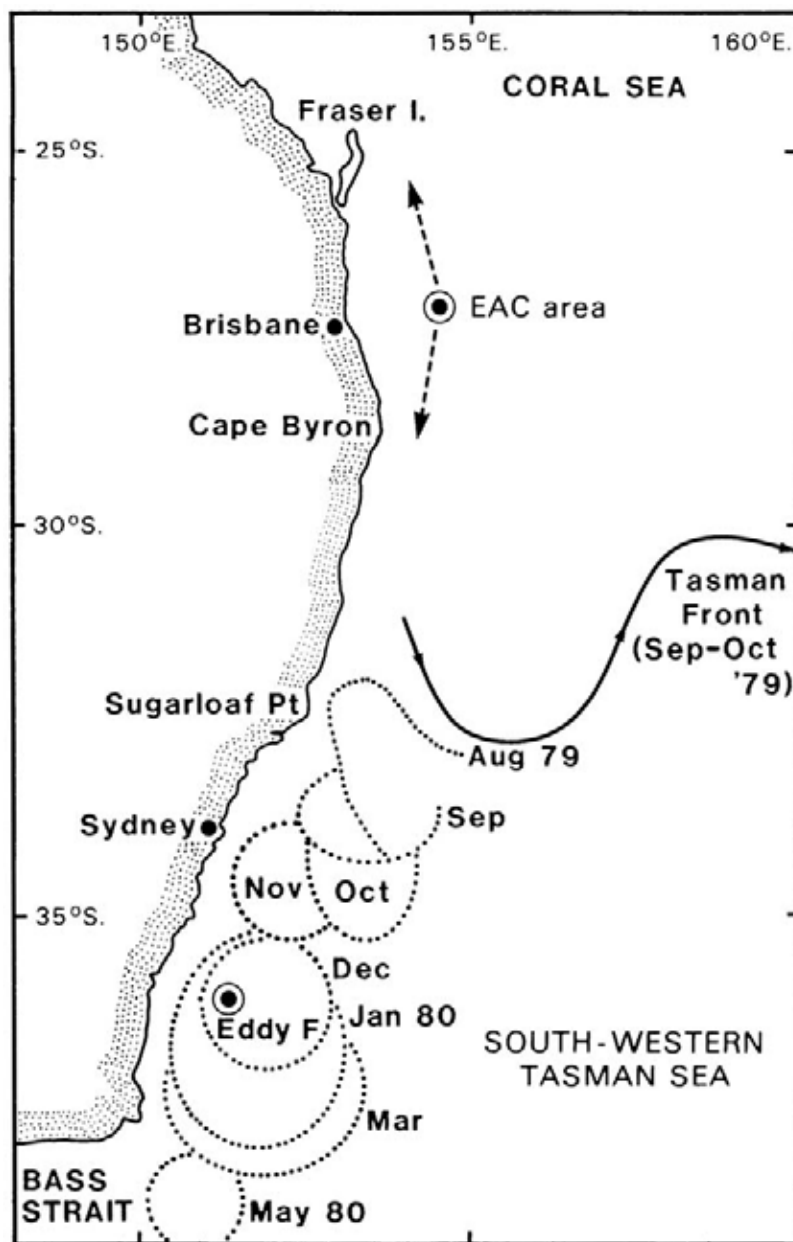


Figure 8.4 Movement of Eddy J and the position of Eddy F during sampling periods (After Tranter et al, 1983).

Results from the Eddy F survey

The Eddy F survey established that there were substantial differences in the communities inside, outside, and—for the fish at least—the eddy edge. The survey also found that the mesopelagic fish, squid and crustacean communities migrated from between 400 and 1000 m depth during the day to close to the upper 250 m at night. The distribution of fish and crustaceans with respect to the eddy are summarised in Table 8.2. Brandt (1981) found that some of the fish distributions correlated well with temperature. For example, the cold-water species outside the eddy did not penetrate into the warm, near-surface layers at night. Individuals of three fish species caught outside the eddy were larger than those caught inside, while only *Ceratoscopelus warmingii* was larger inside the eddy than outside.

Fewer species of crustaceans were caught, probably because the large nets' meshes were too big. However, there were species found only in either the inside or the outside of the eddy, but most were found in different abundances in all the regions. Two species (*Sergia prehensilis* and *Oplophorus spinosus*) were larger outside the eddy, and proportionately more male and female *S. prehensilis* and female *O. spinosus* were in breeding condition outside the eddy than in either the eddy or the eddy edge. Fecundity in *O. spinosus* was greater outside the eddy. Females of *Systellaspis debilis* were larger at the eddy edge than elsewhere, but the proportion of breeding females was greatest inside the eddy.

Pelagic squid were most abundant at night, and none of the five abundant species were restricted to a single region, although *Pterygioteuthis giardi* and *Brachiotheuthis riisei* were more numerous inside the eddy. The length-frequency distributions of *Abraaliopsis gilchristi* and *Pterygioteuthis gemmata* were significantly larger outside the eddy than on the edge or inside.

History of Eddy J

The physics and biology of Eddy J were intensively studied between March 1979 and May 1980. After an eventful lifetime, the eddy finally disappeared east of Bass Strait in July 1980. Cresswell (1983) fully documented the physical oceanographic history of Eddy J.

Eddy J was first surveyed in March 1979 (Figure 8.4), although the eddy had formed some time before this date. It was initially isolated from the EAC between March and October 1979 (winter), during which time the isothermal signature layer of the eddy core developed. The isothermal layer reached a depth of ~350 m in October 1979. In the spring and summer of 1979–1980, Eddy J was overrun by filaments of the EAC and, on one occasion, from the more recently formed Eddy K. These filaments and the interaction with Eddy K injected warm EAC water into Eddy J. The temperature in the signature layer remained relatively constant until February 1980, when the signature layer of Eddy J was found to have moved on top of the cooler, denser signature layer of the previously formed Eddy I, and it appears that the two eddies coalesced (Cresswell 1983). The two eddies remained together until May 1980, but could not be found in July 1980. Coalescence was observed between Eddies Maria and Leo in 1981, so this process may be fairly common.

Decapod crustaceans, myctophid fishes and squid, and hyperiid amphipods were collected on five cruises (in August, September and October 1979, and February and May 1980) inside and outside, and at the edge of Eddy J. The samples were collected with a rectangular midwater trawl which had an 8 m² mouth area (RMT-8) 4.5 mm mesh, and a cod end lined with 0.33 mm mesh (Griffiths et al 1980). The net was fished open, at night, for about 60 minutes at nominal depths of 10, 50, 100, 200, 300 and 350 m at a speed of about 1.5 m sec⁻¹. The crustaceans, myctophids and squid form the basis of this review. Because of the very different mouth areas, mesh size, and towing speeds, the communities caught by the Engle trawl used in Eddy F and the RMT-8 used in the Eddy J study are, at best, only qualitatively comparable.

From a biological viewpoint, the mesopelagic fauna initially inside the eddy may have been changed or added to through the filaments, exchange with Eddy K, and the coalescence with the core of Eddy I. There is little evidence that cooler, Tasman Sea water intruded into the eddy, and hence little evidence for the passive advection of Tasman Sea mesopelagic species into the eddy.

Micronekton distribution in relation to Eddy J structure and age

The distribution of myctophid fishes, mesopelagic crustaceans and squid were investigated on five cruises sampling in and around Eddy J. Some 298 species (45,343 individuals) of the first three groups were analysed. The distribution of copepods was reported by Tranter et al (1983); hyperiid amphipods in August, September and October 1979 was reported by Young and Anderson, (1987) and Young (1989); and phyllosoma larvae and macroplankton by McWilliam and Philips (1983). These

different groups were investigated because they have different thermal habitat requirements, diurnal depth ranges, and swimming abilities. In addition, Brandt (1983a) argues time scales may be important in understanding the biological integrity of communities inside and outside these eddies. The time scales that impact are:

- Time scales associated with sequential changes as the eddy ages including diffusion and mixing processes, species survival and reproduction inside and eddy, migrations to preferred habitats and predation and competition pressures.
- Seasonal time scales when there are large natural changes in species abundances, and
- Time scales associated with random events such as filaments from the EAC or coalescence between two eddies.

Table 8.2 Comparison of the community structure of micronektonic fish (after Brandt & Hodgson, 1981) and crustaceans (after Griffiths and Brandt 1983a) outside, inside and at the edge of Eddy F in November-December 1978.

Mesopelagic fishes	Outside Eddy	Eddy Edge	Inside Eddy
<i>Scopelopsis multipunctatus</i>			
<i>Ceratoscopelus warmingii</i>			
<i>Diaphus meadi</i>			
<i>Hygophum hygomii</i>			
<i>Notoscopelus resplendens</i>			
<i>Diaphus danae</i>	■■■		
<i>Lampanyctus pusillus</i>	■■■		
<i>Electrona risso</i>	■■■		
<i>Diaphus thermophilus</i>	■■■■■		
<i>Lobianchia dofleini</i>	■■■■■		
<i>Diaphus mollis</i>	■■■■■		
<i>Lampanyctus ater</i>		■■■	
<i>Argyropelecus aculeatus</i>		■■■	
<i>Chauliodus sloani</i>		■■■	
<i>Lampanyctus alatus</i>		■■■■■	
<i>Diaphus fragilis</i>	■■■■■		
<i>Vinciguerria</i> sp.		■■■■■	
<i>Howella sherborni</i>			■■■
<i>Lobianchia gemellarii</i>			■■■
<i>Echinostoma barbatum</i>			■■■
<i>Benthosema suborbitale</i>			■■■
<i>Bathylagus argyrogaster</i>			■■■
Micronektonic Crustaceans	Outside Eddy	Eddy Edge	Inside Eddy
<i>Sergia prehensilis</i>	■■■■■		
<i>Oplophorus spinosus</i>	■■■■■		
<i>Systellaspis debilis</i>	■■■■■		
<i>Sergestes armatus</i>	■■■■■		
<i>Sergestes corniculum</i>	■■■■■		
<i>Sergestes disjunctus</i>	■■■		
<i>Acanthephyra quadrispinosa</i>	■■■		
<i>Gennadas gilchristi</i>	■■■■■		
<i>Sergestes stimulator</i>		■■■■■	
<i>Funchalia villosa</i>		■■■■■	
<i>Sergia splendens</i>			■■■

Wadley (1985), using a variety of multivariate techniques, examined the distribution of the myctophids, crustaceans and squid over the-ten month sampling period. The communities sampled in the eddy core were distinct from those from the eddy edge or outside. A separation of the micronekton inside the eddy corresponded to the coalescence of Eddy J with Eddy I: the myctophids and squid in Eddy J became distinct from the crustaceans in Eddy I community. Wadley believes the micronekton has the swimming ability to escape from the eddy, but the evidence that the community remained intact suggests that the animals themselves were actively maintaining their position in the eddy. She notes that the longest a drogued buoy remained in the eddy was five months. Wadley also examined the vertical distribution of these three groups: nearly 50% of the cephalopods and 41% of the fish occurred in the upper 100 m, but only 15% of the crustaceans were in this depth range. The crustacean abundance mode was between 250 and 300 m depth.

Brandt (1983) found marked differences in the myctophid fish community inside and outside the eddy, and there is some consistency in the distribution of individual species between Eddies F and J. Brandt (1983) notes the distributions of individual species in Eddy J were not as precise as those found in Eddy F, but this may be due to the different histories of the eddies, the seasons in which the samples were taken, and the different sampling gear used. He suggested natural variations in fish communities may have overshadowed successional changes. There was little change in the myctophid fauna inside the eddy between successive cruises between August and October, but there was a major change between August–October and February–May. The species both inside and outside the eddy changed at the same time as three major events (formation of the warm summer cap, southward movement of some 500 km, and the coalescence of eddies J and I), each of these events could have markedly influenced the species' distributions. Brandt (1983) suggests the changes outside the eddy may be due to the shift in the geography of the eddy, as it moved southwards into cooler waters in the Tasman Sea. This effectively shifted the outside "reference" stations that were being used as a comparison for the catches inside the eddy. Changes in the seasonal abundance of the fish fauna could be expected because a number of the species have life spans of about one year.

The distribution of the four most abundant myctophids (*Lampanyctus alatus*, *Benthosema suborbitale*, *Hygophum hygomii* and *Diaphus meadi*) was not related to the three regions (inside, on the edge, and outside) of the eddy. However, the highest abundances of each of these coincided with a particular temperature at night. The first three species were found in the upper 60 m at night, while *D. meadi* was found in the 0–300 m depth range. The fifth most abundant species (*Diaphus danae*) was found outside or at the eddy edge only. Brandt concluded that in contrast to the crustaceans, the distributions of the myctophids were related more to night time temperatures than to the physical structure of Eddy J. Wadley found that the patterns in fish communities were determined mainly by the less abundant species, rather than these five very abundant ones.

Griffiths and Brandt (1983b) found the crustacean community inside Eddy J was not replaced by a Tasman Sea community as the eddy aged. They argued that a species succession inside the eddy was initiated, resulting in an inside community that was unlike either the original eddy community or the Tasman Sea community surrounding the eddy. They reported a marked change in community composition after Eddies J and I coalesced in early 1980. The distribution of 9 of the 18 most abundant crustacean species was not related to location inside, outside, or at the eddy edge. The most abundant species, *Sergia prehensilis*, showed no significant differences in abundance among the inside, edge or outside locations. *Gennadas gilchristi* was the second most abundant crustacean, and was significantly more abundant outside the eddy, while the third most abundant species, *Systellaspis debilis*, was significantly more abundant inside and at the edge than outside. There were differences in the size-frequency distributions of *S. prehensilis* and *S. debilis* between locations, which suggests breeding and recruitment were occurring at different times inside and outside the eddy. No differences in the size-frequency distributions of *G. gilchristi* were seen inside or outside the eddy.

Wadley (1985) reanalysed the individual phylum data presented above by grouping the fish, crustaceans and cephalopods and using the log-transformed abundances to classify the 145 stations sampled. She found the same temporal pattern of grouping of the August, September and October

cruises, and the February and May cruises as before. The warm, near-surface samples in the core of Eddy J grouped together over the ten months of the survey. Below 100 m, there was a clear difference between samples taken in Eddy J (August–October), and samples taken after the Eddy J/Eddy I coalescence in February and May. There were differences in the abundance patterns of crustaceans between the cores of Eddy J and Eddy I, although these may have been confounded with vertical distributions of the individuals. Wadley believes that outside the eddy, temporal stability was found only in the August–October period, with the outside samples in February and May not showing any clear patterns. The reasons for this change outside the eddy are not known, but may have been related to a change from the relatively cool water outside the eddy in August–October when near 33 °S to colder water, and the different thermal structures found at 36°S in February and 39°S in May.

In summary, the tropical and subtropical species are transported southwards in the EAC, and remain in the dynamic highs shed by the current that form these warm core eddies. The contrasts across the boundaries of warm-core eddies suggest that eddies may be responsible for much of the large-scale patchiness in pelagic distributions in the western Tasman Sea. The persistence of the tropical and subtropical species (especially the mesopelagic) inside the warm-core eddies for up to a year argues that the warm-water community is actively maintaining itself inside the eddy, and there is little evidence that cooler water species colonised the eddy from the surrounding Tasman Sea. The washovers or filaments from the EAC would serve to reintroduce warm-water species into an eddy. The coalescence of two eddies brought together two warm-water populations, but with little evidence of cold-water species entering the eddies. When attempting to establish bioregionalisation in the pelagic realm, there is a clear need to understand the integrated physical, chemical and biological oceanography, including vertical and horizontal distribution of these properties, in regions with major transport mechanisms.

Tranter et al, (1983) attempted an early version of a bioregionalisation of eddies by using 20 species of copepods to classify 51 stations into 8 groups. It is instructive to summarise their results. Copepods have a much poorer swimming ability than mesopelagic fishes, crustaceans and squid. Tranter et al (1983) found that the basic dichotomy was strongly controlled by temperature: four “warm” habitat groups (18.1°C to 14.4°C), and three “cool” groups (13.9°C to 13.3°C), and one anomalous group (16.0 °C) (which was lumped in with the cool habitat despite being dominated by warm-water species). According to the pattern of surface temperature, this suggests that the two groups split approximately along the central/southern portion of the Tasman Sea and that the anomalous group is located just to the south of the Tasman Front (south of the L2_19 unit in Figure 8.1). Tranter et al (1983) identified groups belonging to the following categories, where “habitat groups” were determined on the basis of a clustering analysis of species:

Feature	“Habitat Group”
Eddy core	I, III
Surrounding Seas	V, VI
Eddy Edge	II, VII

In addition, the following seasonal associations were also observed:

Season	“Habitat Group”
Winter/Summer	III
Spring/Autumn	I

Faunal similarities were observed between groups occurring in EAC waters and those in eddies. Tranter et al (1983) provided the following analyses of associations:

Group	Association
I	East Australian Current waters and eddy water when eddy is near formation region
II	“Frontal Characteristics” – edge/frontal margin of eddies
III	Heterogeneous mix, mainly comprising eddy waters with some EAC and waters outside of eddy; low copepod counts possibly associated with warmer edge of cool cyclonic cell
IV and VIII	Cooler side of eddy edge
V and VI	Cooler seas outside of eddy (Group V mainly in spring)

Ordination analyses using principal components identified species that were characteristic of eddy waters (*Mecynocera clause* and *Lucicutia flavigornis*) as well as those that were seasonal and related to eddy waters. Diurnal variations confounded some analyses but distinctions relative to eddy structure could still be discerned.

An earlier study found high surface-chlorophyll concentrations along the south-eastern margin of a warm-core eddy, towards the crescent of an adjacent cyclonic cool-water structure. An upwelling–downwelling circulation was postulated to occur at the interface between the warm-core and cool-core eddies, leading to nitrate enrichment and high phytoplankton concentrations. These features were postulated to be the basis for empirical correlations between southern bluefin tuna catches and temperature fronts.

Taken together, all of the studies identify various oceanographic aspects of eddies that are related to distinct associations of plankton, zooplankton and higher order species, including commercial fish. At a structural level, several features of eddies can be identified as influencing biological distributions; notably, the core of the eddy, the frontal margin and the surrounding waters. These faunal associations are dependent on the formation stage of the eddy, depth, seasonal mixing and interaction of the eddy with other eddies and with the continental slope or shelf.

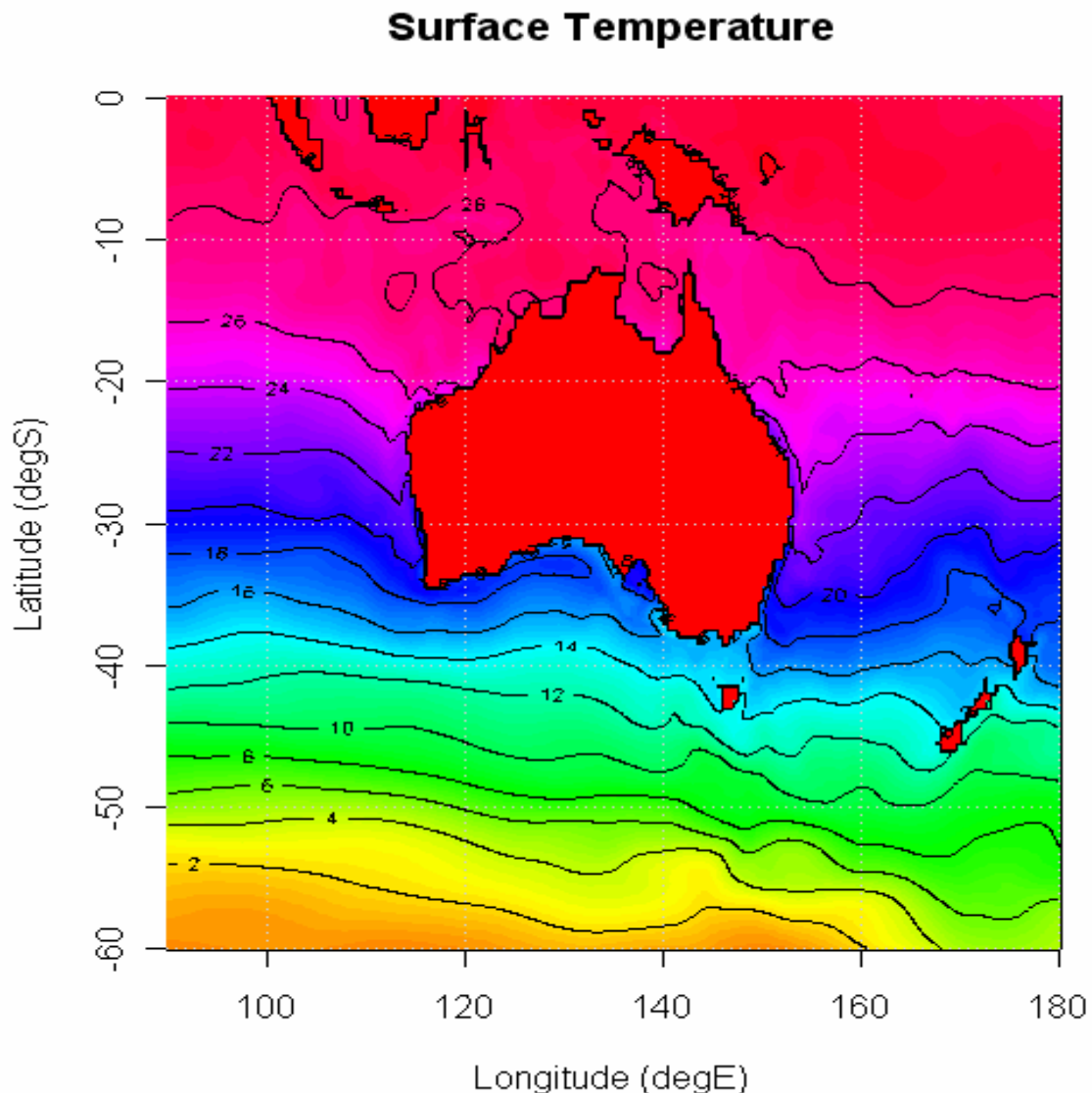


Figure 8.5 Pattern of surface mean temperatures around Australia obtained from the CSIRO CARS oceanographic atlas.

8.9 Zoogeographic Surveys

Eddy P, 1982

Eddy P was sampled in 1982, as part of a zoogeographic study to determine the latitudinal distribution of myctophids and mesopelagic crustaceans. The aim was to try and understand the distributions of species in these groups found in the studies of Eddies F and J.

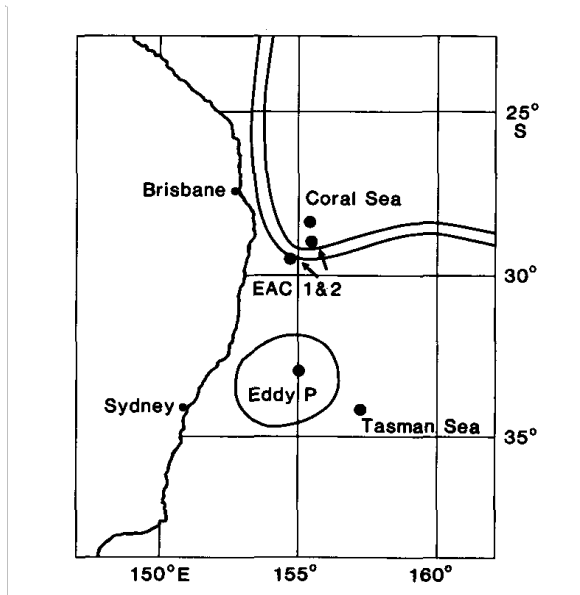


Figure 8.6 Sampling sites (●) during August 1982 on the first zoogeography cruise. The approximate boundaries of warm-core Eddy P, the East Australian Current, and the Coral Sea are shown (After Griffiths and Wadley, 1986).

Griffiths and Wadley (1986) identified four separate domains (Tasman Sea, inside newly formed Eddy P, in the EAC, and in the Coral Sea), separated on the basis of the distribution of temperature and salinity, with depth, in the 1982 voyage (Figure 8.6). A multivariate agglomerative analysis for the crustaceans and the myctophids was performed, grouping similar stations on the basis of species distribution and abundance.

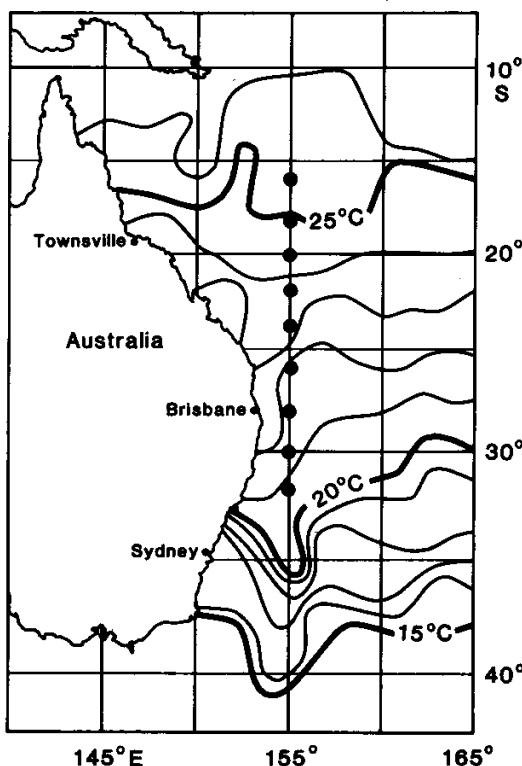
This cruise established that the crustacean fauna in the EAC and the Coral Sea were quite similar, but there were clear differences between these warm-water species assemblages and the “cold-water” species assemblage in the Tasman Sea, based primarily on differences in the relative abundance of species in the different regions (Table 8.3). The crustacean assemblage inside a newly formed eddy (Eddy P) was unique, with the absence of some warm-water species and well as the presence of some cold-water species (Griffiths and Wadley 1986): truly a mix of both Coral Sea and Tasman Sea species. In contrast, only warm-water or widespread species of myctophid fishes were found inside the warm-core eddy. There was no clear separation of the eddy from the Coral Sea or EAC sites, but there was a substantial difference between the warm-water group and the cool-water Tasman Sea assemblage. This separation was due primarily to the absence of three cool-water species found in the Tasman Sea from the warm-water sites, and the absence from the warm-water sites of cold water species from the Tasman Sea.

Table 8.3. Warm and cold water species determined in 1982.

Cold-water species	Warm-water species
<i>Acanthephyra quadrispinosa</i>	<i>Sergestes seminudus</i>
<i>Gennadas gilchristi</i>	<i>Sergia scintillans</i>
<i>Sergia prehensilis</i>	<i>Lucifer typus</i>
<i>Sergestes disjunctus</i>	<i>Centrobranchus nigroocellatus</i>
<i>Lampanyctus australis</i>	<i>Diaphus luetkini</i>
<i>Electrona risso</i>	<i>Myctophum nitidulum</i>
<i>Lobianchia dolfeni</i>	<i>Lobianchia gemellari</i>
<i>Symbolophorus barnardi</i>	<i>Diaphus atlanticus</i>
	<i>Notolychnus valdiviae</i>

Latitudinal Survey 1983

A second zoogeographic cruise was made in 1983, with sampling planned at 2 degrees of latitude intervals between 16°S and 32°S in the Coral and Tasman seas (Figure 8.7).

**Figure 8.7** Sampling sites (●) along 155°E during June and July 1983.

The surface isotherms are taken from a sea-surface temperature map for the week ending 28 June 1982 (after Griffiths and Wadley, 1986).

Unfortunately, the southern stations were sampled in a southwards extension of Coral Sea water, in which two dynamic highs, centred at 25°S and 32°S were found, with the EAC west, or inshore, of the ship's track. Because of this southward extension, no samples were taken in the Tasman Sea domain. The EAC was west, or inshore, of the ship's track.

The latitudinal distributions of crustaceans and myctophids are given in Table 8.4, arranged by the cold- or warm-water affinities found in 1982. Four of the 12 cold-water myctophid species found in 1982 were not caught in 1983, and one myctophid and one crustacean were caught only at 32°S and

28°S respectively. This supported the physical oceanographic evidence that no sampling was done in the Tasman Sea domain. The abundance of another five species increased from their latitude of first capture (24°S to 28°S) towards 32°S, suggesting these species had cold-water affinities.

The results have defined the zoogeographic distribution well enough to be confident that the species assemblage inside warm-core eddies are initially derived from the Coral Sea/EAC source water, and to be able to follow changes in fauna with time as eddies move into the Tasman Sea domain. In addition, these results suggest that the physical oceanographic controls of zoogeographic boundaries are different for myctophid fish and mesopelagic crustaceans. A temperature of 15°C at 250 m apparently separates warm- from cold-water zones for myctophids in this region, but not for crustaceans. There is no similar sharp temperature boundary for the mesopelagic crustaceans.

Table 8.4. Latitudinal distribution of myctophids and crustaceans (as mean catch per hour) during 1983 sampling. The species are listed under their cold- or warm-water affinities determined from the 1982 sampling. Species with no catch-per-hour data listed were not caught in 1983 (after Griffiths and Wadley, 1986).

Affinity	16°S	18°S	20°S	22°S	24°S	26°S	28°S	30°S	32°S
Warm Water									
<i>Lampanyctus alatus</i>		0.5	2.5	24.5	35.5	60.0	14.0	49.0	72.5
<i>Centrobranchus nigroocellatus</i>							0.5	0.5	0.5
<i>Diaphus luetkini</i>	1.5	3.0	3.5	1.5	1.0	1.5	0.5		
<i>Myctophum nitidulum</i>					0.5				
<i>Lobianchia gemellarii</i>	1.0	3.0	0.5		3.0	2.5	0.5	3.5	3.0
<i>Diaphus atlanticus</i>	2.5	4.0	1.0		4.0		0.5	4.0	2.0
<i>Notolynchnus valdiviae</i>	0.5	2.0	6.5	14.5	57.5	23.5	3.0	22.5	17.0
<i>Triphoturus micropterus</i>			1.0	1.5	3.5	8.5	0.5	3.5	13.5
<i>Diaphus mollis</i>	1.0	0.5			1.0	6.5	3.0	0.5	2.5
<i>Benthosema suborbitale</i>	1.0	1.5	0.5	1.0	14.5	2.0	11.5	14.5	9.0
<i>Sergestes seminudus</i>	2.0	7.5	6.0	3.5	3.5	11.0	12.5	28.0	26.5
<i>Sergia scintillans</i>			1.5	1.5	6.0	16.5	5.0	15.0	17.5
<i>Lucifer typhus</i>	0.5				11.5	0.5	1.5		0.5
<i>Gennadas scutatus</i>								1.0	1.0
<i>Sergestes vigilax cf. "bilobe"</i>						1.0			
<i>Sergestes atlanticus</i>						1.0	2.0	8.5	5.0
<i>Sergestes pectinatus</i>	0.5		0.5	6.0	3.0	10.0	2.0	9.0	18.0
<i>Sergia splendens</i>			0.5	1.0	0.5	13.0	0.5	8.5	15.5
Cold Water									
<i>Lampanyctus australis</i>									1.0
<i>Electrona risso</i>									
<i>Lobianchia dolfini</i>							0.5	3.5	7.5
<i>Symbolophorus barnardi</i>							3.0		
<i>Diaphus sp. nov.</i>							6.5	5.5	14.5
<i>Ceratoscopelus warmingii</i>	4.5	9.0	1.5	12.5	19.5	7.5	51.0	41.0	45.5
<i>Hygophyllum hygomii</i>						0.5	3.0	3.5	7.5
<i>Sergia prehensilis</i>					0.5	2.0	6.5	5.5	
<i>Gennadas tinayrei</i>						6.5	10.5	22.5	15.0
<i>Gennadas gilchristi</i>							14.0	25.5	0.5
<i>Sergestes disjunctus</i>							0.5	3.0	6.5
<i>Acanthephyra quadrispinosa</i>							0.5		

8.10 Summary

Warm-core eddies formed by the pinching off of dynamic highs in the East Australian Current carry myctophid, crustacean and squid communities that are characteristic of the region of formation. Most of the species found inside a warm-core eddy originate from the Coral Sea. There was an absence of cold-water myctophids in the Coral Sea water in 1983; however, they were present inside Eddy P in 1982. This repeats the observation by Backus and Craddock (1982), who found more warm-water fish would cross into cold-water regions across the edge of the Gulf Stream than cold-water fish that would cross into warm water. However, the crustaceans did not show this pattern.

The results from the studies of Eddies F and J and from the 1982 and 1983 cruises suggest strongly that the physical oceanographic controls of zoogeographic boundaries are different for these two groups that can swim rapidly. The data from Tranter et al (1983, and see above) suggest that the copepods, who are much less mobile, show a more passive pattern than the larger organisms.

McKelvie (1985) found the distribution of faunal groups in the Labrador Current, Slope Water and in the Gulf Stream off eastern USA were consistent with a gradation of fauna in the regions, rather than abrupt changes in species composition between water masses. The results from the EAC region show similar gradation of species between domains within a single water mass. Brandt (1981) found that myctophids were quite specific about the thermal regimes they inhabited at night, while Griffiths and Brandt (1983) found the crustaceans were less so. The 1983 zoogeographic results, combined with the temperature preferences, suggest a plausible explanation of why more species of “cold-water” crustaceans than “cold-water” fishes were found inside warm-core eddies. Cold-water crustaceans were found as far north as 24°S in 1983, but cold-water fish were not found north of 32°S. Most warm-core eddies form between 26 and 33°S (Boland & Church, 1981), so there would be cold-water crustaceans, but no cold-water myctophids, in the area of formation. Only widespread myctophid species would be found within the eddy. The different night-time depth distributions (fishes, <100 m; crustaceans, 150–400 m) may also contribute to the presence of cold-water crustaceans inside new eddies.

The results from the warm-core eddy studies clearly show that the complexity in species distributions in the pelagic realm cannot be understood without understanding the physical and chemical oceanography background of this realm. Good physical and chemical oceanographic information and an understanding of ocean circulation features such as eddies and currents are the basis for understanding disjunct distributions of animal. There is also a clear need to understand the biology and behaviour of the organisms before applying rigid boundaries in a variable ocean. The distinctiveness of the inside and outside of warm-core eddies is maintained by the behaviour patterns of the species involved. The maintenance of the characteristic physical and biological environment inside eddies due to the forcing dynamics reinforces the maintenance of these separate communities, and complexity in distribution patterns. Community changes inside warm-core Eddy J as the eddy aged were partly driven by changes in nutrient regimes, vertical mixing, primary production, filament washovers and interaction with other eddies. The lifetimes of the mesopelagic fishes and crustaceans are of the order of the lifetime of an eddy, and breeding success was evident in the size-structure of populations inside the eddy.

The principal conclusion of these studies is that, without a good understanding of the physical and chemical environment—the physical dynamics of that environment—the distribution of the biota cannot be understood and neither can rigid boundaries between communities be drawn. It is also true that the dynamic circulation patterns in the offshore ocean probably make a boundary line drawn today not relevant this time next year.

9 Recommendations for Future Research

The 3-D regionalisation that has been produced through the current series of projects relied extensively on the CARS database, a collection of physical and chemical information. The identification of water masses through the regionalisation compares favourably with that obtained experimentally as part of the World Ocean Circulation Experiment (see section 7.3).

One of the obvious gaps in the current bioregionalisation project has been the lack of biological data. The following list highlights the key areas where further research would improve the bioregionalisation.

- Integrate existing shelf and slope demersal fish regionalisations by combining the datasets and analysing the combined set. This would provide the basis for an updated benthic regionalisation.
- Characterisation of Australian offshore islands (excluding Macquarie Island). Collate available fish data, including the NORFANZ data, to characterise demersal and pelagic fish. This would feed into both the Benthic and Pelagic regionalisation.
- There is a wealth of information in existing museum collections on, for example, echinoderms, molluscs and decapods (taxonomically well-known groups). These data should be mined, digitised and verified.
- Biological oceanographic datasets for the Northern Planning Region cover only the Gulf of Carpentaria. Further collections in the Arafura and Timor seas, as well as the Torres Strait are needed.
- Searches for ecosystem surrogates are currently underway for the soft-bottom communities of the Great Barrier Reef and the Gulf of Carpentaria. Once developed, these surrogates may be used for other shallow, soft-bottom communities in tropical Australia.
- Seasonal and inter-annual changes in biological and physical characteristics must be taken into account when applying them to bioregionalisation. More emphasis must be placed on systematic monitoring of both climate variability and climate change around Australia as it pertains to the pelagic domain.
- The design and implementation of Marine Protected Areas must consider the sources, sinks and connectivity of communities through their pelagic larvae and also the links between current regimes, seasonal reproductive activity and recruitment.
- Test surrogacy assumptions that use geomorphic data to predict biological distributions to determine which physical variables are most biologically relevant (e.g. existing projects in the south-east and Great Barrier Reef).
- The valuable synoptic SeaWiFS chlorophyll data reflect the biomass of surface phytoplankton only, and there is a need to carefully assess, region by region, to what extent these data can be used as a proxy for the phytoplankton biomass of the total water column. This applies especially to areas such as the Coral Sea that are known to have persistent deep (75-150 m) chlorophyll maxima.
- Collect more chlorophyll data to characterise the waters around Australia for input into a chlorophyll, CARS-type database. This could be done by asking the National Facility running *Southern Surveyor* to implement a system to routinely include a fluorometer and a full ocean depth PAR sensor on all CTD casts, and to collect samples for chlorophyll analyses to calibrate the fluorometer on each cruise. This should be implemented as a standard oceanographic calibration method similar to the collection of salinity and oxygen samples to calibrate the relevant sensors on the CTD.

- No phytoplankton data appear to ever have been collected from the region between Cape Leeuwin and Port Lincoln. The need for such information relates to, among others, this being the upstream source for phytoplankton communities affecting the lucrative South Australian shellfish and finfish farm aquaculture operations.
- Analyse and map distributions of informative biological groups, e.g. the lanternfishes (Family Myctophidae), to use as primary indicators for Australia's pelagic zones.
- Further development of pelagic bioregionalisation methods with an emphasis on temporal variability, in conjunction with dataset development.
- Development of methods for using a pelagic bioregionalisation in delineating Marine Protected Areas. This work will involve formalising the relationship between design, declaration and management of these areas.

10 Acknowledgments

We thank the National Oceans Office for having the vision to implement and fund this data project – with particular thanks to Miranda Carver (National Oceans Office) and David McDonald (CSIRO Marine Research) for their management of the project. The project involved material from many sources, for which we thank all the contributors, particularly Steve Rintoul and Sergei Solakov for comments and permission to use extracts from their paper in the Water Mass formation and Subduction section. Thanks also to the Commonwealth Bureau of Meteorology and the *Journal of Marine Research* for granting permission to use their material. The entire project team did a fantastic job with the data and we are very grateful for their dedication. We would like to thank Dr Vivienne Mawson for providing editorial comments under very tight time frames. Many thanks to Annabel Ozimec for her continued technical support with managing large Word documents, and Dianne Furlani for her editorial comments.

11 References

- Ajani, P, Lee, R, Pritchard, T and Krogh, M (2001) Phytoplankton dynamics at a long-term coastal station off Sydney, Australia. *Journal of Coastal Research* 34: 60-73.
- Allen, WE and Cupp, EE (1935) Plankton diatoms of the Java Seas. *Annls. Jard. bot. Buitenzorg* 44: 101-174.
- Anderson, OB, Woosworth, PL and Flather, RA (1995) Intercomparison of recent global tide models. *Journal of Geophysical Research* 100(C12): 25261-25282.
- Ayukai, T and Miller, D (1998) Phytoplankton biomass, production and grazing mortality in Exmouth Gulf, a shallow embayment on the arid, tropical coast of Western Australia. *Journal of Experimental Marine Biology and Ecology* 225: 239-251.
- Backus RH and Craddock , JE (1982) Mesopelagic fishes in Gulf Stream cold core rings. *Journal of Marine Research* 40: 1-20.
- Behrenfeld MJ and Falkowski, PG (1997) Photosynthetic rates derived from satellite-based chlorophyll concentration. *Limnology and Oceanography* 42(1): 1-20
- Bingham, FM and Lukas, R. (1995) The distribution of intermediate water in the western Equatorial Pacific during January-February 1986. *Deep-Sea Research* 42(9): 1545-1573
- Bingham, FM and Lukas, R (1995) The distribution of intermediate water in the western equatorial Pacific during January-February 1986. *Deep Sea Research II*, 42(9): 1545-1573.
- Boland FM and Church JA (1981)The East Australian Current 1978. *Deep-Sea Research* 28 (9A): 937-957
- Bolch, CJ and Hallegraeff, GM (1990) Dinoflagellate cysts from Recent marine sediments of Tasmania, Australia. *Botanica Marina* 33: 173-192.
- Brainerd, KE and Gregg, MC (1995) Surface mixed and mixing layer depths. *Deep Sea Research I* 42: 1521-1543
- Brandt, SB (1981) Effects of a warm-core eddy on fish distributions in the Tasman Sea off east Australia. *Marine Ecology Progress Series* 6: 19-33.
- Brandt, SB (1983a) Temporal and spatial patterns of lanternfish (family Myctophidae) communities associated with a warm-core eddy. *Marine Biology* 74: 231-244.
- Brandt, SB (1983b) Pelagic squid associations with a warm-core eddy of the East Australian Current. *Australian Journal of Marine and Freshwater Research* 34: 573-585.
- Brandt, SB and Hodgson, HL (1981) Lanternfishes, oceanic fronts and warm-core eddies. *Australian Fisheries* 40(5): 14-17.
- Burford, MA and Rothlisberg, PC (1999) Factors limiting phytoplankton production in a tropical continental shelf ecosystem. *Estuarine, Coastal and Shelf Science* 48: 541-549.
- Burford, MA, Rothlisberg, PC, and Wang, Y (1995) Spatial and temporal distribution of tropical phytoplankton species and biomass in the Gulf of Carpentaria, Australia. *Marine Ecology Progress Series* 118: 255-266.
- Condie, SA and Dunn, JR (submitted) Seasonal characteristics of the surface mixed layer in the Australasian region: Implications for primary production regimes and biogeography. *Marine and Freshwater Research*

- Condie, SA, Fandry, C, McDonald, D, Parslow J and Sainsbury, K (2003) Linking ocean models to coastal management on Australia's North West Shelf. *Eos, Transactions, American Geophysical Union*, 84: 49-53.
- Condie, SA and Harris, PT (2005) Chapter 35. Interactions between physical, chemical, biological, and sedimentological processes in Australia's Shelf Seas (30, W-S). *The Sea* 14: 1411-1447.
- Cresswell, GR (1983) Physical evolution of Tasman Sea Eddy J. *Australian Journal of Marine and Freshwater Research* 34(4): 495-513.
- Cresswell, GR (1983) Physical evolution of Tasman Sea eddy J. *Australian Journal of Marine and Freshwater Research* 34: 495-513.
- CSIRO Division of Fisheries and Oceanography (1963) Oceanographical observations in the Pacific Ocean in 1961. *HMAS Gascoyne Cruise G 1/61. Oceanographical Cruise Report No. 8*.
- Dakin, WJ and Colefax, A (1933) The marine plankton of the Coastal Waters of New South Wales. 1. The chief planktonic forms and their seasonal distribution. *Proceedings of the Linnean Society of N.S.W.* 58:186-222.
- Dakin, WJ and Colefax, AN (1940) *The Plankton of Australian coastal waters of New South Wales. Part 1. Monographs of the Department of Zoology University of Sydney* 1: 1 – 221.
- Desrosieres, R (1965) Observations sur le phytoplankton superficial de l'océan indien oriental. *Cahiers ORSTOM Oceanographie* 3: 31-37.
- Dodimead, AJ, Favorite, F, and Hirano, T (1963) Salmon of the North Pacific Ocean Part II. Review of the Oceanography of the Subarctic Pacific region. *International North Pacific Fisheries Commission Bulletin No. 13*.
- Dunn, JR and Ridgway, KR (2002) Mapping ocean properties in regions of complex topography, *Deep Sea Research I* 49(3): 591-604
- Egbert, GD, Bennett, AF and Foreman, MGG (1994) TOPEX/POSEIDON tides estimated using a global inverse model. *Journal of Geophysical Research* 99: 28821-24852
- Findlay, CS and Flores JA (2000) Subtropical Front fluctuation south of Australia ($45^{\circ} 09' S$, $146^{\circ} 17' E$) for the last 130 k years based on calcareous nanoplankton. *Marine Micropaleontology* 40(4): 403-416.
- Furnas, MJ and Mitchell, AW (1996) Nutrient inputs into the Great Barrier Reef (Australia) from subsurface intrusions of Coral Sea Waters: a two-dimensional displacement model. *Continental Shelf Research* 16: 1127-1148.
- Furnas, MJ and Mitchell, AW (1999) Wintertime carbon and nitrogen fluxes on Australia's Northwest Shelf. *Estuarine, Coastal and Shelf Science* 49: 165-175.
- Gibbs, CF, Arnott, GH, Longmore, AR and Marchant, JW (1991) Nutrient and plankton distribution near a shelf break front in the region of Bass Strait Cascade. *Australian Journal of Marine and Freshwater Research* 42: 201-217.
- Gordon, AL (1975) An Antarctic oceanographic section along $170^{\circ} E$. *Deep Sea Research* 22: 357-377.
- Gran, HH, and Braarud, T (1935) A quantitative study of the phytoplankton in the Bay of Fundy and the Gulf of Maine (including observations of hydrography, chemistry and turbidity). *Journal of the Biological Board of Canada* 1: 279-433.
- Griffiths, FB and Brandt, SB (1983a) Distribution of mesopelagic decapod Crustacea in and around a warm-core eddy in the Tasman Sea. *Marine Ecology Progress Series* 12(2): 175-184.

- Griffiths, FB and Matear, RJ (2004) Primary production in the Southern Ocean: Comparison between estimates from the Behrenfeld-Falkowski VGPM model and SeaWiFs and MODIS satellite estimates and measurements. Presented to Ocean Optics XVII, 2004.
- Griffiths, FB and Brandt, SB (1983) Mesopelagic Crustacea in and around a warm-core eddy in the Tasman Sea off eastern Australia. *Australian Journal of Marine and Freshwater Research* 34(4): 609-623.
- Griffiths, FB and Wadley, VA (1986) A synoptic comparison of fishes and crustaceans from a warm-core eddy, the East Australian Current, the Coral Sea and the Tasman Sea. *Deep Sea Research* 33: 1907-1922.
- Griffiths, FB, Brandt, SB, and Cavill, GA (1980) A collapsible rectangular midwater trawl—RMT 1+8. CSIRO Division of Fisheries and Oceanography Report 122.
- Hallegraeff, GM (1981) Seasonal study of phytoplankton pigments and species at a coastal station off Sydney; importance of diatoms and the nanoplankton. *Marine Biology* 61: 107-118.
- Hallegraeff, GM (1983) Scale-bearing and lorate nanoplankton from the East Australian Current. *Botanica Marina* 26: 493-515.
- Hallegraeff, GM (1995) Marine phytoplankton communities in the Australian region: Current status and future threats. In: L.Zann (ed.) *State of the Marine Environment Report for Australia* Tech. Annex 1, 85-96.
- Hallegraeff, GM (2002) *Aquaculturists' Guide to Harmful Australian Microalgae*. 2nd edition. The Print Centre, Hobart, 136 pp.
- Hallegraeff, GM and Jeffrey, SW (1984) Tropical phytoplankton species and pigments in continental shelf waters of North and North-West Australia. *Marine Ecology Progress Series* 20: 59-74.
- Hallegraeff, GM and Jeffrey, SW (1993) Annually recurrent diatom blooms in spring along the New South Wales coast of Australia. *Australian Journal of Marine and Freshwater Research* 44: 325-34.
- Hallegraeff, GM and Reid, DD (1986) Phytoplankton species successions and their hydrological environment at a coastal station off Sydney. *Australian Journal of Marine and Freshwater Research* 37: 361-377.
- Hallegraeff, GM and Westwood, KJ (1995) Environmental factors influencing algal blooms of the Derwent River. pp 38-55 in: Proceedings of the Scientific Forum, *The State of the Derwent. Proceedings of a Scientific Forum*, 26th April 1995, Hobart, Tasmania. Published by the Tasmanian Department of Environmental and Land Management, pp 38-55.
- Hanson CE (2004) Oceanographic forcing of phytoplankton dynamics in the Coastal Eastern Indian Ocean. PhD Thesis, University of Western Australia, Perth, WA
- Hanson CE, Pattiaratchi, CB, and Waite, AM (2005) Sporadic upwelling on a downwelling coast: Phytoplankton responses to spatially variable nutrient dynamics off the Gascoyne region of Western Australia. *Continental Shelf Research* 25: 1561-1582
- Harris, PT (1994) Comparison of tropical, carbonate and temperate, siliciclastic tidally dominated sedimentary deposits: examples from the Australian continental shelf. *Australian Journal of Earth Sciences* 41: 241-254.
- Hasselmann, K and WAMDI group, (1998) The WAM model- a third generation ocean wave prediction model. *Journal of Physical Oceanography* 18: 1775-1810.
- Hiramatsu, C and De Decker, P (1996) Distribution of calcareous nanoplankton near the subtropical convergence, south of Tasmania, Australia. *Australian Journal of Marine and Freshwater Research* 47: 707-713.

Holloway, PE, Humphries, SE, Atkinson, M and Imberger, J (1985) Mechanisms for nitrogen supply to the Australian North West Shelf. *Australian Journal of Marine and Freshwater Research* 36: 753-764.

Interim Marine and Coastal Regionalisation for Australia Technical Group (1998) Interim Marine and Coastal Regionalisation for Australia: an ecosystem-based classification for marine and coastal environments. Version 3.3. Environment Australia, Commonwealth Department of the Environment. Canberra, 104pp.

Jeffrey, SW and Hallegraeff, GM (1980) Studies on the phytoplankton species and photosynthetic pigments in a warm-core eddy of the East Australian Current. 1. Summer populations. *Marine Ecology Progress Series* 3: 285-294.

Jeffrey, SW and Hallegraeff, GM (1987) Phytoplankton pigments, species and light climate in a complex warm-core eddy (Mario) of the East Australian Current. *Deep Sea Research* 34: 649-673.

Jeffrey, SW and Hallegraeff, GM (1990) Phytoplankton ecology of Australasian waters. pp. 310-348 in MN Clayton and RJ. King (eds), *Biology of Marine Plants* Longman Cheshire, Melbourne.

Kalnay, E, Kanamitsu, M, Kistler, R, Collins, W, Deaven, D, Gandin, L, Iredell, M, Saha, S, White, G, Woollen, J, Zhu, Y, Leetmaa, A, Reynolds, Chelliah, M, Ebisuzaki, W, Higgins, W, Janowiak, J, Mo, KC, Ropelewski, C, Wang, J, Jenne, Roy, Joseph, Dennis (1996) The NCEP/NCAR 40-Year Reanalysis Project *Bulletin of the American Meteorological Society* 77: 437-471

Komen, G, Cavaleri, L, Donelan, M, Haseleman, S and Janssen, PAEM, (1994) *Dynamics and Modelling of Ocean Waves*. Cambridge University Press, Cambridge. 532 pp.

Lagerloef, GSE, Mitchum, GT, Lukas, RB, Niiler, PP (1999) Tropical Pacific near-surface currents estimated from altimeter, wind, and drifter data, *Journal of Geophysical Research* 104(C10): 23313-23326.

Lee, R, Ajani, P, Krogh, M and Pritchard, TR (2001) Resolving climatic variance in the context of retrospective phytoplankton pattern investigations off the east coast of Australia. *Journal of Coastal Research* 34: 74-86

LeRoi, JM and Hallegraeff, GM (2004) Scale-bearing nanoplankton flagellates from southern Tasmanian coastal waters, Australia. 1. Species of the genus *Chrysochromulina* (Haptophyta). *Botanica Marina* 47: 73-102.

Lewis, RK (1981) Seasonal upwelling along the south-eastern coastline of south Australia. *Australian Journal of Marine and Freshwater Research* 32: 843-854.

Lyne V, Last P, Scott R, Dunn, J, Peters, D, Ward, T (1998) *Large Marine Domains of Australia's EEZ*. CSIRO Marine Research and Department of Environment and Land Management, Tasmania. A report commissioned by Environment Australia, March 1998.

Lyne, V and Hayes, D (2005) *Pelagic Regionalisation. National Marine Bioregionalisation Project*. A report to the National Oceans Office. CSIRO Marine Research. Australia.

Markina, NP (1972) Special features of plankton distribution around northern coasts of Australia during different seasons of 1968-1969 (Russ.). *Izv. Tikhvokean nauchnoissled Inst ryb Khoz. Okeanogr.* 81: 57-68

Markina, NP (1974) Biogeographic regionalisation of Australian waters of the Indian Ocean. *Oceanology* 15: 602-604.

Markina, NP (1976) Ecological diversity of plankton in the Australian region of the Indian Ocean. *Biol. Morya* 3: 49-57

Marshall, SM (1933) The production of microplankton in the Great Barrier Reef region. *Scientific Report of the Great Barrier Reef Expedition* 2: 112-157.

McCartney, MS (1977) *Subantarctic Mode Water. A Voyage of Discovery*, supplement to *Deep Sea Research*, Martin Angel, editor, Pergamon Press pp.103-119

- McCartney, MS (1982) The subtropical recirculation of mode waters. *Journal of Marine Research* 40: (Suppl.): 427-464.
- McCartney, MS and Baringer, MO (1993) Notes on the S. Pacific hydrographic section near 32°S – WHP P6. *WOCE Notes* 5(2): 3-11.
- McKelvie, DS (1985) Discreteness of pelagic faunal regions. *Marine Biology* 88(2): 125-133.
- McMinn, A (1990) Recent dinoflagellate cyst distribution in eastern Australia. *Review of Palaeobotany and Palynology* 65: 305-310.
- McWilliam PS and Phillips, BF (1983) Phyllosoma larvae and other crustacean macrozooplankton associated with eddy J, a warm-core eddy off south-eastern Australia. *Australian Journal of Marine and Freshwater Research* 34(4) 653-663.
- Moestrup, Ø (1979) Identification by electron microscopy of marine nanoplankton from New Zealand, including the description of four new species. *New Zealand Journal of Botany* 17: 61-95.
- Nilsson, CS and Cresswell, GR (1980) Formation and evolution of East Australian Current warm-core eddies. *Progress in Oceanography* 9(3): 133-183.
- Nilsson, CS, Andrews, JC, Scully-Power, P (1977) Observations of eddy formation off east Australia. *Journal of Physical Oceanography* 7(5): 659-669.
- Porter-Smith, R, Harris, PT, Anderson, O, Coleman, R, Greenslade, D and Jenkins, CJ (2004) Classification of the Australian Continental shelf based on predicted sediment exceedance from tidal currents and swell waves. *Marine Geology* 211(1-2): 1-20
- Reid, J L (1965) Intermediate Waters of the Pacific Ocean. Johns Hopkins Oceanography Studies 2. 85 pp
- Revelante, N and Gilmartin, M (1982) Dynamics of phytoplankton in the Great Barrier Reef Lagoon. *Journal of Plankton Research* 4: 47-76.
- Revelante, N, Williams, WT and Bunt, JS (1982) Temporal and spatial distribution of diatoms, dinoflagellates and *Trichodesmium* in waters of the Great Barrier Reef. *Journal of Experimental Marine Biology and Ecology* 63: 27-45.
- Ridgway, KR and Condie, SA (2004) The 5500-km long boundary flow off western and southern Australia. *Journal of Geophysical Research* 109: 4017, doi:10.1029/2003JC001921.
- Ridgway, KR and Dunn, JR (2003) Mesoscale structure of the mean East Australian Current System and its relationship with topography. *Progress in Oceanography* 56: 189-222.
- Ridgway, KR, Dunn, JR and Wilkin, JL (2002) Ocean interpolation by four-dimensional least squares: Application to the waters around Australia, *Journal of Atmospheric and Oceanic Technology* 19(9): 1357-1375
- Riley, GA (1942) The relationship of vertical turbulence and spring diatom flowering. *Journal Marine Research* 5: 67-87.
- Rintoul, SR and Bullister, JL (1998) A late winter hydrographic section from Tasmania to Antarctica. *Deep Sea Research* 46: 1417-1454.
- Rintoul, SR, Donguy, JR and Roemmich, DH (1997) Seasonal evolution of upper ocean structure between Tasmania and Antarctica. *Deep Sea Research I* 44(7): 1185-1202.
- Rothlisberg, P, Condie, S, Hayes, D, Griffiths, B, Edgar, S, and Dunn, J (2005) Collation and analysis of oceanographic datasets for National Marine Bioregionalisation; the Northern Large Marine Domain. A Report to the National Oceans Office.

- Rothlisberg, PC, Pollard, PC, Nichols, PD, Moriarty, DJW, Forbes, AMG, Jackson, CJ, and Vaudrey, D (1994) Phytoplankton community structure and productivity in relation to the hydrological regime of the Gulf of Carpentaria, Australia, in summer. *Australian Journal of Marine and Freshwater Research* 45: 265-282.
- Scott BD (1978) Hydrographic features of a warm core eddy and their biological implications. Australia, Commonwealth Scientific Industrial Research Organisation Division of Fisheries and Oceanography Report 100. 18pp
- Scott, FJ and Marchant, HJ (eds) (2005) *Antarctic Marine Protists*. ABRS and Australian Antarctic Division, 550 pp.
- Solakov, S and Rintoul, S (2000) Circulation and water masses of the Southwest Pacific: WOCE Section P11, Papua New Guinea to Tasmania. *Journal of Marine Research* 58: 223-268
- Stramma, L, Peterson, RG and Tomczak, M (1995) The South Pacific Current. *Journal of Physical Oceanography* 25: 77-91.
- Sverdrup, H.U. (1953). On conditions for the vernal blooming of phytoplankton. *J. Cons. Perm. Int. Explor. Mer.* 18: 287-295.
- Thomson, RORY and Edwards, RJ (1981) Mixing and Water Mass formation in the Australian subantarctic. *Journal of Physical Oceanography* 11: 1399-1407.
- Tranter, DJ (1977) Further studies of plankton ecosystems in the eastern Indian Ocean V. Ecology of the Copepoda. *Australian Journal of Marine and Freshwater Research* 28(5): 593-625.
- Tranter, D J and Kerr, JD (1969) Seasonal variations in the Indian Ocean along 110°E. V. Zooplankton biomass. *Australian Journal of Marine and Freshwater Research* 20: 77-84.
- Tranter, DJ, Parker, RR and Cresswell, GR (1980c) Are warm-core eddies unproductive? *Nature* 284: 540-542.
- Tranter, DJ, Tafe, DJ, and Sandland, RL (1983) Some zooplankton characteristics of warm-core eddies shed by the East Australian Current, with particular reference to copepods. *Australian Journal of Marine and Freshwater Research* 34(4): 587-607.
- Tranter, DJ, Parker, RR and Vaudrey, DJ (1980b) *In vivo chlorophyll a fluorescence in the vicinity of warm-core eddies off the coast of NSW, December 1979*. CSIRO Division of Fisheries and Oceanography Report 113.
- Tranter, DJ, Parker, RR, and Higgins, HW (1979b) *In vivo chlorophyll a fluorescence in the vicinity of warm-core eddies off the coast of NSW, October 1978*. CSIRO Division of Fisheries and Oceanography Report 110.
- Tranter, DJ, Parker, RR, and Vaudrey, DJ (1979a) *In vivo chlorophyll a fluorescence in the vicinity of warm-core eddies off the coast of NSW, September 1979*. CSIRO Division of Fisheries and Oceanography Report 105.
- Tranter, DJ, Parker, RR, Gardner, D and Campbell, R (1980a) *In vivo chlorophyll a fluorescence in the vicinity of warm-core eddies off the coast of NSW, November 1978*. CSIRO Division of Fisheries and Oceanography Report 112.
- Tsuchiya, M and Talley, LD (1996) Water-property distributions along an eastern Pacific hydrographic section at 135W. *Journal of Marine Research* 54: 541-564.
- Wadley, VA (1985) *The community structure of micronekton from an oceanic eddy*. PhD Thesis, University of Sydney, Sydney, Australia.
- Waite, AM (2004) Leeuwin Current meso-scale eddies: death traps or nurseries (a preliminary overview of the 2003 Eddy Voyage). Abstract AMSA 2004 Conference proceedings, p.132
- Wilkinson, C (2004) *Common Phytoplankton of South Australia*. South Australian Shellfish Quality Assurance Program, Port Lincoln Marine Science Centre. Unpublished report. 80pp.

Wood, EJF (1954) Dinoflagellates in the Australian region. *Australian Journal of Marine and Freshwater Research* 5: 171-351

Young, JW (1989) The distribution of hyperiid amphipods (Crustacea: Peracarida) in relation to warm-core Eddy J in the Tasman Sea. *Journal of Plankton Research* 11: 711-728.

Young, JW and Anderson, DA (1987) Hyperiid amphipods (Crustacea: Pericarida) from a Warm-Core Eddy in the Tasman Sea. *Australian Journal of Marine and Freshwater Research* 38: 711-725.

Appendix A Product List

The following tables list the dataset and mapset in the products column. The location column contains the names of the base data, maps and grids. The Neptune record label is contained in the first column.

A.1 NATIONAL (longitude: 90-180E; latitude: 0-60S)

Oceanographic features

Neptune Record	Products	Data Contact donna.hayes@csiro.au	Maps	Grids
DRAFT: Sea Surface Temperature Monthly Means and Variance in the Australian Region (record # 868)	Dataset: Sea-surface Temperature Monthly Means and Variance Mapset: Sea-surface Temperature Quarterly Means and variances (8 Maps) GIS Layer: Monthly Sea-surface Temperature		SST_aprmean.jpg SST_aprmean.pdf SST_janmean.jpg SST_janmean.pdf SST_julmean.jpg SST_julmean.pdf SST_octmean.jpg SST_octmean.pdf SST_aprvar.jpg SST_aprvar.pdf SST_janvar.jpg SST_janvar.pdf SST_julvar.jpg SST_julvar.pdf SST_octvar.jpg SST_octvar.pdf	jan_sst_avg.zip feb_sst_avg.zip mar_sst_avg.zip apr_sst_avg.zip may_sst_avg.zip jun_sst_avg.zip jul_sst_avg.zip aug_sst_avg.zip sep_sst_avg.zip oct_sst_avg.zip nov_sst_avg.zip dec_sst_avg.zip jan_sst_var.zip apr_sst_var.zip jul_sst_var.zip oct_sst_var.zip
DRAFT: Mapset: Sea-surface Temperature Quarterly Means (in the Australian Region) (record # 830)				
DRAFT: GIS Layer: Monthly Sea-surface Temperature in the Australian Region (record # 1031)				

COLLATION AND ANALYSIS OF OCEANOGRAPHIC DATASETS FOR MARINE BIOREGIONALISATION

Neptune Record	Products			
<p>DRAFT: Sea-surface Temperature Monthly Means and Variance in the Australian Region (record # 868)</p> <p>DRAFT: Map: Sea-surface Temperature Total Mean (in the Australian Region) (record # 899)</p> <p>DRAFT: GIS Layer: Sea-surface Temperature in the Australian Region (record # 1032)</p>	<p>Dataset: Sea-surface Temperature Total Means</p> <p>Map: Sea-surface Temperature Total Mean</p> <p>GIS Layer: Sea-surface Temperature</p>	<p>Data Contact donna.hayes@csiro.au</p>	<p>Map SST_totmean.pdf SST_totmean.jpg</p>	<p>Grid all_sst_avg.zip</p>
<p>DRAFT: Wind Stress Monthly Mean Fields in the Australian Region (record # 805)</p> <p>DRAFT: Mapset: Wind Stress on Australian Oceans Quarterly Means (in the Australian Region) (record # 831)</p> <p>DRAFT: GIS Layer: Wind Stress on Australian Oceans in the Australian Region (record # 1033)</p>	<p>Dataset: Wind stress on Australian Oceans Monthly Mean Fields</p> <p>Mapset: Wind stress on Australian Oceans Quarterly Means (4 Maps)</p> <p>GIS Layer: Wind Stress</p>	<p>Data necp_monthly.nc.zip</p>	<p>Maps wind_apr_mean.pdf wind_apr_mean.jpg wind_jan_mean.pdf wind_jan_mean.jpg wind_jul_mean.pdf wind_jul_mean.jpg wind_oct_mean.pdf wind_oct_mean.jpg</p>	<p>Grids/Shapes wind_stress_grds.zip windstress_shp.zip</p>

COLLATION AND ANALYSIS OF OCEANOGRAPHIC DATASETS FOR MARINE BIOREGIONALISATION

Neptune Record	Products			
DRAFT: Wind stress Monthly Mean Fields in the Australian Region (record # 805) DRAFT: GIS Layer: Wind Curl in the Australian Region (record # 815)	Mapset: Wind Curl on Australian Oceans Quarterly Means (4 Maps) GIS Layer: Wind Curl GIS Layer: Wind Stress Dataset: Wind Stress on Australian Oceans Monthly Mean Fields	Data ncep_monthly.nc.zip	Maps curl_apr.pdf curl_apr.jpg curl_jan.pdf curl_jan.jpg curl_jul.pdf curl_jul.jpg curl_oct.pdf curl_oct.jpg	Grids/Shapes wind_curl.zip wind_stress_grds.zip windstress_shp.zip
DRAFT: Mapset: Wind Curl on Australian Oceans Quarterly Means (in the Australian Region) (record # 832)				
DRAFT: GIS Layer: Wind Stress on Australian Oceans in the Australian Region (record # 1033)				
DRAFT: Sea-surface Mean Height and Currents in the Australian Region (record # 818) DRAFT: Mapset: Mean Sea-surface Currents each Quarter (in the Australian Region) (record # 833)	Dataset: Sea-surface Currents Monthly means Mapset: Mean Sea-surface Currents each Quarter (4 Maps) GIS Layer: Sea-surface Currents	Data hgt_10thde.g.nc.gz	Maps surfcur_apr.pdf surfcur_apr.jpg surfcur_jan.pdf surfcur_jan.jpg surfcur_jul.pdf surfcur_jul.jpg surfcur_oct.pdf surfcur_oct.jpg	Grids surf_currents.zip
DRAFT: GIS Layer: Sea-surface Currents in the Australian Region (record # 1034)				

COLLATION AND ANALYSIS OF OCEANOGRAPHIC DATASETS FOR MARINE BIOREGIONALISATION

Neptune Record	Products			
DRAFT: Sea-surface Mean Height and Currents in the Australian Region (record # 818)	Dataset: Sea-surface Mean Height and Currents Mapset: Sea-surface Height Quarterly Means (4 maps)	Data hgt_10thde.g.nc.gz	Maps SSH_apr.pdf SSH_apr.jpg SSH_jan.pdf SSH_jan.jpg SSH_jul.pdf SSH_jul.jpg SSH_oct.pdf SSH_oct.jpg	Grids ssh.zip surf_currents.zip
DRAFT: Mapset: Sea-surface Height Quarterly Means (in the Australian Region) (record # 855)				
DRAFT: GIS Layer: Sea-surface Height in the Australian Region (record # 1035)				
DRAFT: GIS Layer: Sea-surface Currents in the Australian Region (record # 1034)				
DRAFT: Sea-surface Height Monthly Standard Variability in the Australian Region (record # 801)	Dataset: Sea-surface Height Standard Deviation Mapset: Sea-surface Height Monthly Variability (4 maps)	Data std_height_monthly.zip	Maps SSH_aprvar.pdf SSH_aprvar.jpg SSH_janvar.pdf SSH_janvar.jpg SSH_julvar.pdf SSH_julvar.jpg SSH_octvar.pdf SSH_octvar.jpg	Grids ssh_var.zip
DRAFT: Mapset: Sea-surface Height Monthly Variability (in the Australian Region) (record # 834)				
DRAFT: GIS Layer: Sea-surface Height in the Australian Region (record # 1035)				

COLLATION AND ANALYSIS OF OCEANOGRAPHIC DATASETS FOR MARINE BIOREGIONALISATION

Neptune Record	Products			
DRAFT: Sea-surface Height Annual Standard Deviation in the Australian Region (record # 806)	Dataset: Sea-surface Height Annual Standard Deviation Map: Sea-surface Height Annual Variability	Data std_height.zip	Map SSH_totvar.pdf SSH_totvar.jpg	Grids SSH_var_all.zip SSH_var.zip
DRAFT: Map: Sea-surface Height Annual Variability (in the Australian Region) (record # 885)				
DRAFT: GIS Layer: Sea-surface Height in the Australian Region (record # 1035)				
DRAFT: Mixed Layer Depth in the Australian Region (record # 814)	Dataset: Mixed Layer Depth Annual Amplitude Map: Mixed Layer Depth Annual Amplitude	Data mld_10thde.g.nc.gz	Map mld_amp.pdf mld_amp.jpg	Grids mld_amp.zip
DRAFT: Map: Mixed Layer Depth Annual Amplitude (in the Australian Region) (record # 965)	GIS Layer: Mixed layer Annual Amplitude			
DRAFT: GIS Layer: Mixed Layer Depth in the Australian Region (record # 1036)				

COLLATION AND ANALYSIS OF OCEANOGRAPHIC DATASETS FOR MARINE BIOREGIONALISATION

Neptune Record	Products	Data	Map	Grid
DRAFT: Mixed Layer Depth in the Australian Region (record # 814)	Dataset: Mixed Layer Depth Annual Mean Map: Mixed Layer Depth Annual Mean	mld_10thde.g.nc.gz	mld_mean.pdf mld_mean.jpg	mld_mean.zip
DRAFT: Map: Mixed Layer Depth Annual Mean (in the Australian Region) (record # 1004)	GIS Layer: Mixed Layer Annual Mean			
DRAFT: GIS Layer: Mixed Layer Mean in the Australian Region (record # 1036)				

COLLATION AND ANALYSIS OF OCEANOGRAPHIC DATASETS FOR MARINE BIOREGIONALISATION

Neptune Record	Products			
<p>DRAFT: Eddies and Fields Based on Sea-surface Temperatures in the Australian Region (record # 869)</p> <p>DRAFT: Mapset: Eddies and Fields based on Sea-surface Temperature Quarterly (classes 1 - 4) (in the Australian Region) (record # 870)</p> <p>DRAFT: GIS Layer: Eddies and Fields Based on Sea-surface Temperature in the Australian Region (record # 1037)</p>	<p>Dataset: Eddies and Fields Based on Sea-surface Temperatures</p> <p>Mapset: Eddies and Fields based on Sea-surface Temperature Quarterly (classes 1 - 4) (16 maps)</p> <p>GIS Layer: Eddies and Fields Based on Sea-surface Temperatures</p>	Data sst_class.zip	Maps april.zip apr_class1.pdf apr_class1.jpg apr_class2.pdf apr_class2.jpg apr_class3.pdf apr_class3.jpg apr_class4.pdf apr_class4.jpg january.zip jan_class1.pdf jan_class1.jpg jan_class2.pdf jan_class2.jpg jan_class3.pdf jan_class3.jpg jan_class4.pdf jan_class4.jpg july.zip jul_class1.pdf jul_class1.jpg jul_class2.pdf jul_class2.jpg jul_class3.pdf jul_class3.jpg jul_class4.pdf jul_class4.jpg october.zip oct_class1.pdf oct_class1.jpg oct_class2.pdf oct_class2.jpg oct_class3.pdf oct_class3.jpg oct_class4.pdf oct_class4.jpg	Grid sst_class.zip

COLLATION AND ANALYSIS OF OCEANOGRAPHIC DATASETS FOR MARINE BIOREGIONALISATION

Neptune Record	Products			
DRAFT: Wave Height Direction and Period in the Australian Region (record # 859)	Dataset: Mean Wave Height Period Map: Mean Wave Height GIS Layer: Wave Height Direction and Period	Data Contact donna.hayes@csiro.au Porter-Smith_et_al.pdf	Map mean_wave_h.pdf mean_wave_h.jpg	Grid waves.zip
DRAFT: Map: Annual Mean Wave Height (in the Australian Region) (record # 971)				
DRAFT: GIS Layer: Wave Height Direction and Period in the Australian Region (record # 1038)				
DRAFT: Wave Height Direction and Period in the Australian Region (record # 859)	Map: Annual Mean Wave Period Dataset: Annual Mean Wave Period GIS Layer: Wave Height Direction and Period	Data Contact donna.hayes@csiro.au Porter-Smith_et_al.pdf	Map mean_wave_p.pdf mean_wave_p.jpg	Grids waves.zip
DRAFT: Map: Annual Mean Wave Period (in the Australian Region) (record # 973)				
DRAFT: GIS Layer: Wave Height Direction and Period in the Australian Region (record # 1038)				

COLLATION AND ANALYSIS OF OCEANOGRAPHIC DATASETS FOR MARINE BIOREGIONALISATION

Neptune Record	Products	Data Contact donna.hayes@csiro.au Porter-Smith_et_al.pdf	Map max_wave_h.pdf max_wave_h.jpg	Grids waves.zip
DRAFT: Wave Height Direction and Period in the Australian Region (record # 859)	Map: Annual Maximum Wave Height			
DRAFT: Map: Annual Maximum Wave Height (in the Australian Region) (record # 970)	Dataset: Annual Maximum Wave Height			
DRAFT: GIS Layer: Wave Height Direction and Period in the Australian Region (record # 1038)	GIS Layer: Wave Height Direction and Period			
DRAFT: Wave Height Direction and Period in the Australian Region (record # 859)	Map: Annual Maximum Wave Period	Data Contact donna.hayes@csiro.au Porter-Smith_et_al.pdf	Map max_wave_p.pdf max_wave_p.jpg	Grids waves.zip
DRAFT: Map: Annual Maximum Wave Period (in the Australian Region) (record # 972)	Dataset: Annual Maximum Wave Period			
DRAFT: GIS Layer: Wave Height Direction and Period in the Australian Region (record # 1038)	GIS Layer: Wave Height Direction and Period			

COLLATION AND ANALYSIS OF OCEANOGRAPHIC DATASETS FOR MARINE BIOREGIONALISATION

Neptune Record	Products	Data Contact donna.hayes@csiro.au porter-smith_et_al.pdf	Map mean_tidal_vel.pdf mean_tidal_vel.jpg	Grid tides_mean_vel.zip
DRAFT: Half Lunar Cycle Mean and Maximum Tidal Currents in the Australian Region (record # 854) DRAFT: Map: Half Lunar Mean Tidal Currents (in the Australian Region) (record # 968) DRAFT: GIS Layer: Half Lunar Cycle Tidal Currents in the Australian Region (record # 1039)	Dataset: Half Lunar Cycle Tidal Data Map: Half Lunar Mean Tidal Currents GIS Layer: Half Lunar Tidal Currents	Data Contact donna.hayes@csiro.au porter-smith_et_al.pdf	Map mean_tidal_vel.pdf mean_tidal_vel.jpg	Grid tides_mean_vel.zip
DRAFT: Half Lunar Cycle Mean and Maximum Tidal Currents in the Australian Region (record # 854) DRAFT: Map: Half Lunar Tidal Currents (in the Australian Region) (record # 969) DRAFT: GIS Layer: Half Lunar Cycle Tidal Currents in the Australian Region (record # 1039)	Dataset: Half Lunar Cycle Tidal Data Map: Half lunar Maximum Tidal currents GIS Layer: Half Lunar Tidal Currents	Data Contact donna.hayes@csiro.au porter-smith_et_al.pdf	Map max_tidal_vel.pdf max_tidal_vel.jpg	Grid tides_max_vel.zip

Depth structure

Neptune Record	Products	Location		
DRAFT: Sea-surface Silicate in the Australian Region (record # 809)	Dataset: Sea Silicate Mapset: Silicate by Depth Annual Means (5 maps) GIS Layer: Sea-surface Silicate	Data silicate_10thde.g.nc.gz	Maps silicates_0.pdf silicates_0.jpg silicates_1000.pdf silicates_1000.jpg silicates_150.pdf silicates_150.jpg silicates_2000.pdf silicates_2000.jpg silicates_500.pdf silicates_500.jpg	Grids CARS_Silicate.zip silicate_amp.zip silicate_mean.zip
DRAFT: Mapset: Silicate by Depth Annual Means (in the Australian Region) (record # 940)				
DRAFT: GIS Layer: Sea-surface Silicate in the Australian Region (record # 1040)				
DRAFT: Sea-surface Phosphate in the Australian Region (record # 811)	Dataset: Sea Phosphate Mapset: Phosphate by Depth Annual Means (5 maps) GIS Layer: Sea-surface Phosphate	Data phosphate_10thde.g.nc.gz	Maps phosph_0.pdf phosph_0.jpg phosph_1000.pdf phosph_1000.jpg phosph_150.pdf phosph_150.jpg phosph_2000.pdf phosph_2000.jpg phosph_500.pdf phosph_500.jpg	Grids CARS_Phosph.zip phosphate_amp.zip phosphate_mean.zip
DRAFT: Mapset: Phosphate by Depth Annual Means (in the Australian Region) (record # 938)				
DRAFT: GIS Layer: Sea-surface Phosphate in the Australian Region (record # 1041)				

COLLATION AND ANALYSIS OF OCEANOGRAPHIC DATASETS FOR MARINE BIOREGIONALISATION

Neptune Record	Products	Location		
DRAFT: Sea-surface Nitrate in the Australian Region (record # 813)	Dataset: Sea Nitrate	Data Nitrate_10thde.g.ncgz	Maps nitrate_am0.pdf nitrate_am0.jpg nitrate_am1000.pdf nitrate_am150.pdf nitrate_am150.jpg nitrate_am2000.pdf nitrate_am2000.jpg nitrate_am500.pdf nitrate_am500.jpg	Grids CARS_Nitrate nitrate_amp.zip nitrate_mean.zip
DRAFT: Mapset: Nitrate by Depth Annual Means (in the Australian Region) (record # 937)	Mapset: Nitrate by Depth Annual Mean (5 maps)			
DRAFT: GIS Layer: Sea-surface Nitrate in the Australian Region (record # 1042)	GIS Layer: Sea-surface Nitrate			
DRAFT: Sea-surface Dissolved Oxygen in the Australian Region (record # 812)	Dataset: Sea Dissolved Oxygen	Data Oxygen_10thde.g.nc.gz	Maps oxy_0.pdf oxy_0.jpg oxy_1000.pdf oxy_1000.jpg oxy_150.pdf oxy_150.jpg oxy_2000.pdf oxy_2000.jpg oxy_500.pdf oxy_500.jpg	Grids CARS_oxy oxygen_amp.zip oxygen_mean.zip
DRAFT: Mapset: Dissolved Oxygen by Depth Annual Mean 9 in the Australian Region (record # 936)	Mapset: Dissolved Oxygen by Depth Annual Mean (5 maps)			
DRAFT: GIS Layer: Sea-surface Dissolved Oxygen in the Australian Region (record # 1043)	GIS Layer: Sea-surface Dissolved Oxygen			

COLLATION AND ANALYSIS OF OCEANOGRAPHIC DATASETS FOR MARINE BIOREGIONALISATION

Neptune Record	Products	Location		
DRAFT: Sea Temperature at Depth in the Australian Region (record # 808)	Dataset: Temperature at Depth Mapset: Sea Temperature by Depth Annual Means (5 maps)	Data Temperature_10thde.g.nc.gz	Maps temp_0.pdf temp_0.jpg temp_1000.pdf temp_1000.jpg temp_150.pdf temp_150.jpg temp_2000.pdf temp_2000.jpg temp_500.pdf temp_500.jpg	Grids CARS_Temp temp_amp.zip temp_mean.zip
DRAFT: Mapset: Sea Temperature by Depth Annual Mean (in the Australian Region) (record # 941)	DRAFT: GIS Layer: Sea Temperature			
DRAFT: GIS Layer: Sea Temperature in the Australian Region (record # 1044)				
DRAFT: Sea Salinity in the Australian Region (record # 810)	Dataset: Salinity by Depth Annual Mean	Data Salinity_10thde.g.nc.gz	Maps sal_0.pdf sal_0.jpg sal_1000.pdf sal_1000.jpg sal_150.pdf sal_150.jpg sal_2000.pdf sal_2000.jpg sal_500.pdf sal_500.jpg	Grids CARS_salinity salinity_amp.zip salinity_mean.zip
DRAFT: Mapset: Salinity by Depth Annual Means (in the Australian Region) (record # 939)	Mapset: Salinity by Depth Annual Means (5 maps)			
DRAFT: GIS Layer: Sea Salinity in the Australian Region (record # 1045)	DRAFT: GIS Layer: Sea Salinity (record # 1045)			

COLLATION AND ANALYSIS OF OCEANOGRAPHIC DATASETS FOR MARINE BIOREGIONALISATION

Neptune Record	Products	Location
DRAFT: Geostrophic Subsurface Currents in the Australian Region (record # 894)	Dataset: Geostrophic Currents by Depth Monthly Mean	<u>subsurface currents/subsurf currents.nc.gz (84 Mb)</u>

Benthic

	Products	Location	input datasets
DRAFT: Benthic Nutrients and Physical Water Properties Annual Amplitude (0.025 grid) (in the Australian Region) (record # 807)	Bottom temperature, salinity, nutrients (silicate, phosphate and Nitrate), DO at 2km resolution on shelf and slope and 0.1° for rest of EEZ. Delivered to GA as a netcdf file.	Data <u>cars/seafloor.nc.gz (15,248 Kb)</u>	Temperature, salinity, nutrients and Dissolved Oxygen extracted at fine scale for slope. cars\benthic\seafloor.nc Neptune record 'Benthic Physical Water Properties' <u>cars/seafloor.nc.gz (15,248 Kb)</u> location data <u>cars/salt_locs.asc.gz (238Kb)</u> temp_locs.asc.gz (246K) <u>cars/silic_locs.asc.gz (105Kb)</u> <u>cars/phosph_locs.asc (98Kb)</u> <u>cars/oxy_locs.asc.gz (172Kb)</u> <u>cars/nitr_locs.asc.gz (121Kb)</u>
DRAFT: Benthic Nutrients and Physical Water Properties Annual Mean (0.1 grid) (in the Australian Region) (record # 946)	Dataset: Benthic Sea Temperature Dataset: Benthic Silicate Dataset: Benthic Phosphate Dataset: Benthic Nitrate Dataset: Benthic Dissolved Oxygen Dataset: Benthic Salinity	Data seafloor_10thde.g.nc.gz	Bottom temperature

Phytoplankton

Neptune Record	Products	Location		input datasets
DRAFT: Map: Phytoplankton Provinces (in the Australian Region) (record # 879)	GIS layer –phytoplankton Map: Phytoplankton Provinces	Maps Gustaaf_phyto.pdf Gustaaf_phyto.jpg Hallegraeff_phyto.jpg	Shape gutaaf_phyto.zip Hallegraeff_phyto.e00	Phytoplankton database Neptune record 'Phytoplankton Biomass Database'
DRAFT: GIS Layer: Phytoplankton Provinces in the Australian Region (record # 1046)				

Primary Production

Neptune Record	Products	Format			Input datasets
DRAFT: Ocean Colour Monthly Means and Variances (MODIS) in the Australian Region (record # 880)	Dataset: Ocean Colour Data from the Moderate Resolution Imaging Spectroradiometer (MODIS)	Data Chloro_monthly_mean.zip Chloro_monthly_std_d ev.zip	Maps chlormean_april.pdf chlormean_april.jpg chlormean_jan.pdf chlormean_jan.jpg chlormean_jul.pdf chlormean_jul.jpg chlormean_oct.pdf chlormean_oct.jpg		MODIS ocean colour data Neptune record: Ocean Colour Data from the Moderate Resolution Imaging Spectroradiometer (MODIS)
DRAFT: Mapset: Ocean Colour Chlorophyll Quarterly Means (in the Australian Region) (record # 904)	Mapset: Ocean Colour Chlorophyll Quarterly Means (4 maps)				
DRAFT: GIS Layer: Ocean Colour (MODIS) in the Australian Region (record # 1047)	GIS Layer: Ocean colour Chlor_grids.zip				
DRAFT: Incident of Light and Photosynthetically Active Radiation (PAR) Monthly Means in the Australian Region (record # 872)	Dataset: Incident of Light and Photosynthetically Active Radiation (PAR) Monthly Means	Data light_incident_ascii.zip	Maps light_april.pdf light_april.jpg light_jan.pdf light_jan.jpg light_jul.pdf light_jul.jpg light_oct.pdf light_oct.jpg	Girds grids_monthly_light.zip	Monthly PAR and cloud climatology's Neptune Record 'Incident of Light and Photosynthetically Active Radiation (PAR) Monthly Means'
DRAFT: Mapset: incident of Light Quarterly Means (in the Australian Region) (record # 873)	Mapset: Incident of Light Quarterly Means (4maps)				Grids grids_monthly_light.zip
DRAFT: GIS Layer: Incident of Light (PAR) in the Australian Region	GIS Layer: Incident of Light (PAR)				map_template.zip

COLLATION AND ANALYSIS OF OCEANOGRAPHIC DATASETS FOR MARINE BIOREGIONALISATION

Neptune Record (record # 1049)	Products	Format			Input datasets
DRAFT: Primary Production Data from (MODIS) in the Australian Region (record #1057) DRAFT: Mapset: Primary Production each Quarter (in the Australian Region) (record # 906) DRAFT: GIS Layer: Primary Production (MODIS) in the Australian Region (record # 1048)	Dataset: Primary Production Data (Monthly Mean) from Ocean Colour Data (MODIS) Mapset: Primary Production each Quarter (4 maps)	Data MOD_P1_8D_4KM.nc	Maps PP_april.pdf PP_april.jpg PP_july.pdf PP_july.jpg PP_oct.pdf PP_oct.jpg PP_jan.pdf PP_jan.jpg	Grids primary_production.zip	MODIS primary production from ocean colour data Neptune record: Primary Production Data from Ocean Colour Data (MODIS)

COLLATION AND ANALYSIS OF OCEANOGRAPHIC DATASETS FOR MARINE BIOREGIONALISATION

Neptune Record	Products	Format			Input datasets
DRAFT: Primary Production Data from (MODIS) in the Australian Region (record #1057)	Dataset: Primary Production Data (Annual Mean) from Ocean Colour Data (MODIS)	Data MOD_P1_8D_4KM.nc	Maps PP_annmean.pdf PP_annmean.jpg	Grid primary_production.zip	MODIS primary production from ocean colour data Neptune record: Primary Production Data from Ocean Colour Data (MODIS)
DRAFT: Map: Primary Production Annual Mean (in the Australian Region) (record # 929)	Map: Primary Production Annual Mean (1 map)				
DRFAT: GIS Layer: Primary Production (MODIS) in the Australian Region (record # 1048)	GIS Layer: Primary Production				
DRAFT: SeaWiFS movie of surface Chlorophyll, 1997-2001 in the Australian Region (record # 1021)	Movie: Ocean Colour (SeaWiFS)	Movie Ocean_colour.gif			

COLLATION AND ANALYSIS OF OCEANOGRAPHIC DATASETS FOR MARINE BIOREGIONALISATION

Neptune Record	Products	Format		Input datasets	
DRAFT: Primary Production around Australia 1959-1965 (record # 1011) DRAFT: Mapset: Primary productivity in northern Australian waters by northern season (4 maps) Mapset: Primary productivity in Australian waters by season (record # 1050)	Mapset: Primary productivity in northern Australian waters by northern season (4 maps) GIS Layer: Primary Production around Australia by season	Data data-checked_MASTER.xls	Maps PP_North_dec-apr.jpg PP_North_may-june.jpg PP_North_july-aug.jpg PP_North_sept-nov.jpg PP_Legend.jpg	MapInfo PrimProd.ID PrimProd.IND PrimProd.MAP PrimProd.TAB PrimProd.xls	CSIRO Division of Fisheries and Oceanography oceanographica l Cruise Reports
DRAFT: Primary Production around Australia 1959-1965 (record # 1011) DRAFT: Mapset: Primary productivity in southern Australian waters by southern season (4 maps) Mapset: Primary productivity in Australian waters by season (record # 1050)	Mapset: Primary productivity in southern Australian waters by southern season (4 maps) GIS Layer: Primary Production around Australia by season	Data data-checked_MASTER.xls	Maps PP_South_autumn.jpg PP_South_winter.jpg PP_South_spring.jpg PP_South_summer.jpg PP_Legend.jpg	MapInfo PrimProd.ID PrimProd.IND PrimProd.MAP PrimProd.TAB PrimProd.xls	CSIRO Division of Fisheries and Oceanography oceanographica l Cruise Reports

COLLATION AND ANALYSIS OF OCEANOGRAPHIC DATASETS FOR MARINE BIOREGIONALISATION

Neptune Record	Products	Format		Input datasets	
DRAFT: Primary Production around Australia 1959-1965 (record # 1011) DRAFT: Map: Zooplankton Biomass (in the Australian Region) (record # 1006) DRAFT: GIS Layer: Zooplankton Biomass in the Australian Region (record # 1051)	Map: Zooplankton biomass GIS Layer: Zooplankton Biomass	Data data-checked_MASTER.xls	Map All-CB-samples.jpg	MapInfo CB_all-data.ID CB_all-data.MAP CB_all-data.TAB CB_all-data.xls	CSIRO Division of Fisheries and Oceanography oceanographica l Cruise Reports
DRAFT: Primary Production around Australia 1959-1965 (record # 1011) DRAFT: Mapset: Zooplankton Biomass in southern Australian waters by southern season (4 maps) DRAFT: GIS Layer: Zooplankton Biomass in southern Australian waters by southern season (record # 1052)	Mapset: Zooplankton biomass in southern Australian waters by southern season (4 maps)	Data data-checked_MASTER.xls	Maps CBOS.pdf CBO_South_autumn.jpg CBO_South_spring.jpg CBO_South_summer.jpg CBO_South_winter.jpg	MapInfo CB_OH.ID CB_OH.MAP CB_OH.TAB CB_OH.xls	CSIRO Division of Fisheries and Oceanography oceanographica l Cruise Reports

COLLATION AND ANALYSIS OF OCEANOGRAPHIC DATASETS FOR MARINE BIOREGIONALISATION

Neptune Record	Products	Format		Input datasets	
DRAFT: Primary Production around Australia 1959-1965 (record # 1011) DRAFT: Mapset: Zooplankton Biomass in the Timor Triangle by northern season (record # 1009)	Mapset: Zooplankton biomass in the Timor triangle by northern season. (4 maps)	Data data-checked_MASTER.xls	Maps CBHN.pdf CBH_North_dec-apr.jpg CBH_north_july-aug.jpg CBH_North-may-june.jpg CBH_North_sept-nov.jpg CBH_Legend.jpg	MapInfo CB_HH.ID CB_HH.MAP CB_HH.TAB CB_HH.xls	CSIRO Division of Fisheries and Oceanography oceanographica l Cruise Reports
DRAFT: GIS Layer: Zooplankton Biomass in the Timor Triangle by northern season (record # 1053)					
DRAFT: Primary Production around Australia 1959-1965 (record # 1011) DRAFT: Mapset: Zooplankton biomass seasonality (along 110°E) (record # 1010) DRAFT: GIS Layer: Zooplankton Biomass Seasonality (along 110°E) (record # 1030)	Mapset: Zooplankton biomass seasonality (8 maps)	Data data-checked_MASTER.xls	Maps IOSN.pdf IOSN_DM1-63_Mar-Apr.jpg IOSN_DM2-62_Jul-Aug.jpg IOSN_DM2-63_May.jpg IOSN_DM3-62_Sept-Oct.jpg IOSN_DM3-63_Jul-Aug.jpg IOSN_DM4-62_Oct.jpg IOSN_G1-63_Jan-Feb.jpg IOSN_G4-62_Aug.jpg IOSN_Legend.jpg	MapInfo IOSN_VH.ID IOSN_VH.MAP IOSN_VH.TAB IOSN_VH.xls	CSIRO Division of Fisheries and Oceanography oceanographica l Cruise Reports

A.2 The Northern Marine Region

Neptune Record	Products	Location		
DRAFT: Sea-surface Temperature Monthly Means and Variance in the Australian Region (record # 868)	Dataset: Sea-surface Temperature Monthly and Annual Means in the Northern Marine Region	Data Contact donna.hayes@csiro.au	Maps sst_dry.pdf sst_dry.jpg sst_wet.pdf sst_wet.jpg sst_ave.jpg sst_ave.pdf	Grid all_sst_avg.zip jan_sst_avg.zip july_sst_avg.zip
DRAFT: Mapset: Sea-surface Temperature wet/dry season Means in the northern Marine Region (record # 907)	Mapset: Sea-surface Temperature wet/dry season Means in the Northern Marine Region (3 maps)			
DRAFT: GIS Layer: Sea-surface Temperature in the Australian Region (record # 1032)				
DRAFT: Sea-surface Silicate in the Australian Region (record # 809)	Dataset: Sea-surface Silicate	Data Silicate_10thde.g.nc.gz	Maps silicate.pdf	Grids CARS_Silicate.zip silicate_amp.zip silicate_mean.zip
DRAFT: Map: Silicate Annual Means in the Northern Marine Region (record # 889)	Map: Silicate Annual Means in the Northern Marine Region			
DRAFT: GIS Layer: Sea-surface Silicate in the Australian Region (record # 1040)				

COLLATION AND ANALYSIS OF OCEANOGRAPHIC DATASETS FOR MARINE BIOREGIONALISATION

Neptune Record	Products	Location		
DRAFT: Sea-surface Phosphate in the Australian Region (record # 811)	Dataset: Sea Phosphate Map: Phosphate Annual Means in the Northern Marine Region	Data phosphate_10thde.g.nc.gz	Maps Phosphate.pdf	Grids CARS_Phosphorus.zip phosphate_amp.zip phosphate_mean.zip
DRAFT: Map: Phosphate Annual Means in the Northern Marine Region (record # 890)				
DRAFT: GIS Layer: Sea-surface Phosphate in the Australian Region (record # 1041)				
DRAFT: Sea-surface Nitrate in the Australian Region (record # 813)	Dataset: Sea Nitrate Map: Nitrate Annual Means in the Northern Region	Data nitrate_10thde.g.nc.gz	Maps nitrate.pdf nitrate.jpg	Grids CARS_Nitrate.zip nitrate_amp.zip nitrate_mean.zip
DRAFT: Map: Nitrate Annual Means in the Northern Marine Region (record # 891)				
DRAFT: GIS Layer: Sea-surface Nitrate in the Australian Region (record # 1042)				

COLLATION AND ANALYSIS OF OCEANOGRAPHIC DATASETS FOR MARINE BIOREGIONALISATION

Neptune Record	Products	Location		
DRAFT: Sea-surface Dissolved Oxygen in the Australian Region (record # 812)	Dataset: Dissolved Oxygen Annual Mean Map: Dissolved Oxygen in the Northern Marine Region	Data Oxygen_10thde.g.nc.gz	Maps oxygen.pdf oxygen.jpg	Grids CARS_Oxy.zip oxy_mean.zip oxy_amp.zip
DRAFT: Map: Dissolved Oxygen Annual Mean in the Northern Marine Region (record # 849)				
DRAFT: GIS Layer: Sea-surface Dissolved Oxygen in the Australian Region (record # 1043)				
DRAFT: Salinity in the Australian Region (record # 810)	Dataset: Salinity Annual Mean	Data Salinity_10thde.g.nc.gz	Maps salinity.pdf	Grids CARS_Salinity.zip salinity_mean.zip satinity_amp.zip
DRAFT: Map: Salinity in the Northern Marine Region (record # 848)	Map: Salinity Annual Means in the Northern Marine Region			
DRAFT: GIS Layer: Sea Salinity in the Australian Region (record # 1045)				
Draft: Sea Temperature Monthly and Annual Means in the Australian Region (record # 808)	Dataset: Temperature at depth	Data North_temp.asc	Map North_temp_jan.pdf north_temp_jul.pdf	Grid North_temp
DRAFT: Map: Sea Temperature in the Northern	Map: Temperature in the Northern Marine Region			

COLLATION AND ANALYSIS OF OCEANOGRAPHIC DATASETS FOR MARINE BIOREGIONALISATION

Neptune Record	Products	Location		
Marine Region <i>map</i> (record # 933)				
GIS Layer: Sea Temperature in the Australian Region (record #1044)				
DRAFT: Currents from the Northern Region Circulation Model (record # 975)	Dataset: Currents from the Northern Region Circulation Model	Data npfzip.zip	Maps Current_jan.jpg Current_jan.pdf Current_jul.jpg Current_jul.pdf	Grids and shape current_grd.zip current_shape.zip npf_jan_sub.shp npf_jul_sub.shp npf_jancur.grd npf_julcur.grd
DRAFT: Mapset: Currents in the Northern Marine Region (record # 875)				
DRAFT: GIS Layer: Currents from the Northern Region Circulation Model (record #)				
DRAFT: Tidal Range from the Northern Marine Circulation Model (record # 999)	Map: Maximum Tidal Range for the Northern Marine Region Dataset: Tidal Range from the Northern Marine Circulation Model	Data Npf1zip.txt	Maps max_tide.jpg max_tide.pdf	Grids max_tide.zip
DRAFT: Map: Maximum Tidal Range for the Northern Marine Region (record #998)				

COLLATION AND ANALYSIS OF OCEANOGRAPHIC DATASETS FOR MARINE BIOREGIONALISATION

Neptune Record	Products	Location		
DRAFT: Bottom Stress from the Northern Marine Region (record # 874)	Dataset: Bottom Stress from the Northern Region Circulation Model	Data Npf1.txt.gz	Maps max_stress.pdf max_stress.jpg mean_stress.pdf mean_stress.jpg stdev_stress.pdf stdev_stress.jpg	Grids strmax strmn strdev
DRAFT: Mapset: Bottom Stress in the Northern Marine Region (record # 912)	Mapset: Bottom Stress in the Northern Marine Region (3 maps)			
DRAFT: Prawn Larval Distribution in the Gulf of Carpentaria for Wet and Dry Seasons (record # 995)	Dataset: Prawn Larval Distribution in the Gulf of Carpentaria for Wet and Dry Seasons	Data M4870_gen2_w.csv M4870_gen2_d.csv	Maps M4870_totd.jpg M4870_totw.jpg M4870_totd.pdf M4870_totw.pdf	Grids m4870_totw m4870_totd
DRAFT: Mapset: Prawn Larval Distributions in the Gulf of Carpentaria for Wet and Dry Seasons (record # 986)	Map: Prawn Larval Distributions in the Gulf of Carpentaria for Wet and Dry Seasons. (2 maps)			

COLLATION AND ANALYSIS OF OCEANOGRAPHIC DATASETS FOR MARINE BIOREGIONALISATION

Neptune Record	Products	Location		
DRAFT: Prawn Larval Distribution in the Gulf of Carpentaria for Wet and Dry Seasons (record # 995) DRAFT: Mapset: Commercial Prawn Larval Distributions in the Gulf of Carpentaria for Wet and Dry Seasons (record # 983)	Dataset: Prawn Larval Distribution in the Gulf of Carpentaria for Wet and Dry Seasons Map: Commercial Prawn Larval Distribution in the Gulf of Carpentaria for Wet and Dry Seasons (2 maps)	Data M4870_gen2_w.csv M4870_gen2_d.csv	Maps M4870_comd.jpg M4870_comw.jpg M4870_comd.pdf M4870_comw.pdf	Grids m4870_comw m4870_comd

COLLATION AND ANALYSIS OF OCEANOGRAPHIC DATASETS FOR MARINE BIOREGIONALISATION

Neptune Record	Products	Location		
DRAFT: Prawn Larval Distribution in the Gulf of Carpentaria for Wet and Dry Seasons (record # 995)	Dataset: Prawn Larval Distribution in the Gulf of Carpentaria for Wet and Dry Seasons	Data M4870_gen2_w.csv M4870_gen2_d.csv Map: Non-Commercial Prawn Larval Distribution in the Gulf of Carpentaria for Wet and Dry Seasons (2 maps)	Maps M4870_ncomd.jpg M4870_ncomw.jpg M4870_ncomd.pdf M4870_ncomw.pdf	Grids m4870_ncomw m4870_ncomd
DRAFT: Mapset: Non-Commercial Prawn Larval Distributions in the Gulf of Carpentaria for Wet and Dry Seasons (record # 985)				

COLLATION AND ANALYSIS OF OCEANOGRAPHIC DATASETS FOR MARINE BIOREGIONALISATION

Neptune Record	Products	Location		
DRAFT: Zooplankton biomass in the Gulf of Carpentaria for Wet and Dry Seasons (record # 987)	Dataset: Zooplankton Biomass in the Gulf of Carpentaria for the Wet and Dry Seasons	Data M4870_bio_d.csv M4870_bio_w.csv M4870_bi.zip	Maps M4870_bio_w.jpg M4870_bio_d.jpg M4870_bio_w.pdf M4870_bio_d.pdf	Grids m4870_bio_w m4870_bio_d
DRAFT: Mapset: Total Zooplankton biomass in the Gulf of Carpentaria for Wet and Dry Seasons (record # 989)	Map: Total Zooplankton Biomass in the Gulf of Carpentaria for Wet and Dry Seasons (2 maps)			
DRAFT: Ocean Colour Monthly Means and Variances in the Australian Region (record # 880)	Dataset: Ocean Colour Chlorophyll Annual Mean in the Northern Marine Region	Data Chlorophyll_monthly_means.zip Chlorophyll_monthly_std_dev.zip	Maps chlor_dry.pdf chlor_dry.jpg chlor_wet.pdf chlor_wet.jpg	Grids Chloro_means.zip Chloro_std_dev.zip Chlor_grids.zip
DRAFT: Mapset: Ocean Colour Chlorophyll wet/dry Means in the Northern Marine Region (record # 908)	Mapset: Ocean Colour Chlorophyll wet/dry Means in the Northern Marine Region (2 maps)			
DRAFT: GIS Layer: Ocean Colour Chlorophyll (MODIS) in the Australian Region (record: # 1047)				

COLLATION AND ANALYSIS OF OCEANOGRAPHIC DATASETS FOR MARINE BIOREGIONALISATION

Neptune Record	Products	Location		
DRAFT: Incident Light and Photosynthetically Active Radiation (PAR) Monthly Means in the Australian Region (record # 872)	Dataset: Incident of Light and Photosynthetically Active Radiation (PAR) Monthly Means	Data light_incident_ascii.zip	Maps light_wet.pdf light_wet.jpg light_dry.pdf light_dry.jpg	Grids grids_monthly_light.zip
DRAFT: Mapset: Incident Light for the Wet and Dry Seasons in the Northern Marine Region (record # 1055)	Mapset: Incident of Light in Northern Marine Region (2 maps)			
DRAFT: GIS Layer: Incident Light (PAR) in the Australian Region (record # 1049)				
DRAFT: Primary Production Data from (MODIS) in the Australian Region (record #1057)	Dataset: Primary Production Data (Monthly) from Ocean Colour Data (MODIS)	Data MOD_P1_8D_4KM.nc	Maps pp_dry.pdf pp_dry.jpg pp_wet.pdf pp_wet.jpg	Grids primary_production.zip
DRAFT: Mapset: Primary Production wet/dry Seasonal Mean in the Northern Marine Region (record # 948)	Mapset: Primary Production wet/dry Seasonal Mean in the Northern Marine Region (2 maps)			
DRAFT: GIS Layer: Primary Production (MODIS) in the Australian Region (record # 1048)				

A.3 CASE STUDY Albatross Bay

Neptune Record	Products	Format			input datasets
DRAFT: Prawn Larval Distribution in the Albatross Bay for Wet and Dry Seasons (record # 996)	Dataset: Prawn Larval Distribution in the Albatross Bay for Wet and Dry seasons	Data m1663_ab_genus_shp	Maps M1663_genw.jpg M1663_gend.jpg M1663_genw.pdf M1663_gend.pdf	Grids m1663_gend	Prawn larval density from stepped oblique bottom to surface plankton tows M1663_ab_genus.shp m4870_pl.zip (78 Kb) Neptune record 'Prawn Larval Distribution of Commercial and Non-Commercial Species in Albatross Bay'
DRAFT: Mapset: Prawn Larval Distributions in Albatross Bay for Wet and Dry Seasons (record # 976)	Map: Prawn Larval Distributions in Albatross Bay for Wet and Dry seasons (2 maps)	m1663_gend.csv m1663_genw.csv			
DRAFT: Prawn Larval Distribution in the Albatross Bay for Wet and Dry Seasons (record # 996)	Dataset: Prawn Larval Distribution in the Albatross Bay for Wet and Dry seasons	Data m1663_ab_genus_shp m1663_gend.csv m1663_genw.csv	Maps M1663_comd.jpg M1663_comw.jpg M1663_comd.pdf M1663_comw.pdf	Grids m1663_gencomd m1663_gencomw	Prawn larval density from stepped oblique bottom to surface plankton tows M1663_ab_genus.shp m4870_pl.zip (78 Kb) Neptune record 'Prawn Larval Distribution of Commercial and Non-Commercial Species in Albatross Bay'
DRAFT: Mapset: Commercial Prawn Larval Distributions in Albatross Bay for Wet and Dry Seasons (record # 991)	Mapset: Commercial Prawn Larval Distributions in Albatross Bay Wet and Dry Seasons (2 maps)				

COLLATION AND ANALYSIS OF OCEANOGRAPHIC DATASETS FOR MARINE BIOREGIONALISATION

Neptune Record	Products	Format			input datasets
DRAFT: Prawn Larval Distribution in the Albatross Bay for Wet and Dry Seasons (record # 996)	Dataset: Prawn Larval Distribution in the Albatross Bay for Wet and Dry seasons Map: Non-Commercial Prawn Larval Distributions in Albatross Bay. Wet and Dry Seasons (2 maps)	Data m1663_ab_genus_shp m1663_gend.csv m1663_genw.csv	Maps M1663_noncomd.jpg M1663_noncomw.jpg M1663_noncomd.pdf M1663_noncomw.pdf	Grids m1663_noncomw m1663_noncomd	Prawn larval density from stepped oblique bottom to surface plankton tows M1663_ab_genus.shp m4870_pl.zip (78 Kb) Neptune record 'Prawn Larval Distribution of Commercial and Non-Commercial Species in Albatross Bay'
DRAFT: Chlorophyll a concentrations in Albatross Bay (record # 977)	Dataset: Chlorophyll <i>a</i> concentrations in Albatross Bay Map: Chlorophyll <i>a</i> concentrations in Albatross Bay (1 map)	Data m1381_ab_chl.xls	Map M1381_chl.jpg M1381_chl.pdf		M1381_chl
DRFAT: Map: Chlorophyll a concentrations in Albatross Bay (record # 978)					

COLLATION AND ANALYSIS OF OCEANOGRAPHIC DATASETS FOR MARINE BIOREGIONALISATION

Neptune Record	Products	Format		input datasets
DRAFT: Mean Chlorophyll and Primary Production at two sites in Albatross Bay (record # 994)	Dataset: Mean Chlorophyll and Primary Production at two sites Map: Mean Chlorophyll in Albatross Bay. (1 map)	Data m1664_prod.xls	Maps M1664_clor.jpg M1664_chlor.pdf	Northern_data/covers/m1582_phy Coverage M1664_prod
DRAFT: Map: Mean Chlorophyll in Albatross Bay (record # 984)				
DRAFT: Mean Chlorophyll and Primary Production at two sites in Albatross Bay (record # 994)	Dataset: Primary Production and Mean Chlorophyll at two sites in Albatross Bay	Data m1664_prod.xls	Maps M1664_prod.pdf M1664_prod.jpg	¹⁴ C primary productivity incubations at 2 stations over 7 cruises
DRAFT: Primary Production of Chlorophyll at two sites in Albatross Bay (record # 993)	Map: Primary Prduction of Chlorophyll in Albatross Bay at two sites (1 map)			Northern_data/covers/m1664_prod Neptune record 'Primary Productivity Data in Albatross Bay 1988-1991' <u>m1664_prod.zip (16Kb)</u>

COLLATION AND ANALYSIS OF OCEANOGRAPHIC DATASETS FOR MARINE BIOREGIONALISATION

Neptune Record	Products	Format		input datasets
DRAFT: Copepod Abundance in Albatross Bay (record # 979)	Dataset: Copepod Abundance in Albatross Bay Map: Copepod Abundance in Albatross Bay (1 map)	Data m6332_copepods.xls	Maps m6332_cpp.jpg m6332_cpp.pdf	Coverage M6332_cpp
DRAFT: Map: Copepod Abundance in Albatross Bay (record # 980)				
DRAFT: Phytoplankton Abundance in Albatross Bay (record 982)	Dataset: Phytoplankton Abundance in Albatross Bay Map: Phytoplankton Abundance in Albatross Bay (1 map)	Data m1582_phy.xls	Maps M1582_phy.pdf M1582_phy.jpg	Northern_data/covers/m1582_phy
Map: Phytoplankton Abundance in Albatross Bay (record # 981)				Neptune record 'Phytoplankton Biomass in Albatross Bay' <u>m1582_phy.zip (132Kb)</u>

COLLATION AND ANALYSIS OF OCEANOGRAPHIC DATASETS FOR MARINE BIOREGIONALISATION

Neptune Record	Products	Format			input datasets
DRAFT: Zooplankton Biomass in Albatross Bay (record # 988)	Dataset: Zooplankton Biomass in Albatross Bay	Data m1663_ab_biocd.csv m1663_ab_biocw.csv	Maps M1663_ab_biocd.jpg M1663_ab_biocw.jpg M663_ab_biocd.pdf M1663_ab_biocw.pdf	Grids m1663_biocw.zip m1663_biocd.zip	Total zooplankton biomass (dry weight) from stepped-oblique bottom to surface plankton tows Northern_data/covers/m1663_ab_bioc Neptune record ‘Zooplankton Biomass 1986 - 1992 in Albatross Bay’ m1663_bio.zip (108 Kb)
DRAFT: Mapset: Zooplankton Biomass in Albatross Bay (record # 990)	Mapset: Zooplankton Abundance in Albatross Bay				
DRAFT: GIS Layer: Biomass in Albatross Bay (record # 1056)					
DRAFT: Seagrass Sites in the Port of Weipa, Gulf of Carpentaria (record #1003)	Dataset: Seagrass Sites in the Port of Weipa, Gulf of Carpentaria	Data WeipaSeagrassMetadata.zip WeipaGIS.zip			

Appendix B Data Centre Directory Structure

File locations on the National Oceans Office data base Neptune (for internal National Oceans Office use).

\noo_data\ocean_2004\

noo_data\ocean_2004\base_data
noo_data\ocean_2004\base_data\cars
noo_data\ocean_2004\base_data\circulation
noo_data\ocean_2004\base_data\cruise_report
noo_data\ocean_2004\base_data\ga
noo_data\ocean_2004\base_data\ga\ga_sed_grid
noo_data\ocean_2004\base_data\ga\ga_shapes
noo_data\ocean_2004\base_data\ga\metadata
noo_data\ocean_2004\base_data\incident_light
noo_data\ocean_2004\base_data\modis_data
noo_data\ocean_2004\base_data\northern
noo_data\ocean_2004\base_data\northern\chlorophyll
noo_data\ocean_2004\base_data\northern\copepods
noo_data\ocean_2004\base_data\northern\currents
noo_data\ocean_2004\base_data\northern\phytoplankton
noo_data\ocean_2004\base_data\northern\prawn
noo_data\ocean_2004\base_data\northern\zooplankton
noo_data\ocean_2004\base_data\northern_model
noo_data\ocean_2004\base_data\ssh_dev
noo_data\ocean_2004\base_data\ssh+current
noo_data\ocean_2004\base_data\sst_class
noo_data\ocean_2004\base_data\subsurface_currents
noo_data\ocean_2004\base_data>waves
noo_data\ocean_2004\base_data>winds

\noo_public\ocean_2004

noo_public\ocean_2004\arc_grids
noo_public\ocean_2004\arc_grids\tides
noo_public\ocean_2004\arc_grids>waves
noo_public\ocean_2004\arc_grids\wind
noo_public\ocean_2004\arc_grids\wind\stress

noo_public\ocean_2004\arc_shape
noo_public\ocean_2004\arc_shape\metadata
noo_public\ocean_2004\arc_shape\northern

noo_public\ocean_2004\docs

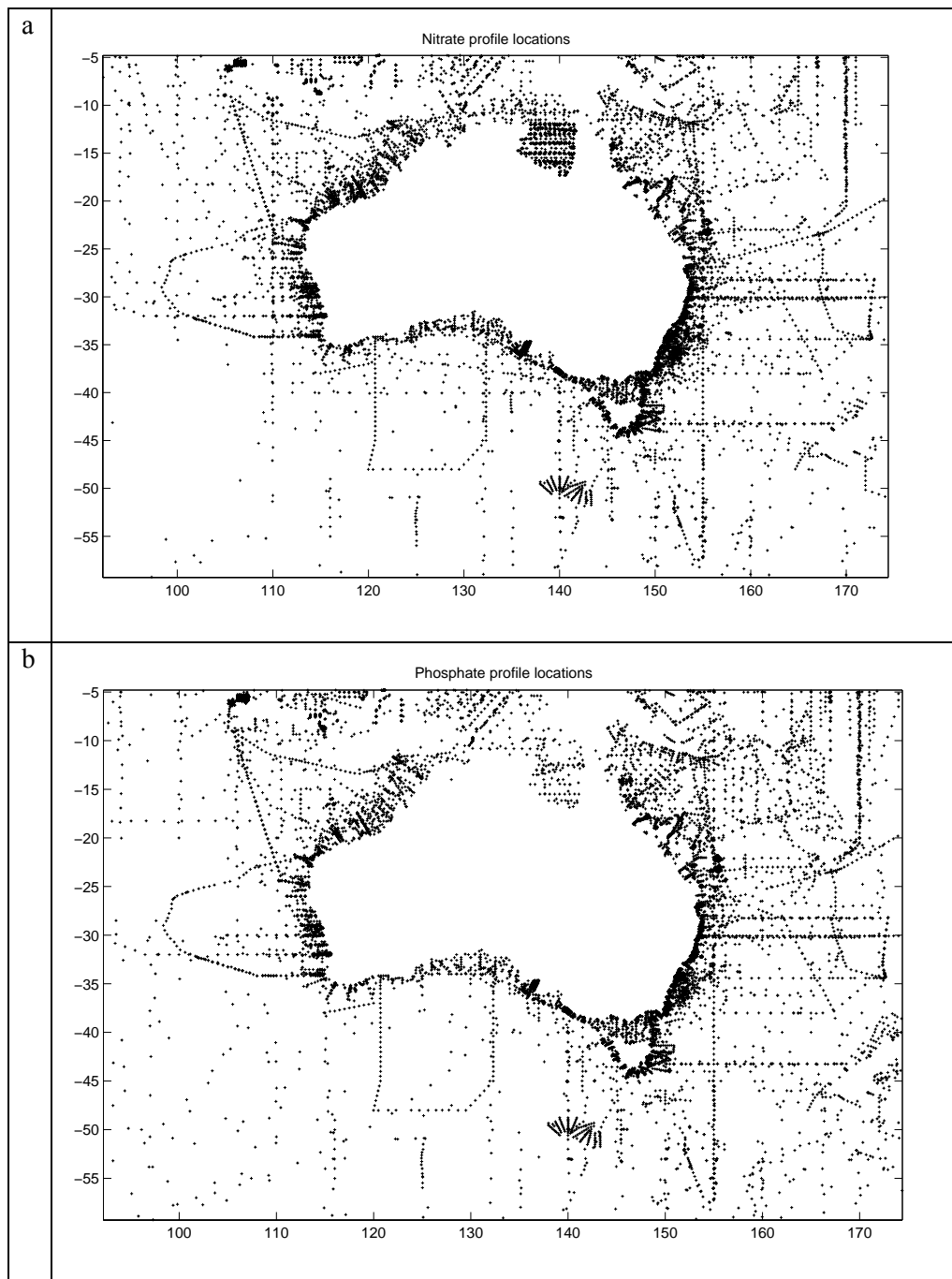
noo_public\ocean_2004\map_info

noo_public\ocean_2004\map_info\primary-production
noo_public\ocean_2004\map_info\primary-production\moved 110line
noo_public\ocean_2004\map_info\zooplankton
noo_public\ocean_2004\map_info\zooplankton\moved 110line

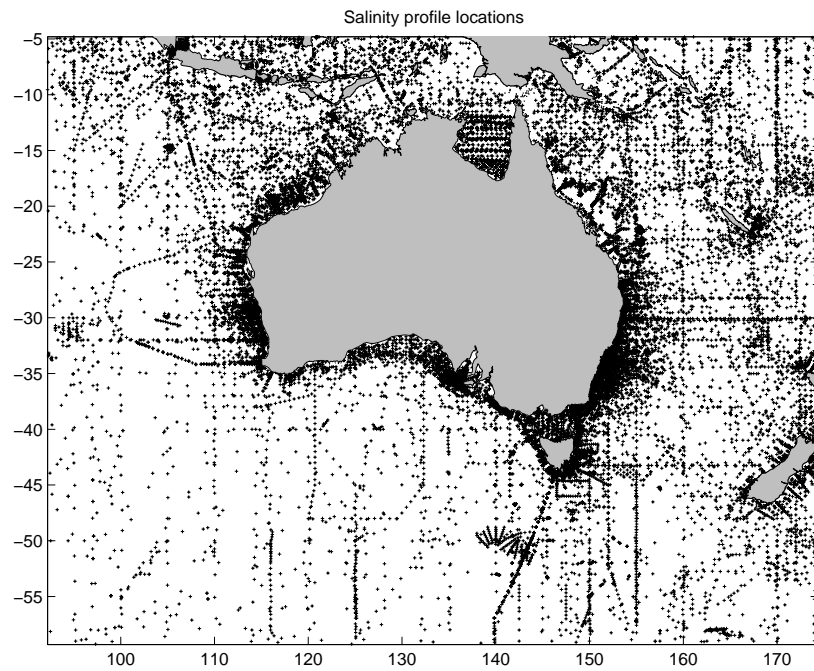
noo_public\ocean_2004\maps
noo_public\ocean_2004\maps\albatross_bay
noo_public\ocean_2004\maps\cars
noo_public\ocean_2004\maps\cars\north
noo_public\ocean_2004\maps\chloro
noo_public\ocean_2004\maps\cruise_report
noo_public\ocean_2004\maps\cruise_report\clarke-bumpus_hor
noo_public\ocean_2004\maps\cruise_report\clarke-bumpus_obl
noo_public\ocean_2004\maps\cruise_report\clarke-bumpus_surface-horizontal
noo_public\ocean_2004\maps\cruise_report\indian_std_net
noo_public\ocean_2004\maps\cruise_report\primary_production
noo_public\ocean_2004\maps\currents
noo_public\ocean_2004\maps\currents\northern
noo_public\ocean_2004\maps\northern
noo_public\ocean_2004\maps\p_prod
noo_public\ocean_2004\maps\phyto_dist
noo_public\ocean_2004\maps\quart_light
noo_public\ocean_2004\maps\ssh
noo_public\ocean_2004\maps\sst
noo_public\ocean_2004\maps\sst_class
noo_public\ocean_2004\maps\template
noo_public\ocean_2004\maps\tides
noo_public\ocean_2004\maps>waves
noo_public\ocean_2004\maps>winds

noo_public\ocean_2004\movie

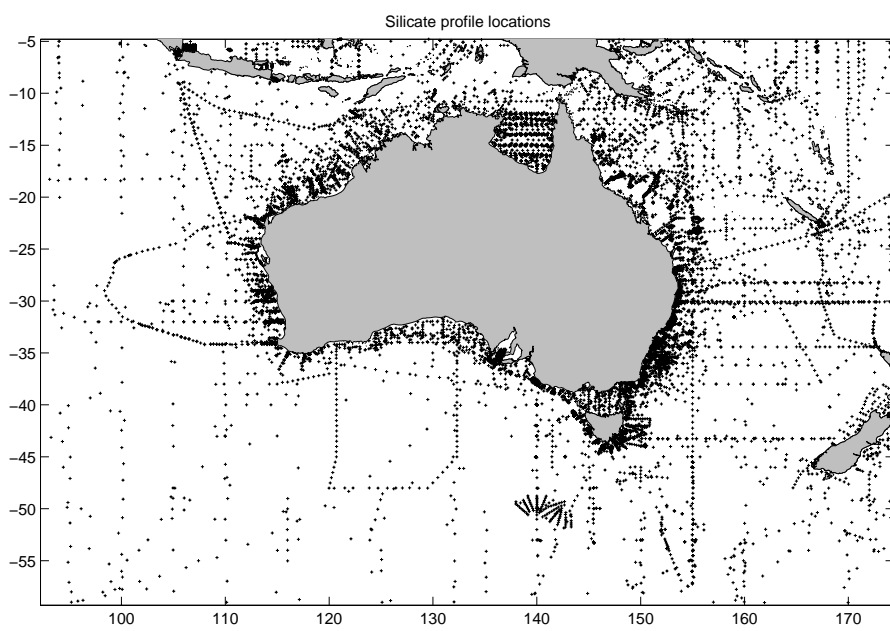
Appendix C CARS Station Locations



c

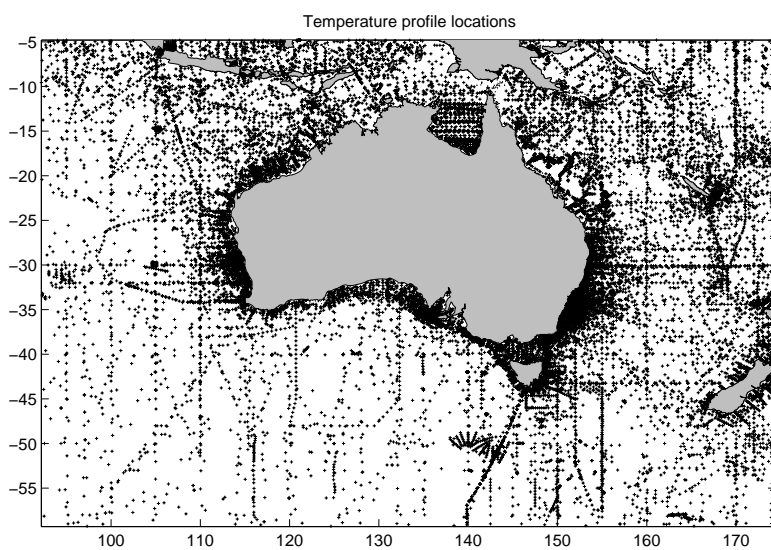


d

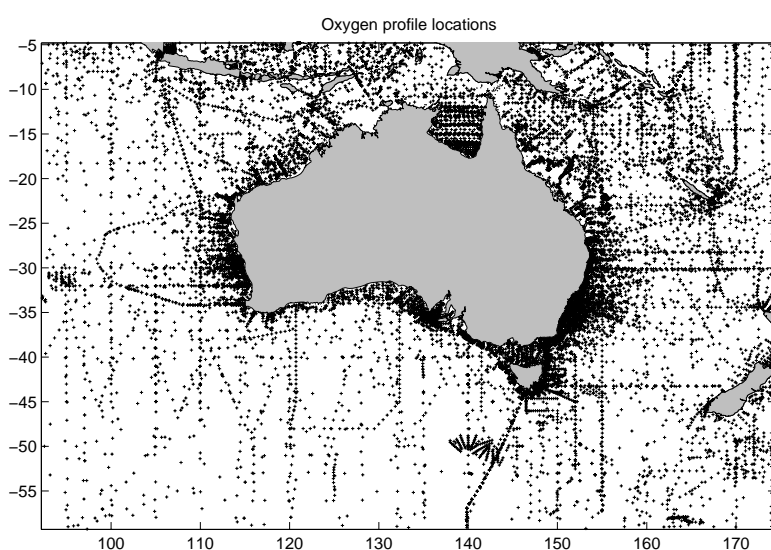


COLLATION AND ANALYSIS OF OCEANOGRAPHIC DATASETS FOR MARINE
BIOREGIONALISATION

e



f



Appendix D Major oceanographic features within the Australian Marine Jurisdiction

Reproduced with permission from Condie *et al.* (2003)

Category	Name of feature	Geographical area	Indicative depth range (m)	Distinguishing properties (relative to local environment)
Water masses	Tropical Surface Water (TSW)	Southwest Pacific	0 – 100	LOW S, HIGH T
	Subtropical Lower Water (SLW)	Southwest Pacific	0 – 200	high S, high T, low O ₂
	Indonesian Throughflow Water (ITW)	Eastern Indian	0 – 1000	low S, high T, low N
	South Indian Central Water (SICW)	Eastern Indian	0 – 200	high S
	Subantarctic Mode Water (SAMW)	North of 50°S	300 – 500	high O ₂ , high N,
	Antarctic Intermediate Water (AAIW)	North of 50°S	800 -1400	low S, high O ₂ , high N
	Subantarctic Zone (SZ)	Southern Ocean	0 – 5000	high N, low Si
	Polar Frontal Zone (PFZ)	Southern Ocean	0 – 5000	high N
	Antarctic Zone (AAZ)	Southern Ocean	0 – 5000	high N, low T, low S
Currents, fronts, & eddies	Hiri Current	Southwest Pacific	0 – 500	high S
	South Equatorial Current	Latitudes 10-15 °S	100 – 800	high S, low T
	Great Barrier Reef Undercurrent	Southwest Pacific	300 – 400	high S, high T
	East Australian Current	Southwest Pacific	0 – 2000	high S, high T, low N
	Tasman Front	Southwest Pacific	0 – 400	high S, med T, low N

	Norfolk Eddy	Southwest Pacific	0 – 2000	high S, high T, low N
	Bass Strait Cascade	Southwest Pacific	80 – 500	high S, low T
	Tasman Outflow	Eastern Indian	0 – 1000	high S, high T
	Zeehan Current	Eastern Indian	0 – 300	high S, high T
	Flinders Current	Eastern Indian	300 – 800	high S, high T
	Leeuwin Current	Eastern Indian	0 – 200	low S, high T
	Leeuwin Undercurrent	Eastern Indian	300 – 400	high S, low T
	Capes Current	Eastern Indian	0 – 100	high S, low T, high N
	Ningaloo Current	Eastern Indian	0 – 100	low T
	Subtropical Front	Latitudes 40-45 °S	0 – 400	high S, high T
	Subantarctic Front	Southern Ocean	0 – 5000	high S, high T
	Polar Front	Southern Ocean	0 – 5000	strong T/S gradients
	Antarctic Slope Front	Southern Ocean	0 – 500	strong T/S gradients
Semi-enclosed seas	Bass Strait	Southwest Pacific	0-80	low T, high S
	South Australian Gulfs	Eastern Indian	0 – 100	high S, inverse estuary
	Shark Bay	Eastern Indian	0 – 20	high S, inverse estuary
	North West Shelf	Tropical Shelf Seas	0 – 200	large tidal range
	Exmouth Gulf	Tropical Shelf Seas	0 – 30	high S, inverse estuary
	Timor Sea / Joseph Bonaparte	Tropical Shelf Seas	0 – 150	strong tidal currents
	Arafura Sea / Gulf of Carpentaria	Tropical Shelf Seas	0 – 70	seasonally stratified
	Torres Strait	Tropical Shelf Seas	0 – 40	strong tidal currents
	Great Barrier Reef Lagoon	Tropical Shelf Seas	0 – 80	low N

Appendix E 3-D/4-D Data Issues

Simon Pigot
Spatial Information Scientist
Department of Primary Industries, Water and Environment

E.1 Executive Summary

An examination of the data and system needs of the National Oceans Office has been carried out with respect to a critical need of the National Oceans Office: visualisation and communication of the results of the pelagic and benthic regionalisations as part of the National Bioregionalisation of the Australian Marine Jurisdiction project. Given the variety of oceanographic data underlying the regionalisations it is expected that the recommendations in this report could be applied to visualisation and communication of other oceanographic data by the National Oceans Office.

The main recommendations of this report follow:

Spatial data formats:

- (i) That 3-D and 4-D data from CSIRO Marine Research and others received in NetCDF or HDF formats be kept in those formats, since these data formats are sufficient, reasonably space efficient, generally standardised, self-documenting, non-proprietary, portable and readily integrated with existing visualisation tools such as OpenDX and the fly-through VisKit system developed at DPIWE.
- (ii) That 3-D and 4-D data not in NetCDF or HDF data formats (e.g. movie loops) be provided with an accurate description and/or existing extraction tools so that these data sources can be interpreted correctly when required for visualisation and analysis. No specific format is preferred, although it would obviously be preferable if the formats used supported fast subsetting and extraction for ease of integration with existing visualisation tools.

Computer systems:

- (i) That National Oceans Office purchase 32-bit (and as they mature, 64-bit) Intel workstations with the latest Nvidia GeForce professional series graphics boards with either AGP or PCI-X interfaces in order to do visualisation work in OpenDX and/or VisKit under Linux.
- (ii) That the National Oceans Office purchase immersive virtual reality equipment to effectively communicate visualisations of oceanographic data.

The overall aim of these recommendations is that resources should be spent on developing informative and imaginative visualisations rather than the traditional over-emphasis on the format of the data.

E.2 Introduction

CSIRO Marine Research (CMR) and the National Oceans Office have recently begun a project on the regionalisation of the pelagic (open ocean) and benthic (ocean floor) ecosystems of Australia's Marine Environment. The results of the regionalisation process will be a subdivision of these two ecosystems into distinct bioregions based on the available physical and biological data.

As part of its wider support role in Australian ocean management, the National Oceans Office needs to be able to impart an understanding of these regionalisations to their clients, most of whom are not scientists, but managers, policy makers, industry stakeholders and the wider community.

This report will focus on two of the fundamental tasks that the author believes the National Oceans Office will need to do in preparation for imparting an understanding of these regionalisations to its clients:

ingest the scientific data (provided by CSIRO Marine Research in a variety of formats) from both the physical and biological characterisation processes that underlie the regionalisations.

visualise the key physical and biological processes that are taking place in one or more bioregions, using appropriate computer software and hardware.

The first section of the report will deal with the basic properties of the 3-D and 4-D data that will be provided to the National Oceans Office by CSIRO Marine Research and data format recommendations. The second section will deal with the issue of visualising this data by examining the available software options currently used in both oceanographic applications and those that the author has contributed to within DPIWE for similar tasks. The third section will examine the various options for computer hardware that can be used to run these visualisations together with some estimates of cost.

Addressing these two fundamental tasks within the context of this project should give National Oceans Office a general basis on which to impart understandings of other data within its purview because of the need to deal with a wide variety of physical and biological oceanographic data that underly the regionalisations.

Two additional issues were mentioned at the various meetings I attended with CSIRO Marine Research staff and National Oceans Office staff. These issues will not be addressed in this report beyond their discussion in the following two subsections because I believe they are logically distinct and that none of the decisions recommended in this report will restrict the options available to implement them. The two issues are:

Evolution of the regionalisations

As the client understanding of the regionalisations developed by National Oceans Office and CSIRO Marine Research improves, it may make sense at some stage for the National Oceans Office to revisit the regionalisation process and recombine the underlying physical and biological data to modify the regionalisations or even produce new regionalisations. In terms of the underlying scientific data, these modifications could either be driven by a new understanding of some physical process or the biological data and/or the relationships

between the two or by some outside political imperative. It seems likely that the principles of the scenario-based model developed for the Regional Forestry Agreement could be employed to address this problem.

Distribution of the regionalisations and other oceanographic data through web based portals

In the context of this work a portal is a web-based service that integrates spatial data and metadata queries to provide an organised view of spatial data from one or more agencies. In the past, implementing portal services usually required all the spatial data within an organisation to be converted to some standard format before it could be used. By the insistence on the use of a standard format, this method of distributing spatial data adds an unnecessary and onerous burden to the task of making spatial data available to users outside an organisation. It also largely ignored, or at best failed to take advantage of, the existence of often very efficient routines that were used within the organisation to subset and/or extract data from the native format.

Realising these shortcomings and the imperfect nature of any translation between two different spatial data file formats, the trend now through movements such as [OpenGIS](#) (Open Geographic Information Systems) and [DODS/OpenDAP](#) (Distributed Oceanographic Data System/Open Data Access Protocol) is to provide a standard language rather than a standard data format. The advantages of this approach are that a standard language in the form of a programmer's interface is much more flexible than a standard file format and the data can remain in its native format, eliminating the often huge burden of translating data to the standard format.

Access to multiple data sources without the need to download them to local storage is achieved by implementing networked data servers that can exchange data using this standard language. The program that extracts the data or a subset of the data from its native format to the standard language becomes just one more client amongst many.

Given that such designs are now becoming the norm (e.g. ESRI's ArcIMS version 9.0 with the data delivery option, OpenDAP servers with clients for NetCDF and other formats) and that templates for adding client data format readers are becoming ubiquitous, it is expected that the recommendations in this report will not constrain the provision of such a data-distribution service.

E.3 3-D/4-D Data Properties and Data Formats

E3.1 Types of 3-D/4-D Spatial Data to be provided

From the documentation provided by CSIRO Marine Research and the National Oceans Office on data products, and data formats it would appear that most 3-D and 4-D data are gridded and time series of gridded data respectively.

Although not specifically mentioned, some of the gridded data may be on non-uniform grids (e.g. rectilinear grids with varying intervals or non-rectilinear grids) and some data will likely be provided as 3-D points.

E3.2 Spatial Data Formats

Assuming that a data format can actually represent the data and in a reasonably space efficient manner, there are a number of criteria that should be examined when considering possible data formats:

fast extraction of subsets: fast subsetting capabilities are essential for rapid analysis and data filtering/preparation for visualisation.

portability of both the format and the extraction routines: essential so that the data and the extraction routines can moved between platforms as required.

proprietary versus non-proprietary: proprietary formats tend to be expensive, slow to evolve and difficult to support. Non-proprietary formats are usually free and evolve with at least some community support.

standardised and self-documenting: a flexible data format should have clearly defined conventions governing its use as well as the facility to incorporate information on its structure and meaning (metadata).

can be readily integrated with other tools: in this case visualisation software such as OpenDX or the VisKit fly-through software.

The NetCDF and HDF formats as used by CSIRO-DMR meet these criteria (with adherence to profile standards such as COARDS in the case of netCDF). Given that they support fast and flexible extraction of subsets and thus can be easily integrated with visualisation toolkits and packages, it seems unlikely that any advantage would be gained by converting them to other formats. I believe the focus should instead be on using the data that these formats contain to develop informative and imaginative visualisations that will help impart an understanding of the regionalisations.

E.4 Software to visualise the data

Visualisation is the process of forming a mental picture of something that is not actually in sight.

Data in the spatial formats described above are usually visualised via a three-stage process. In the first stage a subset of the data is extracted and possibly filtered. Next, the filtered subset is mapped to OpenGL graphics objects and finally the OpenGL graphics objects are rendered on some form of visual display unit (e.g. CRT/LCD screen, data projector(s)).

A brief overview of the origins and status of some possible candidates for the National Oceans Office visualisation task will now be given. This will be followed by a small table comparing their volume-rendering capabilities (since these are most applicable to the visualisation of oceanographic data in a three-dimensional setting), support for preferred input data formats and a number of other features the software should have to visualise the oceanographic data.

OpenDX: is a comprehensive suite of visualisation tools, which originated as IBM's Data Explorer package. The source was released for community development 4-5 years ago and development has continued. The data model is structured around gridded data and the visualisation tools can be incorporated in a stand-alone application. Paid support is available if required. Currently limited to 32-bit datasets.

Vis5D: originated at the University of Wisconsin. Vis5D allows volumetric visualisation of five dimensions of gridded data. Although it is now quite old, it has a simple user interface optimised for atmospheric weather models. Open source. 32 bit datasets.

VisAD: also originates from the University of Wisconsin plus a number of other developers. Unlike the other visualisation toolkits described in this document, VisAD has a data model that uses the metadata to describe the mathematical types of the actual data. These types can then be mapped to data display types to produce the visualisation. Uses Java Components. Open source.

AVS: Advanced Visual Systems Express/Vis is another comprehensive suite of visualisation tools, somewhat similar to OpenDX in functionality and design but still proprietary. 64-bit support.

VTK: Visualisation Tool Kit is a C++ library with interfaces in higher-level languages such as Python. Myriad of advanced features and the data model supports a number of formats besides gridded data. Open source.

VisKit (DPIWE software): Fly-through visualisation system designed around textured terrain applications. Can be used with Silicon Graphics Volumizer software to add paged access to large Volumetric datasets.

<i>Name</i>	<i>Basic volumetric visualisation facilities of interest</i>	<i>Supports NetCDF and HDF?</i>	<i>Fly-through facility?</i>	<i>Non-uniform grids?</i>
<u>OpenDX</u>	Isosurface extraction, horizontal and vertical slicing, coloured surface shading, animated 3-D and 2-D grids, textual annotations	Yes	Yes	Yes
Vis5D	Isosurface extraction, horizontal and vertical slicing, coloured surface shading, animated 3-D grids	No	No	No
<u>VisAD</u>	Isosurface extraction, horizontal and vertical slicing, coloured surface shading, animated 3-D and 2-D grids, textual annotations with the Integrated Data Viewer (IDV) from NCAR.	Yes	No*	Yes
<u>AVS</u>	Isosurface extraction, horizontal and vertical slicing, coloured surface shading, animated 3-D and 2-D grids, textual annotations	Yes	Yes	Yes
VTK	Isosurface extraction, horizontal and vertical slicing, coloured surface shading, animated 3-D and 2-D grids, textual annotations	No*	No*	Yes
VisKit	Can be added using SGI Volumizer software.	No*	Yes	No*

* - Can be added.

From the above, I would recommend OpenDX and VisKit because:

OpenDX is freely available, fully featured and has the additional ability to partition its compute load across different computers. OpenDX has native support for NetCDF and HDF file formats.

VisKit is already specialised around the visualisation of large textured surfaces such as bathymetry. Volume visualisation capabilities can be added using SGI's Volumizer software or even OpenDX. VisKit was demonstrated to National Oceans Office staff in 2003 and would be a useful even in its current form for a number of the tasks described in the requirements document supplied by National Oceans Office for the later phases of the regionalisation project.

E.5 Computer hardware to run these visualisations

From discussions with National Oceans Office staff, it would appear that there is a requirement for both on-line visualisation to interactively explore the oceanographic datasets and off-line or canned visualisation where a viewer travels along a pre-programmed path through the data and the trip is rendered to a video for later display.

On-line visualisation of large, interesting datasets will place heavy demands on computer system memory, CPU and disk. Off-line or canned visualisations are much less demanding on these resources, but are only useful when a fair bit of knowledge has already been built up from interactive explorations of the datasets.

Fortunately, some useful on-line visualisation is now possible from desktop PC systems. Indeed, over the last 10 years the amount of CPU and graphics compute power available to the desktop user has increased dramatically. As an example, in 1996 DPIWE purchased a second-hand Silicon Graphics Onyx rack with 4 x 200 mhz R10000 processors and InfiniteReality graphics (the graphics pipe consists of four 30 cm x 30 cm circuit boards). This was not a desktop machine, yet users of today can obtain desktop machines with processors at least five times faster than the Onyx, which are coupled with a graphics pipe (on a standard PC peripheral board) that is 10-15x faster than InfiniteReality. This migration of compute and graphics power to the desktop has taken place largely because of the development of the interactive entertainment and movie businesses.

E5.1 32-bit Intel Pentium 4 Workstations for average visualisation tasks

Machines that give these capabilities are desktop PCs (2.8GHz Pentium 4 and above plus 1Gb or more RAM) with an AGP or PCI-X graphics slot and an NVidia graphics adaptor, of which the latest incarnation is the GeForce 6. National Oceans Office users will need hardware-accelerated 3-D textures in order to explore three-dimensional oceanographic data, so any purchases must specify the FX or Quadro line of Nvidia graphics adaptors.

Given that visualisation systems such as OpenDX and software such as VisKit can make use of multiple processors when preparing data for visualisation, it might also make sense if National Oceans Office were to purchase a multiple processor Intel IA64 or Xeon 64-bit machine. If in addition, this machine was purchased with two or more PCI-X slots, it would be possible to run two Nvidia Quadro or FX cards, effectively doubling the amount of graphics processing unit power available to be used in visualisations.

Lastly, the National Oceans Office should be aware that the Linux operating system is in general more robust and makes better use of compute resources than Microsoft Windows does for applications such as these. There is also a fairly major commitment to the Linux platform from Silicon Graphics, Nvidia and other companies involved in visualisation for tasks such as these.

E5.2 Virtual Reality to improve understanding of the visualisation

Thoughtful application of virtual reality equipment and techniques to the National Oceans Office visualisations would open up more possibilities in the investigation, understanding and exploration of oceanographic datasets. The basic components for a virtual reality setup are as follows:

A computer system with multiple graphics pipes (such as the dual Nvidia Quadro/FX multiple processor IA-64 or Xeon machine described above or a Silicon Graphics Onyx4 UltimateVision with two or more ATI Radeon-based graphics pipes). Each graphic pipe is used to display part of the visualisation. When projected next to the images from the other graphic pipes it gives a group of users an immersive experience. Stereo glasses and either a head-mounted or hand-held tracking device to control movement through the visualisation.

[Silicon Graphics](#) and [Fakespace systems](#) are the main manufacturers and proponents of this technology and it is likely that the Immersadesk from Fakespace systems or RealityDesk from Silicon Graphics would be best suited to the National Oceans Office needs.

E.6 Conclusions

See Executive Summary on page 222.

E.7 References

AVS Website: <http://www.avs.com>

Lichtenbelt, BR Crane, S Naqvi (1998) Introduction to Volume Rendering, HP Professional books, Prentice Hall

National Oceans Office (2004) Data Transfer Formats Document

National Oceans Office (2004) Building the tools for ecosystem-based management: A conceptual framework for the National Bioregionalisation of the Australian Marine Jurisdiction

OpenDAP/DODS Website: <http://www.opendap.org>

OpenDX Website: <http://www.opendx.org>

OpenGIS Website: <http://www.opengis.org>

Reitinger, B (2001) On-line Program and Data Visualisation of Parallel Systems in a Monitoring and Steering Environment, Diploma Thesis, Johannes Kepler University, Linz, Austria.

Rees, T (2004) Metadata and Database Issues for Oceanographic Bioregionalisation Project, Paper provided at meeting with CSIRO-DMR.

Schroeder, WK Martin, B Lorensen, 1998, The Visualisation Toolkit VTK, Prentice Hall

VisAD Website: <http://www.ssec.wisc.edu/~billh/visad.html>

Volumizer (Silicon Graphics software product) information:
<http://www.sgi.com/software/volumizer>